THE ROLE OF THE TETRASPANIN6 (TSPAN6) IN REGULATING THE IMMUNE MICROENVIRONMENT IN INFLAMMATORY BREAST CANCER (IBC)

by

JING ZHANG

A thesis submitted to the University of Birmingham for the degree of

DOCTOR OF PHILOSOPHY

Institute of Cancer and Genomics

College of Medical and Dental Sciences

University of Birmingham

September 2022

ABSTRACT

Inflammatory breast cancer (IBC) is a rare and aggressive type of invasive breast cancer with poor outcomes. Previous studies demonstrated that IBC is characterised by an abundance of tumour-infiltrating immune cells. However, the mechanism(s) underlying the IBC-controlling accumulation of various immune cells remained unclear. By performing standard trans-well experiments under two time intervals (4-hour and 16-hour), we demonstrated that the medium conditioned by IBC cells (CM-IBC) was chemotactic for B lymphocytes. More importantly, we discovered that Tspan6, a poorly-studied tetraspanin, strengthened the chemoattractive potential of IBC for B cells. Through "immune cell depletion and supplementation" experiments, we uncovered the cellular pathways (i.e. monocyte-dependent, monocyte/CD8+ T lymphocyte-dependent and Pertussis Toxin (PTX)-sensitive pathways) by which Tspan6-expressing IBC cells enhanced the migration of B cells. With regard to the molecular pathway, we identified that syntenin-1, the only known partner protein of Tspan6, played a vital role in regulating the Tspan6-dependent migration of B cells. The disassociation of Tspan6 and syntenin-1 significantly attenuated the chemoattractive potential of IBC cells for B lymphocytes. In addition, the downstream effector, Src kinase and p38 MAPK, appeared to involve in the Tspan6-syntenin-1-dependent migration of B cells. In conclusion, we uncovered intracellular and extracellular pathways by which Tspan6-expressing IBC cells could enhance the migration of B cells. These findings may provide more insights into the complicated immune networks in IBC and provide novel targets for anti-tumour therapeutics.

ACKNOWLEDGEMENTS

This PhD is undoubtedly one of the most significant challenges for me. The whole journey has brought me many memorable moments, mixed with disappointment, doubt, pain and frustration, but also excitement, joy, success and pride. Along this route, I have received unselfish help from many people. First and foremost, I would like to thank my supervisors, Dr Fedor Berditchevski and Dr Abeer Shaaban. They have provided me with a great deal of guidance and encouragement, which has helped me develop my confidence in my research project and build my critical thinking. I still remember the second day in the lab when Dr Fedor Berditchevski showed me how to perform a western blot and instructed me to write down all the steps. He told me that details frequently determine the success or failure of an experiment. Also, I would like to express my gratitude to Dr Elena Odintsova for encouraging me to practice my presentation skills and helping me collect cell images.

I am grateful to the members of my lab, Steven and Yikun. We support each other all the time. Both of you were always there to help in any way you could when problems arose. I would also like to thank Maryam, Regina and Vera for their help in the early stages of my PhD and for telling me how to adjust myself to the new environment and the PhD life.

I would like to thank all my friends in Birmingham. Although most of you do not know or understand my field of study, you have shown great enthusiasm for my subject and have supported my research unconditionally for a long time.

Finally, I would like to thank my family, my mother, my father and my boyfriend, for your unconditional love and support that has brought me this far. You have always comforted me when I was discouraged and encouraged me to keep going. Thank you all for always being there for me.

TABLE OF CONTENTS

LIST OF FIGURES

LIST OF TABLES

ABBREVIATIONS

5-LO	5-Lipoxygenase
AA	Arachidonic Acid
Ab	Antibody
ABC	ATP-Binding Cassette
ABCC1	ATP Binding Cassette Subfamily C Member 1
AD	Alzheimer'S Disease
ADCC	Antibody-Dependent Cell-Mediated Cytotoxicity
AJCC	American Joint Committee on Cancer
AKT/PKB	Protein Kinase B
ALDH	Aldehyde Aehydrogenases
ALIX	ALG-2-Interacting Protein X
AMPA	A-Amino-3-Hydroxy-5-Methyl-4-Isoxazolepropionic Acid
AP	Adaptor Protein
APCs	Antigen-Presenting Cells
APP	Amyloid Precursor Protein
AR	Androgen Receptor
Areg	Amphiregulin
AREs	Au-Rich Elements
Arg	Arginine
Aβ	B-Amyloid Peptide
BAFF	B-cell Activating Factor
BAFFR	B-cell Activating Factor Receptor
Bax	Bcl-2-Associated X Protein
BBD	Benign Breast Disease
BCSS	Breast Cancer-Specific Survival
BL1	Basal-Like 1
BL2	Basal-Like 2
BrdU	Bromodeoxyuridine
Bregs	B Regulatory Cells
BSA	Bovine Serum Albumin
CCG motif	Cys-Cys-Gly Motif
CCL2	Chemokine (C-C motif) Ligands 2

CCL3	Chemokine (C-X-C motif) Ligand 3
CCL4	Chemokine (C-C motif) Ligands 4
CCL5	Chemokine (C-C motif) Ligands 5
CCL8	Chemokine (C-C motif) Ligands 8
CCL9	Chemokine (C-C motif) Ligands 9
CCL10	Chemokine (C-C motif) Ligands 10
CCL11	Chemokine (C-C motif) Ligands 11
CCL18	Chemokine (C-C motif) Ligands 18
CCL19	Chemokine (C-C motif) Ligands 19
CCL20	Chemokine (C-C motif) Ligands 20
CCL21	Chemokine (C-C motif) Ligands 21
CCL22	Chemokine (C-C motif) Ligands 22
CCR2	C-C Chemokine Receptor Type 2
CCR7	C-C Chemokine Receptor Type 7
CD	Cluster of Differentiation
CI	Confidence Interval
CIMC	Canine Inflammatory Mammary Carcinoma
c-Jun	Transcription factor Jun
CK	Cytokeratin
CM	Conditioned Medium
c-Met/HGFR	Tyrosine-protein Kinase Met/Hepatocyte Growth Factor Receptor
CM-IBC	Medium Conditioned by IBC Cells
COX-1	Cyclooxygenase-1
COX-2	Cyclooxygenase-2
CRC	Colorectal Cancer
CREB	cAMP Response Element-Binding Protein
CSC	Cancer Stem-Like Cells
CSF-1/M-CSF	Colony Stimulating Factor 1
CTC	Circulating Tumour Cells
CTD	C-Terminal Domain
CTSB	Cysteine Protease Cathepsin B
CX3CL1	C-X3-C Motif Chemokine Ligand 1
CXCL1	Chemokine (C-X-C motif) Ligand 1
CXCL4	Chemokine (C-X-C motif) Ligand 4
CXCL7	Chemokine (C-X-C motif) Ligand 7
CXCL8	Chemokine (C-X-C motif) Ligand 8

CXCL12	Chemokine (C-X-C motif) Ligand 12
CXCL13	Chemokine (C-X-C motif) Ligand 13
CXCL16	Chemokine (C-X-C motif) Ligand 16
CXCR3	CXC Chemokine Receptor Type 3
CXCR4	C-X-C Chemokine Receptor Type 4
CXCR4	CXC Chemokine Receptor Type 4
CysLTR1	Cysteinyl Leukotriene Receptor 1
DAPI	4'6-Diamidino-2-Phenylindole
DCIS	Ductal Carcinoma *In Situ*
DCs	Dendritic Cells
DDR	Discoidin Domain Receptor
DFS	Disease-free Survival
DKK1	Dickkopf-related Protein 1
DMEM	Dulbecco's Modified Eagle's Medium
DMFS	Distant-metastasis-free Survival
DNA	Deoxyribonucleic Acid
DUSP1	Dual Specificity Protein Phosphatase 1
EBI2	Epstein-Barr virus-induced G-protein Coupled Receptor 2
EC1	Small Extracellular Loop
EC2	Large Extracellular Loop
ECM	Extracellular Matrix
EDTA	Ethylenediamine Tetraacetic Acid
EGF	Epidermal Growth Factor
EGFR	Epidermal Growth Factor Receptor
ELISA	Enzyme-linked Immunoassay
EMT	Epithelial-mesenchymal Transition
EP4	Prostaglandin E2 Receptor 4
ER	Estrogen Receptor
ErbB family	Epidermal Growth Factor Receptor Family
ERK	Extracellular Signal-regulated Kinase
EVs	Extracellular Vesicles
EWI-2/IgSF8	Immunoglobulin Superfamily Member 8
EZH2	Enhancer of Zeste Homolog 2
FACS	Fluorescence Activated Cell Sorting
FAK	Focal Adhesion Kinase
FALP	5-Lipoxygenase-Activating Protein

Fas	FS-7-associated Surface Antigen
FasL	Fas Ligand
FCS	Fetal Calf Serum
FcγRIIB	Fc fragment of IgG Receptor Iib
FEVR	Familial Exudative Vitreoretinopathy
FGFR	Fibroblast Growth Factor Receptor
FOXP3	Forkhead Box P3
FZD4	Frizzled-4
GC	Germinal Center
GFP	Green Fluorescent Protein
GM3	Monosialodihexosylganglioside
GPCR	G Protein-coupled Receptor
GRO	Growth-regulated Oncogene
GTP	Nucleotide Guanosine Triphosphate
Gαi	G_i Protein Alpha Subunit
H3	Histone 3
HCC	Human Hepatocellular Carcinoma
HCV	Hepatitis C Virus
HER1/2/3/4	Human Epidermal Growth Factor Receptor1/2/3/4
HGF	Hepatocyte Growth Factor
HLA	Human Leukocyte Antigen
HMEs	Human Mammary Epithelial Cells
HMGB1	High Mobility Group Box 1
HR	Hormone Receptor
H-Ras	Harvey Rat Sarcoma Viral
HRP	Horseradish Peroxidase
HSP27	Heat Shock Protein
IBC	Inflammatory Breast Cancer
IDC	Invasive Ductal Carcinoma
IFNα	Interferon Alpha
IFNγ	Interferon Gamma
IgA	Immunoglobulin A
IgG	Immunoglobulin G
IκB	Nuclear Factor of Kappa Light Polypeptide Gene Enhancer in B-cells Inhibitor
IκB-α	Nuclear Factor of Kappa Light Polypeptide Gene Enhancer in B-cells Inhibitor Alpha

IκB-β	Nuclear Factor of Kappa Light Polypeptide Gene Enhancer in B-cells Inhibitor Beta
ILC	Invasive Lobular Carcinoma
ILK	Integrin-Linked Kinase
ILVs	Intraluminal Vesicles
IL-1	Interleukin 1
IL-1a	Interleukin 1 Alpha
IL-4	Interleukin 4
IL-5	Interleukin 5
IL-6	Interleukin 6
IL-7R	Interleukin 7 Receptor
IL-8	Interleukin 8
IL-10	Interleukin 10
IL-12	Interleukin 12
IL-13	Interleukin 13
IL-23	Interleukin 23
IM	Immunomodulatory
IMCs	Inflammatory Mammary Carcinomas
ITIMs	Immunoreceptor Tyrosine-Based Inhibition Motifs
JAK	Janus Kinase
JNKs	c-Jun N-terminal Kinases
JNK1/2/3	c-Jun N-terminal Kinases 1/2/3
KAI-1	Tetraspanins27
KD	Knock Down
Ki-67	Nuclear Protein
K-Ras	Kirsten Rat Sarcoma Virus
LABC	Locally Advanced Breast Cancer
LAR	Luminal Androgen Receptor
LECs	Lymphatic Endothelial Cells
LFA-1	Leukocyte Function Associated Antigen-1
LPS	Lipopolysaccharides
LRP1	Low-Density Lipoprotein Receptor-Related Protein 1
LRP5	Low-Density Lipoprotein Receptor-Related Protein 5
LTD4	Leukotriene D4
LXR	Liver X Receptor
Lys	Lysine
Lyn	Tyrosine-Protein Kinase Lyn

M	Mesenchymal
MAb	Monoclonal Antibody
MAPK	Mitogen-Activated Protein Kinase
MaSCs	Mammary Stem Cells
MAVS	Mitochondrial Antiviral Signalling Protein
MCP-1/CCL2	Monocyte Chemoattractant Protein-1
MDR1	Multidrug Resistance Protein 1
MDSCs	Myeloid-Derived Suppressor Cells
MET	Mesenchymal to Epithelial Transition
MFSD2B	Major Facilitator Superfamily Transporter 2b
MG	Growth Factor Reduced Matrigel
MHC I/II	Major Histocompatibility Complex I/II
MIF	Macrophage Migration Inhibitory Factor
MIP-1β	Macrophage Inflammatory Protein-1 Beta
miRNA	microRNA
MK2	MAPK Activated Protein Kinase 2
MK3	MAPK Activated Protein Kinase 3
MMP1/3/9/10	Matrix Metalloprotease 9
MMTs	Malignant non-IMC Mammary Tumours
MNK	MAPK-Interacting Kinase
MSCs	Mesenchymal Stem/Stromal Cells
MSK1/2	Mitogen and Stress-Activated Kinases 1/2
MVB	Multivesicular Body
NAC	Neoadjuvant Chemotherapy
NCCN	National Comprehensive Cancer Network
NET-6	Tetraspanin-13
NF-κB	Nuclear Factor Kappa B
NK Cells	Natural Killer Cells
NMT1	N-myristoyl Transferase 1
NST	No Special Type
OD	Optical Density
OS	Overall Survival
PBMCs	Peripheral Blood Mononuclear Cells
PBS	Phosphate Buffered Saline
pCR	Pathological Complete Response
PD1	Programmed Cell Death-1
PD-L1/2	Programmed Cell Death Ligand 1/2

PEI	Polyethyleneimine
PFS	Progression-Free Survival
PGs	Prostaglandins
PGD	Prostaglandin D
PGE	Prostaglandin E
PGE2	Prostaglandin E2
PGF	Prostaglandin F
PGF2a	Prostaglandin F2 Alpha
PGH2	Prostaglandin H_2
PGI2	Prostacyclin
PI3K	Phosphoinositide-3 Kinase
PICK1	Protein Interacting with C Kinase 1
PKC	Protein Kinase C
PKCα	Protein Kinase C Alpha
PLCγ	Phospholiase C Gamma
PR	Progesterone Receptor
PTN	Pleiotrophin
PTX	Pertussis Toxin
Ras	Rat Sarcoma Virus
RDS	Peripherin-2
RelA	A Key Member of NF-κB Family
RFS	Recurrence-free Survival
RGS16	Regulator of G Protein Signaling 16
Rho family	Ras Omologous Family
Rho-GTPase	Rho-Guanosine Triphosphate Hydrolase
RhoA	Ras Homolog Family Member A
RHOB	Ras Homolog Family Member B
RhoC GTPase	RhoC-Guanosine Triphosphate Hydrolase
RLRs	Retinoic Acid-inducible Gene I-like Receptors
RNA	Ribonucleic Acid
RPN2	Ribophorin II
RTKs	Receptor Tyrosine Kinases
S1P	Sphingosine-1-Phosphate
S1P1	Sphingosine 1-Phosphate Receptor Type 1
S1P2	Sphingosine 1-Phosphate Receptor Type 2
S1P3	Sphingosine 1-Phosphate Receptor Type 3
S1P4	Sphingosine 1-Phosphate Receptor Type 4

S6	Serine 6
p-SAPK	Phospho-Stress-Activated Protein Kinase
SAPK4	Stress-Activated Protein Kinase 4
SD	Standard Deviation
SDS-PAGE	Sodium Dodecyl Sulfate-Polyacrylamide Gel Electrophoresis
SEM	Standard Error Mean
Ser	Serine
SH2	Src Homology 2
SHIP-1	Src Homology 2-containing Inositol Phosphatase-1
SHP-1	Src Homology Region 2 Domain-containing Phosphatase-1
SHP-2	Src Homology Region 2 Domain-containing Phosphatase-2
siRNA	Small Interfering RNA
SLOs	Secondary Lymphoid Organs
SPHK1	Sphingosine Kinase 1
SPNS2	Spinster 2
STAT1/2/3/4/5A/5B/6	Signal Transducer and Activator of Transcription1/2/3/4/5A/5B/6
SV40	Simian Virus 40
TACI	Transmembrane Activator and CAML Interactor
TAMs	Tumour-Infiltrating Macrophages
TAZ	Transcriptional Co-activator with PDZ-binding motif
TBST	Tris-Buffered Saline with 0.05% Tween-20
Tc cells	T Cytotoxic Cells
TDEs	Tumour-Derived Exosomes
TEMs	Tetraspanin-Enriched Microdomains
Tfh	T follicular helper cells
TGF-β	Transforming Growth Factor Beta
TGF-β1	Transforming Growth Factor Beta 1
TβRI	Transforming Growth Factor β Receptor I
Th cells	T helper cells
Thr	Threonine
TIG1	Tazarotene-Induced Gene-1
TILs	Tumour-Infiltrating Lymphocytes
TIL-B	Tumour-Infiltrating B Lymphocytes

TIME	Tumour Immune Microenvironment
TIMP-1	Tissue Inhibitor of Metalloproteinase-1
TLR	Toll Like Receptors
TLR7/8	Toll Like Receptors 7/8
TLSs	Tertiary Lymphoid Structures
TM2	Transmembrane Domain 2
TM3	Transmembrane Domain 3
TMB	Tetramethylbenzidine
TNBC	Triple-Negative Breast Cancer
TNF-a	Tumor Necrosis Factor Alpha
TNFAIP3	Tumor Necrosis Factor Alpha Induced Protein 3
TNFR2	Tumor Necrosis Factor Alpha Receptor 2
TN-IBC	Triple Negative Inflammatory Breast Cancer
TN-non-IBC	Triple Negative non Inflammatory Breast Cancer
Tregs	Regulatory T cells
TSPAN7	Tetraspanin 7
TSPAN12	Tetraspanin 12
TTP	Tristetraprolin
TXA2	Thromboxane
TYK2	Tyrosine Kinase 2
UTR	Untranslated Region
UV	Ultraviolet
VEGF	Vascular Endothelial Growth Factor
VEGF3	Vascular Endothelial Growth Factor 3
VEGF-A	Vascular Endothelial Growth Factor-A
VEGF-D	Vascular Endothelial Growth Factor-D
VEGFR	Vascular Endothelial Growth Factor Receptors
VEGFR3	Vascular Endothelial Growth Factor Receptor 3
WHO	World Health Organization
XIAP	X-linked Inhibitor of Apoptosis Protein
Xq22	Chromosome
Y	Tyrosine
YAP	Yes-Associated Protein, a transcription factor

1. INTRODUCTION

1.1. Breast Cancer

1.1.1. Definition

The mammary gland development is a sequential process elaborately regulated by many evolutionary factors (Feng Y *et al.*, 2018). A mature human mammary gland typically consists of epithelial components and stroma components. The epithelial components originate from mammary stem cells (MaSCs), differentiating into luminal and basal stem cells. The luminal stem cells further develop into ductal and alveolar cells, while basal stem cells differentiate into myoepithelial cells. Alveolar cells subsequently form lobules that are responsible for milk production. Milk is then drained by ducts that are constituted by ductal cells. The milk-secreting system is supported and surrounded by myoepithelial cells. Stroma tissue, such as vessels, connective tissues and adipose tissues, exert supportive function, providing nutrition, the tissue connecting and protection (WHO classification of tumours, 5th edition, breast tumours). The term "breast cancer" refers to a malignant tumour arising from breast epithelial or stroma tissue due to accumulating genetic and epigenetic abnormalities, causing an uncontrolled, non-programmed proliferation in the breast (Chu PY *et al.*, 2019). Breast cancer originates from epithelial cells and stroma cells called carcinoma and sarcoma. Because breast sarcoma is rare, "breast cancer" typically refers to breast carcinoma (Figure 1-1).

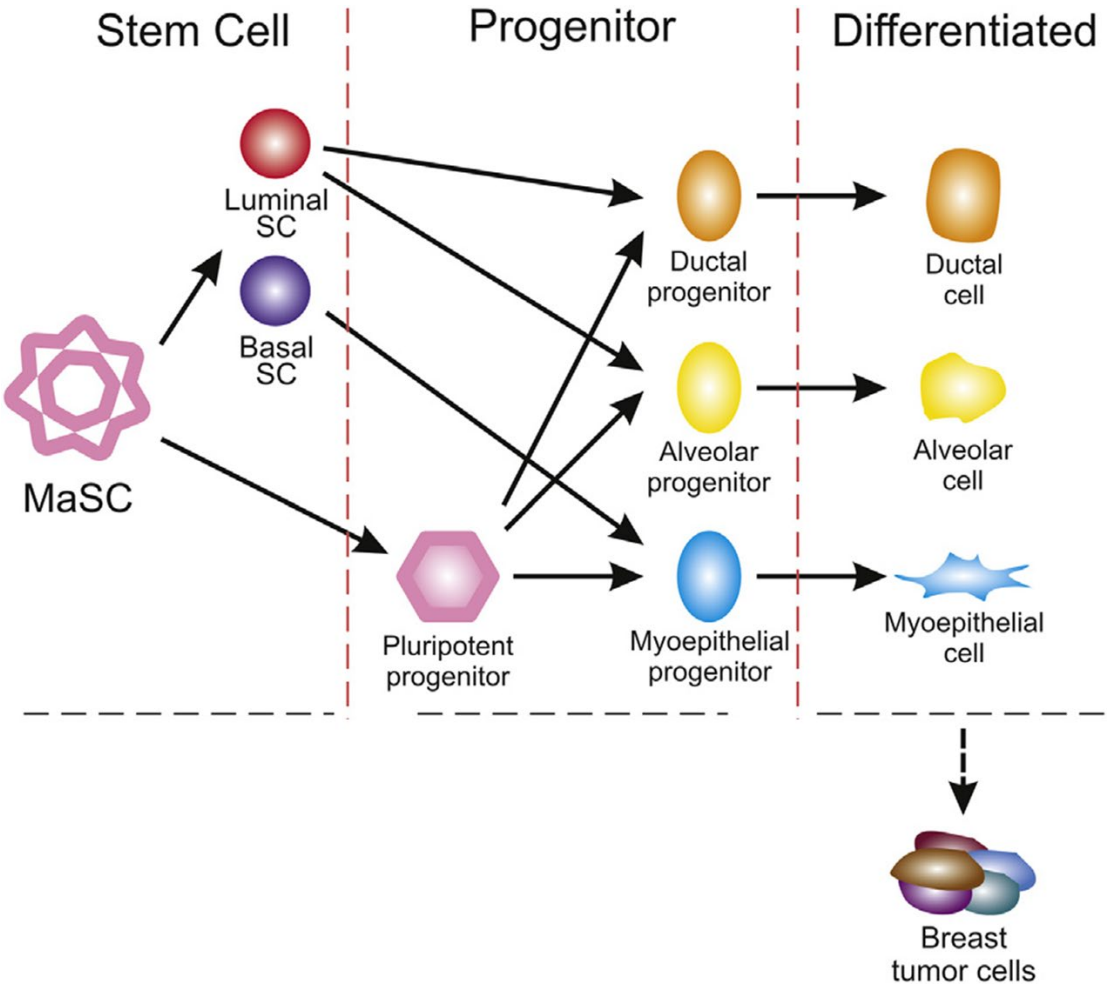

Figure 1-1. Mammary cell hierarchy and origins of breast carcinoma. Multipotent mammary stem cells (MaSCs) undergo symmetric and asymmetric divisions to generate progenitor cells (luminal and basal stem cells) and achieve self-renewal. Luminal stem cells subsequently develop into alveolar progenitors and ductal progenitors, which eventually differentiate into alveolar and ductal cells that are responsible for milk production and draining. In contrast, basal stem cells develop into myoepithelial progenitors, further differentiating into myoepithelial cells and exerting supportive and protective functions. Breast carcinogenesis can occur at any stage of mammary gland development, giving rise to heterogeneous breast cancer cells. The figure is reproduced and modified from (Feng Y *et al.*, 2018).

1.1.2. Pathology classification

Depending on the presence of cancer cells invasion into the basement membrane, breast cancer is generally categorised into two subtypes: non-invasive breast carcinoma (carcinoma *in situ*) and invasive breast carcinoma (WHO 5th 2019, AJCC,8th).

1.1.2.1. *In situ* Carcinomas

Since lobular carcinoma *in situ* was considered a benign entity and has been removed from the breast carcinoma family, currently, breast carcinoma *in situ* refers to ductal carcinoma *in situ* (DCIS) and a special type, Paget disease (WHO 5th 2019, AJCC,8th). DCIS develops from ductal cells and does not affect the surrounding tissue. Therefore, DCIS is considered an early carcinoma in the breast and possesses the potential to become an invasive breast carcinoma. Therefore, an early diagnosis is vital to stop its progression to invasive breast carcinoma. Paget disease is a rare type of breast carcinoma, and it typically presents with eczema-like skin of the nipple and areola. Delayed therapeutic intervention is quite common in Paget disease patients due to misdiagnosis with other skin diseases.

1.1.2.2. Invasive breast cancer

Invasive breast carcinomas are a heterogeneous group of malignant epithelial neoplasms affecting the glandular components of the breast. Based on different morphologies, invasive

breast cancers are categorised into: 1) special type, those present special histological features in >/=90% of the tumour (e.g. lobular, mucinous tubular histological patterns); 2) no special type (NST), which do not have specific histological features and account for a majority of invasive breast cancer cases. Below, we described one representative carcinoma from each type.

Invasive ductal breast cancer (invasive ductal carcinoma, IDC)

IDC is the most common type of breast cancer, accounting for 40%–75% of invasive breast carcinoma cases (Makki J, 2015). It is currently more known as invasive breast carcinoma of NST (WHO Classification of Tumours, 5th). IDC is a broad and heterogeneous family of invasive breast cancer that cannot be categorised morphologically as any special subtype. The histological architecture of IDC varies dramatically. Tumours can develop several growth patterns, such as cords, clusters and trabeculae, and in some cases, tumours exhibit a predominant solid or syncytial infiltrative pattern (WHO Classification of Tumours, 5th).

Invasive lobular breast cancer (invasive lobular carcinoma, ILC)

ILC is the second most prevalent invasive breast cancer histopathologically separate from IDC. It accounts for 5-15% of breast cancer cases (WHO Classification of Tumours, 5th) and is the most common special type of breast carcinoma. ILC is typically composed of cells that lack cohesion and appear singly scattered or grouped in a single-file linear pattern (WHO

Classification of Tumours, 5th). Like IDC, ILC can damage the normal structure of the breast and metastasise to other organs.

1.1.3. Molecular classification

Over the past decade, molecular classification of breast cancer has gradually become a vital indicator for therapeutics. Compared to pathology classification, molecular classification emphasises the intrinsic properties of breast cancer, which could provide more biological information on the behaviours of cancer cells. There are four molecular subtypes of breast cancer defined by the expression levels of estrogen receptor (ER), progesterone receptor (PR) (both ER and PR are hormone receptor HR), the amplification of the HER2 oncogene, and the degree of the Ki-67 index (Perou CM *et al.*, 2000; Cheang MC *et al.*, 2009; Goldhirsch A *et al.*, 2011). Specifically, breast cancer can be categorised into: luminal A (ER/PR+, HER2-, Ki-67<14%), luminal B (ER/PR+, HER2-/+, Ki-67>/=14%), HER2 overexpressing (ER/PR-, HER2+), basal-like (ER/PR-, HER2-) (Table 1-1). It is worth noting that there is a high proportion of overlap between basal-like breast cancer and triple-negative breast cancer (ER/PR-, HER2-, TNBC), hence the basal type is sometimes referred to as TNBC (Goldhirsch A *et al.*, 2011).

MOLECULAR SUBTYPE				
IMMUNOPROFILE	**LUMINAL A**	**LUMINAL B**	**HER2/*NEU***	**BASAL-LIKE**
ER, PR	ER and/or PR+	ER and/or PR+	ER–, PR–	ER–, PR–
HER2 and others	HER2–Low Ki-67 (<14%)	HER2+ or HER2– Ki-67 = 14% or more	HER2+	HER2– CK5/6 and/or EGFR+

Table 1-1. Molecular classification of breast cancer. Clinically defined subtypes of breast cancer. ER, estrogen receptor; PR, progesterone receptor; HER2, human epidermal growth factor receptor 2; CK, cytokeratin; EGFR, epidermal growth factor receptor. The table is reproduced from (Makki J, 2015).

Due to the heterogeneity of TNBC, a further genetic classification was applied to divide TNBC into six distinct subtypes: basal-like 1 (BL1), basal-like 2 (BL2), mesenchymal (M), mesenchymal stem-like (MSL), immunomodulatory (IM), and luminal androgen receptor (LAR) (Lehmann BD *et al.*, 2011; Wang DY *et al.*, 2019). Each subtype is characterised by distinct gene expression. For example, the LAR subtype is enriched with the expression of genes linked to the androgen receptor (AR) signalling pathway (Lehmann BD *et al.*, 2011). Others, like BL1 and BL2 subtypes, express significant levels of cell cycle and DNA damage response genes, and the M and MSL subtypes have an abundance of genes involved in epithelial-mesenchymal transition (EMT) and growth factor pathways (Lehmann BD *et al.*, 2011).

1.2. Inflammatory Breast Cancer (IBC)

1.2.1. Definition

IBC, as a special subtype of breast carcinoma, is a rare and lethal disease. The term IBC was initially used by Lee and Tannenbaum in 1924 (Lee BJ and Tannenbaum NE, 1924). IBC is defined by the 8th edition of the American Joint Committee on Cancer (AJCC 8th edition) as 'Inflammatory carcinoma is a clinical-pathologic entity characterised by diffuse erythema and oedema (peau d'orange) involving a third or more of the skin of the breast.' However, the criteria are questioned as the measurement of lesion area is relatively subjective; thus, the UK IBC working group definition did not include specified criteria for the proportion of breast involvement or size of erythema (or oedema) (Rea D *et al.*, 2015). The primary IBC is classified as T4d, and the stage of IBC is determined by the extent of nodal involvement and distant metastases, ranging from stage IIIB to stage IV (AJCC 8th edition).

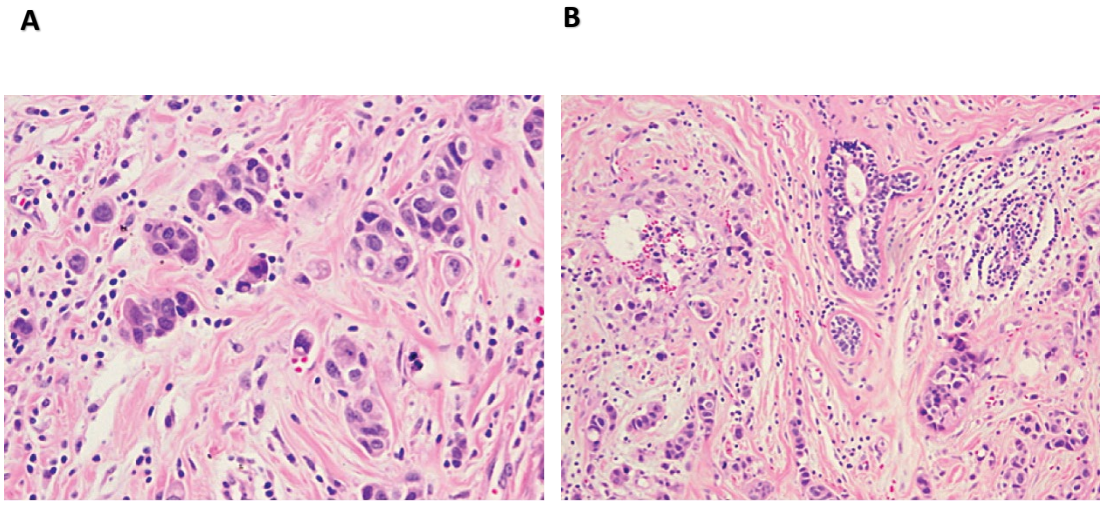

Figure 1-2. Haematoxylin and eosin stains of inflammatory breast cancer. (A) Invasive inflammatory breast cancer stained with haematoxylin and eosin. **(B)** A representative image

of inflammatory breast cancer tumour cells at high magnification. The figures are reproduced from (Woodward WA, 2015).

1.2.2. Clinical and pathological characteristics of IBC

IBC is a unique clinical entity, typically presenting with diffuse redness (brownish or dark purple skin might appear occasionally) and oedema with apparent dermal hair follicles (peau d'orange) involving affected breast skin. Warm and asymmetric breast size is also common, as well as nipple retraction (Ellis DL and Teitelbaum SL, 1974; Robertson FM *et al.*, 2010; Fouad TM *et al.*, 2017). Intriguingly, despite prominent skin changes, palpable mass underlying the breast is typically not detectable in IBC cases. Consequently, IBC is often misdiagnosed as mastitis or other infectious diseases (Robertson FM *et al.*, 2010; Fouad TM *et al.*, 2017).

Although the aforementioned clinical features characterise IBC, it is not a distinct histological subtype of breast carcinoma. IDC remains the most common type of IBC (65.5% ~ 89.8%), followed by ILC (3.4% ~ 10.2%) and the mixed type (1.4% ~ 5.6%) (Raghav K *et al.*, 2016; Copson E *et al.*, 2018; Kupstas AR *et al.*, 2020). The most common histopathological feature of IBC is the presence of lymphovascular tumour emboli in the papillary and reticular dermis of the skin overlying the breast, which mainly contributes to the swelling and erythema in IBC patients (Figure 1-3). The formation of emboli is a product of a series of well-orchestrated steps. Tumour cells disassociate from the primary tumour as a small cluster, and then invade vascular

and lymphatic vessels enriched in IBC. The cluster of cells survives and evades the surveillance of immune cells, eventually forming a blockage in the vessels (Jolly MK *et al.*, 2017; Lim B *et al.*, 2018). Another hallmark of IBC is the high expression of E-cadherin (Levine PH *et al.*, 2012). Intriguingly, E-cadherin is thought to function as a suppressor of tumour metastasis in non-IBC, while in IBC, E-cadherin is widely expressed by cancer cells at the primary lesion, tumour emboli and metastatic sites. Furthermore, it is thought that the expression of E-cadherin by IBC cells facilitates tumour emboli formation (Robertson FM *et al.*, 2010; Jolly MK *et al.*, 2017).

While the molecular subtypes of IBC are identical to non-IBC, subtype proportions are slightly different between these two cancers. Hormone receptor-positive (HR+) remains the most prevalent type, but IBC has higher proportions of HER2+ and TNBC cases compared to non-IBC (IBC: HR+ 30%~56.2%, HER2+ 23.1%~40% and TNBC 25.1%~30%; non-IBC: HR+ 60%~84%, HER2+ 2.5%~25% and TNBC 5%~15%) (Masuda H *et al.*, 2014; Mullooly M *et al.*, 2017; Copson E *et al.*, 2018; Alwan NAS and Al-Okati D, 2018; Mesa-Eguiagaray I *et al.*, 2020). In addition, patients with IBC are more likely to have poorer outcomes than molecular subtype-matched non-IBC, which implies an aggressive nature of IBC (Li J *et al.*, 2011; Masuda H *et al.*, 2014).

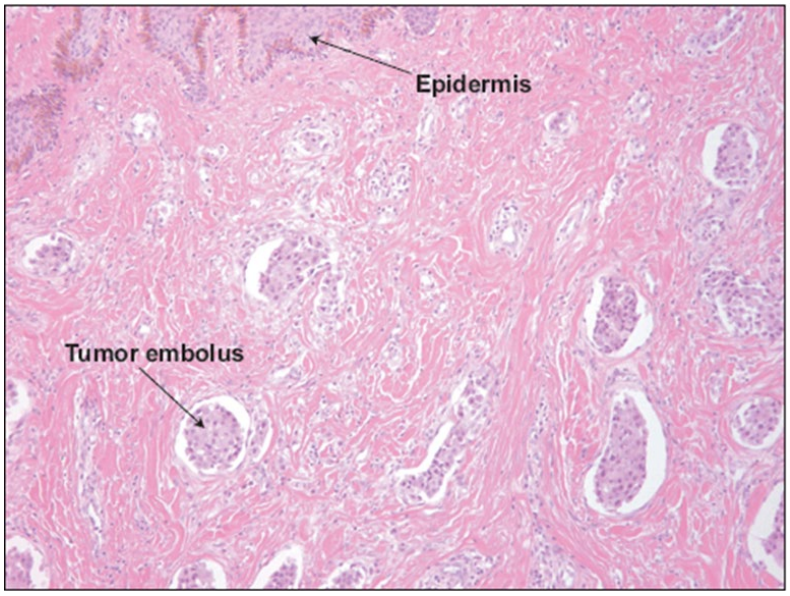

Figure 1-3. Tumour emboli in IBC tissues. A representative HE-stained histologic section of the IBC specimen. This figure is adopted from (Houchens NW and Merajver SD, 2008).

1.2.3. Epidemiology of IBC

A retrospective review of IBC cases in the UK demonstrated that IBC accounts for 0.4-1.8% of invasive breast cancer (Copson E *et al.*, 2018). The median age of IBC patients was 56 years (range 26-92 years old), compared to 62 years for unselected UK invasive breast cancer cases (Copson E *et al.*, 2018). Approximately 88% of IBC patients were white/Caucasian, followed by Asian and black, 5.2% and 4.8%, respectively (Copson E *et al.*, 2018). Though there is a low incidence of IBC, patients diagnosed with IBC have unfavourable survival than those with non-IBC. The median overall survival (OS) of stage III and stage IV were 7.5 years and 1.9 years, respectively (Copson E *et al.*, 2018). Five-year OS rates of IBC stage III and IV are 61% and 21.4% (Copson E *et al.*, 2018), while for non-IBC, are 73.9% and 26.6%, respectively

(public health England 2020). In addition, approximately 40% of IBC patients in stage III develop distant metastasis within five years since their first diagnosis (Copson E *et al.*, 2018). A slightly higher incidence of IBC is observed in the USA (2%-4%). The difference may be attributed to the difference in the population structure of the UK and the US (Hance KW *et al.*, 2005). Despite a low incidence, IBC contributes to 7-10% of breast cancer-associated deaths, resulting in 4,000 deaths per year in the USA (Hance KW *et al.*, 2005). Furthermore, similar to the UK, IBC patients in the USA also have a poorer prognosis when compared to non-IBC patients (Schlichting JA *et al.*, 2012).

The prognosis of IBC differs greatly depending on the molecular subtype. Statistics of the UK showed that HR+/HER2+ patients had the most favourable outcome (the five-year OS), whereas the TN-IBC cohort had the worst outcome: HR+/HER2+ 76.9%, HR+/HER2− 70%, HR−/HER2+ 66.2%, and HR−/HER2− 37.7% (Copson E *et al.*, 2018), which is in line with the data of the IBC patients in the Netherlands (IBC five-year OS: HR+/HER2+ 45.8%, HR+/HER2− 36.5%, HR−/HER2+ 31.8%, and HR−/HER2− 15.2%) (van Uden D *et al.*, 2019).

1.2.4. Current treatments of IBC

Due to the rarity of the disease, there are no large, randomised trials to optimise the therapeutics for IBC. The guidelines for systemic treatment are mainly based on evidence

from retrospective analysis, small prospective studies, and findings from non-IBC, locally advanced breast cancer (LABC) patients. Trimodal therapy is strongly recommended for patients with IBC, which comprises systemic cytotoxic chemotherapy that is more likely to be initiated before surgery (neoadjuvant chemotherapy, NAC), an aggressive mastectomy, and radiotherapy (NCCN, 2021) (Rea D *et al.*, 2015). A chemotherapy regimen involving the anthracycline-based treatment with a taxane was reported to improve the progression-free survival (PFS) and OS of ER-negative IBC (Cristofanilli M *et al.*, 2004). Another study indicated that the anthracycline-taxane combination significantly improved the treatment response rate of IBC patients with axillary lymph node metastasis (Hennessy BT *et al.*, 2006). The molecular status also determines therapy for IBC patients. HR+ IBC patients are strongly recommended endocrine therapy after completing the preoperative systemic therapy (Rea D *et al.*, 2015). IBC patients with HER2+ are recommended to receive anti-HER2 therapy, such as trastuzumab, for up to one year (Gianni L *et al.*, 2010). IBC patients without distant metastasis who respond well to preoperative systemic therapy could consider a mastectomy. Otherwise, additional systemic chemotherapy and/or preoperative radiation should be carried out. Postoperation radiotherapy is also necessary for IBC patients unless some people have clear contraindications.

1.2.5. Signalling pathways in IBC

1.2.5.1. Overview of signalling pathways in IBC

Over the last two decades, an increasing number of investigations focused on identifying specific molecules and signalling pathways that contributed to the high malignancy of IBC. Below, we summarised vital molecules and signalling pathways linked to IBC development and progression.

1.2.5.2. EGFR pathway in IBC

The epidermal growth factor receptor (EGFR, also called ErbB1 or HER1), belongs to the ErbB family of receptors, which comprises HER1, HER2, HER3, and HER4. The ligand binding to EGFR induces homo- or heterodimerisation of the receptor with other ErbB proteins. Ligand-bound EGFR complexes activate multiple downstream signalling molecules, including PI3K/AKT, Ras/MAPK, PLCγ/PKC and STAT, which control cell proliferation, migration, invasion and differentiation (Zhang D *et al.*, 2009; Sigismund S, Avanzato D and Lanzetti L, 2018).

A previous study showed that a higher level of EGFR transcripts was detected in 58% of IBC samples compared to only 39% of non-IBC (Guérin M *et al.*, 1989). IBC patients expressing high levels of EGFR have poorer OS than EGFR-negative patients (3-year estimate: EGFR-

positive 67% vs. EGFR-negative 50%; p = 0.01). In addition, EGFR-positive IBC patients are more likely to have a higher cumulative incidence of breast cancer-related death than EGFR-negative patients (breast cancer-specific death of 5-year: EGFR-positive 91.7% vs EGFR-negative: 48.2% ; p =0.09) (Cabioglu N *et al.*, 2007).

Wang *et al*. found that EGFR regulated the stemness of IBC cells via cyclooxygenase-2 (COX-2) which plays a crucial role in inflammatory responses (Wang X *et al.*, 2017). Specifically, they reported that the COX-2-dependent pathway modulated the cancer stem-like (CSC) phenotype of IBC *in vitro* via Nodal, a member of the TGF-β superfamily (Wang X *et al.*, 2017). Stimulation with EGF significantly increased Nodal expression, ultimately promoting cell migration and invasion, and increasing the cell population expressing CSC markers (Wang X *et al.*, 2017). Another growth factor, amphiregulin (Areg), was also reported to promote the proliferation of IBC *in vitro* via an Areg-EGFR autocrine loop (Willmarth NE and Ethier SP, 2006). In turn, the activity of EGFR in IBC contributed to the synthesis of Areg (Willmarth NE and Ethier SP, 2006). Baillo *et al*. found that the knockdown of Areg not only slowed down the proliferation of IBC cells but also decreased their EGFR-dependent invasiveness (Baillo A, Giroux C and Ethier SP, 2011). Areg knockdown was shown to affect cell movement and invasion via changes in integrin-linked kinase and focal adhesion kinase signalling, caveolar-mediated endocytosis signalling, and Wnt and Notch signalling (Baillo A, Giroux C and Ethier SP, 2011). In parallel, negative regulators of cell motility DKK1 and RHOB were upregulated at transcription and protein levels after Areg knockdown (Baillo A, Giroux C and Ethier SP,

2011). Willmarth *et al*. found that tumour cells growing in the presence of Areg became more invasive and migratory than those growing in an EGF-containing medium, indicating that the Areg-EGFR signalling network may contribute to a more aggressive cancer phenotype (Willmarth NE and Ethier SP, 2006). The difference could be attributed to an Areg-induced membranous accumulation of EGFR on IBC cells. Compared to EGF, EGFR simulated by Areg was more likely to locate on the cell surface and had less phosphorylation and ubiquitination, which dramatically decreased the internalisation and degradation of EGFR (Willmarth NE *et al.*, 2009).

Further evidence for the importance of the EGFR-dependent pathway in the proliferation and migration of IBC cells was reported by Zhang *et al*., who found that Erlotinib, an EGFR tyrosine kinase inhibitor, suppressed the growth of IBC *in vitro*. They also found that erlotinib inhibited the invasiveness and EMT of IBC cells and reduced lung metastasis (Zhang D *et al.*, 2009). In another study, injection of mesenchymal stem/stromal cells (MSCs) into IBC xenograft tumours resulted in increased phosphorylation of EGFR in cancer cells and led to skin invasion and metastasis (Lacerda L *et al.*, 2015). Notably, both invasion and metastasis were blocked by erlotinib (Lacerda L *et al.*, 2015), thus demonstrating the critical role of intercellular communication in regulating the activation of EGFR in IBC.

1.2.5.3. VEGF pathway in IBC

It was shown that IBC had higher expression of angiogenic factors than non-IBC (Shirakawa K *et al.*, 2002; Van der Auwera I *et al.*, 2004) and had a higher number of tumour-infiltrating endothelial cells or their precursors in stroma than in non-IBC stroma (Shirakawa K *et al.*, 2002). A high level of tumour stromal VEGF-A in IBC was reported to associate with worse breast cancer-specific survival (BCSS) ($P<0.01$) and disease-free survival (DFS) ($P<0.01$) (Arias-Pulido H *et al.*, 2012). Clemente *et al*. compared levels of angiogenic factors in inflammatory mammary carcinomas (IMCs) and malignant non-IMC mammary tumours (MMTs) using canine samples. They found that VEGF-A, VEGF-D and VEGFR3 in IMCs and MMTs were all significantly increased compared to normal mammary glands. Of those, only VEGF-D and VEGFR3 were expressed at higher levels in IMCs compared to MMTs. This correlated with higher microvascular density and the lymphangiogenic proliferation index of IMCs compared to MMTs (Clemente M *et al.*, 2013). In addition to its role in angiogenesis, VEGF was also involved in promoting the migration and invasion of IBC. Little *et al.* found that VEGF cooperated with CCL18 (both derived from tumour-infiltrating macrophages (TAMs)), which promoted the migration of IBC *in vitro* via activating the Rho-GTPase (Little AC *et al.*, 2019).

1.2.5.4. MAPK pathway in IBC

The mitogen-activated protein kinases (MAPKs) are activated by a large variety of external stimuli and represent key elements of various intracellular signalling networks that control cell

growth, proliferation, differentiation, migration, apoptosis and inflammation response in mammalian cells. Canonical activation of a MAPK cascade involves consecutive phosphorylations of mitogen-activated protein kinase kinase kinase (MAPKKK), MAPK kinase (MAPKK: MEK1/2/3/4/5/6), and MAPK (Dhillon AS, Hagan S, Rath O and Kolch W, 2007). There are three main classes of MAPKs: ERKs (ERK1 and ERK2), p38 MAPKs (p38α, p38β, p38γ, and p38δ) and JNKs (JNK1, JNK2 and JNK3) (Dhillon AS, Hagan S, Rath O and Kolch W, 2007).

It has been reported that upregulation of the ERK1/2 pathway was linked to a more aggressive phenotype in IBC (Mohamed HT *et al.*, 2020). IL-8 and CCL2, two chemokines highly expressed by TN-IBC tissues compared to TN-non-IBC tissues, were reported to induce the activation of ERK/1/2, leading to the increased expression of cysteine protease cathepsin B (CTSB), which promoted proteolytic activity and cell invasion of TN-IBC *in vitro* (Mohamed HT *et al.*, 2020). The authors also demonstrated that higher levels of IL-8 and CCL2 detected in TN-IBC tissues correlated with increased lymphovascular invasion in IBC tissues (Mohamed HT *et al.*, 2020). Interestingly, ERK1 and ERK2 may function differently in IBC. Gagliardi *et al*. found that high mRNA expression of ERK1 positively correlated with OS and distant-metastasis-free survival (DMFS) of IBC patients. In contrast, overexpression of ERK2 mRNA in IBC was significantly associated with reduced OS and DMFS (Gagliardi M *et al.*, 2020). In further experiments, the authors found that knockdown of ERK2 inhibited the anchorage-independent growth and the formation of mammospheres of IBC cells and reduced

cell migration and invasion *in vitro*. Consequently, these ERK2-knockdown cells had less lung metastasis than ERK1-knockdown or control cells *in vivo* (Gagliardi M *et al.*, 2020).

Similarly, p38 MAPKs have also been implicated in IBC tumorigenesis. Mueller *et al*. found that p38 MAPK mediated the EGFR/Src-induced proliferation and transformation of IBC *in vitro* (Mueller KL *et al.*, 2012). Specifically, mutation at EGFR tyrosine 845 or treatment with the Src family kinase inhibitor abrogated the p38 MAPK-induced proliferation and transformation of SUM149 cells. Interestingly, the autophosphorylation and kinase activity of EGFR or canonical downstream of EGFR (PI3K-AKT or ER1/2 pathways) were not affected in these cells, which was indicative of a specific contribution of p38 MAPK to the malignancy of IBC (Mueller KL *et al.*, 2012). Another study has identified p38 MAPK and ERK1/2 as upstream activators of MAPK-interacting kinase (MNK), which triggered the activation of NF-κB and promoted the CSC phenotype of IBC *in vivo* (Evans MK *et al.*, 2018). Specifically, the authors found that MAPK-dependent activation of MNK increased the cellular level of XIAP, which facilitated the nuclear translocation of NF-κB and, subsequently, increased the transcription of NF-κB target genes associated with cell proliferation, motility and ALDH-positivity (a CSC marker) (Evans MK *et al.*, 2018). In addition, Moor *et al*. showed that p38 MAPK mediated the effects of the enhancer of zeste homolog 2 (EZH2), a polycomb group protein, on the EMT of IBC cells. Specifically, these authors demonstrated that EZH2 binding to phosphorylated p38 MAPK increased the activation of p38 MAPK, leading to the elevated expression of MAPKAPK-2 (MK2) and heat shock protein 27 (HSP27) (Moore HM *et al.*,

2013). Conversely, the knockdown of EZH2 triggered a mesenchymal to epithelial transition (MET) of IBC cells and reduced cell invasion *in vitro* (Moore HM *et al.*, 2013).

It has been reported that JNK regulated the CSC phenotype of IBC. Knockdown of both JNK1 and JNK2 significantly reduced cell proliferation, mammosphere formation and the percentage of IBC cells expressing CSC markers *in vitro* and *in vivo*. The underlying mechanisms likely involve the activation of c-Jun and Notch-1 transcriptional networks (Xie X *et al*., 2017). In another study, Deng *et al*. found that activated JNK had a suppressing role in tumour initiation, growth and metastasis. Mechanistically, the endoplasmic reticulum stress and oxidative stress caused by the knockdown of N-myristoyl transferase (NMT1, an enzyme responsible for catalytic protein myristoylation) activated JNK, which enhanced cell autophagy and decreased cell proliferation (Deng L *et al.*, 2018).

1.2.5.5. NF-κB pathway in IBC

It has been evidenced that the nuclear factor-κB (NF-κB) transcription factor family plays a central role in inflammation activities and is a vital transportation regulator in innate and adaptive immune events. NF-κB is comprised of five members, p50, p52, RelA (p65), c-Rel, and RelB; but only RelA, c-Rel, and RelB possess the capability of activating the target genes, whereas p50 and p52 do not have this ability unless they form heterodimers with RelA, c-Rel, and RelB (Liu T, Zhang L, Joo D and Sun SC, 2017). The canonical pathway responsible for

activating the NF-κB dimers comprises RelA and p50. In the inactivated state, the complex p50/RelA is ineffective due to the restrain from IκB. In the activated state, ligand binding with the corresponding receptor activates and recruits the IκB kinase (IKK) complex, which subsequently phosphorylates IκB and launches the degradation of IκB. The absence of IκB leads to a discharge of complex p50/RelA, which then translocates to nuclear targets to initiate a transcriptional regulation (Liu T, Zhang L, Joo D and Sun SC, 2017).

It has been evidenced that the nuclear factor-κB (NF-κB) transcription factor family plays a central role in inflammation and is a critical regulator in innate and adaptive immunity (Liu T, Zhang L, Joo D and Sun SC, 2017). Transcriptionally active NF-κB pathway is more commonly observed in IBC than in non-IBC (Van Laere SJ *et al.*, 2006). Lerebours *et al*. found that 60 NF-κB -related genes were significantly enhanced in IBC than in non-IBC (Lerebours F *et al.*, 2008), implying that the NF-κB pathway may play a critical role in IBC development. Indeed, Streicher found that NF-κB was implicated in promoting the proliferation of IBC cells by modulating the production of IL-1, an inflammatory molecule implicated in innate and adaptive immunity. Inhibition of NF-κB signalling by Parthenolide (an inhibitor of IκB kinase complex) significantly decreased the secretion level of IL-1 in IBC and reduced tumour cell proliferation (Streicher KL *et al.*, 2007). Similarly, suppressing NF-κB by exogenously introducing dominant-negative IκBα reduced the production of VEGF, IL-1a, and IL-8, partially suppressing the invasive/motile phenotype of IBC cells (Pan Q, Bao LW and Merajver SD,

2003). The authors also found that inhibiting NF-κB led to slower cell growth and less metastasis *in vivo* (Pan Q, Bao LW and Merajver SD, 2003).

1.3. Tumour immune microenvironment of IBC

1.3.1. Overview

Emerging evidence reveals that the tumour immune microenvironment (TIME) is involved in IBC development and progression (Lim B *et al.*, 2018; Gong Y *et al.*, 2021). Infiltration of monocytes/tumour-associated macrophages (TAMs) and tumour-infiltrating lymphocytes (TILs) into IBC tissues have been reported in several studies (Liu X *et al*., 2017; Arias-Pulido H *et al.*, 2018; Reddy SM *et al.*, 2019; Fernandez SV *et al.*, 2020; Arias-Pulido H *et al.*, 2021; Bertucci F *et al.*, 2021; Gong Y *et al.*, 2021). Herein, we will discuss IBC-infiltrated immune cells separately, particularly emphasising the B cell accumulation in cancerous tissues.

1.3.2. Monocytes/TAMs

Monocytes are typically divided into classic (CD14+/CD16-) and non-classic (CD14-/CD16+) subsets based on their distinct functions (Olingy CE, Dinh HQ and Hedrick CC, 2019). Classic monocytes are the most prevalent monocyte subset, with high CCR2 (CCL2 receptor) expression, having pro-inflammatory and mobile capabilities. In contrast, non-classic monocytes are thought to exert patrolling function (Shi C and Pamer EG, 2011).

Monocytes migrate into tissues in response to chemoattractants such as CSF-1, CCL2, and VEGF, and subsequently differentiate into macrophages (Qian BZ *et al.*, 2011; Tariq M *et al.*, 2017). Orlikowski *et al*. first adopted the terms "M1" and "M2" to distinguish the macrophages that are activated by IFNγ (M1 phenotype) from those activated by IL-10 (M2 phenotype) (Orlikowsky T *et al.*, 1999). M1 macrophages express CD68, CD80, and CD86. They produce pro-inflammatory cytokines and chemokines, such as IL-12, IL-1, IL-23, TNF-α, CXCL9, CXCL10, and CXCL11, as well as reactive oxygen intermediates (Squadrito ML and De Palma M, 2011) (Fiure 1-4). M2 macrophages are characterised by the high expression of CD163 and CD206. They secrete immunosuppressive factors such as IL-10 and TGF-β to facilitate tissue regeneration, angiogenesis and wound healing (Tariq M *et al.*, 2017). M2 macrophages can be further subdivided into M2a, M2b, and M2c phenotypes in response to different microenvironmental stimuli (Tariq M *et al.*, 2017) (Figure 1-4).

In 2014, Mohamed *et al*. discovered that IBC tissues are characterised by a high number of infiltrating CD14+ cells (monocytes/macrophages) compared to non-IBC tissues (Mohamed MM *et al.*, 2014). In the same study, they detected a higher representation of CD14+ cells in the blood from IBC patients (collected from axillary tributaries during surgeon) than non-IBC patients (Mohamed MM *et al.*, 2014), suggesting that IBC has an increased chemoattractive potential for monocytes/macrophages than non-IBC. Similarly, recent data from our lab demonstrated that IBC tissues were characterised by an abundance of macrophage infiltration (Badr NM *et al.*, 2022). Macrophages remained the most prevalent immune cells when

analysing the epithelial component of IBC tissue and the cancer stroma (Badr NM *et al.*, 2022). Recent genetic profiling data also demonstrated that macrophages were one of the most abundant immune cells in IBC tissues (the others were CD8+T cells and plasma cells) (Bertucci F *et al.*, 2021). When compared with non-IBC tissues, M1 macrophages were significantly more prevalent in IBC tissues (Bertucci F *et al.*, 2021). Furthermore, it has been suggested that the higher activity of macrophages in TN-IBC may contribute to the shorter survival of IBC patients (Funakoshi Y *et al.*, 2019).

In terms of pathological features, data from our laboratory showed that the enrichment of macrophages in the stroma of IBC tissues was more common in grade 3 tumours than in grade 1 tumours (p=0.031) (Badr NM *et al.*, 2022). In addition, a decreased trend of macrophage accumulation was observed in HER2+ tumours compared to TN-IBC samples (p =0.075) (Badr NM *et al.*, 2022). However, there was no difference in the accumulation of M1 or M2 macrophages between IBC subtypes (Reddy SM *et al.*, 2019).

With regard to the therapeutic response, our previous study discovered a positive correlation between macrophage accumulation in naïve IBC tissues with the pathological complete response (pCR) to neoadjuvant chemotherapy (NAC) (p =0.023) (Hayward S *et al.*, 2020). Similarly, Reddy *et al*. found that patients who achieved pCR were characterised by a higher level of M1 macrophage infiltration (p =0.004), while a decreased accumulation of M2

macrophages was correlated with poor response to NAC (Reddy SM *et al.*, 2019). Interestingly, higher infiltration of macrophages in naïve IBC tissues did not correlate with OS (Hayward S *et al.*, 2020), but in post-treatment tissues, increased accumulation of macrophages was associated with improved PFS (p =0.004) (Reddy SM *et al.*, 2019). Even in the non-pCR cohort, a higher level of macrophage infiltration in post-treatment tissues appeared to link to a better OS (p=0.084) (Reddy SM *et al.*, 2019).

It is worth noting that the co-accumulation of macrophages with specific immune subsets appears to predict treatment resistance. For example, macrophages co-infiltrating with CD4+ T cells or B cells predicted resistance to NAC (Badr NM *et al.*, 2022). Similarly, Reddy *et al.* found that a higher level of co-accumulation of M2 macrophages with mast cells was significantly associated with treatment resistance (Reddy SM *et al.*, 2019).

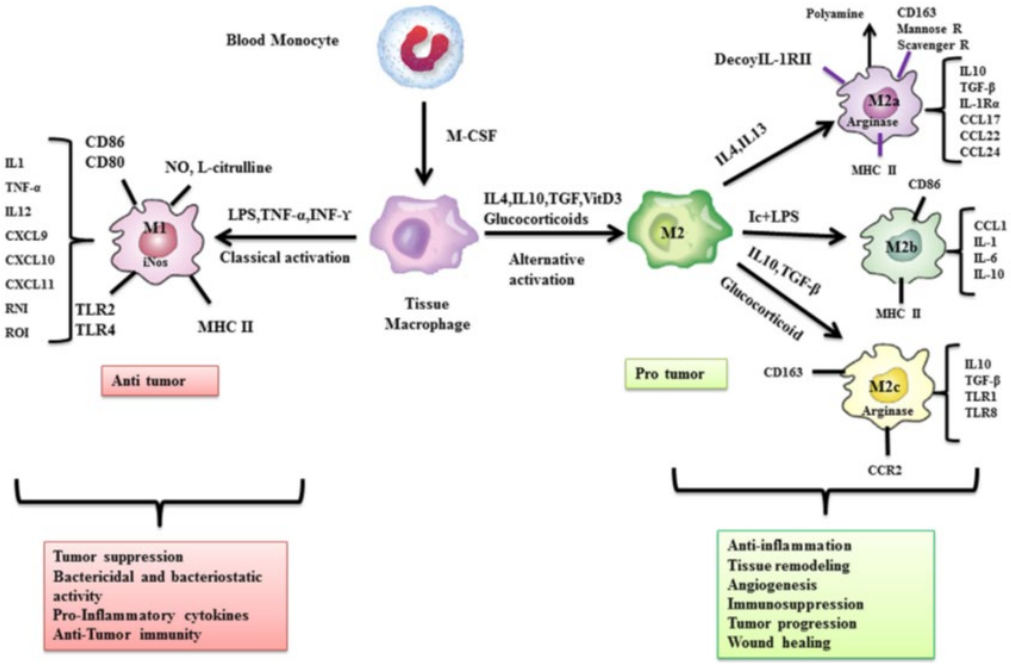

Figure 1-4. Polarisation of macrophages in TIME. Chemoattractants secreted by tumours induce the recruitment of monocytes. Monocytes subsequently differentiate into macrophages in tissues. Different stimuli in tumour environment contribute to different macrophage phenotypes (M1 and M2), which exert distinct functions in regulating tumour progression. The figure is reproduced from (Tariq M *et al.*, 2017).

1.3.3. Lymphoid cells

Tumour-infiltrating lymphocytes (TILs): TILs in IBC are typically comprised of natural killer cells (NK cells), T cells (CD4+ and CD8+ T cells) and B cells. The accumulation level of TILs has been reported to correlate with therapeutic response to NAC (Campedel L *et al.*, 2020) and survival of IBC patients (Van Berckelaer C *et al.*, 2019). In this section, we discussed the TILs within the TIME of IBC, with a particular focus on B cells.

1.3.3.1. Natural killer cells (NK cells)

NK cells are critical players in innate anti-tumour activities. They can be classified into two subsets depending on the expressions of CD56 and CD16. Most NK cells in peripheral circulation are mature NK cells characterised by a high expression of CD16 and a low expression of CD56. These cells exert cytolytic effects on tumour cells by releasing perforin, granzymes and cytolytic granules (Fernandez SV *et al.*, 2020). In comparison, immature NK cells ($CD56^{high}CD16^{-}$) are more abundant in the tissues and superior in cytokine production (Fernandez SV *et al.*, 2020). Although NK cells did not exhibit subtype-biased distribution, it may vary among stages of IBC. Specifically, Reddy *et al*. observed an increased accumulation

of NK cells in stage III tumours than in stage IV samples in the HR+ IBC cohort (Reddy SM *et al.*, 2019).

Further study demonstrated that though IBC patients diagnosed with IV stage have decreased numbers of circulating NK cells (total NK cells) than healthy donors, the absolute counts of circulating immature NK cells from tumour patients was significantly increased compared to healthy donors (Fernandez SV *et al.*, 2020). More importantly, these immature NK cells also express some maturation signatures, such as CD16, granzyme B and perforin (Fernandez SV *et al.*, 2020), which is indicative of a rapid maturation process of NK cells occurring in IBC patients. With regard to treatment response, the level of total NK cell accumulation in naïve IBC tissues did not associate with pCR, while its infiltration in post-treatment samples positively correlated with pCR ($p<0.001$) (Reddy SM *et al.*, 2019).

1.3.3.2. T lymphocytes

T lymphocytes are the backbone of adaptive cell immunity. Most T lymphocytes are CD3+ T lymphocytes, which can be classified into two main subtypes depending on the expression levels of CD4+ and CD8+. CD4+ T lymphocytes, typically referred to as “T helper (Th) cells”, play vital roles in the maturation of B lymphocytes and the activation of T cytotoxic cells as well as natural killer (NK) cells. CD8+T lymphocytes, referred to as “T cytotoxic (Tc) cells”, kill target cells directly by secreting perforin, granzyme and granulysin, and trigger apoptosis

of target cells via Fas/FasL pathway. Depending on distinct differentiation stimuli, CD4+ T cells could be further classified into seven subtypes, Th1, Th2, Th9, Th17, Th22, T regulatory cells (Tregs) and T follicular helper cells (Tfh) (Golubovskaya V and Wu L, 2016; Tay RE, Richardson EK and Toh HC, 2021) (Figure 1-5). Similarly, CD8+ T lymphocytes could be divided into five subtypes, Tc1, Tc2, Tc9, Tc17 and Tc22 (St Paul M and Ohashi PS, 2020) (Figure 1-5). Different CD4+ or CD8+ T lymphocyte subtypes exert specific functions in TIME (Kim HJ and Cantor H, 2014; St Paul M and Ohashi PS, 2020).

Recent data from our laboratory showed that CD4+ T lymphocytes were the second most abundant immune cells infiltrating IBC tissues (Badr NM *et al.*, 2022). An analysis profiled the Th cell subsets isolated from axillary tributaries of IBC and non-IBC patients and demonstrated lower frequencies of the Th1 and Th2 subsets in the IBC cohort compared to the non-IBC cohort (Th1: 29.6 ± 3.9% in non-IBC, vs 11.38 ± 0.7% in IBC patients, p = 0.01; Th2: 28.29 ± 3.87% in non-IBC, vs 12.28 ± 1.43% in IBC patients, p= 0.03) (Saleh ME *et al.*, 2019). This study suggested that suppressed Th1- and Th2- responses contributed to the IBC phenotype. Indeed, Th1 cells are characterised by the secretion of IFNγ, TNF-α, CCL2, and CCL3 (Kim HJ and Cantor H, 2014). They promote the priming and expansion of CD8+ T lymphocytes and enhance the recruitment of NK cells or macrophages to exert tumour-suppressive effects (Kim HJ and Cantor H, 2014). Th2 cells are characterised by the secretion of IL-4, IL-5 and IL-13 (Kim HJ and Cantor H, 2014). Compared to Th1 cells, the role of Th2 cells in anti-tumour host immune response is depended on the context. On the one hand, Th2 cells activate humoral

immunity and promote the infiltration of eosinophils to the tumour site to exert tumour suppression (Zhu X and Zhu J, 2020); on the other hand, Th2 cells are known to stimulate the tumour cell transformation and growth (Kim HJ and Cantor H, 2014). Investigations addressing the effect of Th1 and Th2 on IBC showed that a Th1-biased cytotoxic effector function tended to be associated with better survival of IBC patients (Bertucci F *et al.*, 2015). This finding is supported by microarray data showing that gene signatures related to the Th1-responses correlated with a better pathological response to NAC in IBC patients (Bertucci F *et al.*, 2014). By contrast, the Th2- responses (secretion of TNF-α, IL-6, and TGF-β) correlated with the EMT of IBC cells (Cohen EN *et al.*, 2015). These studies suggest that directing an anti-tumour immune response to Th1 and away from Th2 could be a promising strategy for future IBC treatment.

Hamm *et al*. found that 11 of 12 IBC samples displayed CD8+ T cell infiltration, 5 of which were defined as “high” CD8+ T cell infiltration (infiltrating cells occupying >/=5% of tumour area occupied by tumour cells) (Hamm CA *et al.*, 2016), suggesting that CD8+ T cells are one of the predominant immune cells accumulating in IBC. This finding is in line with a genetic profile, which revealed that CD8+ T cells were the second most abundant infiltrates in IBC tissues (Bertucci F *et al.*, 2021). Interestingly, the frequency of CD8+ T cells in the peripheral blood of IBC patients was lower than that in healthy donors (Fernandez SV *et al.*, 2020). Further analysis revealed that only the numbers of CD8+ effector memory and central memory T cells decreased dramatically ($p = 0.035$, $p = 0.005$, respectively), while the numbers of CD8+ naïve

and effector T cells were not affected (Fernandez SV *et al.*, 2020). In addition, it was demonstrated that infiltration of CD8+ T cells in IBC varied among different subtypes. The HER2+ IBC appeared to have the highest accumulation level, whereas HR+ IBC had the lowest level (Reddy SM *et al.*, 2019; Badr NM *et al.*, 2022). Finally, the HER2+ cohort demonstrated an increased level of CD8+ T cells in stage III patients than in stage IV ($p = 0.008$), suggesting a compromised cytotoxic immunity contributes to a more malignant phenotype (Reddy SM *et al.*, 2019).

It was demonstrated that gene expressions associated with CD8+ T lymphocyte activation in treatment-naïve IBC tissues were positively correlated with pCR to NAC (Bertucci F *et al.*, 2014, 2021). This observation is supported by one previous study (Reddy SM *et al.*, 2019) and our recent data (Badr NM *et al.*, 2022), which showed that high CD8+ T cell infiltration within naïve IBC tissues correlated with a better treatment response to therapy. In contrast, post-treatment IBC tissues from patients who had pCR displayed a dramatic decrease ($p<0.001$) in the level of CD8+ T cell infiltration after NAC (Reddy SM *et al.*, 2019). In short, these data indicated that IBC patients with a high level of baseline CD8+ T cell infiltration and a reduction in this accumulation after NAC were more likely to achieve pCR.

It is worth noting that gene expression of PD-L1 is more common in IBC than in non-IBC (38% vs 28%) (Bertucci F *et al.*, 2015), implying a more robust immune suppression in IBC. This

may, in part, explain the aggressiveness of IBC. Indeed, overexpression of PD-L1 in IBC tissues was found to correlate positively with the infiltration of CD8+ T lymphocytes (Bertucci F *et al.*, 2015; Gong Y *et al.*, 2021) and associated with pCR to NAC (Bertucci F *et al.*, 2015). Hamm *et al*. found that almost 41% of IBC cases have CD8+ T cell infiltration (Hamm CA *et al.*, 2016), and the IBC mutation rate was positively correlated with CD8+/PD-L1+ lymphocyte infiltration. These results support the concept that a CD8+ T lymphocyte-dominant cytotoxic immunity triggered by the IBC-produced neoantigens was progressively suppressed by PD-L1 (Hamm CA *et al.*, 2016).

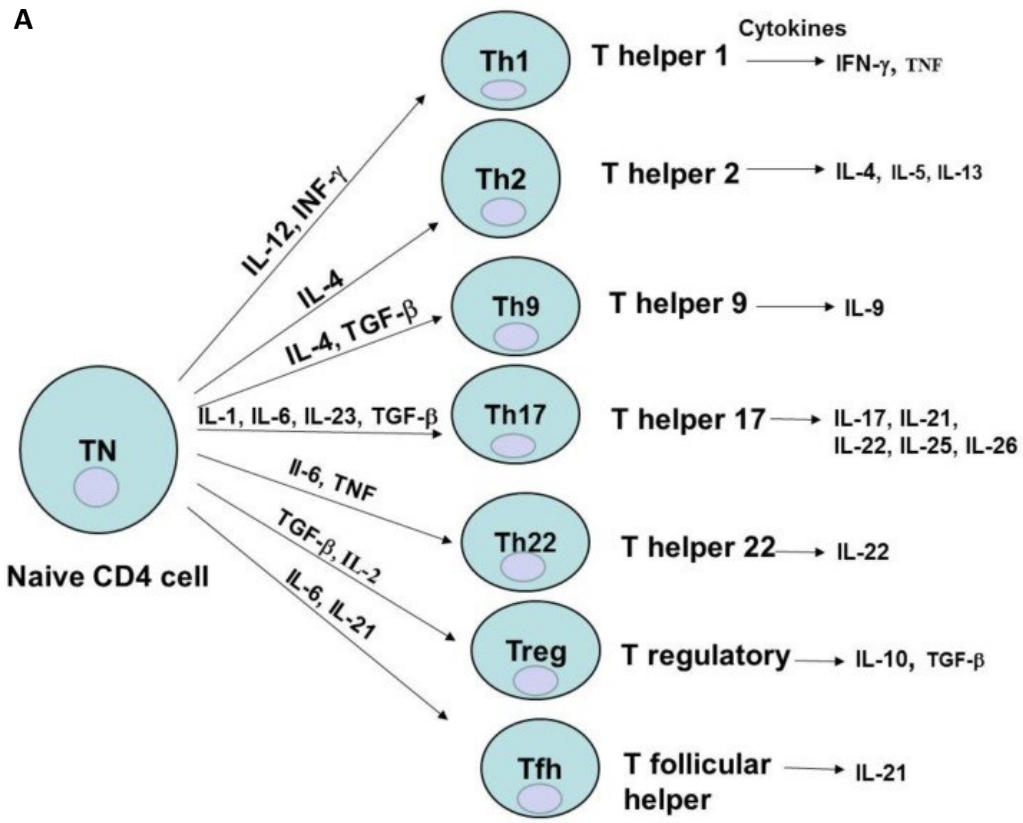

B

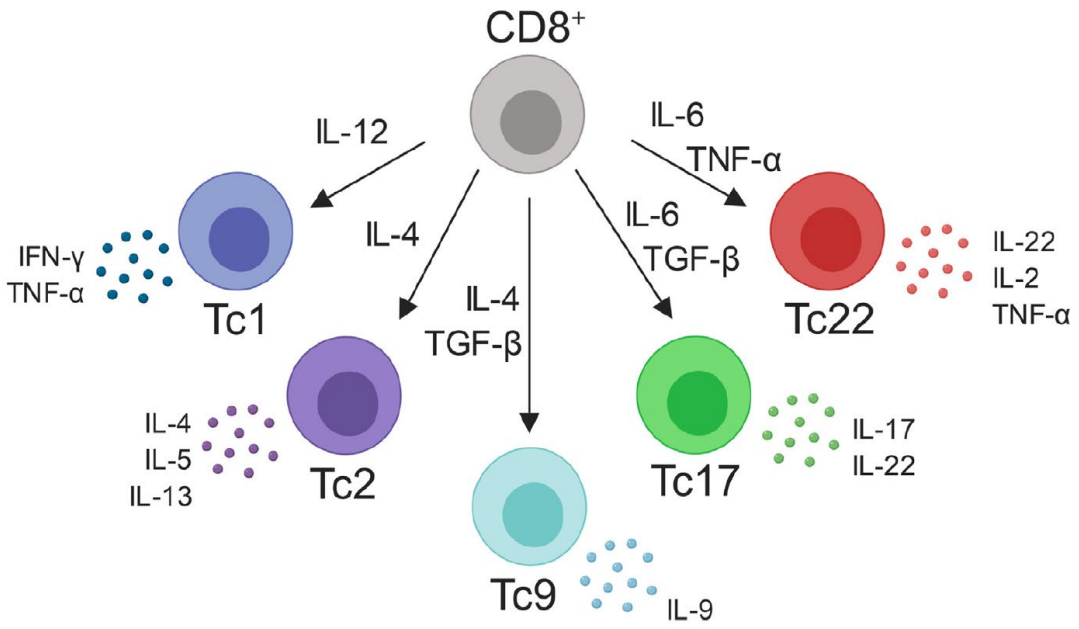

Figure 1-5. Subsets and functions of CD4+ and CD8+ T cells. (A) The development of different CD4+ T cell subsets. **(B)** The development of different CD8+ T cell subsets. Figures reproduced and modified from (Golubovskaya V and Wu L, 2016).

1.3.3.3. B lymphocytes

B lymphocytes are important components of adaptive immunity that play a role in host immune responses to cancer. In this subchapter, we provided an overview of what is currently known about the functions of tumour infiltration of B cells (TIL-B) in breast cancer (including IBC). In addition, we reviewed and summarized the mechanisms underlying B cell recruitment.

1.3.3.3.1. **B lymphocytes in breast cancer**

Degnim *et al*. discovered a significant decrease in the density of CD20+ B lymphocytes in breast cancer tissues that had developed from benign breast disease (BBD), with zero counts of CD20+ B cells found in 41.4% of BBD-developed breast cancer samples and 27.7% of BBD sample (Degnim AC *et al.*, 2017). This observation suggests that suppressed humoral immunity contributes to breast cancer initiation. Interestingly, these authors also found that BBD-developed tumour samples had an increased CD20+ B cell infiltration compared to normal breast tissues (Degnim AC *et al.*, 2017). These results are in agreement with a study performed by Ruffell *et al*., who found that breast cancer tissues had increased CD20+ infiltrates compared to matched-ipsilateral nonadjacent normal tissues (Ruffell B *et al*., 2012). These findings suggest that a protective humoral immune response, triggered by the abnormal breast cells, functions throughout the process but is suppressed in the later stages. This change consequently contributes to breast cancer initiation. Therefore, functional B cell immunity is essential to prevent the development of breast cancer.

Several studies assessed the predictive value of B cell infiltration in different breast cancer subtypes. Kuroda *et al*. evaluated the infiltration of CD20+ TILs and CD38 TILs (a marker for germinal centre B cells) in TNBC tissues, the most lymphocyte-predominant breast cancer subtype. They found that the density of CD20+ TILs in tumour stroma was positively correlated with relapse-free survival (RFS) and OS ($p=0.043$, $p=0.027$, respectively), and the increased

CD38+ TILs in tumour stroma were significantly associated with a longer RFS (p=0.042) (Kuroda H *et al.*, 2021). In the HER2+ subtype, baseline infiltration of intratumoral CD20+ cells in patients receiving dual anti-HER2 neoadjuvant therapy (lapatinib plus trastuzumab) was positively associated with a higher pCR rate (p=0.030) (De Angelis C *et al.*, 2020). This observation is in agreement with a transcriptomic analysis which found that B cell-related gene expression (IgG-signature) correlated with the pCR rate in HER2+ breast cancer patients (Fernandez-Martinez A *et al*, 2019). The predictive value of B cell infiltration in HR+/HER2- breast cancer remains unclear, mainly because it is the least lymphocyte-predominant subtype (Iglesia MD *et al.*, 2014), and enrichment of B cells is more related to the negative expression of HR (Guan H *et al.*, 2016).

As for the role of B cells in predicting breast cancer survival, a recent meta-analysis reported that an increased CD20+ B lymphocyte infiltration was significantly associated with improved OS (pool HR = 0.42, 95% CI 0.24-0.60), better BCSS (pooled HR = 0.66, 95% CI 0.47-0.85), and better DFS/RFS (pooled HR = 0.41, 95% CI 0.27-0.55) (Qin Y *et al.*, 2021). In particular, B cell infiltration predicted favourable invasive DFS (iDFS) and OS for HER2+ and TNBC cohorts (HER2+: iDFS p=0.03, OS p=0.04; TNBC: iDFS p=0.002, OS p=0.01) (Garaud S *et al.*, 2019). Notably, TNBC and HER2+ patients with TIL-B positivity reached the plateau of iDFS and OS within the first five years and maintained this plateau until the tenth year. This indicates that humoral immunity was initiated early following diagnosis and maintained long-lasting effects (Garaud S *et al.*, 2019).

Although the above studies suggest an anti-tumour role of B cells in breast cancer, other reports suggest that B cells may facilitate tumour development (Zhang Z *et al.*, 2017). Specifically, it was found that the density of CD19+ B cells is associated with higher histological grade, lymph node metastasis, advanced clinical stage, and the HR-negative status of breast cancer (Guan H *et al.*, 2016). In addition, it has been suggested that the development of breast tumours is accompanied by a progressive activation of B cell immunity, as invasive breast cancer tissues display the highest density of CD19+ B lymphocytes, followed by tissues from benign breast disease and the lowest is in nonadjacent non-tumour tissues (Garaud S *et al.*, 2019). With regard to survival, the enrichment of plasma cells in breast cancer tissues was reported to correlate with a poorer OS ($p = 0.038$) (Wei H *et al.*, 2016). A higher infiltration of CD138+ B-lymphocytes (plasmablasts or plasma cells) independently predicts a shorter RFS in patients with invasive ductal carcinoma (Mohammed ZM *et al.*, 2013). Even in ductal carcinoma *in situ*, an increased accumulation of CD20+/CD19+ cells was reported to correlate with a shorter PFS ($p = 0.04$) (Miligy I *et al.*, 2017). In conclusion, the role of B cells in breast cancer development and progression remains controversial, and those inconsistent findings are likely to be related to the nonuniform evaluation methods, different criteria for study enrollment, and distinct sample sources.

1.3.3.3.2. **B lymphocytes in TIME of IBC**

Only a few studies examine the role of B cells in IBC. Two studies suggested alterations in the number of infiltrating B cells were associated with tumourigenesis of IBC. The early one demonstrated that the number of CD20+ B-cell infiltration was significantly increased in IBC tissue compared to normal tissue ($p < 0.001$) (Arias-Pulido H *et al.*, 2018). The recent one reported that B cells and plasma cell expression signatures are higher in IBC tissues when compared to non-IBC samples ($p < 0.05$, $p = 0.107$, respectively) (Bertucci F *et al.*, 2021).

Infiltration of B cells is also associated with clinicopathological features of IBC. Recent data from our lab showed that a higher grade of IBC tissues was characterised by fewer intratumoral CD20+ cells ($p=0.047$) (Badr NM *et al.*, 2022). Further analysis showed a co-accumulation of CD20+ B cells with other immune infiltrates, which was more frequently observed in higher-grade tumours. Specifically, a co-accumulation of CD20+ cells with CD4+ T cells was observed in grade 2 and 3 tumours, and a co-accumulation of CD20+ cells with CD8+ cells and TAMs was frequently seen in grade 3 tumours (Badr NM *et al.*, 2022). Concerning clinical stages, a previous finding demonstrated that IBC patients with stage III generally exhibited a higher level of CD20+ cell infiltration compared to IBC patients with stage IV, though this difference did not reach statistical significance (Reddy SM *et al.*, 2019). It is worth noting that the level of B cell infiltration varied among different IBC subtypes. The TN-IBC subtype has the highest level, followed by the HR-/ HER2+ subtype, and the HR+/HER2- subtype has the lowest number of

B lymphocytes (Reddy SM *et al.*, 2019). The co-accumulation of CD20+ cells with TAMs, Tregs and CD4+ T cells is also observed in TNBC (Badr NM *et al.*, 2022).

The role of B cells in predicting the outcome of IBC patients was also investigated. Arias-Pulido *et al*. found that increased infiltration of CD20+ cells in IBC tissues was positively associated with pCR and DFS, and negatively associated with relapses (Arias-Pulido H *et al.*, 2018). Two studies supported these findings, in which the level of CD20+ cell accumulation in IBC tissues was associated with improved treatment response ($p = 0.054$, $p = 0.003$, respectively) (Arias-Pulido H *et al.*, 2018; Reddy SM *et al.*, 2019). Interestingly, increased accumulation of B cells is also correlated with PD-L1 positive TILs (Gong Y *et al.*, 2021), and a co-accumulation of CD20+ cells and PD-L1+ TILs can predict a better DFS and BCSS in IBC (Arias-Pulido H *et al.*, 2018). Therefore, the authors proposed that B lymphocytes executed an anti-tumour response within the TIME of IBC, which was progressively suppressed by PD-1 regulation (Arias-Pulido H *et al.*, 2018). In another study, the enrichment of CD20+/PD-L1+ TILs was shown to be an independent predictive factor for treatment response and survival for IBC but not LABC (locally advanced breast cancer, non-IBC) patients (Arias-Pulido H *et al.*, 2021), implying that B cells may behave differently in the IBC microenvironment compared to in non-IBC.

1.3.3.3.3. **Mechanisms of B lymphocytes recruitment**

Direct regulation: Both non-IBC and IBC cells are known to produce inflammatory factors that stimulate B-cell chemotaxis, such as CXCL12 and CXCL13 (Lerebours F *et al.*, 2008; Tan P *et al.*, 2018). Furthermore, some chemokines are able to induce the migration of a specific B cell subset, for instance, the CXCL9 (Liang YK *et al.*, 2021) and CXCL10 (Kim M *et al.*, 2021) (ligands for CXCR3+ B cells (D Jones RJB and Shahsafaei A, 2000; Liu RX *et al.*, 2015)). In addition to chemokines, cytokines exert a pro-migration effect on B cells. TNF-α is capable of upregulating the recruitment of B cells (Ghods A *et al.*, 2019; Mercogliano MF, Bruni S, Elizalde PV and Schillaci R, 2020; Shaul ME *et al.*, 2021). And, MIF also stimulates the migration of B cells by binding with its receptors CD74 (HLA class II histocompatibility antigen gamma chain) and CXCR4 (receptor for CXCL12) (Calandra T and Roger T, 2003). Notably, breast cancer cells generate both TNF-α (García-Tuñón I *et al.*, 2006) and MIF (Richard V, Kindt N and Saussez S, 2015).

Indirect regulations: Recruitment of B cells to cancerous tissues in IBC may be regulated indirectly. In this regard, data from our lab showed a co-accumulation of CD20+ B cells and FOXP3+ T cells (a marker for regulatory T cells) in all IBC samples (Badr NM *et al.*, 2022). The analysis of grade 2 and grade 3 IBC samples showed that increased CD20+ B cells positively correlated with the accumulation of CD4+ T cells. Moreover, grade 3 tumours

showed a higher number of CD20+ B cells correlating with an increased accumulation of CD8+ T lymphocytes and CD68+ macrophages (Badr NM *et al.*, 2022).

The co-accumulation of B cells with different immune cells shows tumour subtype specificity. Specifically, the co-enrichment of FOXP3+ T cells with CD20+ B cells was predominantly in HR+ IBC tumours, whereas TN-IBC tumours were characterised by co-accumulation of CD20+ B cells with CD68+ macrophages, FOXP3+ T cells, and CD4+ T cells. Others reported similar results for both non-IBC and IBC (Garaud S *et al.*, 2019; Gong Y *et al.*, 2021; H Kuroda TJ and Yamaguchi R, 2021). These observations suggest that the recruitment of B cells to breast cancer (including IBC) may involve a well-orchestrated interaction between tumour cells and non-tumour cells within TIME. Indeed, unlike macrophages and T cells, which are found both in the parenchymal and stromal areas, accumulation of B cells is more likely to be found in the tumour stroma rather than the intratumoral area (Degnim AC *et al.*, 2017; Arias-Pulido H *et al.*, 2018).

Though the mechanism of B cell infiltration mediated by non-B cells has not been elucidated yet, current findings may provide some clues. Mohamed and colleagues reported that TAMs of IBC were characterised by high expression of inflammatory cytokines, such as TNF-α (Mohamed MM *et al.*, 2014). Likewise, macrophages in non-breast cancer were also found to secret a high level of TNF-α (Chow A *et al.*, 2014). As for the contributions of T cells, CD8+

T cells, collected from tumour-draining lymph nodes of breast cancer, have been identified to produce IL-17 and IL-4 (Faghih Z *et al.*, 2013). While IL-4 is a potent stimulus for B cell activation (Nelms K *et al.*, 1999), IL-17 has been identified to upregulate the sensitivity of B cells to CXCL12 and CXCL13 (Ferretti E, Ponzoni M, Doglioni C and Pistoia V, 2016), indirectly enhancing the migration of B cells.

Tertiary lymphoid structures (TLSs): It has been suggested that B cells were critical players in the formation of TLS that resembles the second lymphoid organs (spleen, tonsils, and lymph nodes). TLSs, a consequence of chronic inflammations and the development of cancerous lesions, are typically located in non-lymphoid tissues (Sautès-Fridman C, Petitprez F, Calderaro J and Fridman WH, 2019). TLSs are found in the stroma, peritumoral, and intratumoral areas and are distinguished by a zone enriched with T cells, DCs, and a B cell follicle with germinal centre (GC) features (Sautès-Fridman C, Petitprez F, Calderaro J and Fridman WH, 2019). Diverse immune cells are found in TLSs, such as B cells, plasma cells, DCs, Th1 cells, Tfh cells, Treg cells, and macrophages (Sautès-Fridman C, Petitprez F, Calderaro J and Fridman WH, 2019). In addition, a panel of high expression of chemokines (CCL2/3/4/5/8/18/19/21 and CXCL9/10/11/13) was detected in TLSs (Prabhakaran S *et al.*, 2017). TLSs are associated with better treatment response and favourable survival in breast cancer (Sautès-Fridman C, Petitprez F, Calderaro J and Fridman WH, 2019; Zhang NN *et al.*, 2021). It also positively correlates with TILs in breast cancer (Zhang NN *et al.*, 2021), indicating that TLSs represent a potential hub for recruiting immune cells to the proximal cancerous lesion. In invasive breast cancer, the

presence of TLS was positively associated with tumour grade ($p<0.001$), necrosis ($p<0.001$), lymphovascular invasion ($p=0.045$) and a higher level of TILs ($p<0.001$) (Liu X *et al.*, 2017). It is worth noting that IBC had a higher expression of TLS gene signature than non-IBC, which was irrelevant to the clinicopathological features (e.g., the molecular subtypes) (Bertucci F *et al.*, 2021), suggesting a more immunogenic environment created by IBC.

1.4. Tetraspanins

1.4.1. Overview of tetraspanins

Tetraspanins are a family of small transmembrane proteins first described in 1988 (Hotta H *et al.*, 1988). To date, 33 members have been identified in mammals, 37 in *Drosophila melanogaster*, and 20 in *Caenorhabditis elegans* (Titu S *et al.*, 2021). Tetraspanins are widely involved in many biological events, ranging from reproduction, infections, immune response to cancer regulation (Charrin S, Jouannet S, Boucheix C and Rubinstein E, 2014; Lang T and Hochheimer N, 2020).

1.4.2. Structure of tetraspanins

Tetraspanins are characterised by: 1) Two extracellular loops: the small extracellular loop (EC1) contains 13-31 amino acids, and the large extracellular loop (EC2) contains 69-132 amino acids. EC2 comprises two regions, a conserved region with three helices and a variable region that

varies across different tetraspanins and is thought to be responsible for specific interactions between tetraspanins and their non-tetraspanin partners. The variable region includes the Cys-Cys-Gly (CCG) motif and two-six additional cysteine residues, which form disulfide bonds to stabilise the folding of EC2 (Charrin S, Jouannet S, Boucheix C and Rubinstein E, 2014; Lang T and Hochheimer N, 2020). 2) A short cytoplasmic sequence between TM2 and TM3 (Charrin S, Jouannet S, Boucheix C and Rubinstein E, 2014; Lang T and Hochheimer N, 2020). 3) Four transmembrane domains (TM1-4) with a relatively high homology across most tetraspanins are critical for the configuration of tetraspanins (Zimmerman B *et al.*, 2016; Termini CM and Gillette JM, 2017; Umeda R *et al.*, 2020). 4) Two short N-terminal and C-terminal cytoplasmic portions. These two portions contain cysteine and lysine residues which can be palmitoylated and ubiquitinated in different tetraspanins (Seigneuret M, 2006; Lineberry N, Su L, Soares L and Fathman CG, 2008) (Figure 1-6 A). The crystal structure of three tetraspanin proteins revealed a cone-like shape (Min G, Wang H, Sun TT and Kong XP, 2006; Zimmerman B *et al.*, 2016; Umeda R *et al.*, 2020). This cone-like shape can assume an “open” or “closed” conformation depending on the absence or presence of cholesterol (Figure 1-6 B) (Zimmerman B *et al.*, 2016).

A

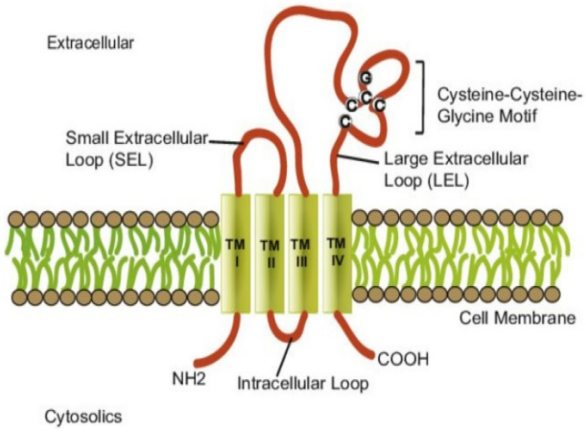

B

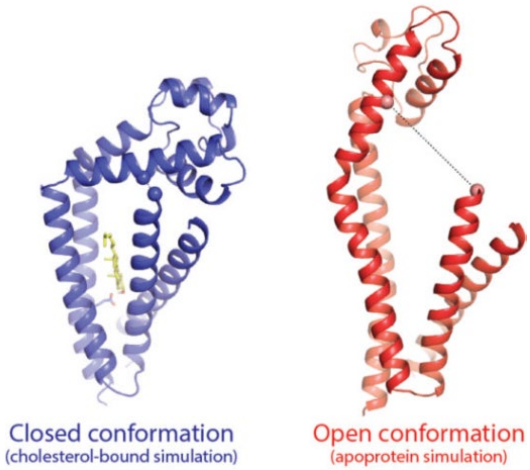

Figure 1-6. Representative model of tetraspanin structure. (**A**) The structure of tetraspanin consists of two extracellular loops, EC1 and EC2, four transmembrane domains TM1-4, two tails (N-terminal and C-terminal), and one small intracellular loop connecting TM2 and TM3. (**B**) Cholesterol molecule (yellow) binding with the cavity of CD81 triggers a closed conformation of CD81 (blue). Conversely, the absence of cholesterol induces open conformation of CD81 (red). The figures are adapted from (Zimmerman B *et al.*, 2016; Titu S *et al.*, 2021).

1.4.3. Post-translational modifications of tetraspanins

Tetraspanins are known to undergo post-translational modifications (Figure 1-7). Glycosylation, palmitoylation and ubiquitination were found in most tetraspanins (Termini CM and Gillette JM, 2017). Palmitoylation seems vital for stabilising the interaction of tetraspanins with each other, and it is thought to be one of the critical steps in the assembly of tetraspanin-enriched microdomains (TEMs/TERMs) (Yang X *et al.*, 2002, 2004). In addition, the palmitoylation of tetraspanins links their partner proteins to TEMs/TERMs, thus regulating the downstream signalling pathways (Berditchevski F, Odintsova E, Sawada S and Gilbert E, 2002). Protein ubiquitination is important for directing transmembrane proteins along various endocytic routes and for protein degradation (Foot N, Henshall T and Kumar S, 2017). Lysines on the cytoplasmic portions of tetraspanins may represent the sites for ubiquitination (Lineberry N, Su L, Soares L and Fathman CG, 2008; Wang Y *et al.*, 2012). Ubiquitination downregulates the expression of tetraspanins on the cell surface and may affect signalling pathways modulated by tetraspanins (Lineberry N, Su L, Soares L and Fathman CG, 2008; Wang Y *et al.*, 2012). Tetraspanins can be N-linked glycosylated on asparagine residues (Termini CM and Gillette JM, 2017); however, the role of glycosylation in tetraspanin function remains relatively unexplored. Previous and recent evidence suggests that glycosylation on tetraspanins may affect the properties of tumour cells differently. CD63 glycosylation potentiates the drug resistance and invasion of breast cancer cells *in vitro* (Tominaga N *et al.*, 2014), whereas glycosylation of CD82 significantly inhibits the migration and metastasis of ovarian cancer cells *in vitro* and *in vivo* (Li J *et al.*, 2020).

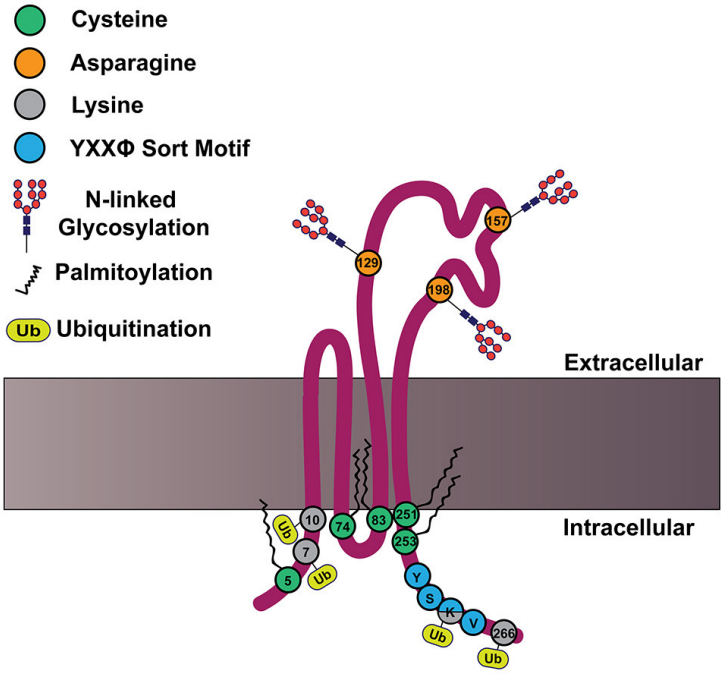

Figure 1-7. Schematic model of post-translational modification in tetraspanin. CD82 is shown here as a model to display the specific sites for tetraspanin post-translational modifications. Membrane proximal cysteine residues (green) are responsible for palmitoylation. Asparagine residues located in EC2 are related to glycosylation. Lysine residues on the cytoplasmic side of CD82 are relevant to ubiquitination. The figure is reproduced from (Termini CM and Gillette JM, 2017).

1.4.4. Functions of tetraspanins and tetraspanin enriched domain (TEM)

Functional roles of tetraspanins were initially identified from observations of tetraspanin-deficient phenotypes in human and animal models. Peripherin/RDS, a retina-specific tetraspanin in humans, is a fundamental scaffolding protein for the photoreceptor outer segment. It has been reported that mutation of RDS caused blindness due to the dysfunction of the outer segment which failed to transduce light signals (Goldberg AF, 2006). Mutations of Tspan12 also lead to an inherited vision disorder called familial exudative vitreoretinopathy (FEVR),

characterised by the improper development of retinal vasculature (Poulter JA *et al.*, 2010). In addition to RDS and Tspan12, mutations in tetraspanin CD151 result in the abnormal assembly of epithelial cell basement membranes, consequently leading to kidney dysfunction and pretibial epidermolysis bullosa (a severe disorder of skin) (Karamatic Crew V *et al.*, 2004). Another tetraspanin, CD81, is a vital component of the co-stimulatory receptor of B lymphocytes. Thus, the activation of B cells would be impaired once CD81 mutated (van Zelm MC *et al.*, 2010).

To date, a growing number of studies demonstrated that tetraspanins directly interacted with their partner proteins, such as integrins, adhesion receptors, immunoglobulin (Ig)-domain-containing factors, growth factor ligand or receptors, cytokine receptors, exopeptidases and metalloproteinases (Hemler ME, 2005; Termini CM and Gillette JM, 2017). Furthermore, serving as scaffolding proteins, tetraspanins establish a web that organises and clusters tetraspanins and their partner proteins, called tetraspanins enriched microdomain (TEM) (Figure 1-8) to regulate the inter-or intracellular activities (Hemler ME, 2005).

Direct or primary interactions of tetraspanins with partner proteins play the basis of TEM, which is resistant to harsh detergents such as 1% Triton-X100 (Hemler ME, 2005). For example, the interaction of CD151 with the laminin-binding integrin α3β1 is mediated by the variable domain of EC2 in CD151 (Nishiuchi R *et al.*, 2005). Dissociation of this interaction

significantly affected the activation of integrin α3β1 and reduced its binding capability to laminin, a principal constituent of the basement membrane, leading to impaired cell adhesion (Nishiuchi R *et al.*, 2005) and decreased cell migration (Fei Y *et al.*, 2012). Another example is the interaction of CD81 and EWI-2, a member of the immunoglobulin superfamily. It was reported that the EWI-2 inhibited the hepatitis C virus (HCV) infection by impeding the binding of HCV envelope glycoproteins to CD81 (Rocha-Perugini V *et al.*, 2008; Montpellier C *et al.*, 2011). It is worth noting that the sites for associating with the same partner protein may vary among different tetraspanins. For example, the interaction of tetraspanin CD81 with EWI-2 is mediated by the EC2 and transmembrane 3 and 4 of CD81 (Montpellier C *et al.*, 2011), whereas the interaction of tetraspanin CD9 with EWI-2 is mediated by the EC2 and transmembrane 2 and 3 of CD9 (Charrin S *et al.*, 2003). In addition, several tetraspanins were shown to interact with other cellular proteins via their intracellular regions. For example, CD63 and Tspan6 interact with syntenin-1 via their C-terminal regions and the PDZ domain of syntenin-1 (Latysheva N *et al.*, 2006; Guix FX *et al.*, 2017; Andrijes R *et al.*, 2021).

Secondary interactions occurring among tetraspanins are mainly mediated by palmitoylation at membrane-proximal cysteine residues and are resistant to milder detergents such as 1% Brij97 (Hemler ME, 2005). This tetraspanin-tetraspanin interaction is not as solid as direct interactions (Berditchevski F, Zutter MM and Hemler ME, 1996). For example, a palmitoylation deficiency in CD151 could impair its associations with CD63 and CD81, but failed to affect the direct interaction of CD151 with integrin α3β1 (Martin F et al., 2005). Similarly, palmitoylation of

CD9 and CD81 was identified to be vital for their interaction, and mutations in these palmitoylated sites of CD9 could badly interrupt this tetraspanin/tetraspanin interaction (Charrin S *et al.*, 2002).

Tertiary interaction refers to a broader cluster of interactions between tetraspanins/partner proteins, tetraspanin/tetraspanin, and partner protein/partner protein. For instance, integrin α3β1 could interact with CD9 through direct interaction with CD151. And, integrin α3β1 could interact with CD9P-1 (partner protein of CD9) on the condition of CD9-CD151 interaction (Charrin S *et al.*, 2003). This large-scale complex is only preserved in Brij58, Brij98 and CHAPS, but not in Brij97 (Martin F *et al.*, 2005).

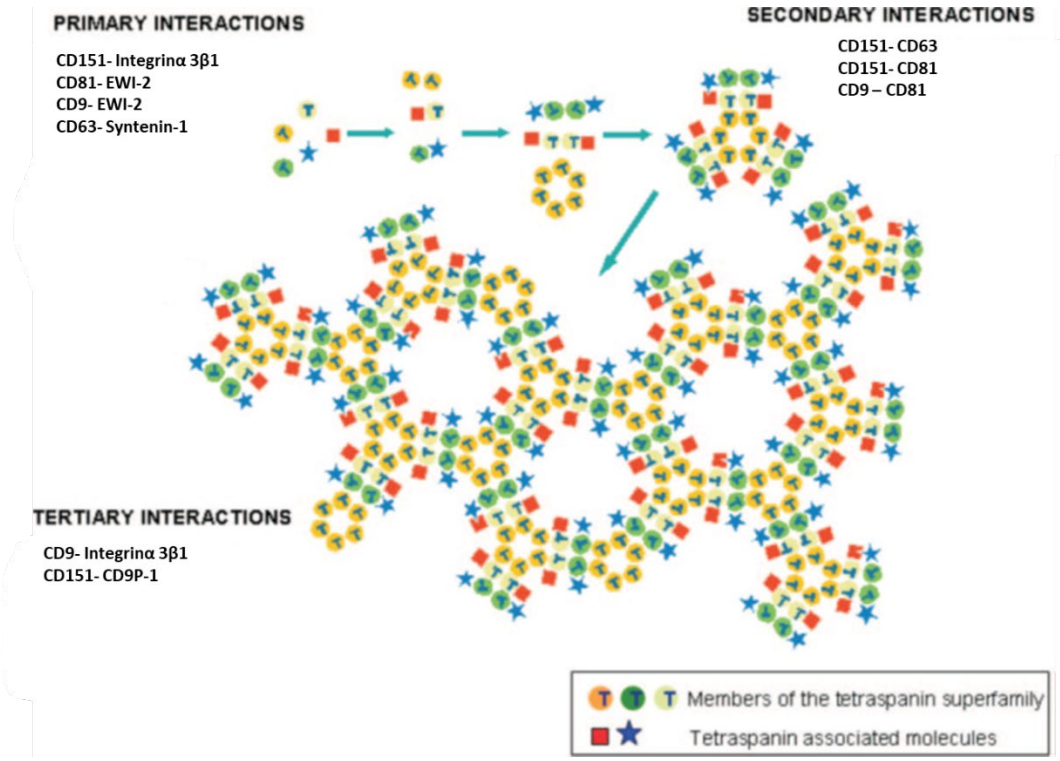

Figure 1-8. Multi-level of tetraspanin enriched domain (TEM). Primary interactions of tetraspanins with their partner proteins are the most robust associations which constitutes the first level of TEM. The secondary interactions occur between different tetraspanins via palmitoylation, connecting more primary interactions to establish the second level of TEM. Tertiary interactions are more likely to be a consequence of upgraded secondary interactions, which are only resistant to the mildest detergent. The figure is modified and reproduced from (Martin F *et al.*, 2005).

1.4.5. Tetraspanins in breast cancer

It has been established that some tetraspanins were involved in tumour development, growth, and metastasis. Here, we summarise what is known about the involvement of tetraspanins in the development of breast cancer (Table 1-2).

Table1-2. Tetraspanins in breast cancer

Name	Main function(s) in Breast cancer
CD151/Tspan24	CD151 potentiated EGFR-dependent signalling in breast cancer via α6β4, which was associated with early tumour onset, increased cell survival, motility and invasion (Deng X *et al.,* 2012); CD151 cooperated with intergins to regulate the sensitivity of breast cancer to Herceptin treatment (Novitskaya V *et al.,* 2014; Mieszkowska M *et al.,* 2019); CD151 enhanced the chemotactic effects of IBC cells on monocytes (Hayward S *et al.*, 2020).
CD9/Tspan29	CD9 differently modulated the migration and metastasis of breast cancer by associating with distinct partners, such as tanlin1 (Powner D *et al.*, 2011) and DDRs (Castro-Sanchez L *et al.*, 2010).
CD82/Tspan27/KAI-1	CD82 weakened the EGFR signalling pathway by increasing the ligand-induced internalisation and attenuating dimerisation and ubiquitination of the receptor (Odintsova E, Sugiura T and Berditchevski F, 2000; Odintsova E, Voortman J, Gilbert E and Berditchevski F, 2003; Wang XQ *et al.*, 2007; Odintsova E *et al.*, 2013); CD82 attenuated mammary tumour cell migration by enhancing actin polymerisation and favouring focal adhesion formation (Ordas L *et al.*, 2021); Truncated CD82 lost its association with the integrin αvß3, which resulted in the increased activation of FAK and enhanced migration of breast cancer cells *in vitro* (Miller J *et al.*, 2018).

CD81/Tspan28	Silencing CD81 diminished the proliferation and migration of breast cancer cells *in vitro* and *in vivo* (Vences-Catalán F *et al.*, 2015; Zhang N *et al.*, 2018; Uretmen Kagiali ZC *et al.*, 2019); In contrast, CD81 expression is increased during the EMT process, indicating its metastasis-promoting effect (Uretmen Kagiali ZC *et al.*, 2019); Deficiency of CD81 in tumour hosts (CD81 knockout mice) not only decreases tumour growth and metastasis but also attenuates the immunosuppressive effect of myeloid-derived suppressor cells (MDSCs) and Tregs (Vences-Catalán F *et al.*, 2015).
CD63	CD63 contributed to the drug resistance of breast cancer (Tominaga N *et al.*, 2014); CD63 increased the proliferation of breast cancer cells (Ando T *et al.*, 2018); The reduced expression of CD63 in EVs markedly decreased the EV-loading of CD63-associated cargos, ILK and β-integrin, attenuating the process of EMT (Pederson PJ, Liang H, Filonov D and Mooberry SL, 2021).
Tspan12	TSPAN12 prevents the degradation of β-catenin and stabilised the association of FZD4 and LRP5 (key components of Wnt receptor), enhancing the expression of genes associated with tumour development and lowering the expression of genes involved in tumour suppression (Knoblich K *et al.*, 2014).

Tspan13/NET-6	Tspan13 promoted the expression of tumour apoptotic factors p53, Bax, Bak and caspase 3, exerting an anti-proliferation effect on tumour cells (Huang H, Sossey-Alaoui K, Beachy SH and Geradts J, 2007); Tspan13 inhibits tumour invasion by downregulating matrix metalloproteinases MMP1 and MMP3 (Huang H, Sossey-Alaoui K, Beachy SH and Geradts J, 2007).

1.4.6. Tspan6

1.4.6.1. Overview of Tspan6

Tspan6 protein is encoded by the gene located on chromosome Xq22.1. The mRNA and protein expression of Tspan6 has been detected in various human organs and tissues with different expression levels (Maeda K *et al.*, 1998).Tspan6 mRNA and protein are highly expressed in the liver and gallbladder system and male and female reproductive organs (including the breast). Tspan6 protein was also detected in respiratory organs, proximal digestive and urinary systems, skin, bone marrow, and lymphoid tissues (https://www.proteinatlas.org/).

The biological functions of Tspan6 in development, tissue maintenance and various pathological conditions remain largely unknown. In 2017, two studies suggested a regulatory role of Tspan6 in neurological disease development. Salas *et al*. discovered that the knockout of Tspan6 strengthened basal synaptic transmission and reduced long-term potentiation (Salas

IH *et al.*, 2017). Guix *et al*. found that Tspan6 may contribute to the development of non-familial Alzheimer's disease (AD) by facilitating the accumulation of β-amyloid peptide (Aβ) peptides in the extracellular environment (Guix FX *et al.*, 2017).

More recently, several reports suggest that Tspan6 may play a role in carcinogenesis. An earlier study reported that the overexpression of Tspan6 was more common in colorectal cancer (CRC) tissues than adjacent non-tumour tissues. CRC patients with overexpression of Tspan6 were likely to have worse survival (Chiang SF *et al.*, 2014). In contrast, patients of locally advanced rectal cancers with overexpression of Tspan6 were more likely to have a complete response to neoadjuvant therapy (Chauvin A *et al.*, 2018). Findings from our laboratory demonstrated that the decrease or deficiency of Tspan6 in the CRC cohort correlated with poor survival (Andrijes R *et al.*, 2021). Furthermore, overexpression of Tspan6 in CRC was associated with a better therapy response to EGFR-targeted treatment (Andrijes R *et al.*, 2021). Apart from CRC, a reduced expression of Tspan6 was also found to correlate with shorter survival and increased levels of EMT signatures in lung and pancreatic cancer patients (Humbert PO *et al.*, 2022). The same study suggested that Tspan6 was a tumour suppressor for Ras-driven cancer, and knockdown of Tspan6 greatly enhanced the tumourigenesis in breast epithelial cells (Eph4) transformed with H-Ras mutant (Humbert PO *et al.*, 2022). These effects may be due to the interaction of Tspan6 with EGFR, resulting in the downregulation of the EGF-dependent activation of Ras/ Erk1/2/p38 MAPK signalling (Humbert PO *et al.*, 2022).

In another molecular study, Tspan6 was shown to negatively regulate the immune signalling pathway against RNA virus infection, which is primarily mediated by retinoic acid-inducible gene I-like receptors (RLRs). Tspan6 underwent ubiquitination and was associated with mitochondrial antiviral signalling protein (MAVS). This prevented MAVS from interacting with RLRs and interfered the MAVs-involved formation of signalosome, consequently inhibiting the RLRs pathway-induced expression of IFN (Wang Y *et al.*, 2012).

1.4.6.2. Tspan6 and syntenin-1, and exosomes

Typically, tetraspanins exert their regulatory function by associating with their partner proteins. In the case of Tspan6, the only known partner protein is syntenin-1 (Guix FX *et al.*, 2017), which was first identified as a product of the melanoma differentiation-association gene *mda-9* (Lin JJ, Jiang H and Fisher PB, 1998). Syntenin-1 comprises 298 amino acids and is highly conserved across various species. The structure of syntenin-1 consists of an N-terminal domain, followed by two tandem PDZ domains (PDZ1 and PDZ2) and a C-terminal domain.

The interaction of Tspan6 and syntenin-1 was first identified in a study investigating Alzheimer's disease (Guix FX *et al.*, 2017). This interaction was shown to regulate the metabolism of amyloid precursor protein (APP), the precursors of Aβ peptides that cause non-

familial Alzheimer's disease (AD) (Guix FX *et al.*, 2017). This study demonstrated that the Tspan6/syntenin-1 complex regulated the composition of exosomes (Guix FX *et al.*, 2017), which are cell-derived extracellular vesicles involved in intercellular communication in normal tissues and pathological conditions (van Niel G, D'Angelo G and Raposo G, 2018). On the one hand, Tspan6 enhanced the loading of APP C-terminal fragments into intraluminal vesicles (ILVs) for exosomal release; on the other hand, Tspan6 inhibited lysosomal degradation of APPs by affecting the autophagosome-lysosomal fusion (Guix FX *et al.*, 2017).

Exosomes are a subtype of extracellular vesicles (EVs). Exosomal cargoes in early endosomes are derived from the Golgi apparatus or internalised plasma membrane. Subsequently, the limited membrane of early endosome bud inward, along with selective cargoes to form ILVs, which contributes to the formation of the multivesicular body (MVBs). With assistance from cytoskeletal and microtubule networks, MVBs reach the plasma membrane and fuse with it, giving rise to the release of ILVs, later called exosomes (van Niel G, D'Angelo G and Raposo G, 2018). The regulatory function of Tspan6 in exosomal cargo sorting was also confirmed by Ghossoub *et al.* Overexpression of Tspan6 on MCF7 (breast cancer cell line) inhibited the loading of syntenin-1 and syndecan-4, a scaffolding protein, into ILVs while promoting the lysosomal degradation of the same cargos (Wang Y *et al.*, 2012). Finally, our recent study demonstrated that the Tspan6-syntenin-1 complex inhibited the sorting of a transmembrane form of TGF-α (tm TGF-α) to EVs, thus diminishing the secretion of tm TGF-α and suppressing the carcinogenesis of CRC (Andrijes R *et al.*, 2021).

In addition to Tspan6, syntenin-1 is known to interact with many other proteins, such as Src (Figure 1-9) (Shimada T, Yasuda S, Sugiura H and Yamagata K, 2019). In the human melanoma model, the syntenin-1/c-Src complex positively regulated the NF-κB activation. Mechanistically, syntenin-1 interacted with c-Src through its PDZ domains, with PDZ2 being the dominant one. This interaction upregulated the activation of p38 MAPK and induced the NF-κB nucleus translocation, eventually enhancing anchorage-independent growth, motility and invasion of melanoma cells (Boukerche H *et al.*, 2010).

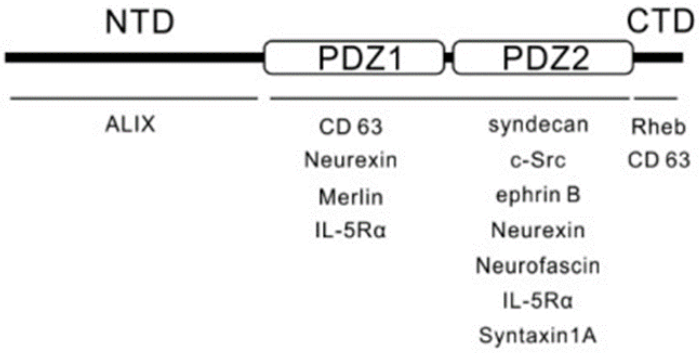

Figure 1-9. A schematic diagram of syntenin-1 and its partners. Syntenin-1 is a PDZ-containing adaptor protein with an N-terminal and a C-terminal domain (CTD). The structural domains of syntaxin-1 responsible for bindings to different proteins are shown, and the target proteins are listed below the specific structural domains. Figure reproduced from (Shimada T, Yasuda S, Sugiura H and Yamagata K, 2019).

1.5. Research Aims

IBC is a rare and fatal disease with fewer targeted therapies, which results in a higher mortality rate for IBC than for non-IBC. Accumulating evidence showed that the TIME is relevant to the

development and progression of IBC, and unpublished data from our lab demonstrated that Tspan6, a poor-studied tetraspanin, was relevant to the B cell infiltration of IBC. However, the underlying mechanisms have not been elucidated. Thus, this project aims to examine the chemoattractive potential of IBC for B cells and how Tspan6 regulates this B cell-biased chemotactic effect of IBC. To this end, both IBC extracellular and intracellular molecules and pathways are investigated.

2. MATERIALS AND METHODS

2.1. Cell lines and Cell culture

2.1.1. Cell lines

Table 2-1. Human cell lines used in this study

Cell line	Tissue	Molecular type	Tumour
SUM149	Human Breast	ER-, PR-, HER2-	Ductal Carcinoma, IBC
BCX010	Human Breast	ER-, PR-, HER2-	Ductal Carcinoma, IBC
SUM190	Human Breast	ER-, PR-, HER2+	Ductal Carcinoma, IBC
MD-IBC3	Human Breast	ER-, PR-, HER2+	Ductal Carcinoma, IBC
KPL4	Human Breast	ER-, PR-, HER2+	Ductal Carcinoma, IBC
HEK293T	Human Embryonic Kidney	NA	NA

2.1.2. Cell culture

The SUM149 and SUM190 cell lines were kind gifts from Dr Stephen P. Ethier (now available from Asterand, Detroit, MI, USA). The human IBC cell line BCX010 was established in the laboratory of Dr Funda Meric-Bernstam (MD Anderson Cancer Center, Houston, TX, USA) (McAuliffe PF *et al.*, 2015). MD-IBC3 and KPL4 cells were provided by Dr Cristofanilli and Dr van Laere, respectively. All cells were routinely grown in T25 and T75 flasks (Corning). SUM149, BCX010, SUM190 and MD-IBC3 cells were grown in Ham's F12 Nutrient Mix containing 5% (v/v) Fetal Calf Serum (FCS) (Gibco), 5 U/ml Penicillin/Streptomycin (Gibco), 5ug/ml insulin (Sigma), and 1μg/ml hydrocortisone (referred to as Ham's F12). KPL4 were

cultured in Advanced Dulbecco's Modified Eagle's Medium/Nutrient Mixture F-12 Ham containing 10% (v/v) FCS (Gibco) and 5U/ml penicillin/streptomycin (Gibco) (referred to as ADF++). HEK293T cells were maintained in Dulbecco's Modified Eagle's Medium (DMEM) containing 10% (v/v) FCS (Gibco) and 5U/ml penicillin/streptomycin (Gibco). All cell lines were cultured at 37°C, 5% CO2, in humidified conditions.

Cells were routinely sub-cultured when they reached ~90% confluency. The growth medium was removed and cells were washed with 1x phosphate-buffered saline (PBS) twice. Cells were detached by incubating with 0.05% Trypsin-EDTA (Gibco) or TrypLE™ Express Enzyme 1X (Gibco) for 3 minutes at 37°C. A complete growth medium was then added to prevent the over-treatment of cells. The cell suspension was transferred to a 15ml Falcon tube and centrifuged at 300g for 3 minutes. Supernatants were discarded and cells were resuspended in fresh complete growth medium and sub-cultured in the required proportion.

2.1.3. Cryopreservation of cell lines

Cells were detached and pelleted as described in section 2.1.2. Cellular pellets were resuspended in a freezing medium (see APPENDIX). The suspension containing the required number of cells ($1x10^6$ ~ $3x10^6$ cells) was aliquoted 1ml in a CryotTube™ vial (Nunc). Vials were kept at -80°C freezer for short-term durations (</=6 months) and transferred to liquid nitrogen for long-term storage (>6 months).

When thawing cells from liquid nitrogen or -80°C freezer, vials with frozen cells were placed in a water bath at 37°C for 2-3 mins. The thawed cell suspension was quickly transferred to a 15ml Falcon tube containing 9ml pre-warmed complete growth medium, then pelleted at 300g for 3 minutes. Resuspended cells with a fresh complete growth medium and aliquoted into T25 flasks. Cells were incubated under standard culture conditions (at 37°C, 5% CO2, in humidified conditions). The culture medium was changed the next day.

2.1.4. Production of lentiviral particles and lentiviral gene transduction

Lentiviral transduction was used to establish IBC cells expressing different tetraspanins (Tspan4, Tspan6, Tspan13, CD63, CD82 and CD151). To produce lentiviral particles, HEK 293T cells (60mm dish, Corning) at ~70% confluency were transfected with a combination of two types of plasmids: packing plasmids (psPAX2, pMD 2.G) and transferring plasmids (pLVx-IRES-puro, pLVx-IRES-Tspan6-Flag-puro, pLVx-IRES-Tspan6 V/G-Flag-puro and pLVx-IRES-tetraspanin-GFP-puro) (Figure 2-1). The packing plasmids were provided by D. Trono (Geneva, Switzerland). Dr Berditchevski provided the transferring plasmids. Plasmids encoding GFP-tagged tetraspanin proteins (GFP-Tspan4, GFP-Tspan6, GFP-Tspan13, GFP-CD63, GFP-CD82 and GFP-CD151) were constructed by GenScript. For transduction with the virus encoding Flag-tagged Tspan6 or Flag-tagged Tspan6 V/G, 8 μg plasmid DNAs (3.6 μg psPAX; 1.8 μg pMD2.G; 2.6 μg pLVx-Tspan6-Flag or pLVx -Tspan6 V/G-Flag) were mixed in 800 μl of serum-free, antibiotics-free DMEM and was supplemented with 12 μl polyethyleneimine (PEI). For transduction with the virus encoding GFP-tagged tetraspanins, 8

µg Plasmid DNAs (3 µg psPAX; 1µg pMD2.G; 4 µg pLVx-tetraspanin-GFP) were mixed in 800 µl of serum-free, antibiotics-free DMEM and was supplemented with 12 µl PEI. After brief vortexing, the DNA/PEI mixture was incubated at room temperature for 10 minutes, followed by the addition of 3.2 ml of fresh DMEM/10% (v/v) FCS before applying it to HEK 293T cells. After 10-16 hours, the DMEM medium was replaced with Ham's F12 medium and incubated for 24 hours to generate viral particles. Supernatants containing lentiviral particles were collected and supplemented with polybrene (1-2 µg/ml). Subsequently, the supernatants were filtered through a 0.45 µm membrane (Sartorius) and added to target cells (SUM149 or BCX010 cells) for additional 24 hours. The infection cycle was repeated to increase the efficiency of lentiviral gene transduction. Selection with 2 µg/ml Puromycin started 48 hours after the last infection cycle and lasted 2 weeks. All transduced cells were maintained and subcultured in Ham's F12 medium.

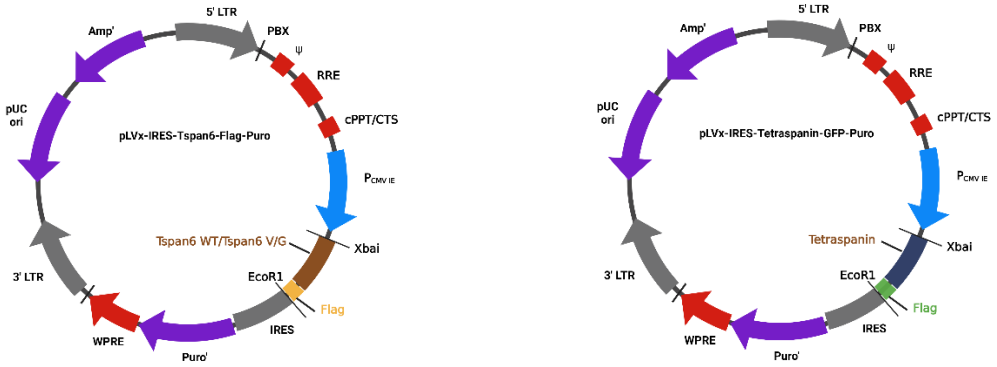

Figure 2-1. Plasmid maps of transferring plasmids.

2.1.5. Three-dimensional (3D) cell culture

For the preparation of 3D cell culture, a well of a 48-well plate was coated with 70% (v/v) Growth Factor Reduced Matrigel (MG) (BD Bioscience) in Ham's F12 and incubated at 37°C for 15mins to solidify the MG. This process facilitated the formation of a high MG-meniscus in the well. Meanwhile, detached cells (described in section 2.1.2) were quantified and resuspended in fresh Ham's F12 medium at 25,000 cells/ml. Two hundred microliters of cell suspension (5000 cells) were mixed with 200 µl 8% MG in Ham's F12 at a 1:1 ratio and were added to the MG-coated well. Cells were cultured at 37 °C, 5% CO2, in humidified conditions and refed with fresh Ham's F12 growth medium containing 4% MG every three days. The growth of colonies was assessed using phase-contrast microscopy (Nikon), and images from 10 fields were captured for subsequent analysis.

2.1.6. Proliferation assay

BrdU cell proliferation ELISA (ab12556, Abcam) was performed to assess cell growth. Cells of interest were seeded in a 96-well tissue culture plate (Corning) at different cell densities (1000, 2000, 4000 cells/100 µl per well) and grown under standard cell culture conditions for 24 and 72 hours. Cells were plated in triplicates for each experimental setting. Controls were also set up, including wells that do not receive cells (medium alone) and wells containing cells but do not receive BrdU reagent (assay background). For better sensitivity and signal-to-noise ratio, BrdU (20 µl/well) was added to the wells containing cells 21 hours before the end of the

culture period. During the incubation, BrdU would be incorporated into proliferating cells. The detection of BrdU was achieved by cell fixation and an anti-BrdU mAb. Cells were subsequently incubated with horseradish peroxidase-conjugated goat anti-mouse antibody, and the binding was visualised after adding TMB peroxidase substrate. The optical density (OD) was measured using an iMark™ microplate reader (Bio-Rad) at a wavelength of 450 nm. All the procedures were carried out according to the manufacturer's instructions. The absolute OD of proliferating cells was determined by subtracting two controls from the measurement of the experimental well.

2.2. Cell biology techniques

2.2.1. Flow cytometry analysis

The required number of cells ($1X10^6 \sim 3X10^6$ cells/4ml) were seeded in a 30 mm^2 dish (Corning) and cultured until they reached ~70% confluency. Cells were detached and pelleted as described in section 2.1.2, then resuspended in MojoSort™ Buffer (Biolegend). The cell suspension was divided into three equal portions for preparing the control and experimental groups and aliquoted to FACS tubes (Stemcell Falcon). Cells were pelleted at 300g for 5 mins and supernatants were removed. Subsequently, cells were incubated with appropriate primary antibodies separately (See Table 2-2) at 4 °C for 45 mins. Cells were then washed with MojoSort™ Buffer (0.5% BSA and 2mM EDTA in PBS) (Biolegend) prior to the second incubation with fluorochrome-labelled secondary antibody (See Table 2-2) at 4 °C for 45 mins

in the dark. Following a second wash, cells were resuspended in 300 µl MojoSort™ Buffer (Biolegend) per tube. The anti-Tspan6 Ab and secondary antibodies were all pre-diluted with 3% Bovine Serum Albumin (BSA) in 1x Tris-buffered saline with 0.05% Tween-20 (TBST). For BD LSR II flow cytometry investigations, cells were maintained at 4°C.

Table 2-2. Antibodies used for flow cytometry

Antibody	Species	Catalogue number	Manufacturer	Volume
Tspan6	Mouse	N/A	In-house generated	500 µl (dilution: 1:1000)
CD81 (M38) (positive control)	Monoclonal Mouse	10630D	Thermo Fisher Scientific	100 µl
Type II PI 4-kinase (4C5G) (negative control)	Mouse	N/A	customised	100 µl
Goat anti-Mouse IgG, Alexa Fluor 488 (Secondary)	Polyclonal Goat	A11017	Thermo Fisher Scientific	500 µl (dilution: 1:500)

2.2.2. Fluorescence Activated Cell Sorting (FACS)

The preparation of cells for cell sorting was carried out under sterile conditions. Cells of interest were harvested and labelled with fluorescence as described in section 2.2.1. Cells were sorted using Beckman Coulter MoFlo Legacy FACS and collected in 2 ml 100% sterile FCS. Sorted cells were pelleted (300g for 5 mins) and grown in 20% (v/v) FCS in Ham's F12 medium supplemented with 2.5 µg/ml anti-fungal antibiotic (Funghizone) in a T25 flask. The growth

medium was exchanged with fresh Ham's F12 medium (5% FCS) after 2-3 days when cells resumed growth.

2.2.3. Cell migration assay

2.2.3.1. Preparation of medium conditioned by IBC cells (CM-IBC)

The required number of cells (SUM149 isogenic pair: $1X10^6$ ~ $1.5X10^6$ cells, BCX010 isogenic pair: $0.4X10^6$ ~ $0.5X10^6$ cells) were cultured in T25 flasks (Corning) with 5 ml fresh Ham's F12 medium for 72 hours (Hayward S *et al.*, 2020). Culture supernatants were collected into a 15 ml Falcon tube and centrifuged for 10 minutes at 400 g at 4 ℃. The CM-IBC was then filtered using a 0.2 μm membrane (Sartorius) and kept on ice for further use and analysis.

2.2.3.2. Preparation of extracellular vesicle (EV)-depleted CM-IBC

The CM-IBC was prepared according to section 2.2.3.1, excluding filtration. The unfiltered CM-IBC was centrifuged for 35 minutes at 4 °C with a fixed-angle rotor spinning at 10000 rpm (SS34 rotor, 70Ti-Beckman). Subsequently, EVs were depleted by another ultracentrifugation at 24000 rpm 4 °C for 2 hours with a fixed angle rotor (SW40Ti rotor, 70Ti-Beckman). The supernatants were then filtered sterilely through a 0.2 μm membrane (Sartorius) and kept on ice for future use. This EV depletion protocol is widely used and the efficacy has been examined by our lab (Hayward S *et al.*, 2020).

2.2.3.3. Preparation of CM of IBC cells for siRNA transfection

Transfection by siRNA duplexes was performed using Lipofectamine RNAiMAX reagent (Invitrogen) following manufacturer instructions in a 6-well format. All siRNAs employed in this study are listed in Table 2-3. For each well to be transfected, 25 pmol siRNA was diluted in 500 µl Opti-MEM I Medium and mixed gently. Following that, 5 µl Lipofectamine RNAiMAX was added to each well containing diluted siRNAs. The siRNA-Lipofectamine mixture was incubated at room temperature for 15-20 minutes. Target cells were detached using a standard protocol (see section 2.1.2) and resuspended in a complete growth medium without antibiotics at $2x10^5$ cells/ml concentration. Two millilitres of cell suspension ($4x10^5$ cells) were added to siRNA-Lipofectamine complexes and mixed gently. This resulted in a final siRNA concentration of 10 nM. After 24 hours of transfection, the medium was changed and the cells were allowed to further condition the newly added growth medium for 72 hours. Medium conditioned by knockdown cells was applied for PBMC transmigration as follows.

Table 2-3. siRNA used for gene slicing

siRNA	Targeted sequence	Manufacturer
Syntenin-1	5’-GCUAUAGCAUAGCUGCUUAtt-3’ (siRNA sequence)	(Predesigned) Eurofins MWG Operon
p38α MAPK	5’-CTCAGTGATACGTACAGCCAA-3’ 5’-CAGAGAACTGCGGTTACTTAA-3’ 5’-AACTGCGGTTACTTAAACATA-3’ 5’-CTGGGAGGTGCCCGAGCGTTA-3’	Qiagen
p38β MAPK	5’-CTGAGCGACGAGCACGTTCAA-3’ 5’-CAGGATGGAGCTGATCCAGTA-3’ 5’-TCCATCGAGGACTTCAGCGAA-3’ 5’-CAGAACACGCCCGGACATATA-3’	Qiagen

p38γ MAPK	5'-TGGAAGCGTGTTACTTACAAA-3' 5'-CTGGACGTATTCACTCCTGAT-3' 5'-CTGGGAGGTGCGCGCCGTGTA-3' 5'-CCAGTCCGAGCTGTTCGCCAA-3'	Qiagen
RELA	5'-ATGGAGTACCCTGAGGCTATA-3' 5'-CCGGATTGAGGAGAAACGTAA-3' 5'-AAGATCAATGGCTACACAGGA-3' 5'-CATGGATTCATTACAGCTTAA-3'	Qiagen
Negative control siRNA	5'-AAT TCT CCG AAC GTG TCA CGT-3'	Qiagen

2.2.3.4. Purification of peripheral blood mononuclear cells (PBMCs)

Peripheral blood mononuclear cells (PBMCs) were purified using Ficoll-Paque plus (GE Healthcare) density gradient centrifugation protocol. Briefly, fresh blood (approximately 40 ml) collected from consented healthy donors was diluted with RPMI-1640 (SIGMA) at a 1:1 ratio. Each 40 ml of the blood/RPMI-1640 mixture was gently transferred to a 50 ml Falcon tube containing 10 ml Ficoll-Paque plus (GE Healthcare). Centrifugation was performed at 400 g for 22 mins to facilitate blood separation. PBMCs (concentrated within a thin layer between plasma and Ficoll-Paque plus) were carefully transferred to a new 50 ml Falcon tube and diluted with fresh RPMI-1640 at a 1:2 ratio. Cells were pelleted at 400 g for 10 mins. PBMCs were subsequently washed with an additional 20 ml 1640 RPMI. Following the second wash, PBMCs were counted using a Neubauer hemocytometer and pelleted again. Cells were diluted with fresh RPMI-1640 to achieve a final concentration of $1x10^7$ cells/ml and kept at room temperature before being used in migration experiments.

2.2.3.5. Chemotactic cell migration

CM-IBC and control medium (complete growth medium, Ham's F12 or ADF++) were aliquoted into 24 wells plate (800 µl/well). Two hundred microliters of PBMCs suspension ($2x10^6$ cells/insert) were seeded in the upper chamber of 5 µm pore trans-well insert (Corning) and allowed to migrate towards the control medium or CM-IBC in the lower well for 4 or 16 hours at 37 °C, 5% CO2, in humidified conditions. Migrated PBMCs were collected from the lower chamber. The total number of migrated PBMCs was counted using a Neubauer hemocytometer. Subsequetnly, cells were transferred to FACS tubes and pelleted by centrifugation at 400g for 5 mins. One microlitre violet fluorescent reactive dye (Invitrogen) was added to each tube to identify live cells. Cells were incubated at room temperature for 15 mins, followed by a wash with MojoSort™ Buffer (Biolegend). A general panel of antibodies (see Table 2-4) was then added to each tube and incubated for at least 30 minutes at 4 °C in the dark. Following that, cells in each tube were washed with MojoSort™ Buffer (Biolegend) again and fixed with 200 µl 4% paraformaldehyde (see Appendix) at room temperature in the dark for 30 mins. After the final wash, the cells were resuspended in 350 µl MojoSortTM Buffer (Biolegend) and kept at 4 °C before the analysis by flow cytometry.

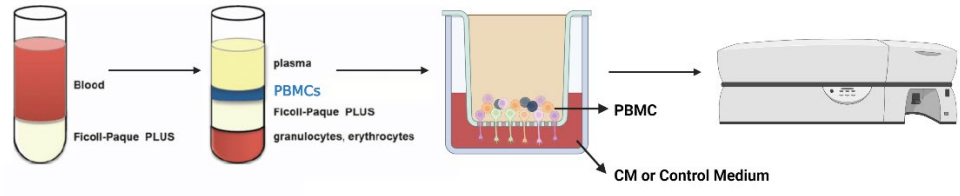

Figure 2-2. Experimental design for cell migration assay. Each 5 µm pore trans-well insert containing $2x10^6$ PBMCs was deposited in an exploratory well-containing control medium or

CM-IBC to allow PBMCs to migrate towards chemoattractant in the lower chamber for 4 or 16 hours.

Table 2-4. Antibodies used for flow cytometry

Marker	Clone	Species	Catalogue number	Manufacturer	Dilution
AmCyan-conjugated CD3	SK7	Monoclonal Mouse	339186	BD Biosciences	1:50
PE-Texas Red-conjugated CD4	SFCI12T4D11	Monoclonal Mouse	6604727	Beckman Coulter	1:100
PE-conjugated CD8	RPA-T8	Monoclonal Mouse	555367	BD Biosciences	1:50
APC-conjugated CD14	HCD14	Monoclonal Mouse	325608	BioLegend	1:100
PE-Cy7-conjugated CD19	HIB19	Monoclonal Mouse	302216	BioLegend	1:100

2.2.3.6. Gating strategies and analysis software

Migrated cells were profiled by flow cytometry using a BD LSR II and analysed by FlowJo® software. Initially, only live and singlet cells could be selected. Cells of interest were gated on size and granularity. Monocytes and subpopulations of lymphocytes were distinguished by using anti-CD3, CD4, CD8, CD14, and CD19 antibodies conjugated to fluorophores. Gating strategies are shown below (Figure 2-3). This gating strategy assessed the proportions of individual subpopulations. The absolute number of an individual subpopulation was calculated by multiplying the ratio with the total number of migrating cells.

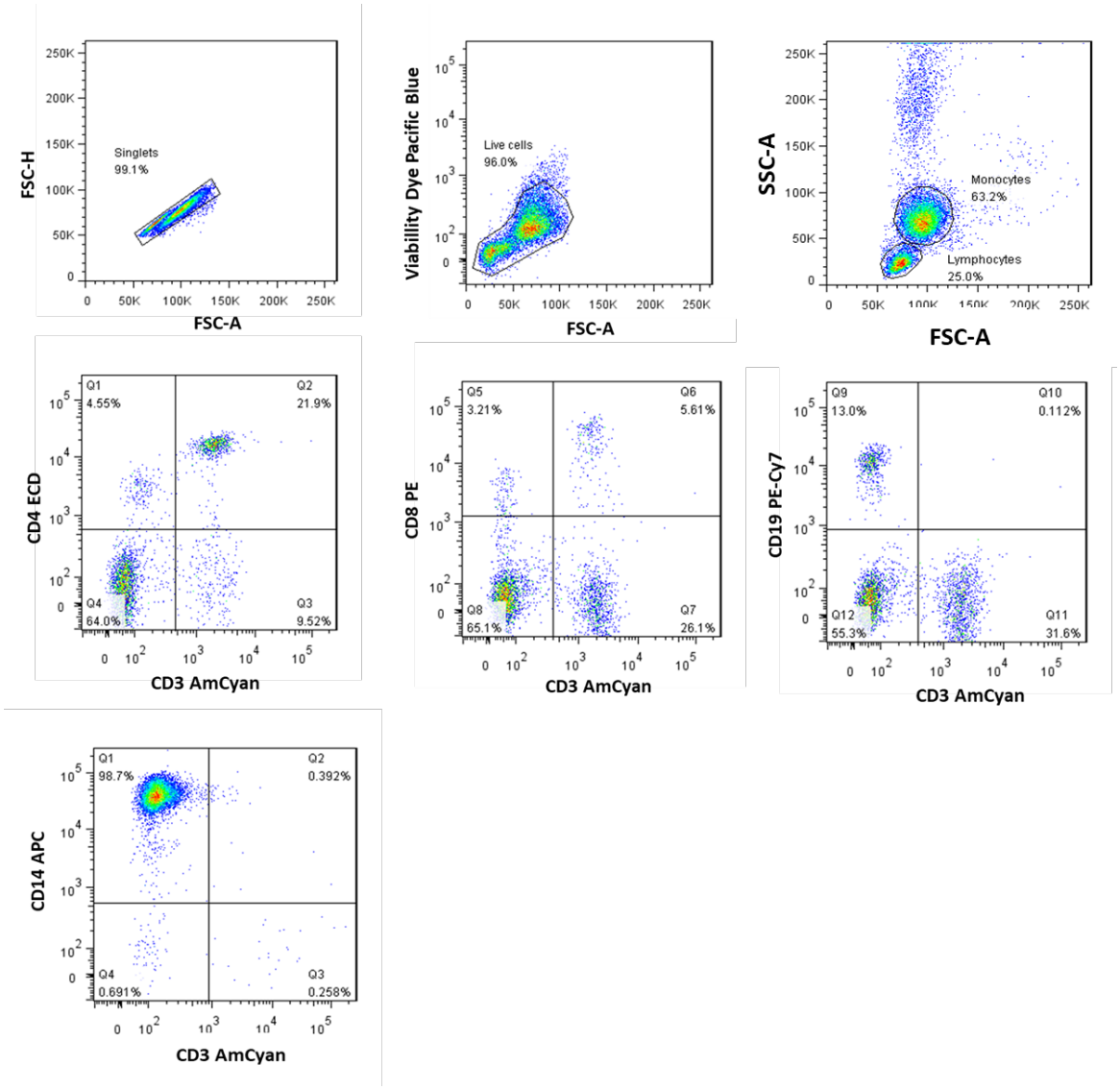

Figure 2-3. Gating strategies for immune subset identification.

2.2.4. Separation of immune subpopulations

2.2.4.1. B cell and CD8+ T cell isolation (negative selection)

PBMCs were purified as described in section 2.2.3.4 and resuspended in MojoSort™ Buffer (Biolegend) at $10x10^7$ cells/ml. B cells were negatively selected by employing MojoSort™

Human B Cell (CD43-) Isolation Kit (Table 2-5). Mechanistically, non-B cells were removed by incubating $10x10^6$ PBMCs with 10~12 µl biotin-conjugated antibody cocktail for 15 mins on ice, followed by incubation with magnetic Streptavidin Nanobeads on ice (equal volume as antibody cocktail) for 15 mins. The amount of antibody cocktail and nanobeads were increased when more PBMCs were processed. B lymphocytes were separated from the nanobeads-labelled cells using a magnetic separator (5 mins, room temperature). Two rounds of magnetic separation have been used. All procedures were performed according to the manufacturer's instructions. B cells were counted before centrifugation and resuspended in RPMI-1640 medium at $10~20x10^5$ cells/ml. The purity of negatively selected B cells (Figure 2-4). For pure B cell migration assay, 200 µl B cell suspension ($2x10^5$ cells/insert) was loaded per insert, while for monocyte or CD8+ T cell supplementation cell migration, 100 µl pure B cell suspension ($2x10^5$ cells/insert) was loaded per insert. Migration assay was performed as described in sections 2.2.3.5.

The protocol for negatively selecting CD8+ T cells was identical to that for B cells, but using MojoSort™ Human CD8 T Cell Isolation Kit (Table 2-5). Purified CD8+ T cells were then resuspended in RPMI-1640 medium at $10x10^5$ cells/ml. The purity of negatively selected CD8+ T cells was assessed (Figure 2-4). For CD8+ T cell supplement cell migration, 100 µl CD8+ T cell suspension ($1x10^5$ cells) was added to an insert containing 100 µl pure B cell suspension ($2x10^5$ cells/insert) to commence cell migration assay.

2.2.4.2. CD14+ monocytes isolation (negative seletion)

PBMCs were purified as described in section 2.2.3.4 and resuspended in MojoSort™ Buffer (Biolegend) at $10x10^7$ cells/ml. Monocytes were negatively selected by employing MojoSort™ Human CD14+ Monocytes Isolation Kit (Table 2-5). Specifically, $10x10^6$ PBMCs were initially blocked with 5~7 µl Human TruStain FcX™ (Fc Receptor Blocking Solution, Biolegend) at room temperature for 10mins. Non-CD14+ monocyte cells were then labelled by incubating PBMCs ($10x10^6$ cells) with 10~12 µl biotin-conjugated antibody cocktail for 15 mins on ice, which was followed by incubation with magnetic Streptavidin Nanobeads for 15 mins on ice (equal volume as antibody cocktail). Scale up the amount of all solutions when more PBMCs are processed. Cells were then washed with MojoSort™ Buffer (Biolegend). The supernatant was removed and cells were resuspended in 2.5 mL of MojoSort™ Buffer (Biolegend). CD14+ Monocytes were isolated using a magnetic separator (5 mins, room temperature). Two rounds of magnetic separation were carried out. All procedures were performed following the manufacturer's instructions. Isolated CD14+ monocytes were centrifuged and resuspended in RPMI-1640 medium at $20x10^5$ cells/ml. The purity of CD14+ monocytes was examined (Figure 2-4). For monocyte supplement cell migration, 100 µl of monocyte suspension ($2x10^5$ cells) was added to an insert containing 100 µl purified B cell ($2x10^5$ cells/insert) to commence the cell migration assay.

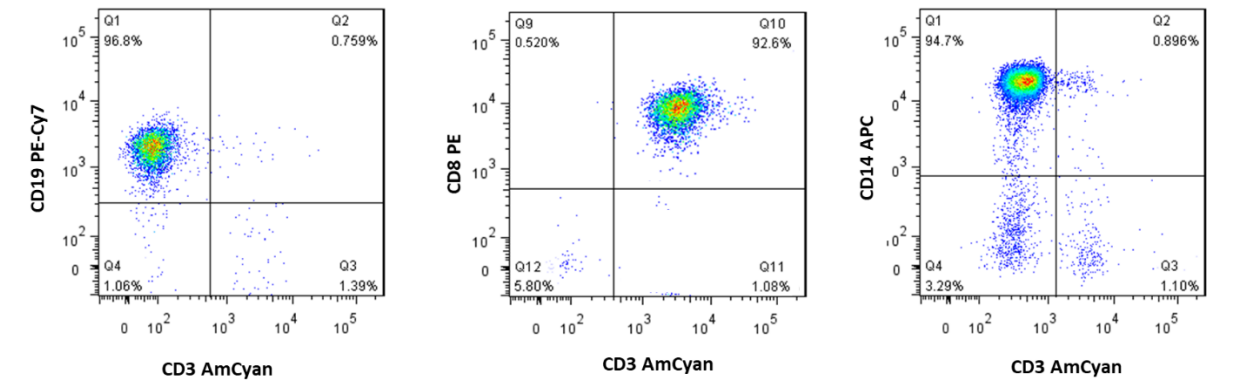

Figure 2-4. The purities of human B cells, CD14+ monocytes and CD8+ T cells after Mojo™ negative selection.

2.2.4.3. Double-conditioned medium (Dou CM-IBC)

CM-IBC was prepared as described in section 2.2.3.1 and kept on ice while the purification of monocytes was carried out (described in section 2.2.4.2). The CD14+ monocytes were then pelleted at 400 g for 6 minutes, resuspended in CM-IBC at $2x10^5$ cells/ml, and incubated for 4 hours at 37°C in 5% CO2 to generate Dou CM-IBC. Dou CM-IBC was then filtered through a 0.45 µm membrane (Sartorius) to remove CD14+ monocytes before keeping this medium on ice for further use.

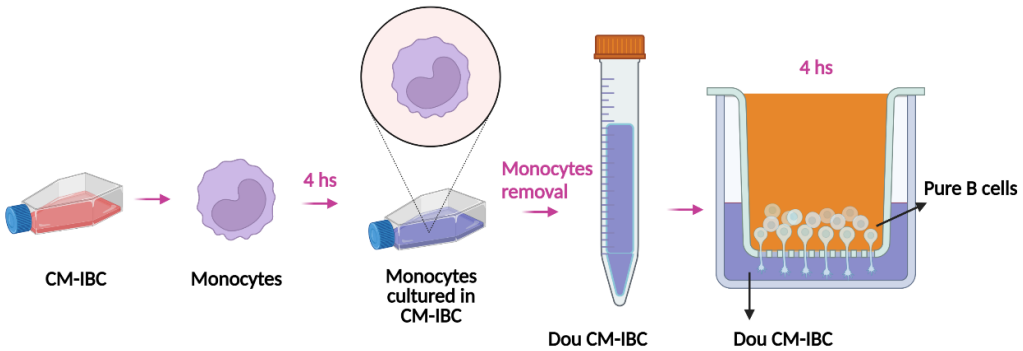

Figure 2-5. The flow diagram shows the processes of generating a double-conditioned medium (Dou CM-IBC). Purified CD14+ monocytes (described in section 2.2.4.2) were incubated in CM-IBC for 4 hours at 37 °C in 5% CO_2. CD14+ monocytes were removed prior to the further use of Dou CM-IBC.

2.2.4.4. CD14+ monocytes/ CD8+ T lymphocytes depletion (positive selection)

PBMCs were purified as described in section 2.2.3.4 and resuspended in MojoSort™ Buffer (Biolegend) at $10x10^6$ cells/ml. For monocyte depletion, PBMCs ($10x10^6$ cells) were incubated with 5-7 µl Human TruStain FcX™. Subsequently, purified PBMCs ($10x10^6$ cells) were incubated with biotin-labelled anti-human CD14 (or anti-CD8) antibody conjugated to nanobeads for 15 mins on ice and washed cells with MojoSort™ Buffer (Biolegend) (see Table 2-5). Targeted cells (CD14+ or CD8+ T cells) were subsequently removed by two rounds of magnetic separation (5 mins, room temperature). Scale up the amount of solution when more PBMCs are processed. Untargeted cells (PBMCS depleted of CD14+ or CD8+ cells) were collected and centrifuged at 400 g for 8 mins. Resuspended cells with RPMI-1640 medium at $10x10^6$ cells/ml and kept them at room temperature. The efficacy of depletion was assessed (Figure 2-6). All procedures were performed following the manufacturer's instructions.

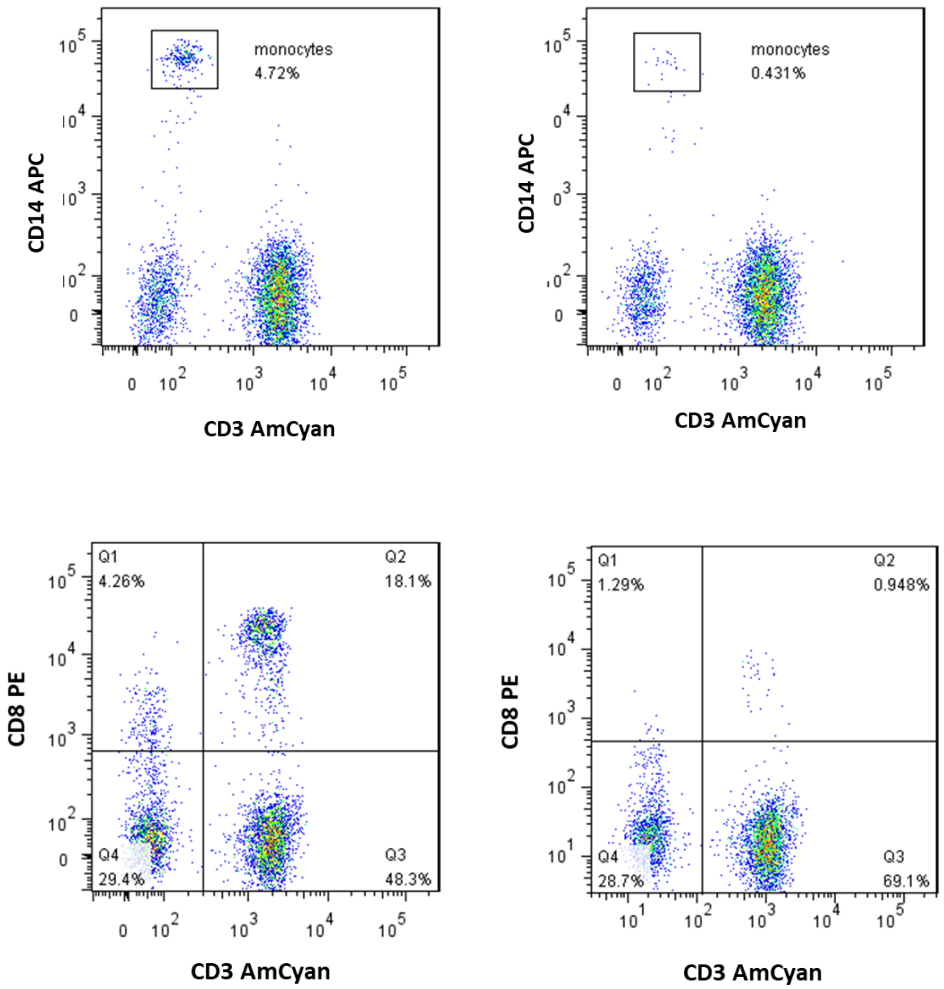

Figure 2-6. The efficacy of cell depletion (up: monocyte depletion; bottom: CD8+ T lymphocyte depletion).

Table 2-5. Commercial kits used for cell separation

Target cells	Application	Manufacturer	Catalogue number
Human B lymphocytes	Negative cell separation	Biolegend	480061
Human CD14+ monocytes	Negative cell separation	Biolegend	480047
Human CD8+ lymphocytes	Negative cell separation	Biolegend	480011

Human CD14+ monocytes	Positive cell separation	Biolegend	480093
Human CD8+ T lymphocytes	Positive cells separation	Biolegend	480107

2.2.5. Midkine stimulation assay

CM-IBC was prepared as described in section 2.2.3.1. Recombinant human Midkine (generously provided by Lyramid (Sydney, NSW, Australia)) was added to CM-IBC/pLVx or control medium (Ham's F12) to reach different concentrations (0, 1, 5, 20 ng/ml). PBMCs were purified in section 2.2.3.4.and the cell migration assay was conducted as described in section 2.2.3.5.

2.2.6. Midkine neutralisation assay

CM-IBC was prepared as described in section 2.2.3.1. Neutralisation antibody to Midkine (IP14, Cellmid) was added to CM-IBC/Tspan6 and CM-IBC/pLVx with different concentrations (0, 1, 5, 20 μg/ml). Isotype mouse antibody (IgG2a) was applied as a negative control. PBMCs were purified in section 2.2.3.4.and the cell migration assay was conducted as described in section 2.2.3.5.

2.2.7. Pure B cell migration assay supplemented with Pertussis Toxin (PTX)

Pure B cells (as described in section 2.2.4.1) were pre-treated with different concentrations of

PTX (0, 200 and 500 ng/ml) at 37 °C and 5% CO_2 for 1 hour prior to the onset of the migration experiments. Pre-treated B cells were then loaded into inserts (Corning) ($2x10^5$ cells/insert), and inserts were placed onto wells containing the control medium or CM-IBC to initiate the migration assay as described in sections 2.2.3.5.

In order to investigate PTX's influence on monocyte-dependent B cell migration, suspended pure B cells were pre-treated with PTX (working concentration: 200 ng/ml) at 37 °C and 5% CO2 in a Falcon tube. Following 1-hour treatment, the pre-treated B cells were washed with MojoSort™ Buffer (Biolegend) and were mixed with pure CD14+ monocytes (as described in 2.2.4.2) at a ratio of 1:1. The mixed cells were loaded into inserts ($4x10^5$ cells/insert). Inserts were placed onto wells containing control medium or CM-IBC to initiate the migration assay.

2.2.8. Immunofluorescence staining

Ten-millimetre round glass coverslips (VWR) were sterilised with ethanol and UV irradiation in a 24-well plate (Corning). Cells were plated on coverslips and grown until they reached ~60% confluency. The growth medium was discarded, and coverslips were rinsed twice with PBS. Cells were fixed with 2% paraformaldehyde/PBS (see APPENDIX) for 10 mins. Coverslips were subsequently rinsed thrice with PBS before permeabilisation with 0.1% Triton X-100/PBS (see APPENDIX) for 20 seconds. Coverslips were then placed onto a coverslip holder, and cells were blocked with 20% goat serum/PBS (see APPENDIX) for 1 hour at room temperature. Subsequently, cells were incubated with appropriate primary antibodies (see Table 2-6) for 1h

at room temperature. Following that, cells were washed with PBS for three times with 10 mins intervals on a rotating platform and incubated with fluorescent secondary antibodies (see Table 2-6) for an additional 1hour in the dark. After the final wash (i.e. cells were washed with PBS for 3 times with 10 mins intervals on a rotating platform), the coverslips were rinsed with distilled water and allowed to dry overnight. Coverslips were put on slides upside down in the drop of anti-FADE (SlowFade™ Gold Antifade Mountant with DAPI, Invitrogen), sealed with nail polish, and then preserved at -20 °C. Staining was analysed, and images were collected using a fluorescence microscope (Nikon ECLIPSE E600). Representative images were processed by Adobe Photoshop.

Table 2-6. Antibodies used for immunofluorescence

Antibody	Species	Catalogue number	Manufacturer	Dilution
Anti-Flag (M2)	Monoclonal Mouse	F1804	Sigma	1:2000
Goat anti-Mouse IgG, Alexa Fluor 568 (Secondary)	Polyclonal Goat	A11019	Thermo Fisher Scientific	1:1000

2.3. Biochemical methods

2.3.1. Preparation of whole-protein lysates from cells

To prepare whole protein lysates, SUM149 ($2x10^6$ cells) and BCX010 ($1x10^6$ cells) cells were plated in a 60 mm^2 dish (Corning) for 48 hours until they reached ~100% confluency. The growth medium was removed and cells were rinsed with PBS 4 times. Cells were lysed by

adding 200 µl 1X Laemmli buffer (5 % w/v SDS, 25 % glycerol, 0.25 M Tris-Cl pH 6.8 in dH2O) supplemented with β-mercaptoethanol (Sigma) (1:20 ratio) and 1X Protease/Phosphatase Inhibitor Cocktail (Cell Signaling Technology). Subsequently, lysates were transferred into Eppendorf tubes and underwent 3-4 cycles of heating-freezing to shear DNA: in each cycle, lysates were heated in a heating block at 95 °C until they lost viscosity and then rapidly transferred to -80 °C for 15 mins. Lysates were centrifuged for 10 mins at 13,000 g at 4 °C. Supernatants were transferred into new Eppendorf tubes and kept at -80 °C until further use.

2.3.2. Immunoprecipitation

Cells were prepared for lysis as described in 2.3.1. The following procedures are performed on ice. Whole cellular protein extraction was accomplished by adding 200 µl ice-cold 1% Brij98 (see APPENDIX) supplemented with 1X Protease/Phosphatase Inhibitor Cocktail (Cell Signaling Technology) onto cells. Cells were scraped and cellular lysates were transferred to Eppendorf tubes and placed on a rotary wheel for 4 hours at 4 °C to complete lysis. Lysates were then centrifuged at 13,000 g for 10 mins at 4 °C and 200 µl supernatants from each tube were collected. Tspan6 protein complexes were pulled down by incubating lysates with 20 µl anti-Flag M2 agarose beads (Sigma-Aldrich) for 4 hours at 4 °C on a rotary wheel. Protein-antibody-beads complex was washed 4 times with lysis buffer (supplemented with 1X Protease/Phosphatase Inhibitor Cocktail). Retained proteins were eluted by 1×Laemmli buffer, followed by boiling at 95 °C for 5 mins, then stored at -80 °C.

For the immunoprecipitation of cell signalling proteins, cells were cultured and lysed as described above. While cell lysis, appropriate mouse monoclonal antibodies (see Table 2-7) were incubated with 20 µl Protein G PLUS-agarose beads for 3 hours at 4 °C on a rotary wheel. The mouse IgG1 isotype (Invitrogen) was used as a negative control. Protein-antibody-agarose complexes were formed by incubating cell lysates with antibody-agarose beads at 4 °C for 2 hours. The immune complexes were washed 4 times with the ice-cold lysis buffer (supplemented with 1X Protease/Phosphatase Inhibitor Cocktail). Retained proteins were eluted with 1X Laemmli buffer, followed by boiling at 95 °C for 5 mins. All protein samples were kept at -80 °C. For cell signalling experiments, samples were reduced by adding 5% v/v β-mercaptoethanol (Sigma-Aldrich).

2.3.3. SDS-PAGE and Western Blot analysis

Equal amounts of protein lysates (~40 µg of total protein) were loaded and resolved on a 10%-12% SDS-PAGE gel (12 mA/gel, 2-3 hours). For the following western blot analysis, proteins were subsequently transferred onto nitrocellulose membranes at 100 V at 4 °C for 1 hour employing 1x Tris/Glycine transfer buffer (Geneflow). Pre-stained protein ladder (NEB) was applied to locate bands of interest. After blocking the membrane with 5% non-fat milk or 3% BSA in TBST (see APPENDIX) for 1 hour at room temperature, the membranes were incubated with diluted primary antibodies (see Table 2-7) overnight at 4 °C. Membranes were washed with TBST (see APPENDIX) 4 times with 10 mins intervals. The membranes were then

incubated with secondary antibodies conjugated to fluorescent dyes (see Table 2-7) at room temperature in the dark for 1 hour. The membranes were washed 4 times with TBST and briefly rinsed with distilled water. The signals were visualised and images were captured and quantified using an LI-COR Odyssey scanning system.

Table 2-7. Antibodies, Sepharose beads and reagents

Antibody	Species	Catalogue number	Manufacturer	Dilution
TSPAN6 Antibody (C-term)	Polyclonal Rabbit	AP9224b	Abgent	1:500
c-Src	Monoclonal Mouse	2110S	Cell signaling	1:50
Src	Monoclonal Rabbit	2123T	Cell signaling	1:1000
Phospho-Src Family (Tyr416)	Polyclonal Rabbit	2101s	Cell signaling	1:1000
Syntenin-1	Monoclonal Rabbit	ab133267	Abcam	1:1000
Phosphor-Syntenin-1	Rabbit	N/A	Customly prepared	1:1000
p-p70 S6 Kinase (Thr 389)	Polyclonal Rabbit	9205S	Cell signaling	1:1000
p-SAPK/JNK	Polyclonal Rabbit	9251S	Cell signaling	1:1000
P-P130-Cas	Polyclonal Rabbit	4011S	Cell signaling	1:1000
p-Paxillin	Polyclonal Rabbit	2541S	Cell signaling	1:1000

p-PKC (pan) (βII Ser660)	Polyclonal Rabbit	9371S	Cell signaling	1:1000
P38 MAPK	Polyclonal Rabbit	9212S	Cell signaling	1:1000
p-p38 MAPK (Thr180/Tyr182)	Monoclonal Rabbit	9215S	Cell signaling	1:1000
p-SAPK/JNK (Thr183/Tyr185)	Polyclonal Rabbit	9251S	Cell signaling	1:1000
p-p44/42 MAPK (Thr202/Tyr204)	Monoclonal Rabbit	4376S	Cell signaling	1:1000
p-p90RSK (Ser380)	Monoclonal Rabbit	11989S	Cell signaling	1:1000
p-eIF4E (Ser209)	Polyclonal Rabbit	9741T	Cell signaling	1:1000
Phospho-NF-κB p65 (Ser536)	Monoclonal Rabbit	3033S	Cell signaling	1:1000
Phospho-AKT (Ser473)	Monoclonal Rabbit	4060S	Cell signaling	1:2000
NF-κB p65	Monoclonal Rabbit	8242S	Cell signaling	1:1000
phospho-AMPK (Thr172)	Monoclonal Rabbit	2535S	Cell signaling	1:1000
Phospho-PKC Substrate	Polyclonal Rabbit	2261S	Cell signaling	1:1000
Phospho-AKT Substrate	Monoclonal Rabbit	9614S	Cell signaling	1:1000
β-Actin	Monoclonal Mouse	A5316	Sigma-Aldrich	1:40000

Anti-mouse IRDye680 RD (secondary)	Donkey	925-68072	LI-COR	1:10000
Anti-rabbit IRDye800 CW (secondary)	Goat	925-3321	LI-COR	1:10000
Mouse IgG1 Isotype Control	Mouse	NCG01	Invitrogen	1:50
ANTI-FLAG M2 Affinity Gel	Monoclonal Mouse	A2220	Sigma	N/A
Protein G PLUS-Agarose	N/A	sc-2002	Santa Cruz	N/A
Protease/Phosphatase Inhibitor Cocktail	N/A	5872s	Cell signaling	1X

2.3.4. Chemokine profiling and ELISA

A human Chemokine Array Kit (see Table 2-8) was used to profile the chemokines of CM-IBC. CM-IBC was prepared as described in section 2.2.3.1. The CM-IBC was collected and analysed per the manufacturer's instructions. Briefly, a membrane array spotted in duplicate with capture antibodies was incubated with blocking buffer in a well of the 4-well multi-dish for 1 hour at room temperature. While the membrane was blocking, one added reconstituted detection antibody to the sample (CM-IBC) and mixed, and incubated the mixture for 1 hour at room temperature. The sample/detection antibody mixture was subsequently added onto the blocked membrane and incubated overnight at 2-8 °C. The membrane was then washed by washing buffer for 10 minutes and repeated twice. Washed membrane was incubated with prepared Streptavidin-HRP solution for 30 minutes at room temperature, followed by an additional wash.

Carefully removed any liquid from the membrane and incubated it with prepared chemi reagent. Following 1-minute incubation, the chemi reagent mix was removed and membrane was transferred to an autoradiography film cassette. A signal proportional to the number of bound chemokines was obtained by visualised chemiluminescence after exposure to the X-ray film.

Sandwich ELISA (see Table 2-8) was employed to precisely evaluate the expression of specific chemokines/cytokines. In general, samples (CM-IBC or Dou CM-IBC) and standards were incubated in ELISA plate wells pre-coated with specific capture antibodies to immobilise the chemokine/cytokine of interest. Subsequently, a specific detection antibody and HRP were added in sequence, followed by incubation with the substrate of HRP. A stopping solution (1M HCL) was applied to terminate the enzyme-substrate reaction. OD was read at the required wavelength using an iMark™ microplate reader (Bio-Rad). The concentrations of samples were calculated based on the curve of standards using Excel programme. Triplicates were used in all tests.

Table 2-8. ELISA kits for chemokines detection

Human Cytokines/Chemokine	Catalogue number	Manufacturer
IL-6	900-TM16	PEPROTECH
IL-8	900-TM18	PEPROTECH
CXCL1	900-K38	PEPROTECH
CXCL10	900-TM39	PEPROTECH
CXCL12	900-M92	PEPROTECH

CXCL13	MBS2600803	MyBioSource
CCL2	900-TM31	PEPROTECH
CCL20	BGK78556	Biogems
Midkine	900-K190	PEPROTECH
PTN	MBS725616	MyBioSource
TGF-α	NBP2-34299	Novus Biologicals
VEGF	900-TM10	PEPROTECH
Amphiregulin	EHAREG	Thermo Fisher
TNF-α	900-TM25	PEPROTECH
Human Chemokine Array	ARY017	R&D Systems

2.4. Statistical analysis

Statistical analysis was performed by Graphpad Prism7 (GraphPad Software Inc). Gaussian data distribution was examined by three tests (D'Agostino-Pearson omnibus, Shapiro-Wilk and Kolmogorov-Smirnov test with Dallal-Wikineson-Lillie for P value). Analysis of two group data with normal distribution was performed using paired two-tailed t-tests or un-paired two-tailed t-tests. Data with non-normal distribution were analysed using non-parametric analysis (Mann-Whitney test or Wiconxon test). Pearson tests (data with normal distribution) or Spearman tests (non-normal distribution data) were employed to analyse the correlation between two data groups. A Fisher exact test was used to compare the proportions of different categories in two group of data. P-value < 0.05 was considered statistically significant.

3. RESULTS CHAPTER I: CHEMOATTRACTIVE POTENTIAL OF IBC CELLS

3.1. Introduction

IBC is an aggressive and rare disease with an unfavourable outcome (Robertson FM *et al.*, 2010). A growing number of studies have demonstrated that TIME was involved in the development and progression of IBC, and the immune infiltrates have either pro-tumourigenic or anti-tumourigenic functions. Furthermore, the specific composition of TIME may be viewed as a potential predictor of the outcome of IBC (Lim B *et al.*, 2018; Reddy SM *et al.*, 2019; Bertucci F *et al.*, 2021; Gong Y *et al.*, 2021). Therefore, the investigations of TIME can provide important insights into the aggressive nature of IBC and potential novel targets for IBC treatment. This chapter aimed to examine the chemoattractive potential of IBC cells for PBMCs *in vitro* and to assess the effect of IBC cells on the migration of each subset of PMBCs.

3.2. Medium conditioned by IBC cells (CM-IBC) is chemotactic for PBMCs and B cells

In this study, we assessed the chemoattractive potential of five IBC cell lines: SUM149, BCX010, SUM190, MD-IBC3 and KPL4. Both SUM149 and BCX010 are representatives of the TN-IBC subtype, whereas SUM190, MD-IBC, and KPL4 represent the HER2+ IBC subtype. Mechanistically, PBMCs collected from consented healthy donors were allowed to migrate through 5 μm-pore membranes towards CM-SUM149, CM-BCX010, CM-SUM190, CM-MD-IBC3, and CM-KPL4 or towards the control medium over two time intervals: four hours (short-

term migration) and sixteen hours (sustained migration). Considering that the growth medium of KPL4 cells is different from that of other IBC cell lines, we used two types of growth medium as controls (Ham' F12 and ADF++, are also referred to as F12 + 5% FCS and F12/DMEM + 10% FCS). The migration of all PBMCs was examined, including migration of monocytes (CD14+), CD4+ T cells (CD3+, CD4+), CD8+ T cells (CD3+, CD8+), and B lymphocytes (CD19+) to various CM-IBCs.

In the 4-hour setting, the total numbers of PBMCs migrating towards different CM-IBC were similar to that migrating towards the control medium (Figure 3-1 A). Next, we analysed the migration of monocytes (CD14+ cells), CD4+ T cells, CD8+ T cells and B lymphocytes (CD19+ cells) during the PBMC migration assay. Compared to the control medium, CM-IBC did not significantly affect the chemotactic migration of monocytes (Figure 3-1 B). Similarly, the migration of CD4+ cells (Figure 3-1 C) and CD8+ cells was unaffected (Figure 3-1 D). Interestingly, unlike monocytes and T lymphocytes, B lymphocytes became more migratory when exposed to CM-IBC (Figure 3-1 E). When compared to the control medium, there was a ~ 47-fold increase in the number of B lymphocytes migrating to CM-SUM190 ($p < 0.001$), ~ 55-fold to CM-KPL4 ($p < 0.01$), ~122-fold to CM-MD/IBC3 ($p < 0.001$), 133-fold to ~ CM-BCX010 ($p < 0.01$), and ~181-fold to CM-SUM149 ($p < 0.01$).

In the 16-hour setting, we observed dramatic increases in the numbers of total PBMCs migrating to CM-SUM149 ($p < 0.05$), CM-BCX010 ($p < 0.05$), CM-SUM190 ($p < 0.05$), CM-

MD-IBC3 ($p < 0.05$) and CM-KPL4 ($p = 0.056$) compared to control medium (Figure 3-2 A). However, the migration of monocytes towards CM-IBC was affected in a cell line–dependent manner. While CM-BCX010 increased the monocyte migration, CM-SUM149, CM-SUM190, CM-MD-IBC3 and CM-KPL4 had no such effect (Figure 3-2B). As for lymphocytes, none of the CM-IBC was chemotactic for CD4+ or CD8+ T cells (Figure 3-2 C, D). In contrast, CM-IBC remained chemotactic for B cells, similar to the 4-hour setting results. Compared to the control medium, there was a ~ 5-fold increase in the number of B lymphocytes migrating to CM-BCX010 ($p < 0.05$), ~ 13-fold to CM-SUM190 ($p < 0.001$), ~ 14-fold to CM-SUM149 ($p < 0.001$), ~ 22-fold to CM-MD/IBC3 ($p < 0.001$), and ~ 44-fold to CM- KPL4 ($p < 0.0001$) (Figure 3-2 E).

Taken together, we observed a selective effect of CM-IBC on the migration of immune cells. Compared to monocytes and T cells, B cells became more migratory when exposed to the CM-IBC.

A

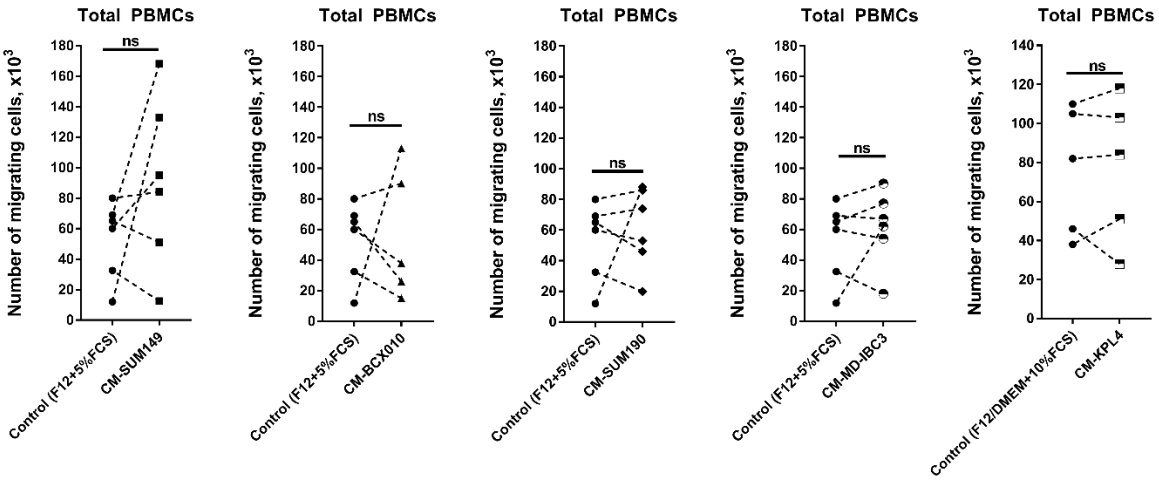
Total PBMCs
Number of migrating cells, x10^3
ns
Control (F12+5%FCS)
CM-SUM149
Total PBMCs
Number of migrating cells, x10^3
ns
Control (F12+5%FCS)
CM-BCX010
Total PBMCs
Number of migrating cells, x10^3
ns
Control (F12+5%FCS)
CM-SUM190
Total PBMCs
Number of migrating cells, x10^3
ns
Control (F12+5%FCS)
CM-MD-IBC3
Total PBMCs
Number of migrating cells, x10^3
ns
Control (F12/DMEM+10%FCS)
CM-KPL4

B

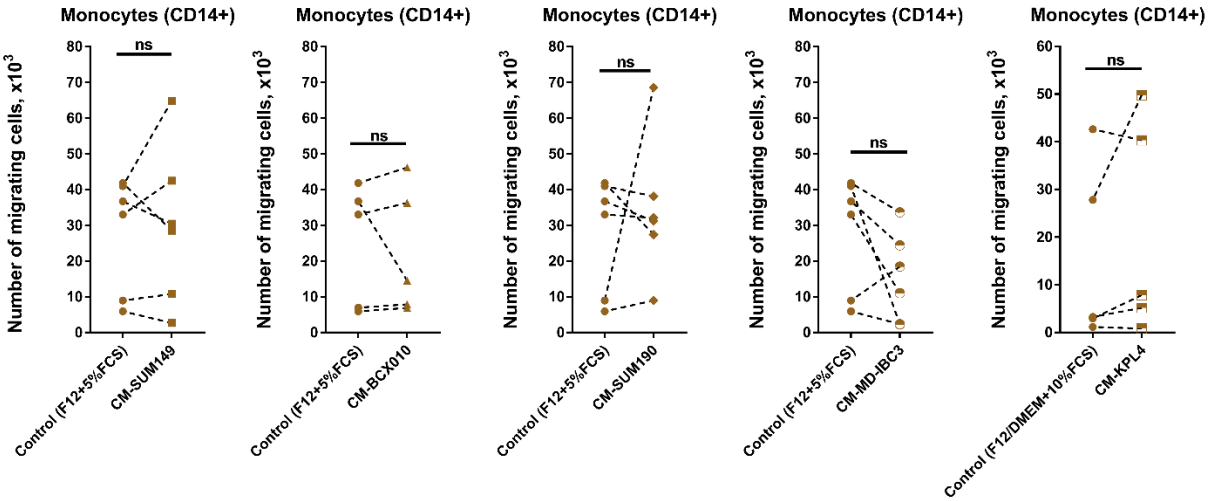
Monocytes (CD14+)
Number of migrating cells, x10^3
ns
Control (F12+5%FCS)
CM-SUM149
Monocytes (CD14+)
Number of migrating cells, x10^3
ns
Control (F12+5%FCS)
CM-BCX010
Monocytes (CD14+)
Number of migrating cells, x10^3
ns
Control (F12+5%FCS)
CM-SUM190
Monocytes (CD14+)
Number of migrating cells, x10^3
ns
Control (F12+5%FCS)
CM-MD-IBC3
Monocytes (CD14+)
Number of migrating cells, x10^3
ns
Control (F12/DMEM+10%FCS)
CM-KPL4

C

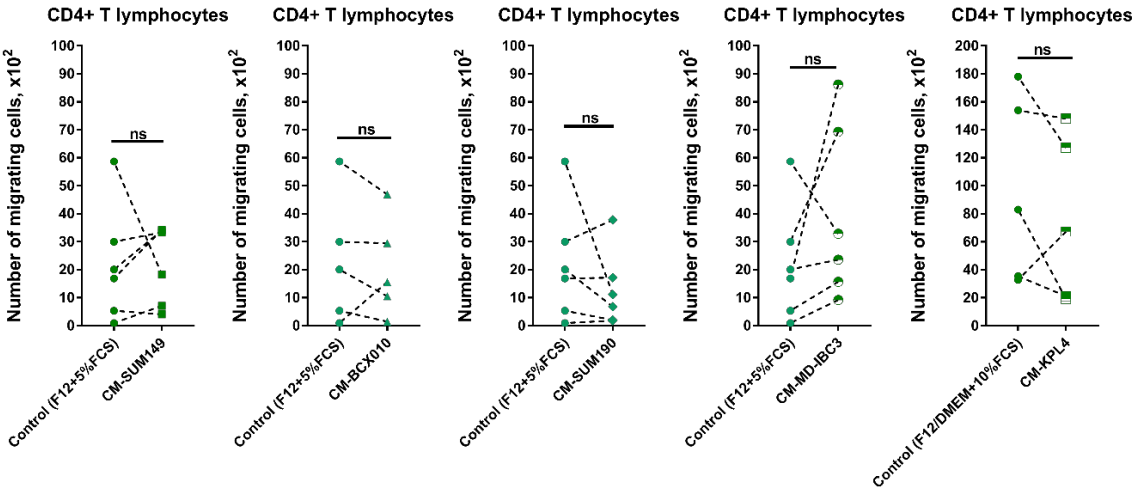
CD4+ T lymphocytes
Number of migrating cells, x10²
ns
Control (F12+5%FCS)
CM-SUM149
CD4+ T lymphocytes
Number of migrating cells, x10²
ns
Control (F12+5%FCS)
CM-BCX010
CD4+ T lymphocytes
Number of migrating cells, x10²
ns
Control (F12+5%FCS)
CM-SUM190
CD4+ T lymphocytes
Number of migrating cells, x10²
ns
Control (F12+5%FCS)
CM-MD-IBC3
CD4+ T lymphocytes
Number of migrating cells, x10²
ns
Control (F12/DMEM+10%FCS)
CM-KPL4

D

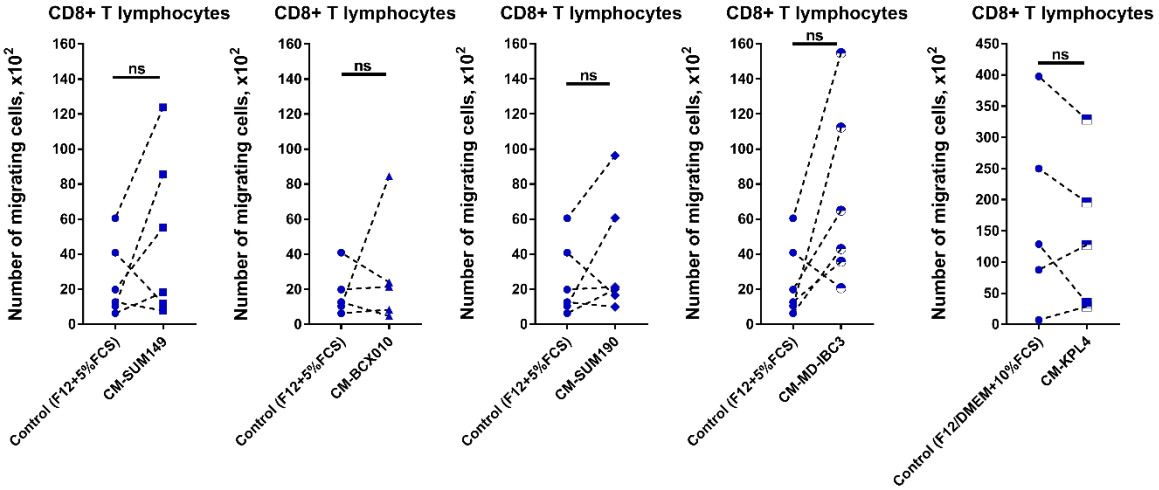
CD8+ T lymphocytes
Number of migrating cells, x10²
ns
Control (F12+5%FCS)
CM-SUM149
CD8+ T lymphocytes
Number of migrating cells, x10²
ns
Control (F12+5%FCS)
CM-BCX010
CD8+ T lymphocytes
Number of migrating cells, x10²
ns
Control (F12+5%FCS)
CM-SUM190
CD8+ T lymphocytes
Number of migrating cells, x10²
ns
Control (F12+5%FCS)
CM-MD-IBC3
CD8+ T lymphocytes
Number of migrating cells, x10²
ns
Control (F12/DMEM+10%FCS)
CM-KPL4

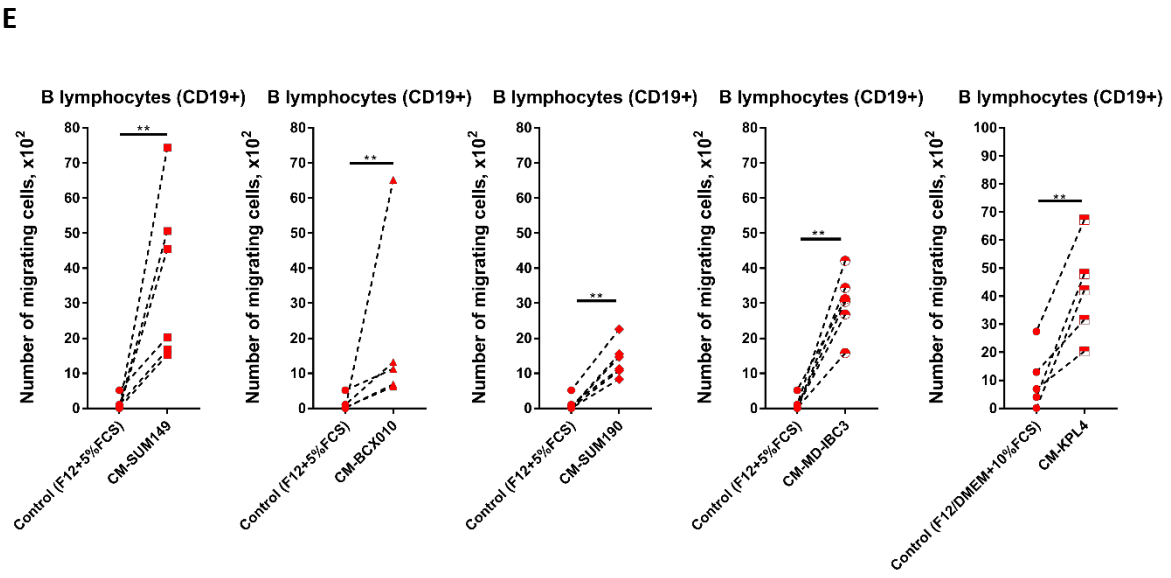

Figure 3-1. Chemoattractive potential of IBC (4-hour setting). (A-E) The short-term migration of total PBMCs (A), monocytes (B), CD4+ T cells (C), CD8+ T cells (D), and B cells (E) to each CM-IBC. A panel of IBC cell lines (SUM149, BCX010, SUM190, MD-IBC3 and KPL4) were adopted to evaluate their chemoattractive potential for PBMCs. PBMCs were collected from 5-6 healthy donors. PBMCs ($2x10^6$ cells/200 μl) were allowed to migrate to CM-SUM149, CM-BCX010, CM-SUM190, CM-MD-IBC3, CM-KPL4, and control medium (F12+5% FCS or F12/DMEM+10% FCS) for 4 hours. Each dot in the graph represents the total number of migrating cells in an individual trans-well assay. P values were calculated using a two-tailed t-test (normal distribution data) or Mann-Whitney test (non-normal distribution data). The significance of P value is indicated on the graph, *p<0.05, **p<0.01, ***p<0.001.

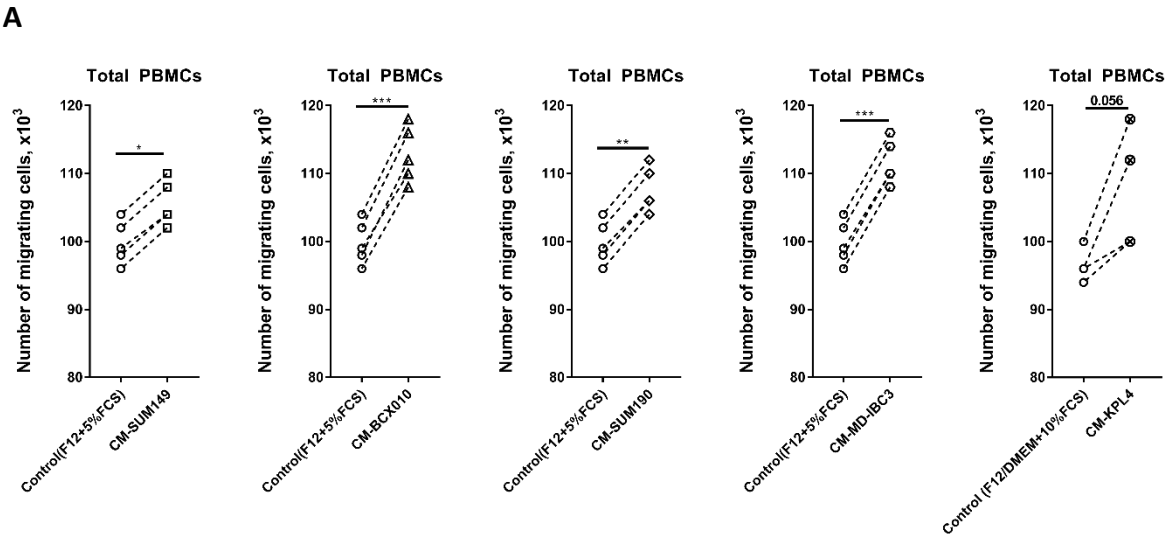

B

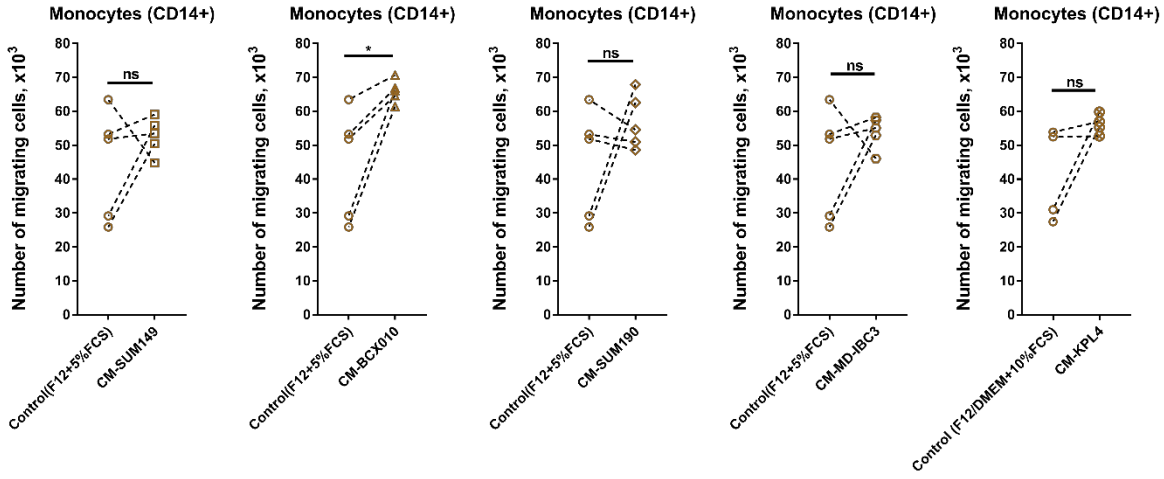
Monocytes (CD14+)
Number of migrating cells, x10³
ns
Control(F12+5%FCS)
CM-SUM149
Monocytes (CD14+)
Number of migrating cells, x10³
*
Control(F12+5%FCS)
CM-BCX010
Monocytes (CD14+)
Number of migrating cells, x10³
ns
Control(F12+5%FCS)
CM-SUM190
Monocytes (CD14+)
Number of migrating cells, x10³
ns
Control(F12+5%FCS)
CM-MD-IBC3
Monocytes (CD14+)
Number of migrating cells, x10³
ns
Control (F12/DMEM+10%FCS)
CM-KPL4

C

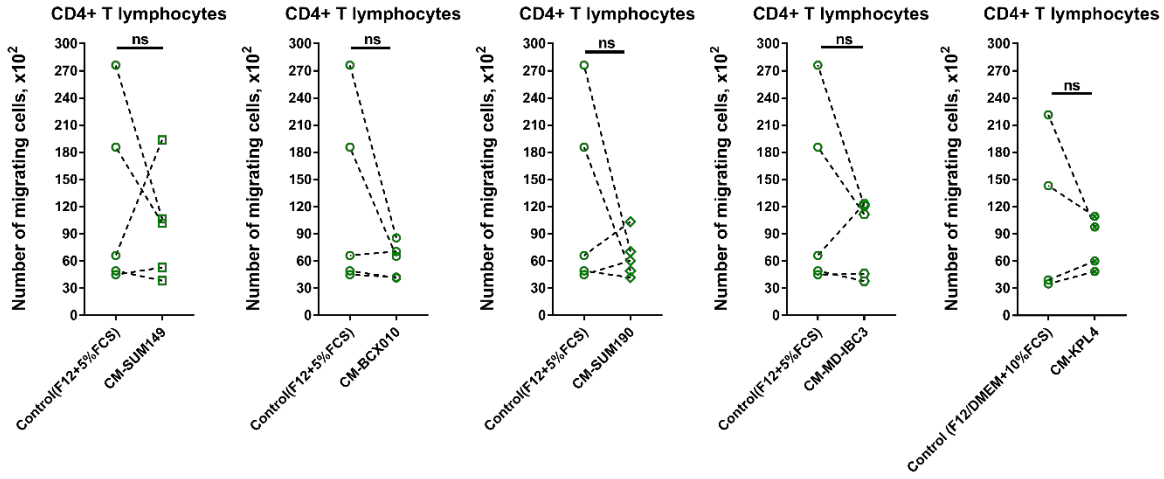
CD4+ T lymphocytes
Number of migrating cells, x10²
ns
Control(F12+5%FCS)
CM-SUM149
CD4+ T lymphocytes
Number of migrating cells, x10²
ns
Control(F12+5%FCS)
CM-BCX010
CD4+ T lymphocytes
Number of migrating cells, x10²
ns
Control(F12+5%FCS)
CM-SUM190
CD4+ T lymphocytes
Number of migrating cells, x10²
ns
Control(F12+5%FCS)
CM-MD-IBC3
CD4+ T lymphocytes
Number of migrating cells, x10²
ns
Control (F12/DMEM+10%FCS)
CM-KPL4

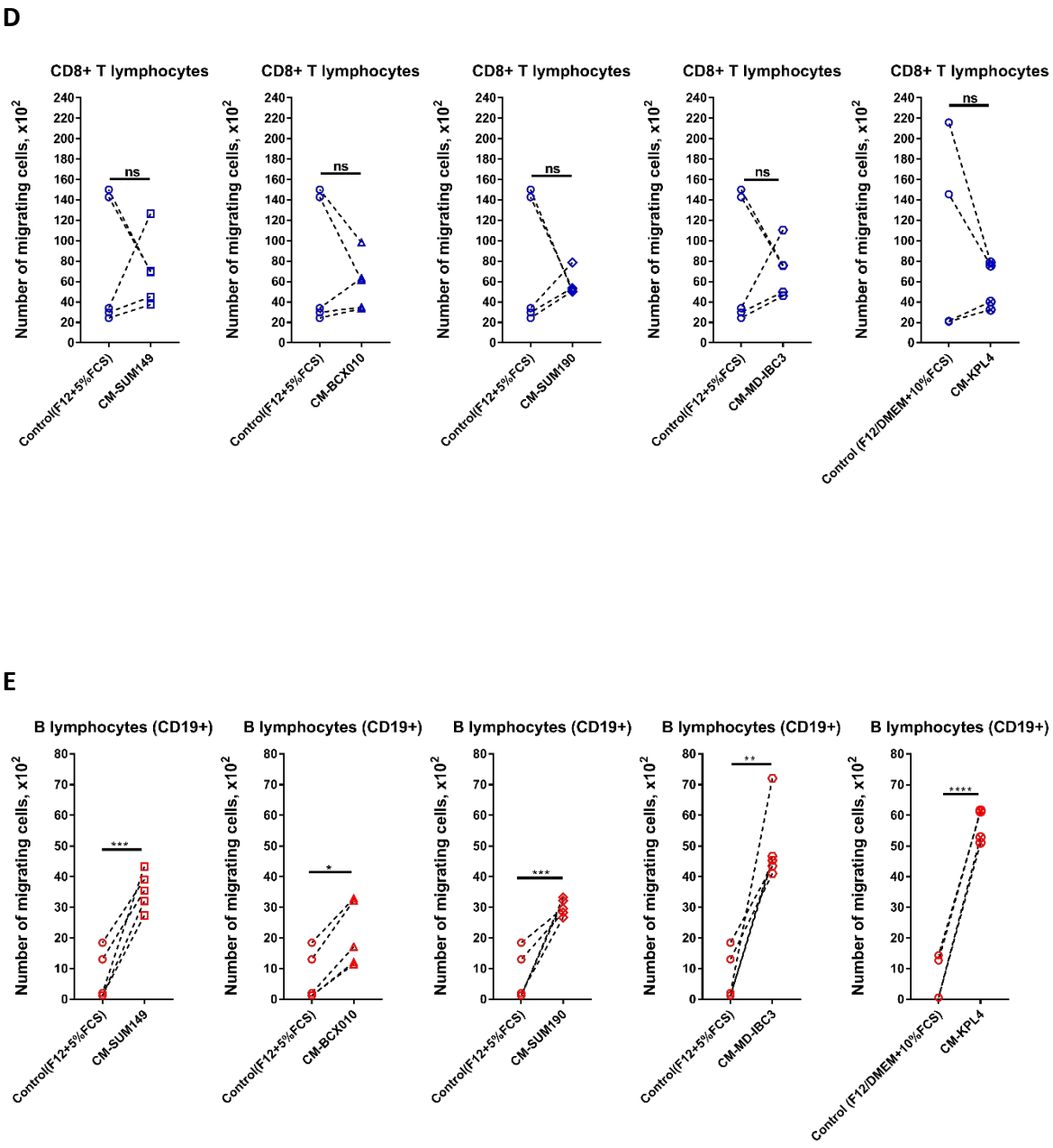

Figure 3-2. Chemoattractive potential of IBC (16-hour setting). (A-E) The sustained migration of total PBMCs (A), monocytes (B), CD4+ T cells (C), CD8+ T cells (D), and B cells (E) to each CM-IBC and control medium (F12+5% FCS). PMBC migration assays were performed as described in Figure 3-1, but for 16 hours. Shown are results of experiments using PBMCs from 4-5 donors. Each dot in the graph represents the total number of migrating cells in an individual trans-well assay. P values were calculated using a two-tailed t-test (normal distribution data) or Mann-Whitney test (non-normal distribution data). The significance of P value is indicated on the graph, *p<0.05, **p<0.01, ***p<0.001.

3.3. Discussion

Accumulating evidence highlights the complexity of TIME, which is controlled at multiple levels, ranging from genetic modulations to intercellular interactions (Plitas G *et al.*, 2016; SE Stanton MLD, 2016; RD Bense CS, 2017; Zhang X *et al.*, 2017; N Linde MC and Sosa MS, 2018; S Garaud LB and C Solinas CG, 2019; Gong Y *et al.*, 2021; Wang Y *et al.*, 2021). Recruitment of immune cells to the cancerous tissues is an important aspect of this process. In our study, we performed standard trans-well migration assays using CM generated by a panel of IBC cells to explore how cancer cells contribute to this. Some studies have shown that the TNBC and HER2+ subtypes are more common in IBC than in non-IBC (Mullooly M *et al.*, 2017; Copson E *et al.*, 2018; Kupstas AR *et al.*, 2020; Mesa-Eguiagaray I *et al.*, 2020), and both of these two subtypes are more immunogenic than the hormone receptor-positive (HR+) subtype (Stanton SE, Adams S and Disis ML, 2016). Therefore, we selected TN-IBC and HER2+ IBC cell lines as representatives to evaluate the chemoattractive potential of IBC for immune cells. We observed a variety of migratory responses of immune cells to different CM-IBC. Interestingly, the most robust and consistent responses were seen for B cells.

A growing number of studies indicate that breast cancer cells may produce and release chemotactic factors into the extracellular environment to induce the chemotaxis of immune cells. For example, the CM of MDA-MB-231 cells overexpressing interferon regulatory factor 5 (a critical immune regulator) was chemotactic for T and B cells, because this CM contained a high concentration of CXCL13 which stimulate the chemotaxis of B cells and a subset of T

cells by binding the CXCR5 (Pimenta EM *et al.*, 2015). Similarly, the CM of TM40D cells (a mammary tumour cell line) triggered the migration of Tregs via COX-2-dependent PGE2 production (Karavitis J *et al.*, 2012). Extracellular stress may also induce chemotactic factor production by tumour cells. For example, radiotherapy induces the apyrase-sensitive nucleotide secretion of breast cancer cells, leading to a marked increase in monocyte recruitment (Hennel R *et al.*, 2014). As for IBC cells, one previous finding from our laboratory demonstrated that CM-BCX010 was chemotactic for monocytes (Hayward S *et al.*, 2020), which was also observed in our present study. The chemotactic effect of CM-BCX010 was mediated by midkine associated with EVs (Hayward S *et al.*, 2020).

However, no published data is available on the chemoattractive potential of IBC for B cells. Here, our results indicate a robust and prominent effect of IBC cells on B cell migration. This finding is supported by some pathological evidence that IBC tissues are characterised by an abundance of B cell infiltration (Arias-Pulido H *et al.*, 2018; Badr NM *et al.*, 2022). Even compared to non-IBC tissues, IBC tissues also display higher numbers of infiltrating memory B cells ($p < 0.05$) (Bertucci F *et al.*, 2021). Currently, no published studies elucidate the mechanism(s) underlying this phenomenon. Various soluble factors, such as cytokines/chemokines (e.g. CXCL13 and TNF-α) (Pimenta EM *et al.*, 2015; Tan P *et al.*, 2018; Ghods A *et al.*, 2019; Mercogliano MF, Bruni S, Elizalde PV and Schillaci R, 2020; Shaul ME *et al.*, 2021) and bioactive lipids (e.g. sphingosine-1-phosphate (S1P) (Aoyagi T, Nagahashi M, Yamada A and Takabe K, 2012; Sic H *et al.*, 2014) are known to be produced by non-IBC cells

and may potentially contribute to the B cell migration.

Here, we also observed a delayed but significant increase in the number of total PBMCs migrating to CM-IBC (sustained experiments). Two reasons may explain these delayed increases: 1) CM-IBC has a time-dependent chemotactic impact on PBMCs, i.e. the longer the duration of the exposure to CM-IBC, the more PBMCs migrate. Indeed, compared to short-term migration, we did observe some enhancements in the sustained migration of PBMCs to certain CM-IBC (Supplementary Figure 1-1 A). 2) Migration of certain subpopulation(s) was (were) enhanced dramatically during the sustained experiments. We noticed that more monocytes were attracted to CM-IBC during sustained experiments compared to short-term experiments (Supplementary Figure 1-1 B). This observation indicates that a transcription-dependent (16 hours) mechanism, instead of a transcription-independent (4 hours) mechanism, may contribute to monocyte migration. For example, the IL-4-induced transcription factor FoxQ1 is overexpressed by monocytes and enhances the migration of monocytes to CCL2 (a typical chemokine for monocyte chemotaxis) (Ovsiy I *et al.*, 2017). Mechanistically, the FoxQ1 expression was elevated in monocytes as early as 3 hours after they were exposed to IL-4, and this expression increased dramatically between 6 and 25 hours. At the genetic level, elevated expression of FoxQ1 was associated with increased expression of CCR2 (receptor for CCL2) and also with reduced expression of genes that negatively regulate cell migration (e.g. claudin 11 and plexin C1) (Ovsiy I *et al.*, 2017). Therefore, in our case, an RNAseq on 4h vs 16 migrating monocytes may provide some clues for us. In addition to monocytes, other immune

cells, such as NK cells, may also migrate during the late stage. Although we did not evaluate the migration of NK cells here, we could not rule out their contribution to the overall increase in PBMC migration.

To determine whether a time-dependent impact of CM-IBC on B cell migration, we compared the absolute numbers of migrating B cells under two different time experimental settings (4 and 16 hours). Surprisingly, the absolute numbers of migrating B cells to CM-SUM149, CM-BCX010, and CM-KPL4 did not significantly increase after 16 hours (Supplementary Figure 1-1 E). This finding suggests that CM-IBC-induced B cell migration occurs mainly in the early stage, thus the first four hours appeared to be a critical period for B cell migration.

In summary, we uncovered a B cell-targeted chemoattractive potential of IBC cells. CM-IBC has a rapid and long-lasting effect on B cell migration. More research on the mechanism behind the early chemotactic effect of CM-IBC on B cells is needed.

4. RESULTS CHAPTER II: B LYMPHOCYTES AND IBC

4.1. Introduction

We have demonstrated that the CM produced by different IBC cell lines had consistent chemotactic effects on B cells. To date, many biologically active molecules produced by tumour cells have been identified to mediate the chemotaxis of immune cells, such as cytokines/chemokines (Berraondo P *et al.*, 2019; Ozga AJ, Chow MT and Luster AD, 2021; Kohli K, Pillarisetty VG and Kim TS, 2022), growth factors (Lynn KD, Roland CL and Brekken RA, 2010; Yang J, Yan J and Liu B, 2018), and bioactive lipids (Raccosta L *et al.*, 2013; Choi C and Finlay DK, 2020). In this chapter, we aimed to assess the involvement of some potential chemotactic factor(s) in regulating the B cell migration towards CM-IBC and examined the contribution of other immune cells in this phenomenon. Specifically, we focused on investigating regulatory mechanisms that control B cell migration within the first four hours from the onset of the experiment.

4.2. Characterising the cytokines/chemokines in CM-IBC

Since chemokines/cytokines are critical players in regulating the chemotaxis of immune cells (Mantovani A *et al.*, 2004), we assessed the expression of some selective soluble chemokines and cytokines in CM-IBC by ELISA. Those chemokines/cytokines are reportedly related to IBC cells or B cell chemotaxis. SUM149 is the most widely-used IBC cell line, and BCX010 has been demonstrated to possess a chemoattractive potential for immune cells (Hayward S *et*

al., 2020). Therefore, we choose SUM149 and BCX010 as representatives. We discovered that only pleiotrophin (PTN) and amphiregulin (Areg) (both are growth factors) were abundantly produced by SUM149 and BCX010 cells (Figure 4-1). Specifically, SUM149 cells produced more than 13000pg/ml of PTN and over 4000pg/ml of Areg, while BCX010 cells secreted more than 5000pg/ml of PTN and approximately 270pg/ml of Areg. However, chemokines/cytokines that involved in B cell chemotaxis, including TNF-α, CXCL-12, CXCl-13 and CCL-20, were virtually undetectable in CM-SUM149 and CM-BCX010. While we cannot exclude the contribution of PTN and Areg to communication between cancer cells and immune cells, we have chosen not to investigate them further in our experimental setup for the following reasons. Firstly, B cells do not express EGFR, the only known receptor for Areg. Secondly, the data from our study (see CHAPTER III) has shown that midkine, a close relative of PTN (the range of receptors for both proteins completely overlap) (Sorrelle N, Dominguez A and Brekken RA, 2017), does not stimulate the migration of B cells. These results suggest that other biological mediators regulate the B cell migration to CM-IBC.

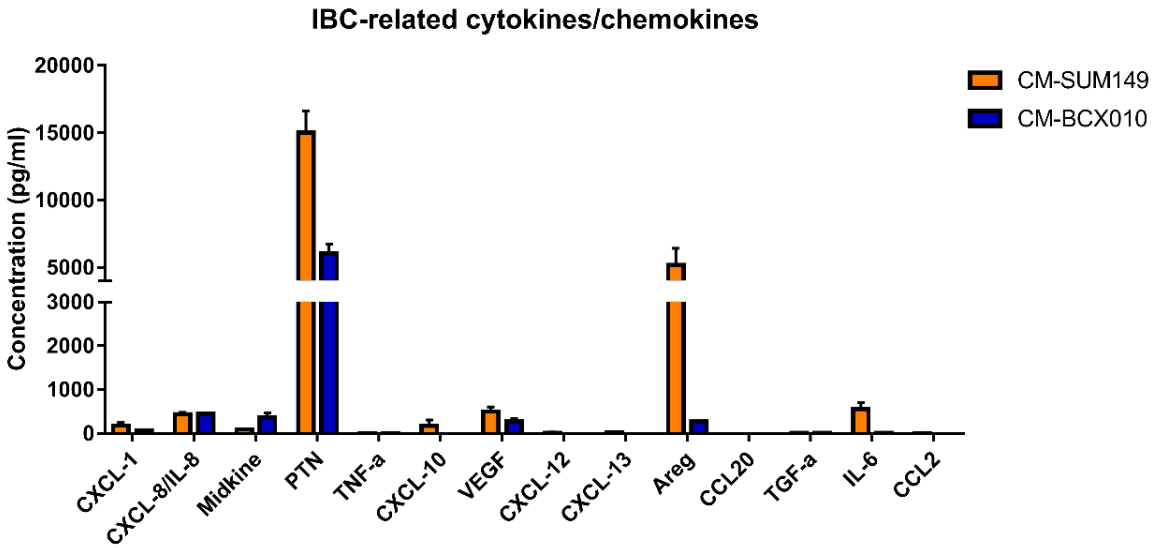

Figure 4-1. Cytokines/chemokines profiles of CM-SUM149 and CM-BCX010. The concentrations of IBC-related or B cells chemotaxis-related cytokines/chemokines in CM-SUM149 and CM-BCX010 were assessed by ELISA. CM has been conditioned for 72 hours before ELISA experiments. Shown are means with SD of the results of 2-3 independent experiments.

4.3. The direct impact of IBC cells on B cell migration

To further investigate the chemoattractive effect of CM-IBC for B cells, we purified B cells by depleting non-B cells using biotin-conjugated antibody cocktails followed by magnetic separation (this process could eliminate the impact of non-B cells on B cells). The chemotactic migration of pure B cells (above 90% purity) to CM-SUM149 and the control medium (F12+5%FCS) was assessed. In the 4-hour setting, there was an ~3.1-fold increase ($p < 0.05$) in the number of migrating pure B lymphocytes to CM-SUM149 compared to the control medium (Figure 4-2 A). Similarly, when migration experiments were carried out over 16 hours, we observed an ~2.4-fold increase in the number of pure B lymphocytes migrating to CM-SUM149 ($p < 0.05$) when compared to control medium (Figure 4-2 B). These findings show that the chemoattractants from IBC cells can directly regulate the B cell migration and this direct modulation starts at the first 4 hours.

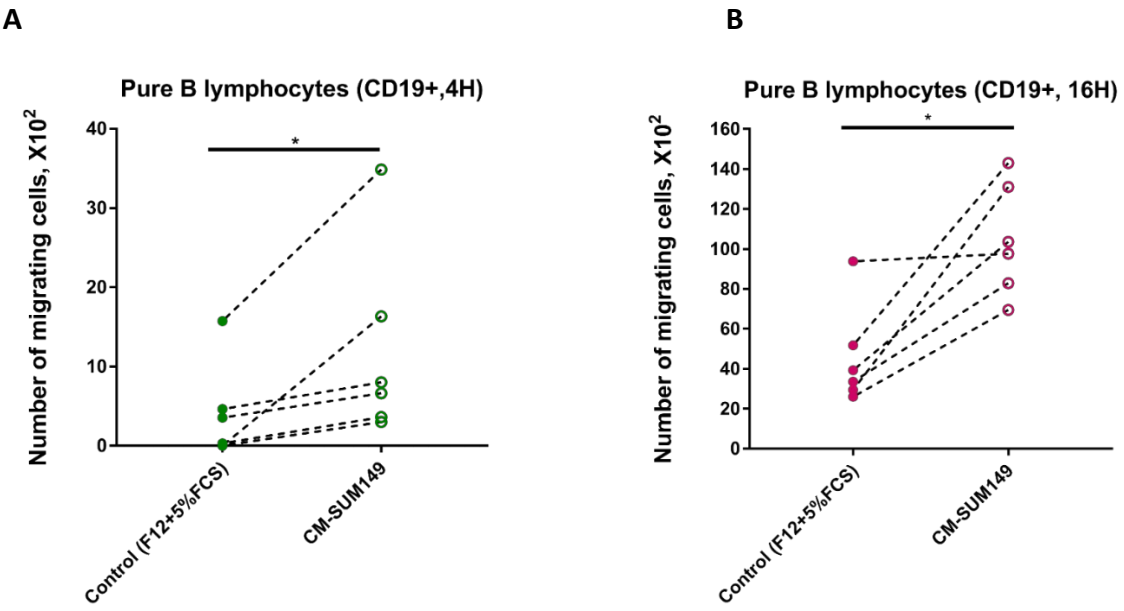

Figure 4-2. The chemoattractive potential of IBC cells for pure B lymphocytes. (A-B) The short-term and sustained migration of pure B cells to CM-SUM149 and control medium. Pure B lymphocytes were purified using biotin-conjugated antibody cocktails followed by magnetic separation. Pure B cells ($2x10^5$ cells/200 µl) were allowed to migrate to CM-SUM149 for 4 hours and 16 hours. The migration of pure B cells to the growth medium (F12+5% FCS) as control. Dots linked together represent a donor-matched comparison. Shown are the results of 6 individual experiments. P values were calculated using a two-tailed t-test (normal distribution data) or Mann-Whitney test (non-normal distribution data). The significance of P value is indicated on the graph, *$p<0.05$.

4.4. The contribution of Pertussis Toxin (PTX)-sensitive factor(s) to pure B cell migration was donor-dependent

Having identified the direct effect of CM-IBC on B cell migration commenced at the first 4 hours, we attempted to elucidate the mechanism underlying this phenomenon. Since most chemotactic factors act via PTX-sensitive GPCRs (Sun L and Ye RD, 2012), we could evaluate the role of GPCR-bound ligands in regulating B cell migration by PTX treatment. Pure B lymphocytes pre-treated with different concentrations of PTX (0, 200, 500 ng/ml) were allowed

to migrate to CM-SUM149 for 4 hours. The results showed that neither low nor high concentrations of PTX (200, 500 ng/ml) significantly impeded B cell migration, though a decreasing trend in B cell migration was observed at high concentration PTX treatment (Figure 4-3). The non-significant effect of PTX may be due to the insufficient number of experimental replicates. Therefore, the role of PTX-sensitive factors in regulating B-cell migration remains to be determined, and more experiments will be required to confirm this.

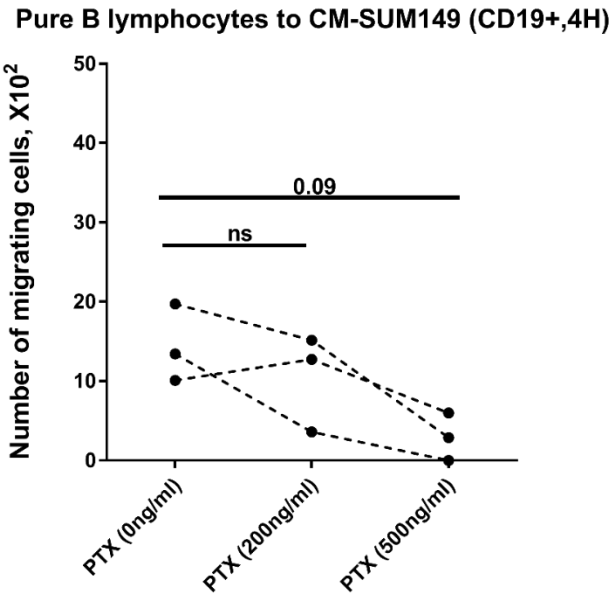

Figure 4-3. The role of PTX-sensitive factors in modulating pure B cell short-term migration remains elusive. Pure B lymphocytes were pre-treated with different concentrations of PTX and allowed to migrate to CM-SUM149 for 4 hours. Pure B cell migration assays were performed as described in Figure 4-3. Each dot shown in the graph represents the total number of migrating pure B cells in an individual trans-well assay. Separate dots connected by a dotted line indicates a donor-matched comparison. Shown are the results of 3 individual experiments. P values were calculated using a two-tailed t-test (normal distribution data) or Mann-Whitney test (non-normal distribution data).

4.5. Non-B cells contribute to the B cell short-term migration to CM-IBC

While determining the direct chemotactic effect of IBC cells on B cells, we questioned if non-B cells could potentially contribute to the B cell short-term migration. To address this question, we compared the migration trends of B cells before and after non-B cell removal. In this instance, PBMCs' B cells refer to B cells before non-B cell depletion, while pure B cells refer to B cells after non-B cell depletion. We found that the number of migrating B cells to CM-SUM149 was reduced by 20% - 90% after non-B cell depletion (Figure 4-4 A). In contrast, the migration of B cells to the control medium was not significantly affected by the absence of non-B cells (Figure 4-4 B). These data strongly suggest that the presence of non-B cells is essential for B cells to migrate towards the CM-IBC at an early stage.

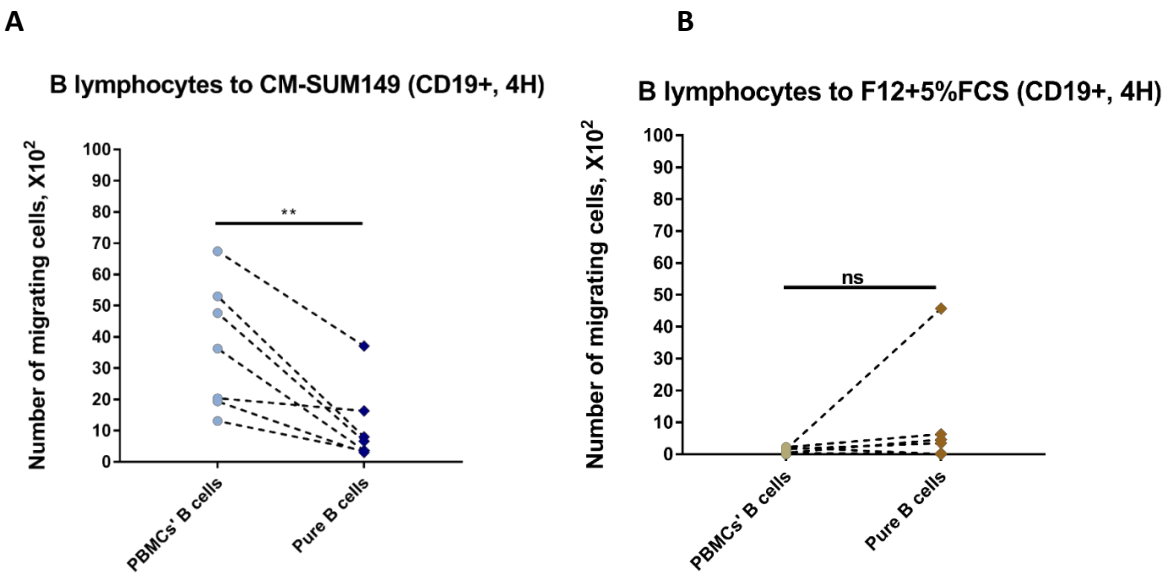

Figure 4-4. Non-B cells are critical for B lymphocyte short-term migration. (A, B) The comparison of B cell migration before and after non-B cell depletion. PBMCs ($2x10^6$ cells/200 µl) and donor-matched pure B lymphocytes ($2x10^5$ cells/200 µl) were allowed to migrate to CM-SUM149 (A) and control medium (F12+5% FCS) (B) for 4 hours. Shown are the results of 7

individual experiments. P values were calculated by a two-tailed t-test and are indicated on the graph, **p<0.01.

4.6. Monocytes potentiate the chemotactic migration of B lymphocytes

Our data suggested that non-B cells in PBMCs may regulate the short-term migration of B cells. However, whether a subpopulation of non-B cells specifically participates in this regulation remains to be determined. We started this investigation by analysing the contribution of monocytes, as macrophages are the most abundant immune infiltrates in IBC tissues (Badr NM *et al.*, 2022), and monocytes/macrophages in the TIME of IBC are characterised by the secretion of various chemokines and cytokines (Rossol M *et al.*, 2011; Mohamed MM *et al.*, 2014; Valeta-Magara A *et al.*, 2019; Hayward S *et al.*, 2020). In addition, we recently found that monocytes became more migratory when exposed to CM-IBC (Hayward S *et al.*, 2020). Thus, we questioned whether monocytes function as intermediates in the communication between IBC cells and B cells. To address this question, we evaluated the B cell migration after monocyte depletion. These experiments showed that the number of B cells migrating to CM-SUM149 decreased by 22% - 75% upon monocyte depletion (Figure 4-5 A). However, monocyte depletion did not significantly affect the migration of B cells towards control medium ($p = 0.06$) (Figure 4-5 B).

To confirm the key role of monocytes in modulating B cell migration, we performed reverse experiments in which we evaluated the change in B cell migration upon monocyte supplementation. As anticipated, the presence of monocytes significantly boosted the migration

of B lymphocytes towards CM-SUM149 (~ 4-fold increase) (Figure 4-5 C). In contrast, monocyte supplementation did not affect B cell migration to the control medium (Figure 4-5 D). Data from "loss and gain" experiments demonstrate that monocytes are essential in conveying the chemotactic effect of IBC cells on B cells.

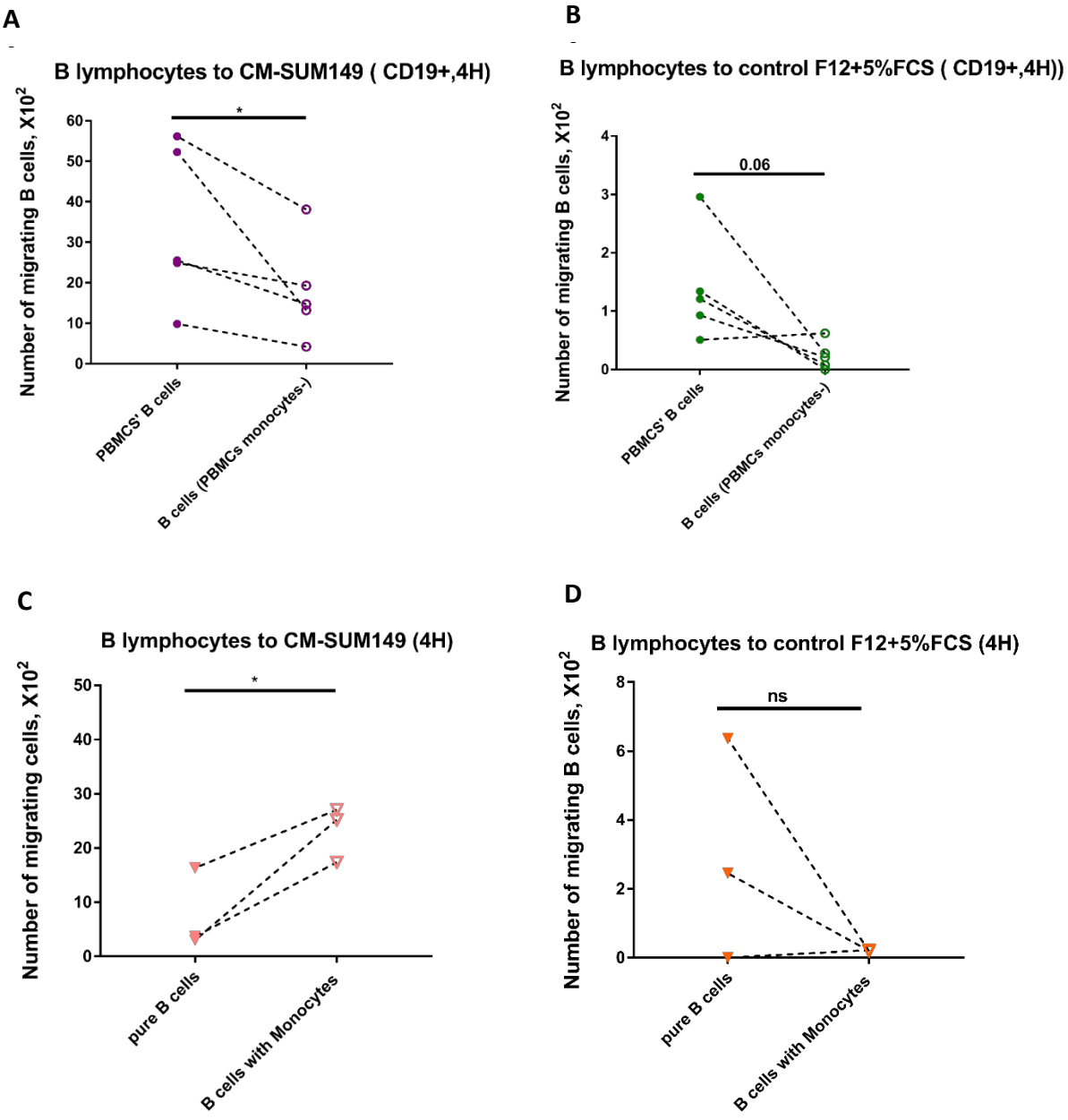

Figure 4-5. Monocytes mediate the migration of B lymphocytes to CM-IBC. (A, B) The absence of monocytes reduced the number of migrating B cells to CM-SUM149. Cells were collected from 5 healthy donors. Monocytes were depleted by using biotin-conjugated antibody cocktails, followed by magnetic separation. The non-monocyte PBMCs ($2x10^6$ cells/200 µl) and donor-matched PBMCs ($2x10^6$ cells/200 µl) were allowed to migrate to CM-SUM149 and control medium (F12+5% FCS) for 4 hours separately. **(C, D)** Monocytes promoted the migration of B lymphocytes to CM-SUM149. Cells were collected from 3 healthy donors. Monocyte purification was performed similarly to B cell isolation but with a monocyte-specific antibody cocktail. The cell mixture of pure B cells and monocytes was allowed to migrate towards CM-SUM149 and the control medium (F12+5% FCS) for 4 hours. Pure B cells under the same conditions were applied as controls. Numbers of B lymphocytes migrating to individual CM with or without monocytes were assessed. Dots linked together represent a donor-matched comparison. P values were calculated using a two-tailed t-test (normal distribution data) or Mann-Whitney test (non-normal distribution data). The significance of P value is indicated on the graph, *$p<0.05$.

4.7. Discussion

To date, no published studies have elucidated the mechanism of B cell infiltration into IBC tissues. Here, we sought to examine one of the possible pathways underlying the accumulation of B cells in cancerous tissues in IBC. As the B cell chemotactic migration commenced at the first hours in our study, we specifically investigated how IBC cells regulate the short-term migration (i.e. migration over 4 hours) of B cells.

We initially observed a chemotactic effect of IBC cells on pure B cell migration, which suggests a direct stimulation of CM-IBC to B cell motility. To determine the chemoattractant(s) responsible for this migration, we inhibited GPCRs on B cells by PTX, which was expected to suppress GPCR-bound ligand(s)-mediated migration of pure B cells. Basically, we did not

observe a PTX-dependent decline in pure B cell migration to CM-SUM149 (Although there was a tendency for B cell migration to decrease in the PTX high concentration group). Additional repetitions and higher PTX concentration treatment are required to confirm the contribution of PTX-sensitive factor(s) to pure B cell recruitment to CM-IBC. In parallel, one cannot exclude the involvement of non-GPCR–dependent pathways. For example, macrophage migration inhibitory factor (MIF) was reported to exert its chemokine-like effect on B cells by binding with CD74 (HLA class II histocompatibility antigen gamma chain) (Calandra T and Roger T, 2003). Knockdown of CD74 completely abrogated the MIF-induced B cell recruitment *in vivo* (Klasen C *et al.*, 2014). Interestingly, CXCR4 (the receptor for CXCL12) was shown to be an alternative receptor for MIF, and inhibition of CXCR4 also significantly reduced the chemotaxis of B cells. The authors, therefore, proposed a cooperation model of CD74 and CXCR4, a non-CPCR and a GPCR, for MIF-induced migration of B cells (Klasen C *et al.*, 2014). To be noted, both breast cancer cell lines and human breast cancer tissues express MIF (Calandra T and Roger T, 2003; Xu X *et al.*, 2008; Richard V, Kindt N and Saussez S, 2015).

In addition to the direct effect of CM-IBC on B cell migration, we next showed that monocytes, as the precursors of macrophages, mediated the chemotactic effect of IBC cells on B cells. It has been demonstrated that monocytes/macrophages collected from the axillary tributaries of IBC patients secret a diverse range of cytokines and chemokines (Mohamed MM *et al.*, 2014), including TNF-α, a known promigratory factor for B cells (Ghods A *et al.*, 2019; Mercogliano

MF, Bruni S, Elizalde PV and Schillaci R, 2020; Shaul ME *et al.*, 2021). Furthermore, it was suggested that monocytes might possess the potential to modulate immune cell chemotaxis indirectly (Badr G *et al.*, 2005; Hansmann L *et al.*, 2008; Lourda M *et al.*, 2014; Ferretti E, Ponzoni M, Doglioni C and Pistoia V, 2016). For instance, peripheral monocytes are one of the principal producers of IFNα (Hansmann L *et al.*, 2008). IFNα downregulates the ligand-induced internalisation of receptors of CCL20, CCL2 and CXCL12 on B cells and upregulates the activation of these ligand-induced signalling pathways (ERK1/2, PI3K/AKT and IκBα) (Badr G *et al.*, 2005), which may enhance the chemotaxis of B cells.

Though we did not further investigate how monocytes enhance the migration of B cells, there is no doubt that monocytes' behaviour is altered when exposed to CM-IBC (Hayward S *et al.*, 2020). A previous finding from our laboratory demonstrated that IBC-produced midkine (a heparin-binding growth factor involved in monocyte chemotaxis) strengthened the chemoattractive potential of IBC cells for monocytes (Hayward S *et al.*, 2020). Of interest, in that study, increased expression of CD151, a well-studied tetraspanin, in IBC cells correlated with greater secretion of midkine. This inspired us whether a specific tetraspanin could regulate monocytes and ultimately enhance the chemotactic migration of B cells. Indeed, clinicopathological data from our lab showed that Tspan6 expression in IBC was positively correlated with B cell infiltration (Unpublished data, Supplementary Figure 1-3 C). More importantly, the co-existence of macrophages and B cells was associated with Tspan6 positivity in IBC tissues (Unpublished data, Supplementary Figure 1-3 D).

In general, we preliminarily investigated the mechanism(s) underlying the migration of B cells to CM-IBC and found that monocytes mediated this migration. However, the intrinsic mechanism in IBC regulating the B cell recruitment remained unclear. Molecules expressed by IBC cells, such as Tspan6, may provide new clues for us to explore this filed.

5. RESULTS CHAPTER III: TSPAN6 IN IBC

5.1. Introduction

It was reported that tetraspanins are involved in regulating the tumour microenvironment (Claas C *et al.*, 1998; Detchokul S, Williams ED, Parker MW and Frauman AG, 2014; Sadej R *et al.*, 2014; El Kharbili M *et al.*, 2017; Lu J *et al.*, 2017; Yan W, Huang J, Zhang Q and Zhang J, 2021). As previous data suggested that Tspan6 implicated in B cell infiltration in IBC tissues (unpublished data, Supplementary Figure 1-4) and another finding from our lab demonstrated that CM of non-IBC cells expressing Tspan6 also has chemotactic effect on B cells (unpublished data). Therefore, in this chapter, we examined whether tetraspanins, especially Tspan6, could regulate IBC's chemoattractive potential for B lymphocytes. The influence of Tsapn6 on proliferation and morphology of IBC cells was also assessed.

5.2. Tspan6 promotes the chemoattractive potential of SUM149 for T and B cells

To examine whether the expression of Tspan6 increases the chemoattractive potential of IBC cells, we generated SUM149/Tspan6 cell line. In addition, we established SUM149-based cell lines expressing four other tetraspanins - whose expression has been previously linked with breast cancer – Tspan13, CD63, CD82 and CD151. We also introduced Tspan4 into SUM149 cells. Although there is no published report on the involvement of Tspan4 in the development of breast cancer, this tetraspanin was shown to play a vital role in the formation of "migrosomes" (cellular organelles that form as large vesicle-like structures on retraction fibres of migrating

cells) by breast cancer cells, which may be involved in "relaying spatiotemporal chemical information for cell-cell communication" (Huang Y *et al.*, 2019). SUM149 cells are best suited for the initial screening experiments as they express low endogenous levels of these tetraspanins. All tetraspanins were 3'GFP-tagged to monitor their stable expression in SUM149 cells. We have also generated the control SUM149 cell line expressing GFP – SUM149/GFP. The migration of B lymphocytes towards CM-SUM149/GFP-Tspan4, CM-SUM149/GFP-Tspan6, SUM149/GFP-Tspan13, CM-SUM149/GFP-CD63, CM-SUM149/GFP-CD82, CM-SUM149/GFP-CD151 and CM-SUM149/GFP was assessed using the "short-term migration" (4h) setting. As anticipated, only Tspan6 significantly promoted the chemoattractive potential of SUM149 cells for B lymphocytes (Figure 5-1 D). In parallel, CM-SUM149/GFP-Tspan6 enhanced the CD4+ and CD8+ T cell migration (Figure 5-1 B, C). Interestingly, in contrast to CD151, expression of Tspan6 had no impact on the chemoattractive potential of SUM149 cells for monocytes (Figure 5-1 A).

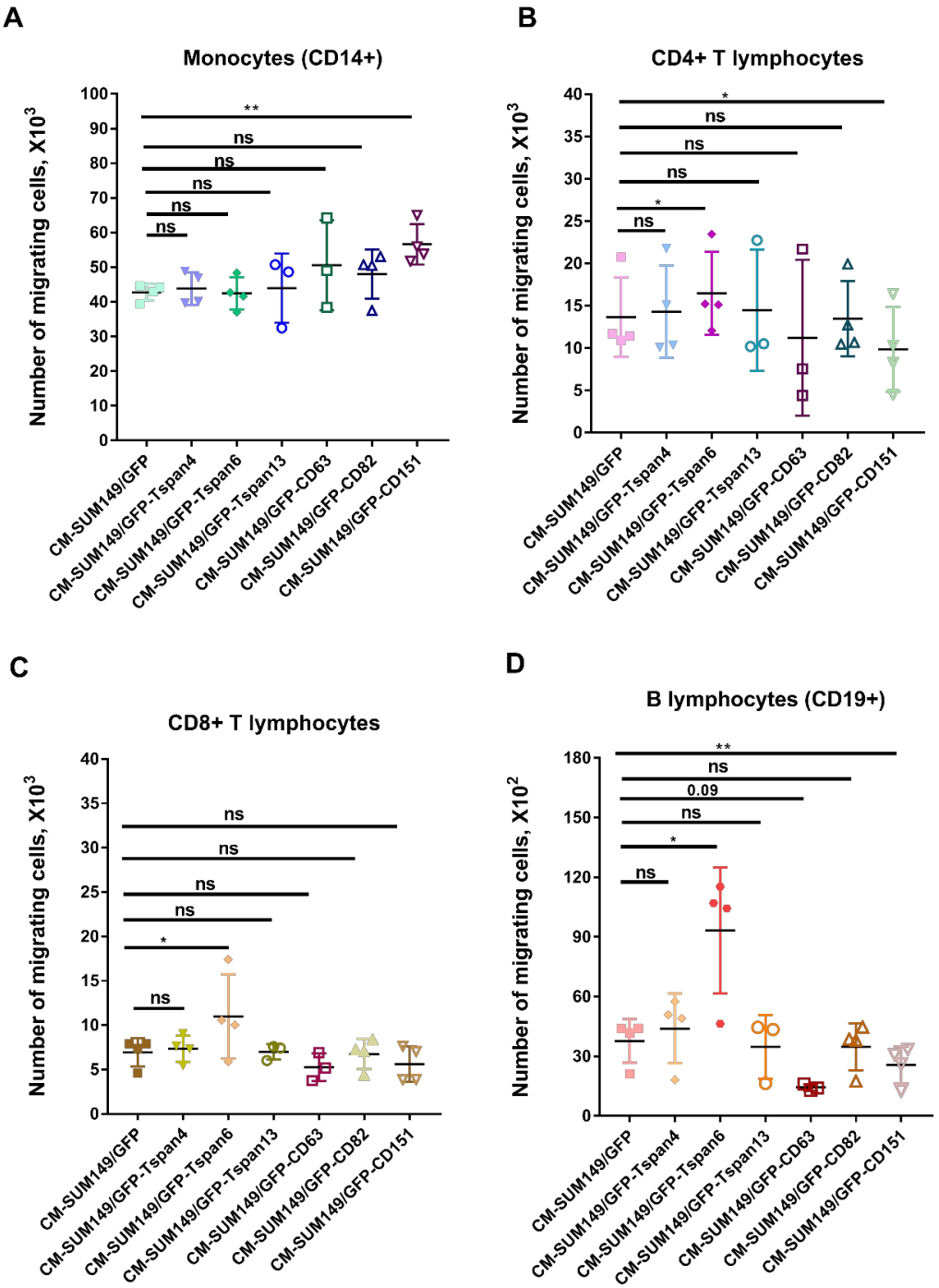

Figure 5-1. The chemoattractive potential of SUM149 is upregulated by the expression of Tspan6. (A-D) The impact of different tetraspanins on the short-term migration of distinct immune subpopulations. A panel of tetraspanins was introduced to SUM149 cells with a lentivirus gene transduction method to establish SUM149/GFP-Tspan4, SUM149/GFP-Tspan6, SUM149/GFP-Tspan13, SUM149/GFP-CD63, SUM149/GFP-CD82, SUM149/GFP-CD151. PBMCs ($2x10^6$ cells/200 µl) were allowed to migrate to CM from these SUM149/tetraspanin cells for 4 hours. Migration of monocytes (A), CD4+ T cells (B), CD8+ T cells (C) and B

lymphocytes (D) to each CM-SUM149/tetraspanin was evaluated. CM-SUM149/GFP was applied as a control. Shown are results of experiments using PBMCs from 4 donors. Each dot in the graph represents the total number of migrating cells in an individual trans-well assay. P values were calculated using a two-tailed t-test (normal distribution data) or Mann-Whitney test (non-normal distribution data). The significance of P value is indicated on the graph, *p<0.05, **p<0.01.

5.3. Establishment of IBC cellular models expressing Tspan6

To further evaluate the effect of Tspan6 on the chemoattractive potential of IBC cells, we established two more IBC cell models stably expressing Flag-tagged Tspan6: SUM149/Tspan6 and BCX010/Tspan6. Similar to SUM149, BCX010 cells express low levels of endogenous Tspan6. Corresponding control cells (SUM149/pLVx and BCX010/pLVx cells) were established by transducing these cells with empty vectors (pLVx-puro, non-flag-tagged). Stable expression of Tspan6 in SUM149/Tspan6 and BCX010/Tspan6 cells was detected by western blot using anti-human Tspan6 polyclonal rabbit (Figure 5-2 A). The plasma membrane expression of Tspan6 was evaluated by flow cytometry using in-house generated mouse serum containing antibody against Tspan6. Peaks of SUM149/Tspan6 and SUM149/pLVx were discrete (Figure 5-2 B), as were the peaks of BCX010/Tspan6 and BCX010/pLVx (Figure 5-2 C). Taken together, we successfully established IBC cellular models expressing Tspan6.

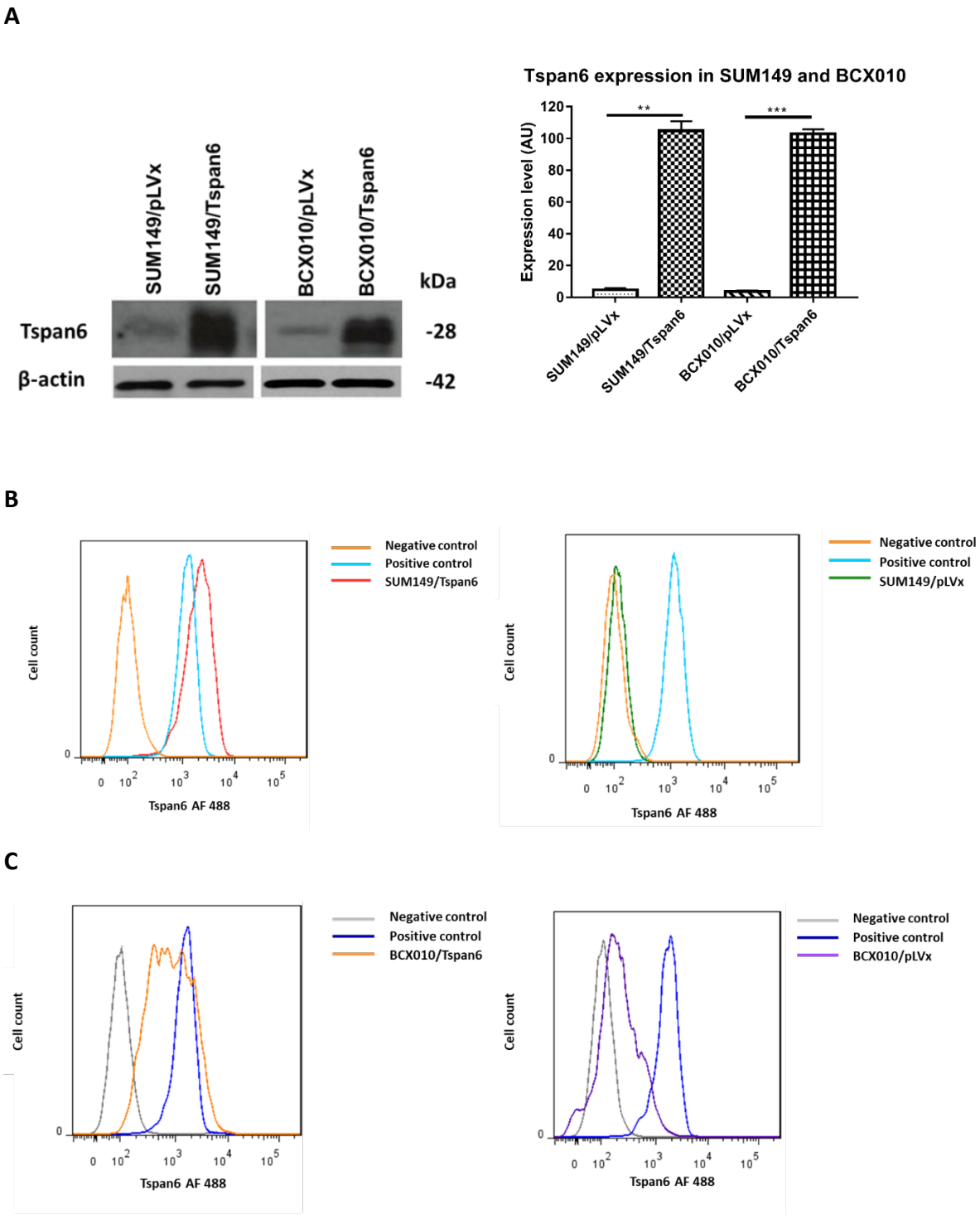

Figure 5-2. Transduced IBC cells strongly and stably express Tspan6. (A) Expression of Tspan6 in SUM149 and BCX010 cells. Tspan6 was detected by western blot with polyclonal antibody against Tspan6. The level of Tspan6 expression was normalised to β-actin expression. SUM149 and BCX010 were transduced with lentiviral plasmids containing flag-Tspan6 (pLVx-Flag-Tspan6) or empty vector (pLVx-puro). Untransduced cells were eliminated by puromycin (2 µg/ml) selection for 14 days. Shown are means with SD of the results of 3 independent

experiments. **(B, C)** Tspan6 expression was assessed by FACS. Tspan6 was detected with an in-house generated mouse antibody against Tspan6. Ab M38 (Anti-CD81) and Ab 4C5G (anti-Type II PI 4-kinase) were applied as positive and negative controls. P values were calculated using a two-tailed t-test and are indicated on the graph, *p<0.05, **p<0.01.

5.4. Characterisation of SUM149/Tspan6 and BCX010/Tspan6 cell lines

To evaluate the distribution of exogenous Tspan6 in IBC cell models, we performed immunofluorescence to visualise FLAG-tagged Tspan6 in SUM149/Tspan6 and BCX010/Tspan6 using mouse anti-FLAG mAb. While Tspan6 was mainly located on the plasma membrane in both SUM149/Tspan6 and BCX010/Tspan6 cell lines, we also detected weak punctate staining in the cytoplasm (Figure 5-3 A and B). As expected, only some non-specific staining was seen in SUM149/pLVx and BCX010/pLVx cells (Figure 5-3 A and B).

Next, we assessed the impact of Tspan6 expression on the IBC cell proliferation by performing BrdU proliferation assays. IBC cells were plated at different cell densities and cultured for 24 and 72 hours. The results demonstrated that the proliferation of SUM149/Tspan6 and BCX010/Tspan6 was comparable to that of SUM149/pLVx and BCX010/pLVx, respectively (Figure 5-3 C).

We also examined whether Tspan6 expression affected the morphological appearance of cells cultured in a 3-dimensional extracellular matrix (3D-ECM). These experiments demonstrated that both SUM149/Tspan6 and SUM149/pLVx cells formed compact round colonies with no apparent difference in the size of SUM149/Tspan6 and SUM149/pLVx colonies (Figure 5-3 D

top panel, Figure 5-3 E). Similarly, the morphology of BCX010 colonies was not affected by the expression of Tspan6 (Figure 5-3 D middle and bottom panels). Intriguingly, regardless of Tspan6 expression, both BCX010/Tspan6 and BCX010/pLVx colonies displayed two distinct morphologies; scattered colonies (Figure 5-3 D middle panel) and irregular compact colonies (Figure 5-3 D bottom panel), indicating the intrinsic heterogeneity of BCX010 cells.

A

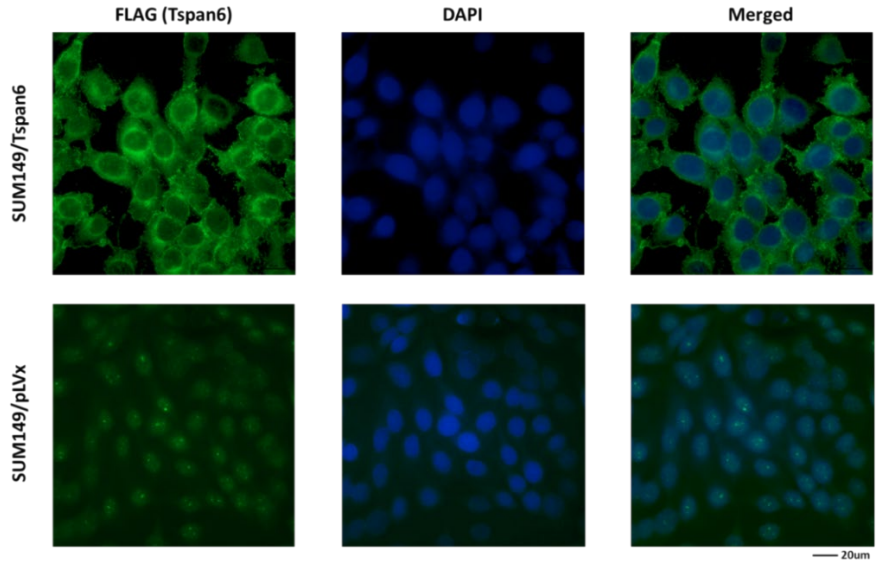

B

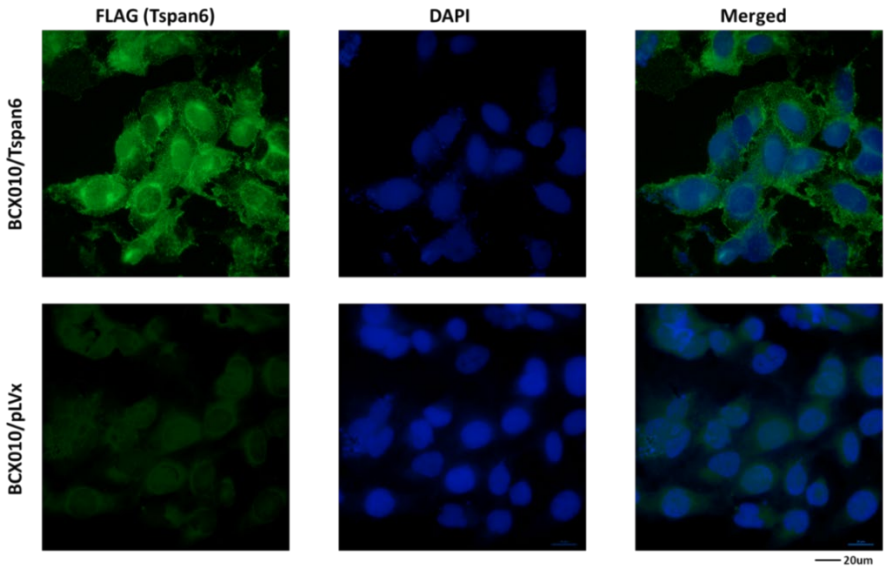

C

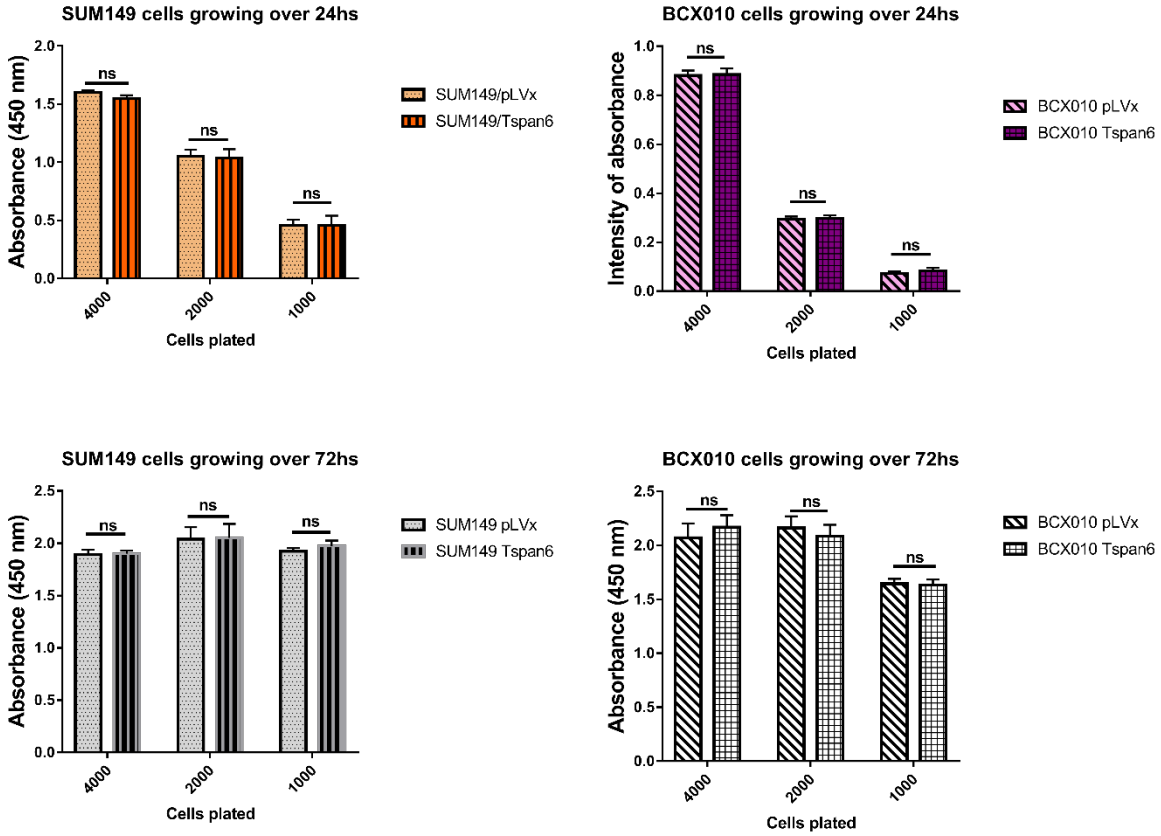
SUM149 cells growing over 24hs
Absorbance (450 nm)
2.0
1.5
1.0
0.5
0.0
ns
ns
ns
4000
2000
1000
Cells plated
SUM149/pLVx
SUM149/Tspan6
BCX010 cells growing over 24hs
Intensity of absorbance
1.0
0.8
0.6
0.4
0.2
0.0
ns
ns
ns
4000
2000
1000
Cells plated
BCX010 pLVx
BCX010 Tspan6
SUM149 cells growing over 72hs
Absorbance (450 nm)
2.5
2.0
1.5
1.0
0.5
0.0
ns
ns
ns
4000
2000
1000
Cells plated
SUM149 pLVx
SUM149 Tspan6
BCX010 cells growing over 72hs
Absorbance (450 nm)
2.5
2.0
1.5
1.0
0.5
0.0
ns
ns
ns
4000
2000
1000
Cells plated
BCX010 pLVx
BCX010 Tspan6

D

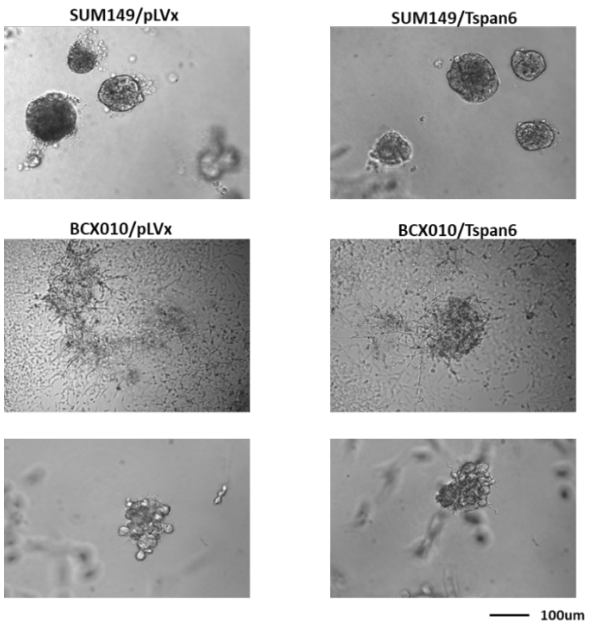
SUM149/pLVx
SUM149/Tspan6
BCX010/pLVx
BCX010/Tspan6
100um

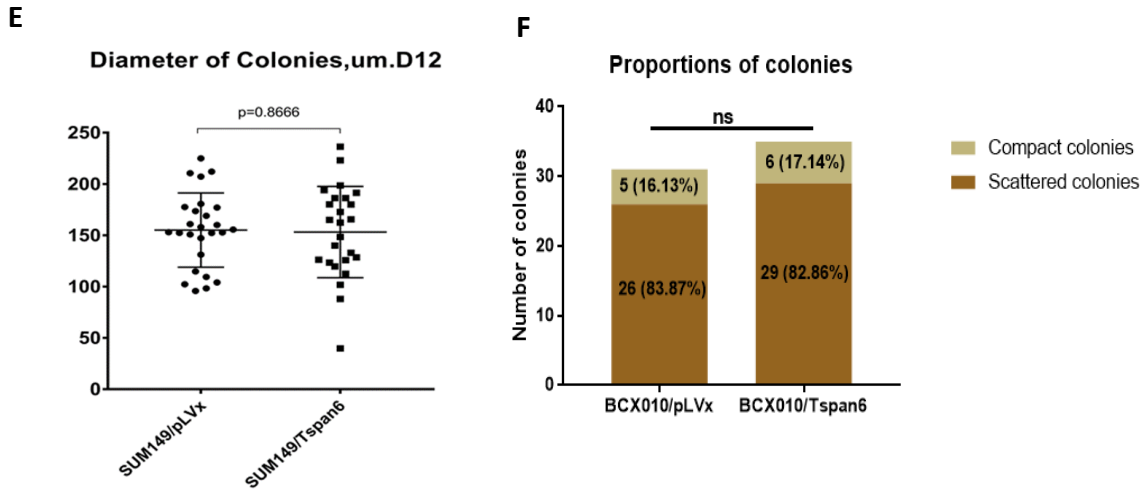

Figure 5-3. Impacts of Tspan6 expression on the characteristics of SUM149 and BCX010 cells. **(A, B)** Representative immunofluorescent images of individual cell lines showed that Tspan6 was predominantly membranous expression. Flag-tagged Tspan6 was detected by mAb anti-Flag and visualised by goat anti-mouse Ab conjugated with AF488. **(C)** Effect of Tspan6 on the proliferation of SUM149 and BCX010 cells. Three biological repeats were performed. Shown are means with SD. **(D)** Representative colonies of SUM149 (top panel) and BCX010 (middle and bottom panels) were grown in 3D ECM (on Day 12). Images were obtained by phase-contrast microscopy. **(E)** Tspan6 did not affect the morphology and growth of SUM149 in 3D cell culture. Diameters of representative colonies were measured by Image J. **(F)** BCX010 displayed two morphologies despite Tspan6 expression. Each morphology was quantified by counting the number of colonies within ten microscope fields and compared using a Fisher exact test. Other P values were calculated using a two-tailed t-test and are indicated on the graph.

5.5. Tspan6 strengthens the chemoattractive potential of SUM149 and BCX010 cells

The results of section 5.2 showed that Tspan6, rather than other tetraspanins, enhanced the chemoattractive potential of IBC cells for B cells. In agreement with the initial observation using cells expressing GFP-tagged proteins, the SUM149/Tspan6 tagged with flag was also more chemotactic compared to SUM149/pLVx cells (Figure 5-4 E left). These results indicated that fusing a relatively large protein tag with Tspan6 does not affect the biological activity of

the tetraspanin in this assay. To verify a universal Tspan6-induced effect on B lymphocyte migration, we conducted additional 4-hour PBMC migration assays by using CM-BCX010/Tspan6 and CM-BCX010/pLVx. As anticipated, the expression of Tspan6 in BCX010 positively correlated with the migration of B lymphocytes, as a ~1.6-fold increase in the number of migrating B lymphocytes to CM-BCX010/Tspan6 as compared to CM-BCX010/pLVx ($p < 0.01$) (Figure 5-5 E).

To confirm a persistent effect of Tspan6 on IBC cells, we carried out 16-hour cell migration assays using CM-SUM149/Tspan6 and CM-SUM149/pLVx. Despite the fact that the expression of Tspan6 in SUM149 cells did not significantly increase the sustained migration of B cells, we detected an upward trend in the migration of B cells to CM-SUM149/Tspan6 as compared to CM-SUM149/pLVx (1.7-fold increase, $p = 0.081$) (Figure 5-4 E right).

In parallel, we observed enhanced CD8+ T cells migration to CM-SUM149/Tspan6 and CM-BCX010/Tspan6 compared to CM-SUM149/pLVx and CM-BCX010/pLVx in 4-hour setting experiments, respectively. Specifically, the expression of Tspan6 in SUM149 and BCX010 increased the number of short-term migrating CD8+ T lymphocytes by ~1.5 ($p<0.01$) and ~1.4 folds ($p<0.01$) compared to CM-SUM149/pLVx and CM-BCX010/pLVx, respectively (Figure 5-4 D left, 5-5 D). In addition, Tspan6 almost significantly enhance the sustained migration (16h) of CD8+ T cells to CM-SUM149/Tspan6 in comparison to CM-SUM149/pLVx ($p = 0.052$) (Figure 5-4 D right).

Unlike B cells or CD8+ T cells, the impacts of Tspan6 on the migration of other immune subpopulations were cell type-dependent and varied between different experimental settings. There were increases in the numbers of CD4+ T cells migrating to CM-SUM149/Tspan6 when compared to CM-SUM149/pLVx in both migration-time settings (Figure 5-4 C), but this phenomenon did not occurre in CM-BCX010/Tspan6. Moreover, Tspan6 also strengthens the effect of BCX010 cells on the short-term migration of monocytes (Figure 5-5 B).

Collectively, while the impact of Tspan6 on the chemoattractive potential of IBC cells varied between different cell lines and experimental settings, it consistently promoted the chemotactic migration of B cells and CD8+ T cells at the first 4 hours. As we have observed a B cell-targeted chemotactic effect of IBC cells, the current results suggested that Tspan6 can strengthen this effect at very early stage (first 4 hours). Therefore, we desire to further analyse the mechanism behind this short-term Tspan6-dependent B cell migration.

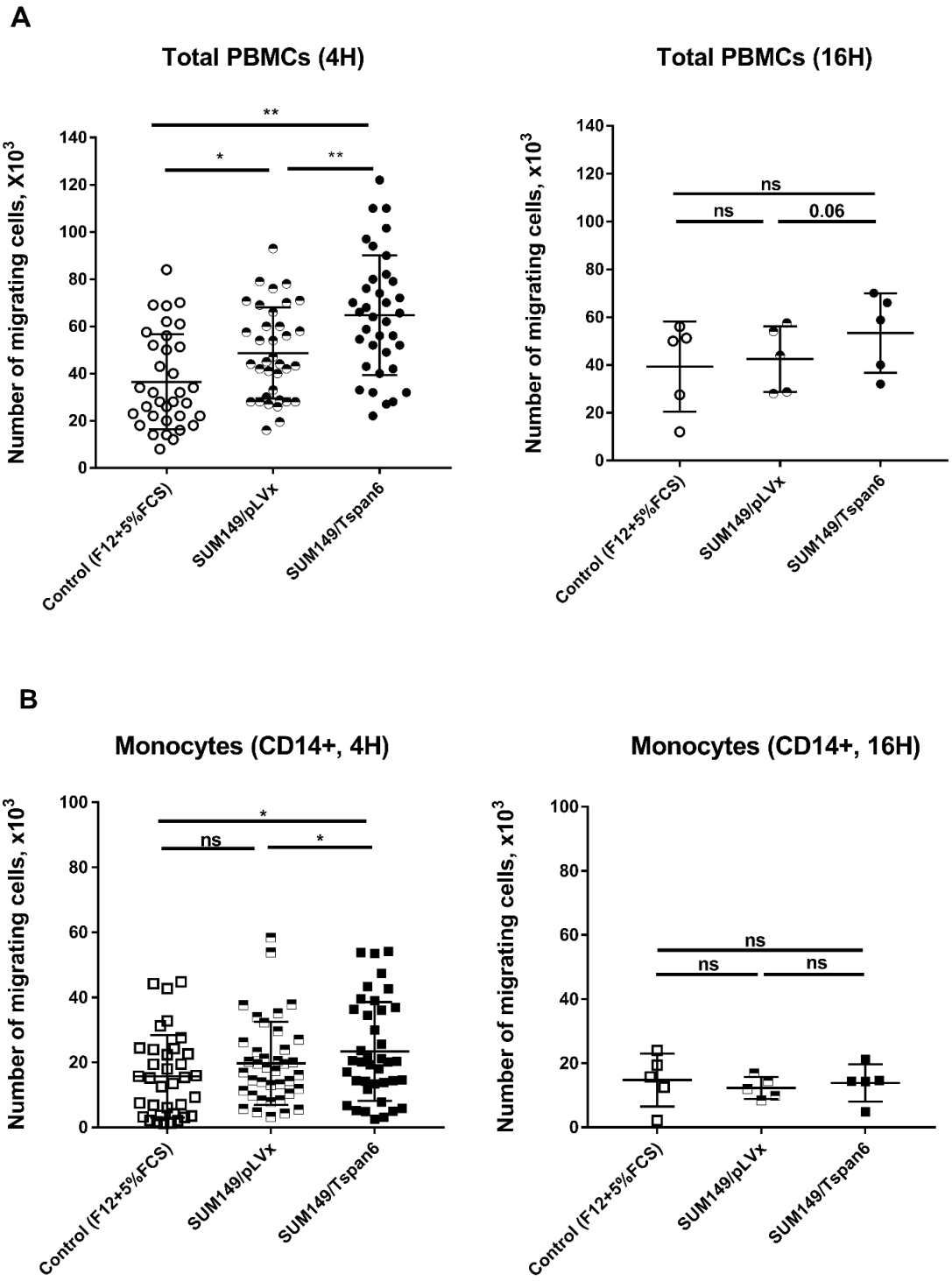
A
Total PBMCs (4H)
Number of migrating cells, X10^3
**
*
**
Control (F12+5%FCS)
SUM149/pLVx
SUM149/Tspan6
Total PBMCs (16H)
Number of migrating cells, x10^3
ns
ns
0.06
Control (F12+5%FCS)
SUM149/pLVx
SUM149/Tspan6
B
Monocytes (CD14+, 4H)
Number of migrating cells, x10^3
*
ns
*
Control (F12+5%FCS)
SUM149/pLVx
SUM149/Tspan6
Monocytes (CD14+, 16H)
Number of migrating cells, x10^3
ns
ns
ns
Control (F12+5%FCS)
SUM149/pLVx
SUM149/Tspan6

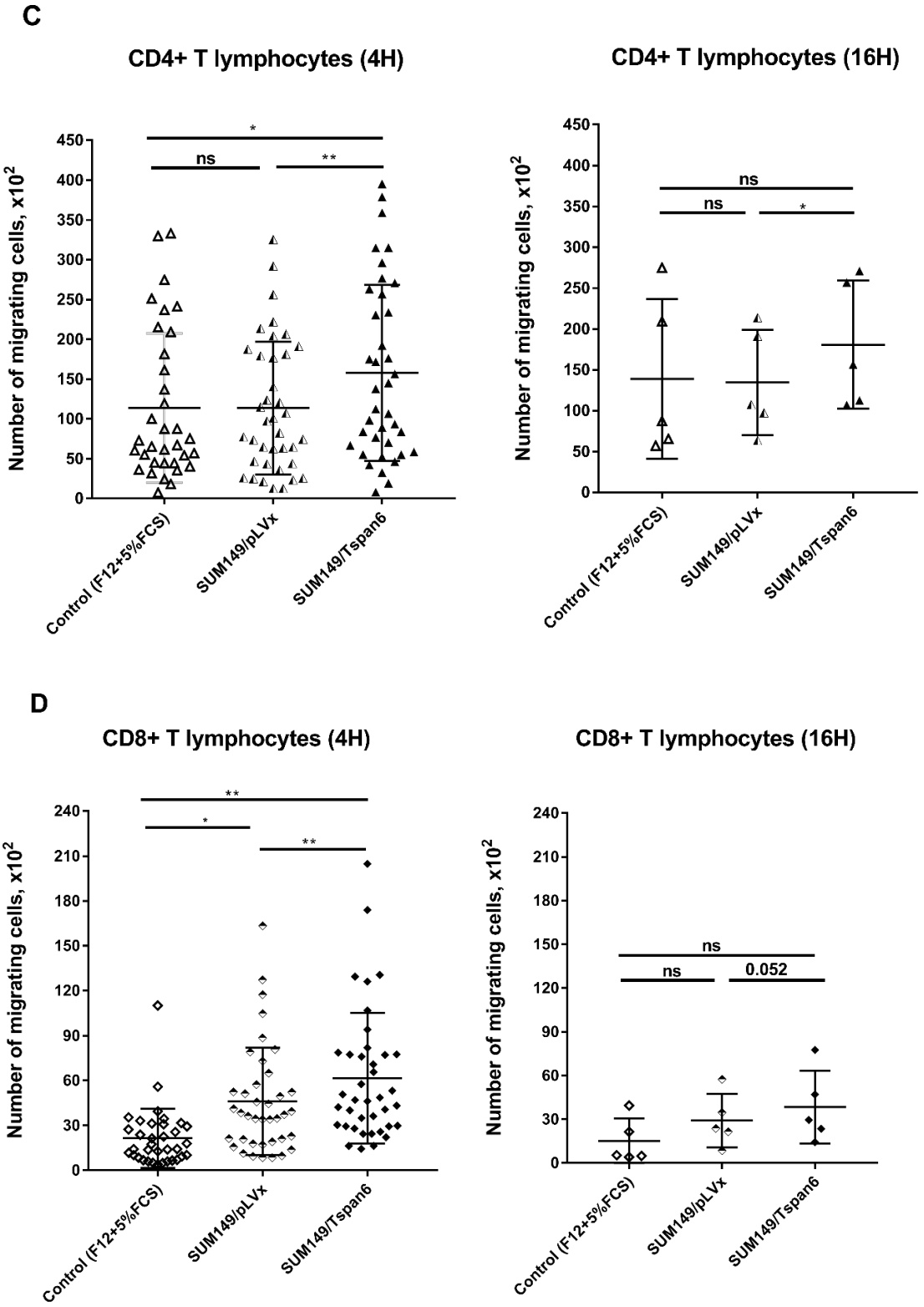
C
CD4+ T lymphocytes (4H)
Number of migrating cells, x10²
450
400
350
300
250
200
150
100
50
0
*
ns
**
Control (F12+5%FCS)
SUM149/pLVx
SUM149/Tspan6
CD4+ T lymphocytes (16H)
Number of migrating cells, x10²
450
400
350
300
250
200
150
100
50
0
ns
ns
*
Control (F12+5%FCS)
SUM149/pLVx
SUM149/Tspan6
D
CD8+ T lymphocytes (4H)
Number of migrating cells, x10²
240
210
180
150
120
90
60
30
0
**
*
**
Control (F12+5%FCS)
SUM149/pLVx
SUM149/Tspan6
CD8+ T lymphocytes (16H)
Number of migrating cells, x10²
240
210
180
150
120
90
60
30
0
ns
ns
0.052
Control (F12+5%FCS)
SUM149/pLVx
SUM149/Tspan6

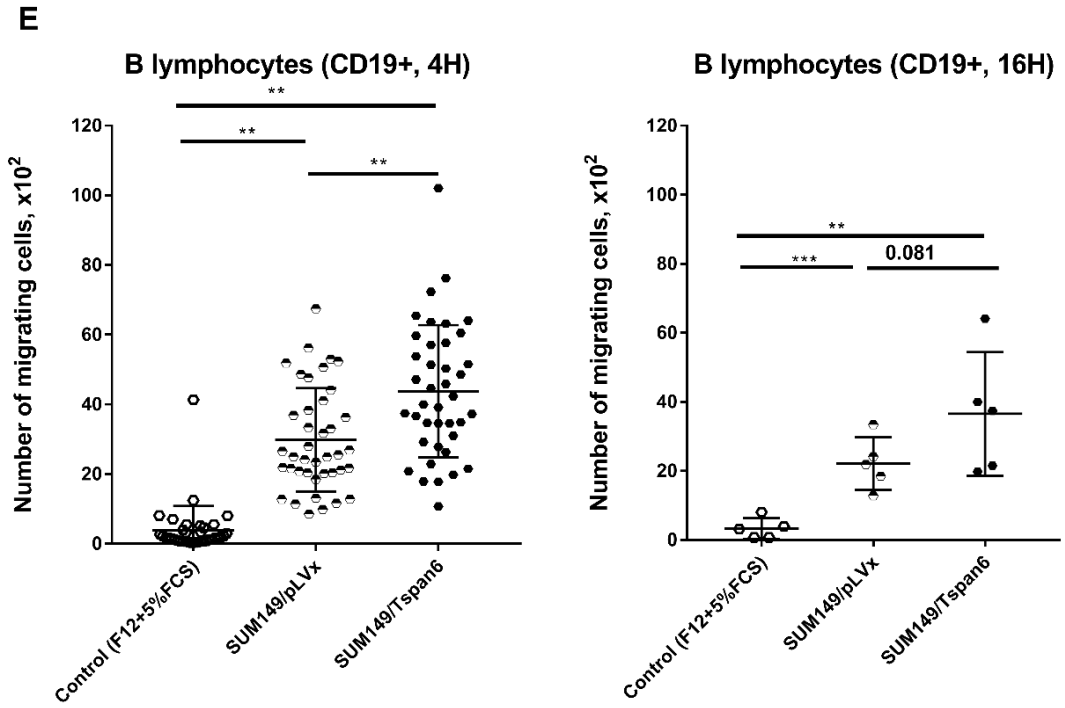

Figure 5-4. Tspan6 strengthens the chemoattractive potential of SUM149 for B cells and CD8+ T cells at first 4 hours. (A-E) The migration of total PBMCs (A), monocytes (B), CD4+T lymphocytes (C), CD8+T lymphocytes (D) and B lymphocytes (E) towards CM-SUM149/Tspan6, CM-SUM149/pLVx and control medium (F12+5% FCS). PBMCs ($2x10^6$ cells/200 µl) were allowed to migrate to the above CM and control medium for 4 or 16 hours. Each dot shown in the graph represents the total number of migrating cells in an individual trans-well assay. Shown are the results of 40 independent experiments under 4-hour migration condition and 5 additional experiments under 16-hour condition. P values were calculated using a two-tailed t-test (normal distribution data) or Mann-Whitney test (non-normal distribution data). The significance of P value is indicated on the graph, *p<0.05, **p<0.01, ***p<0.001.

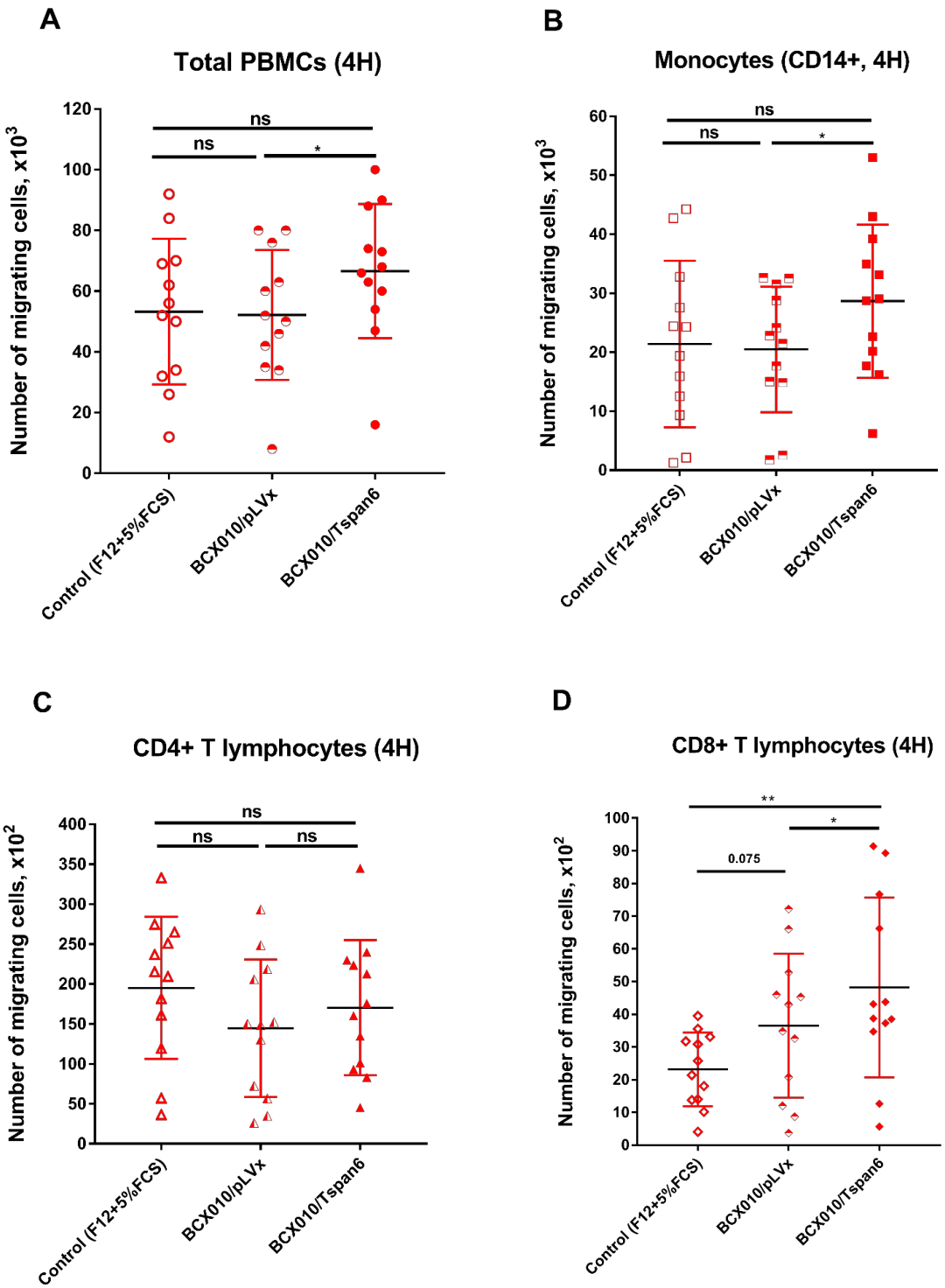
A
Total PBMCs (4H)
Number of migrating cells, x10^3
120
100
80
60
40
20
0
ns
ns
*
Control (F12+5%FCS)
BCX010/pLVx
BCX010/Tspan6
B
Monocytes (CD14+, 4H)
Number of migrating cells, x10^3
60
50
40
30
20
10
0
ns
ns
*
Control (F12+5%FCS)
BCX010/pLVx
BCX010/Tspan6
C
CD4+ T lymphocytes (4H)
Number of migrating cells, x10^2
400
350
300
250
200
150
100
50
0
ns
ns
ns
Control (F12+5%FCS)
BCX010/pLVx
BCX010/Tspan6
D
CD8+ T lymphocytes (4H)
Number of migrating cells, x10^2
100
90
80
70
60
50
40
30
20
10
0
**
*
0.075
Control (F12+5%FCS)
BCX010/pLVx
BCX010/Tspan6

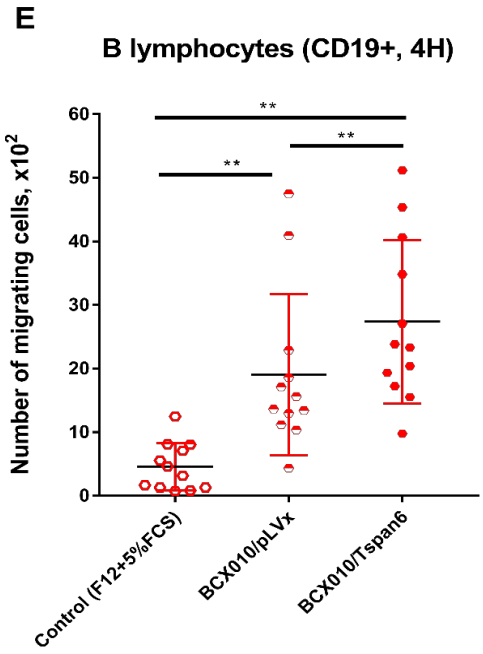

Figure 5-5. Tspan6 strengthens the chemoattractive potential of BCX010 for B cells and CD8+ T cells at first 4 hours. (A-E) The short-term migration of total PBMCs (A), monocytes (B), CD4+T lymphocytes (C), CD8+T lymphocytes (D) and B lymphocytes (E) towards each CM and control medium. PBMC migration assay as described in Figure 5-4. Control medium (F12+5% FCS), CM-BCX010/pLVx, CM-BCX010/Tspan6 were used as chemoattractants. Each dot in the graph represents a total number of migrated cells in an individual trans-well assay. Shown are the results of 12 independent experiments. P values were calculated using a two-tailed t-test (normal distribution data) or Mann-Whitney test (non-normal distribution data). The significance of P value is indicated on the graph, *p<0.05, **p<0.01.

5.6. The role of EVs in Tspan6-dependent migration of B lymphocytes

It has been shown that Tspan6 was involved in changing EV composition (Guix FX *et al.*, 2017; Andrijes R *et al.*, 2021). Furthermore, expression of Tspan6 in immortalised human kidney fibroblasts stimulated EV production (Guix FX *et al.*, 2017). Thus, we questioned whether Tspan6-dependent short-term B cell migration involves EVs produced by IBC cells. To this end, EVs were depleted from CM-SUM149/Tspan6, CM-SUM149/pLVx, BCX010/Tspan6 and

BCX010/pLVx by ultracentrifugation and PBMCs were allowed to migrate towards EV-depleted and intact CM for 4 hours. We observed that EV depletion boosted B cell migration to CM-SUM149/pLVx in four out of six experiments, while the rest two experiments showed a slight decrease (Figure 5-6 A). A similar phenomenon was found in the B cell migration to CM-SUM149/Tspan6 after EV removal (Figure 5-6 B). Compared to SUM149 pair, more consistent impact of EV depletion on B cell migration was shown in experiments using CM-BCX010/Tspan6 and CM-BCX010/pLVx. Specifically, the absence of EVs reduced the B cell migration to CM-BCX010/Tspan6 ($p < 0.05$) (Figure 5-6 D), and produced a downward trend in B cell migration to CM-BCX010/pLVx ($p = 0.063$) (Figure 5-6 C). In general, we did not observe a universal effect of EV depletion on the Tspan6-dependent B cell migration between different IBC cellular models. Therefore, we concluded that the biological activity of Tspan6 in our experimental settings does not rely on EVs.

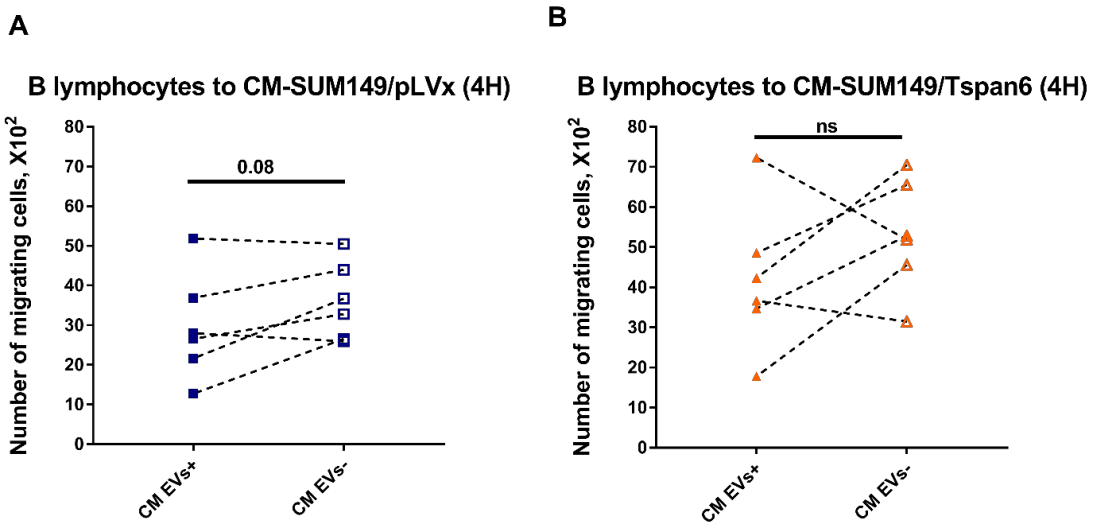

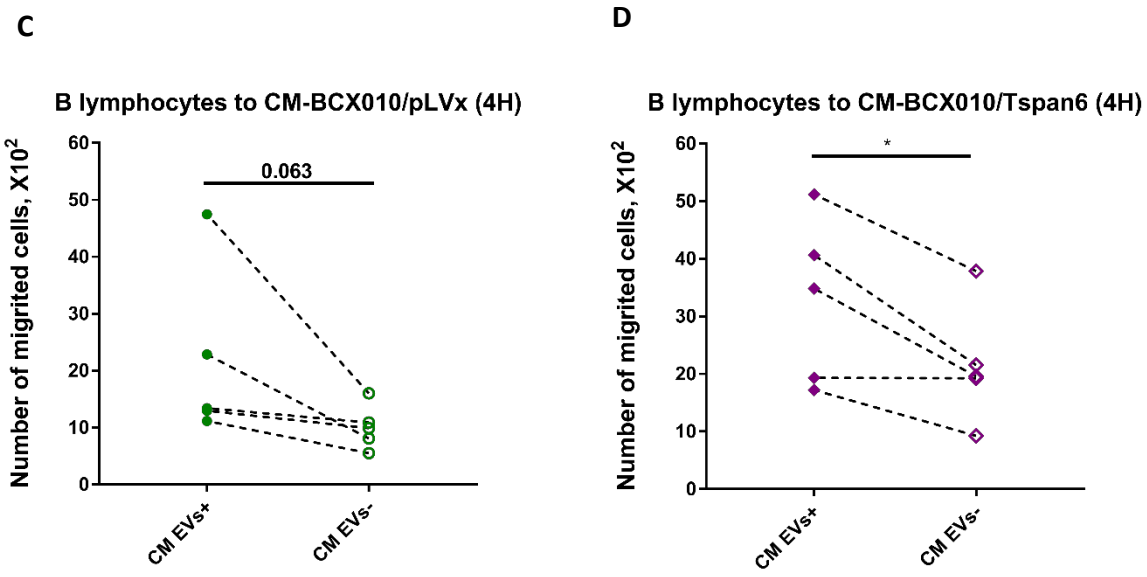

Figure 5-6. EVs differently regulate the short-term migration of B cells to CM of Tspan6-expressing IBC cells. (A, B) EV depletion did not significantly change the chemoattractive potential of SUM149/Tspan6 or SUM149/pLVx for B cells. **(C, D)** EV depletion significantly changed the chemoattractive potential of BCX010/Tspan6 but not BCX010 /pLVx for B cells. EVs were depleted from CM-SUM149/Tspan6, CM-SUM149/pLVx and CM-BCX010/Tspan6, CM-BCX010/pLVx by sequential ultrasound centrifugations. The short-term migration of B lymphocytes towards individual CM with or without EVs was assessed. Each dot in the graph represents the total number of migrating B lymphocytes in an individual trans-well assay. Shown are the results of 5 independent experiments. P values were calculated using a two-tailed t-test (normal distribution data) or Mann-Whitney test (non-normal distribution data). The significance of P value is indicated on the graph, *p<0.05.

5.7. The impact of Tspan6 on the production of cytokines and chemokines

A recent study from our laboratory showed that Tspan6 regulated the secretion of EV-associated transmembrane form of TGF-α (Andrijes R *et al.*, 2021), suggesting that Tspan6 may affect chemotactic factor production. Considering that chemokines are critical players in regulating the recruitment of immune cells, we initially profiled chemokines produced by

SUM149/Tspan6 cells. CM-SUM149/Tspan6 and CM-SUM149/pLVx were analysed using human chemokine antibody arrays. Compared with CM-SUM149/pLVx, the signal intensity of CXCL1 was considerably higher in CM-SUM149/Tspan6 (Figure 5-7 A). To measure the level of CXCL1 more precisely, we performed ELISA. Surprisingly, the level of CXCL1 in CM-SUM149/Tspan6 was comparable to that in CM-SUM149/pLVx (~190 pg/ml) (Figure 5-7 B). Furthermore, the expression levels of CXCL1 in CM-BCX010/Tspan6 and CM-BCX010/pLVx were virtually undetectable in ELISA experiments (Figure 5-7 C). While we cannot explain the discrepancy between our initial profiling and ELISA data, the inconsistent results of the SUM149 and BCX010 pairs indicated that the CXCL1 expression in IBC cells was not Tspan6-dependent.

In addition to CXCL1, we also assessed the concentrations of other cytokines/chemokines by ELISA that are reportedly produced by IBC cells or implicated in the B cell chemotaxis. We found that the expression of Tspan6 in SUM149 cells resulted in a dramatic increase in the secretion of midkine (Figure 5-7 B). The concentrations of midkine in CM-SUM149/Tspan6 and CM-SUM149/pLVx were ~170 pg/ml and ~90 pg/ml, respectively (Figure 5-7 B). A similar trend was observed in the CM-BCX010 pair, but midkine expression was generally higher than that in the CM-SUM149 pair (the concentrations of midkine in CM-BCX010/Tspan6 and CM-BCX010/pLVx were ~790 pg/ml and ~360 pg/ml, respectively) (Figure 5-7 C).

Tspan6 expression also correlated with a high secretion level of Areg in SUM149 cells but did not have the same effect on BCX010 cells. We also detected high levels of PTN (a heparin-binding growth-associated molecule closely related to midkine, see above Chapter II) in all CM-IBC. However, Tspan6 did not appear to affect its expression. In addition, we found that IL-8, TNF-α, and VEGF were detectable in all CM-IBC, while TGF-α and IL-6 were only detectable in CM-SUM149/Tspan6 and CM-SUM149/pLVx. CXCL10, CXCL12 and CXCL13 in CM-SUM149/Tspan6 and CM-SUM149/pLVx were also measured. However, none of them displayed Tspan6-dependent changes in their levels. Furthermore, neither CCL20 nor CCL2 was expressed by SUM149 or BCX010 cells regardless of the Tspan6 expression. Generally speaking, we found a Tspan6-dependent expression of midkine in IBC cells. However, it remained unknown whether midkine could affect B cell recruitment in the context of IBC.

A

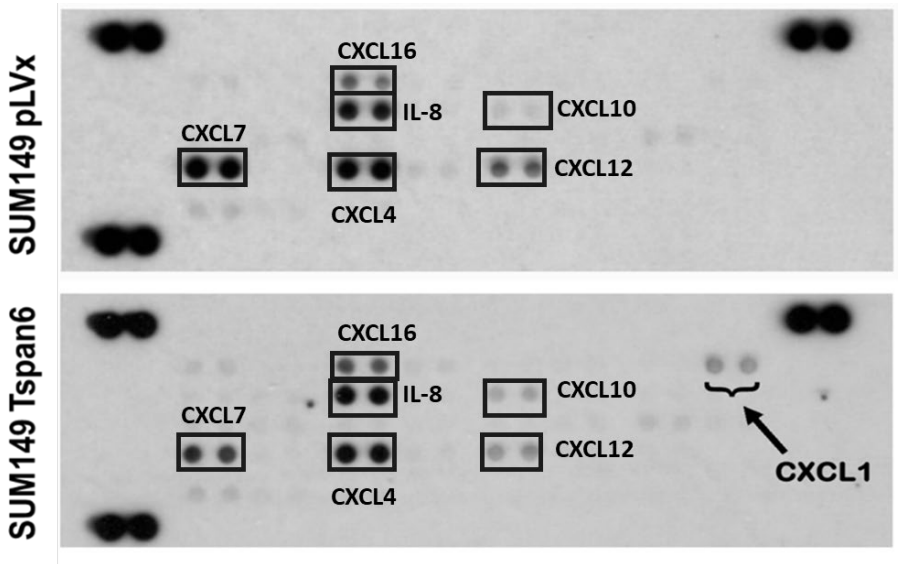

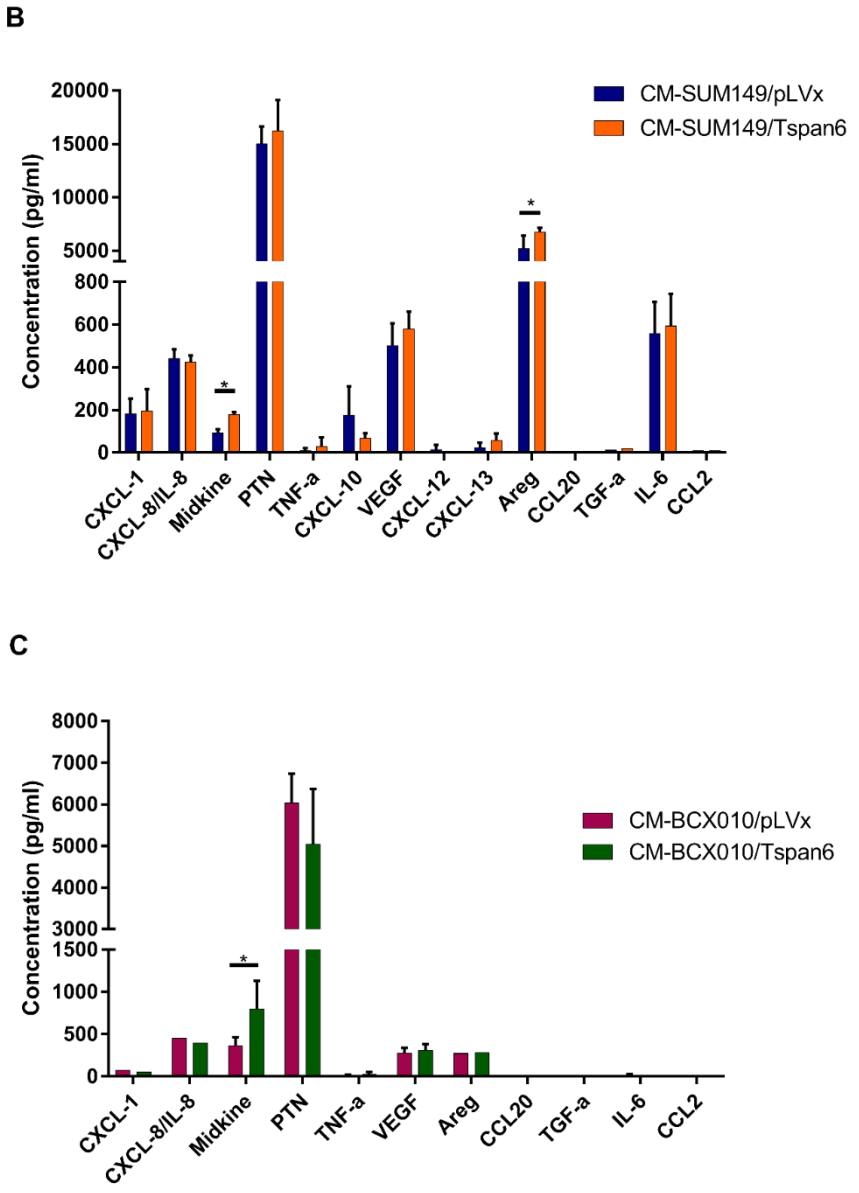

Figure 5-7. Comparisons of cytokine/chemokine expression between CM of Tspan6-expressing IBC cells and control IBC cells. (A) Enhanced expression of CXCL1 was detected in CM-SUM149/Tspan6 compared to CM-SUM149/pLVx. Chemokines in CM-SUM149/Tspan6 and CM-SUM149/pLVx were profiled using human chemokine antibody array membranes. **(B-C)** Midkine expression in IBC cells was Tspan6-dependent, whereas CXCL1 was not. Concentrations of cytokines and chemokines in CM-SUM149/Tspan6, CM-SUM149/pLVx and CM-BCX010/Tspan6, CM-BCX010/pLVx, were measured by ELISA. All CM has been conditioned by 72hours before chemokine array experiments and ELISA. Shown are means with SD of the results of 3 independent experiments. P values were calculated using a two-tailed t-test and are indicated on the graph, *p<0.05.

5.8. Midkine is not involved in regulating the migration of B lymphocytes

A recent study from our laboratory uncovered the role of midkine in mediating the chemotactic migration of monocyte towards CM-IBC (Hayward S *et al.*, 2020). We, therefore, questioned whether this midkine-mediated communication between IBC cells and monocytes also contributed to the Tspan6-dependent migration of B cells. To address this question, we performed PBMC migration assays using control medium (F12+5%FCS) supplemented with different concentrations of recombinant midkine. Unexpectedly, the migration of B lymphocytes towards the control medium was not affected by the addition of midkine (Figure 5-8 A). It should be emphasised that there was minimal B cell migration to the control medium even with midkine supplementation. In contrast, the chemotactic migration of monocytes towards the control medium was increased in a midkine concentration-dependent manner (Figure 5-8 A). These results suggested that midkine could regulate the chemotaxis of monocytes but not B cells. In reverse experiments, we applied antibodies to neutralise midkine in CM-SUM149/Tspan6. Neutralising midkine did not impact the migration of B lymphocytes to CM-SUM149/Tspan6 (Figure 5-8 B). However, perhaps due to a low expression of midkine in CM-SUM149/Tspan6, midkine neutralisation failed to affect the monocyte migration in a concentration-dependent manner (Figure 5-8 B). Though in “gain and loss” experiments, we only performed two replicates for each condition, it seemed that midkine was irrelevant to B cell migration in the context of our study.

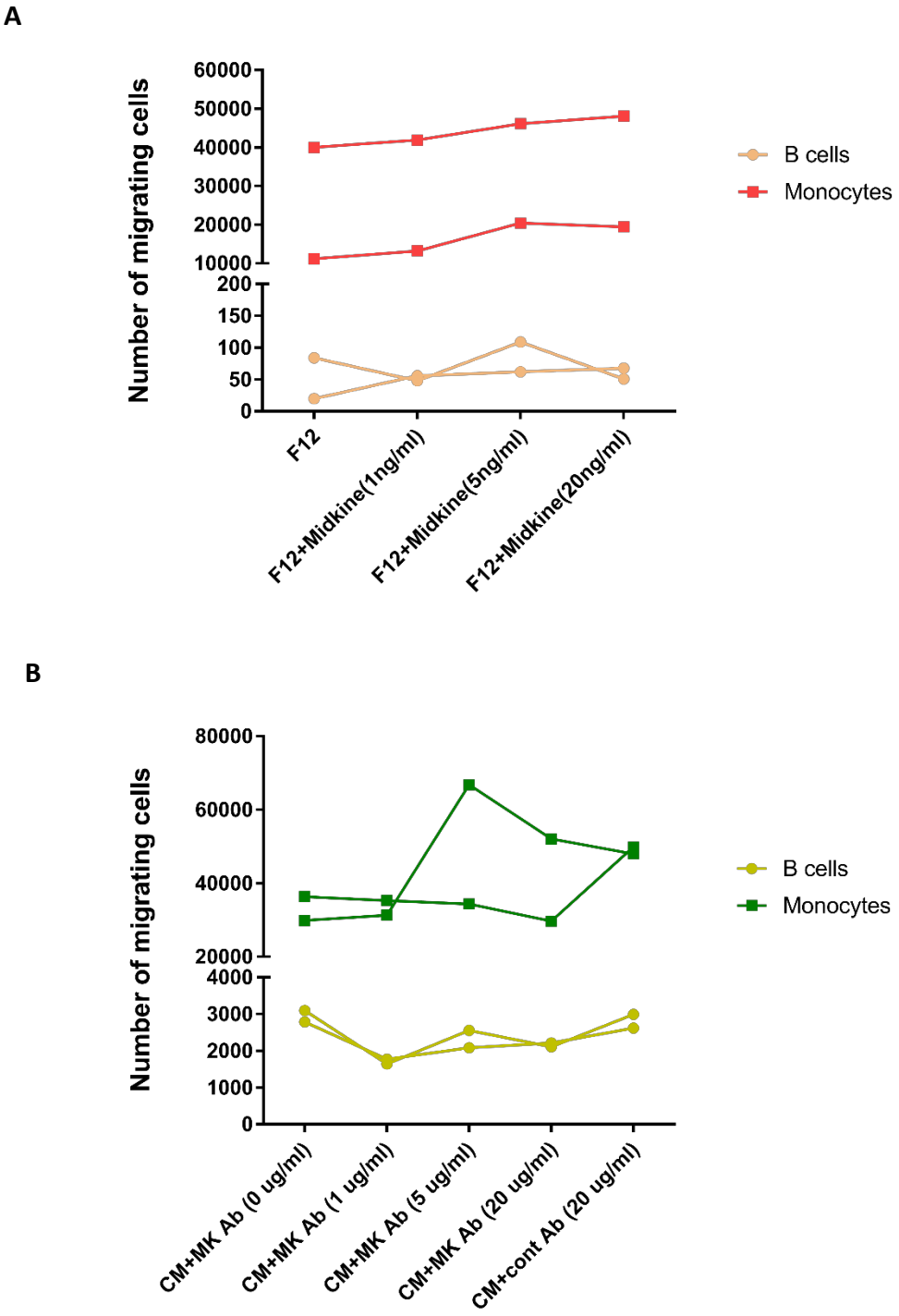

Figure 5-8. Midkine does not mediate the Tspan6-dependent B cell migration. (A) The addition of midkine did not affect B cell migration. PBMCs ($2x10^6$/200 µl) were allowed to migrate to the control medium (F12+5% FCS) supplemented with different concentrations of recombinant midkine for 4 hours. The migration of B cells and monocytes (controls) were analysed. **(B)** Neutralisation of midkine did not significantly and consistently affect the

migration of B cells. PBMCs ($2x10^6$/200 µl) were allowed to migrate to CM-SUM149/Tspan6 supplemented with different concentrations of midkine antibodies (IP14) and isotype control mouse (IgG2a) for 4 hours. The migration of B cells and monocytes (controls) were analysed. Numbers connected by dot lines are donor-matched comparisons.

5.9. Discussion

In this chapter, we discovered that Tspan6 in IBC cells significantly promoted the short-term (4h) chemotactic migration of B cells. To our knowledge, Tspan6 is the first tetraspanin capable of strengthening a B cell-biased chemotactic effect of breast cancer cells. This finding was supported by our analysis of clinical IBC samples which demonstrated that the expression of membranous Tspan6 on naïve IBC tissues correlated with an increased accumulation of intratumoral B cells ($p = 0.02$) (unpublished data).

Tspan6 has been shown to affect EV synthesis and composition; hence, we postulated that Tspan6 altered the IBC's EV production in a manner that modulated B cell migration. However, in our study, we did not obtain robust evidence to support the involvement of EV in mediating the Tspan6-dependent short-term migration of B cells. Unlike short-term migration, the results of sustained migration experiments (16h) indicated that EV mediated the Tspan6-dependent B cell migration (unpublished data). These inconsistent results suggest that the molecular pathways underlying the Tspan6-dependent B cell short-term and sustained migration may vary. In this regard, we compared the absolute numbers of migrating B cells to CM-SUM149/Tspan6 under “short-term” and “sustained” experimental settings (Supplementary Figure 1-2 E) and found that the prolonged exposure of B cells to CM-SUM149/Tspan6 did not significantly

promoted the number of migrating B cells. This finding implies a more complicated or completely different modulation during sustained B cell migration compared to short-term migration. More importantly, this finding also supports our hypothesis that CM of IBC cells expressing Tspan6 can rapidly (in the first 4 hours) exert a powerful chemotactic effect on B cells.

In addition to EVs, we also examined the soluble chemotactic factors (i.e. cytokines and chemokines) existing in CM. Only midkine displayed a Tspan6-dependent increase. Midkine is a heparin-binding growth factor and its elevated expression has been reported in many cancers (Filippou PS, Karagiannis GS and Constantinidou A, 2020). In breast cancer, midkine overexpression is associated with advanced clinical stages and is regarded as an adverse prognostic indicator (Li F, Tian P, Zhang J and Kou C, 2015). One recent work from our laboratory has shown that CD151 expression was relevant to a high expression of EV-associated midkine. Thus, the authors speculated that CD151 might be implicated in the loading of midkine into EVs by associating with midkine-bound proteins (i.e. syndecans, integrins and low-density lipoprotein receptor-related protein 1 (LRP1)) (Hayward S *et al.*, 2020). Here, we found a Tspan6-dependent increased expression of midkine in IBC cells, suggesting a regulatory role of Tspan6 in midkine secretion. Although the mechanism behind this increase was not explored in our study, the possibility that Tspan6 associates with midkine-bound proteins through direct (Tspan6-syndecan) or indirect (TEM/TERMs) bindings cannot be neglected. For example, Tspan6 can directly bind with syndecan (Ghossoub R *et al.*, 2020) or indirectly associate with

it via syntenin (Baietti MF *et al.*, 2012). Through these bindings, Tspan6 increases the loading of midkine to the EVs (similar to the mechanism involving CD151), thus increasing the secretion of midkine. However, neither the prior work nor the current investigation detected midkine-induced B cell migration, indicating that midkine does not appear to play a role in stimulating B cell migration to CM-IBC. Research strategy focusing on the chemotactic factor receptors (e.g. GPCRs) on B cells may be another acceptable way to examine the roles of chemokine and cytokine in regulating Tspan6-dependent B cell migration.

In this study, we also discovered Tspan6-dependent migration of CD8+ cells in short-term experimental settings. This observation encouraged us to examine a possible cross-talk between B cells and CD8+ cells during migration. Interestingly, we only found a correlation between CD8+ T cell and B cell migration towards CM-SUM149/pLVx ($r = 0.344$, $p < 0.05$), but did not find a strong correlation in the context of CM-SUM149/Tspan6 ($r = 0.274$, $p = 0.088$) (Supplementary Table 1-3, 1-4). These findings suggest that Tspan6 in IBC may alter the intercellular communication between B cells and CD8+ T cells. More experiments focusing on the impact of CD8+ T cells on short-term B cell migration are presented in Chapter IV. Intriguingly, the impact of Tspan6 on the short-term migration of CD4+ T cells is cell line-dependent. We found enhanced migration of CD4+ T cells to CM-SUM149/Tspan6, but did not obtained the similar result of CM-BCX010/Tspan6, suggesting variable responses of CD4+ T cells to the Tspan6-induced chemotactic effect. This finding also supports the concept that CD4+ and CD8+ T cells behave differently in the tumour microenvironment (Kim HJ and

Cantor H, 2014; St Paul M and Ohashi PS, 2020). More importantly, the specificity of the Tspan6-induced chemotactic effect on B cells and CD8+ T cells reflects the complexity of tetraspanins in regulating the TIME of IBC, as another tetraspanin, CD151, was reported to regulate the monocyte migration to CM-IBC and this modulation is mediated by EVs (Hayward S *et al.*, 2020).

In this study, we also evaluated the effect of Tspan6 on the proliferation of IBC cells. Humbert et al. found that the expression of Tspan6 suppressed the activation of EGFR, thus reducing the growth and metastasis of pancreatic cancer cells carrying the K-ras mutation (Humbert PO *et al.*, 2022). However, although both SUM149 and BCX010 cells express high levels of EGFR ((Willmarth NE and Ethier SP, 2006) and unpublished data from our laboratory), the expression of Tspan6 did not affect the proliferation of IBC cells under standard culturing conditions. This discrepancy could be attributed to different genetic backgrounds between cancer cell models (pancreatic cancer vs IBC cells). Further work will be required to investigate whether Tspan6-induced changes in the composition of CM can affect EGFR-dependent signalling in IBC cells.

In summary, we, for the first time, discovered that Tspan6 strengthened the short-term chemotactic effect of IBC cells on B cells. However, we did not yet identify the IBC-derived chemotactic factor(s) responsible for Tspan6-dependent B cell migration. In addition to potential direct effects from chemokines and cytokines (due to limited experiments, we could not rule out the contribution of these factors), the involvement of non-B cells is also worth

exploring. Therefore, more investigations concentrating on direct chemotactic effect of chemokines and cytokines, and the intercellular communication between B cells and non-B cells within IBC microenvironment are warranted.

6. RESULTS CHAPTER IV: TSPAN6-DEPENDENT MIGRATION OF B CELLS

6.1. Introduction

IBC and monocytes can produce various kinds of chemotactic factors, and some of them are potential mediators for B cell migration (Rossol M *et al.*, 2011; Tokunaga R *et al.*, 2018; Valeta-Magara A *et al.*, 2019). These chemoattractants may enhance B cell recruitment directly (Klasen C *et al.*, 2014; Farrokhi M *et al.*, 2015; Liu RX *et al.*, 2015; Ghods A *et al.*, 2019) or promote B cell sensitivity to chemokines (Badr G *et al.*, 2005; Ferretti E, Ponzoni M, Doglioni C and Pistoia V, 2016). As we have discovered the Tspan6-dependent enhancement in the chemoattractive potential of IBC for B cells. Here, we described experiments designed to investigate this phenomenon in more detail. By concentrating on the direct effect of IBC cells, and the contribution of monocytes and other non-B cells, we attempted to reveal a communication network in the TIME of IBC that induces B cell migration.

6.2. Direct chemotactic effect of Tspan6-expressing IBC cells on B cells

In our study, we have identified a direct chemotactic effect of CM-IBC on B cells at the first 4 hours (section 4.4), which promoted us to question whether CM of IBC cells expressing Tspan6 would also directly affect B cell migration. To this end, we purified B cells (which eliminate the effect of non-B cells on B cells) and allowed purified B cell to migrate to CM-SUM149/Tspan6 and CM-SUM149/pLVx for 4 hours. Here, PBMCs' B cells refer to B cells

co-cultured with non-B cells (before B cell purification), whereas pure B cells indicate B cells without non-B cells' company. We found that while the absence of non-B cells did reduce the short-term migration of B cells to both CM-SUM149/Tspan6 ($p < 0.01$) and CM-SUM149/pLVx ($p < 0.01$), the CM-SUM149/Tspan6 remained more chemotactic for B cells than CM-SUM149/pLVx ($p < 0.01$) after non-B cell depletion (Figure 6-1 A). These findings indicate that Tspan6 promotes the direct chemotactic effect of IBC cells on B cells.

To further specifically analyse the involvement of chemokines in regulating Tspan6-dependent short-term migration of B cells, we applied PTX to inhibit the GPCRs in B cells. Pure B lymphocytes pre-treated with different concentrations of PTX (0, 200, 500 ng/ml) were allowed to migrate to CM-SUM149/Tspan6 and CM-SUM149/pLVx for 4 hours. We found that neither high-or low-concentration PTX could significantly affect the migration of pure B cells to CM-SUM149/pLVx (Figure 6-1 B). In contrast, the influence of PTX on the migration of pure B cells to CM-SUM149/Tspan6 was more consistent and significant, and even low concentration PTX (200 ng/ml) was sufficient to inhibit the direct chemotactic effect of CM-SUM149/Tspan6 on B cells (Figure 6-1 C). These findings demonstrate that PTX-sensitive mediator(s) is (are) implicated in inducing the Tspan6-dependent direct chemotactic effect on B cells.

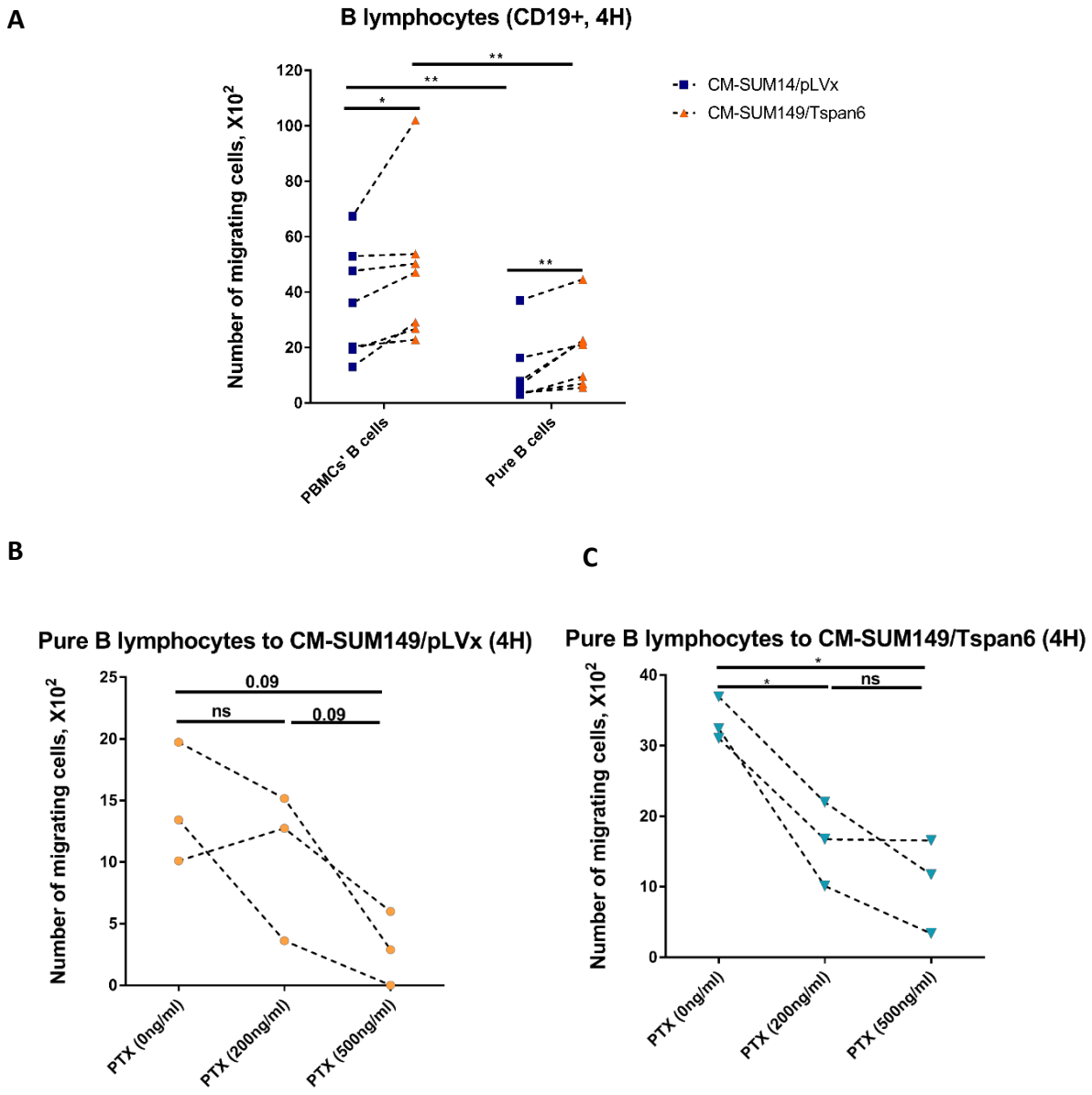

Figure 6-1. The Tspan6-dependent direct chemotactic effect of IBC cells on B cells is mediated by PTX-sensitive mediator(s). (A) CM of IBC cells expressing Tspan6 exerted direct chemotactic effect on B cells even without the help from non-B cells. Pure B lymphocytes (2x105 cells/200 µl) were allowed to migrate to CM-SUM149/Tspan6 and CM-SUM149/pLVx for 4 hours. Donor-matched PBMCs were applied as controls. The migration of PBMCs' B cells and pure B cells to each CM was assessed. Shown are the results of 7 independent experiments. **(B-C)** PTX significantly reduced B cell recruitment to CM-SUM149/Tspan6, while its effect on CM-SUM149/pLVx remained to be determined. Pure B cells (2x10^5 cells/200 µl) were pre-treated with different concentrations of PTX and then allowed to migrate to CM-SUM149/pLVx and CM-SUM149/Tspan6 for 4 hours. Each dot shown in the graph represents

the total number of migrating B cells in an individual trans-well assay. Numbers connected by dot lines are donor-matched comparisons. Shown are the results of 3 independent experiments. P values were calculated using a two-tailed t-test and are indicated on the graph, *p<0.05.

6.3. Monocytes mediate the Tspan6-dependent short-term migration of B cells

Though IBC cells expressing Tspan6 have direct effect on the short-term migration of B cells, we also observed a contribution of non-B cells to this phenomenon (Figure 6-1 A). As we have shown that monocytes mediated the chemotactic effect of IBC cells on B cells at the first 4 hours. Here, we examined whether monocytes mediated the chemotactic effect of IBC/Tspan6 cells on B cells in a similar manner. To this end, monocytes were depleted from PBMCs. The non-monocyte PBMCs (PBMCs monocytes-) were allowed to migrate to CM-SUM149/Tspan6 and CM-SUM149/pLVx for 4 hours, and PBMCs from the same donor were employed as controls. We found that B cells migrating to CM-SUM149/Tspan6 and CM-SUM149/pLVx were both significantly attenuated after monocyte depletion ($p < 0.01$, $p < 0.05$, respectively) (Figure 6-2 A and B). Moreover, the absence of monocytes completely negated the Tspan6-dependent enhancement in the chemoattractive potential of SUM149 cells for B cells at the early stage (Figure 6-2 C). These findings indicate that eliminating monocytes reduced the short-term chemotactic effect of both CM-SUM149/Tspan6 and CM-SUM149/pLVx on B cells, with CM-SUM149/Tspan6 being more affected.

To further confirm the involvement of monocytes in mediating the short-term migration of B cells, we added monocytes to B cells at a ratio of 1:1, and allowed this cell mixture to migrate

to CM-SUM149/Tspan6 and CM-SUM149/pLVx (as control) for 4 hours. The monocyte supplementation substantially increased the migration of B cells to CM-SUM49/Tspan6 and CM-SUM149/pLVx ($p < 0.05$ for both) (Figures 6-2 D and E). Moreover, the effect of monocyte supplementation was more pronounced in CM-SUM149/Tspan6 than in CM-SUM149/pLVx, as the absolute number of B cells migrating to CM-SUM149/Tspan6 increased higher than those migrating to CM-SUM149/pLVx (Figure 6-2 F). The results of "loss and gain" experiments indicate that B cells could not massively migrate to either CM-SUM149/Tspan6 or CM-SUM149/pLVx without the help of monocytes in a short-term time setting. More importantly, monocytes exert a more significant effect on the short-term migration of B cells towards CM-SUM149/Tspan6 than CM-SUM149/pLVx.

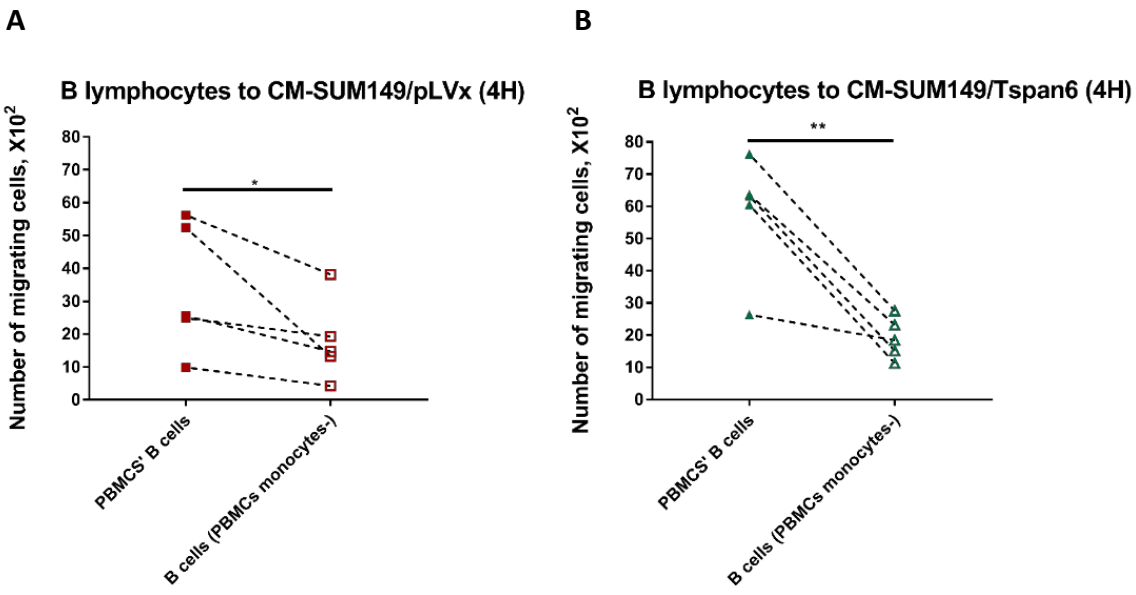

C

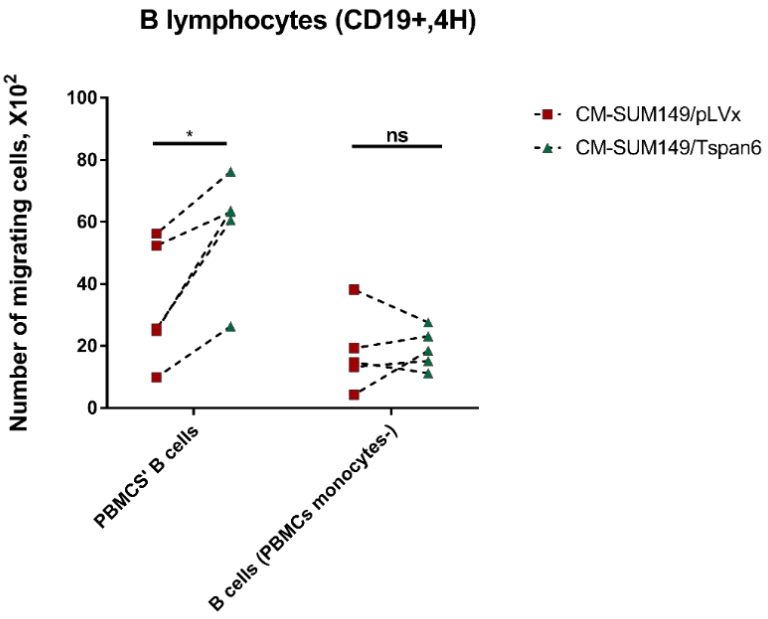
B lymphocytes (CD19+,4H)
Number of migrating cells, X10²
100
80
60
40
20
0
*
ns
CM-SUM149/pLVx
CM-SUM149/Tspan6
PBMCS' B cells
B cells (PBMCs monocytes-)

D

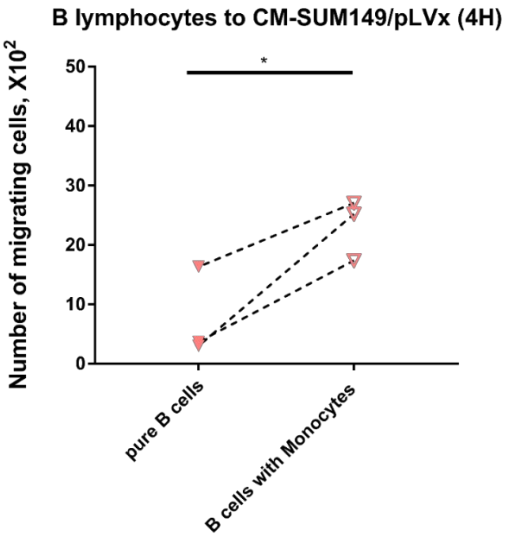
B lymphocytes to CM-SUM149/pLVx (4H)
Number of migrating cells, X10²
50
40
30
20
10
0
*
pure B cells
B cells with Monocytes

E

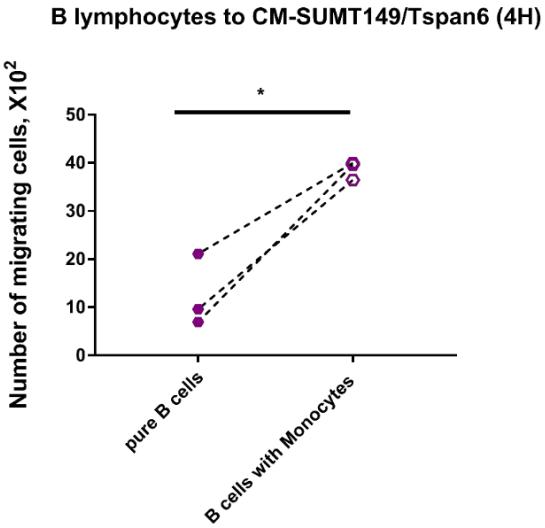
B lymphocytes to CM-SUMT149/Tspan6 (4H)
Number of migrating cells, X10²
50
40
30
20
10
0
*
pure B cells
B cells with Monocytes

F

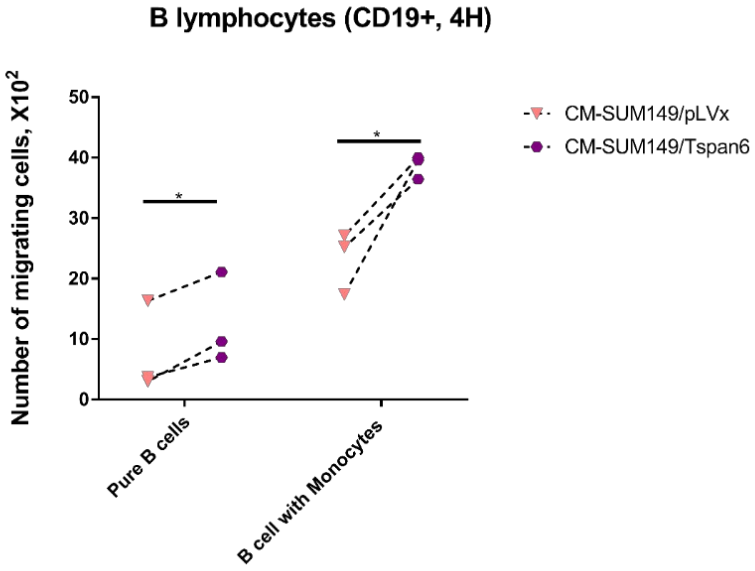

Figure 6-2. Monocytes mediate the Tspan6-dependent short-term migration of B lymphocytes. (A, B) Monocyte depletion decreased B cell migration to CM-SUM149/Tspan6 and CM-SUM149/pLVx. The non-monocyte PBMCs ($2x10^6$ cells/200 µl) and donor-matched PBMCs ($2x10^6$/200 µl) were allowed to migrate to CM-SUM149/pLVx (A) and CM-SUM149/Tspan6 (B) for 4 hours. PBMCs' B cells refer to B cells in PBMCs, whereas B cells in PBMCs monocytes- indicate B cells are in PBMCs without monocyte population. (**C**) The comparison between B cell migration to CM-SUM149/Tspan6 and CM-SUM149/pLVx upon monocyte removal. Shown are the results of 5 independent experiments. **(D, E)** The presence of monocytes significantly increased the B cell migration to CM-SUM149/Tspan6 and CM-SUM149/pLVx. The cell mixture comprising B cells and monocytes (($2x10^5$ monocytes+ $2x10^5$ B cells)/200 µl) was allowed to migrate towards CM-SUM149/pLVx (D) and CM-SUM149/Tspan6 (E) for 4 hours. Pure B cells under the same experimental conditions were controls. (**F**) The comparison between B cell migration to CM-SUM149/Tspan6 and CM-SUM149/pLVx when monocytes were present. Shown are the results of 3 independent experiments. The numbers of B lymphocytes in individual CM under different circumstances were assessed. Numbers connected by dot lines are donor-matched comparisons. P values were calculated using a two-tailed t-test (normal distribution data) or Mann-Whitney test (non-normal distribution data). The significance of P value is indicated on the graph, *$p<0.05$, **$p<0.01$.

6.4. The physical presence of monocytes is required for Tspan6-expressing IBC cells to enhance the B lymphocyte migration

Having discovered the relevance of monocytes in regulating the short-term migration of B cells, and Tspan6 expression increased the significance of this effect. We next attempted to understand the mechanism(s) underlying this phenomenon. We hypothesised that monocytes exposed to the CM of Tspan6-expressing IBC cells (T6-monocytes) secreted more potent stimuli for B cells than monocytes exposed to CM of control IBC cells (pLVx-monocytes). This could result in more B cells migrating to the CM of Tspan6-expressing cells than to the CM of control IBC cells. To prove our hypothesis, we incubated monocytes in CM-SUM149/Tspan6 or CM-SUM149/pLVx for 4 hours to generate double CM (Dou CM-SUM149/Tspan6 and Dou CM-SUM149/pLVx): double CM should contain chemoattractants secreted by both IBC cells and monocytes. Subsequently, monocytes were removed by filtration, and pure B cells (eliminating the impacts of other non-PBMCs on B cells) were allowed to migrate towards double CM for a further 4 hours (Figure 6-3 A). Unexpectedly, B cell migration to Dou CM-SUM149/Tspan6 was not improved compared to Dou CM-SUM149/pLVx. We even observed a trend toward a reduction in the number of B cells moving to Dou CM-SUM149/Tspan6 relative to Dou CM-SUM149/pLVx, though more replicates are needed to confirm this (Figure 6-3 B). These findings indicate that monocytes are essential for Tspan6 to increase the short-term migration of B cells.

A

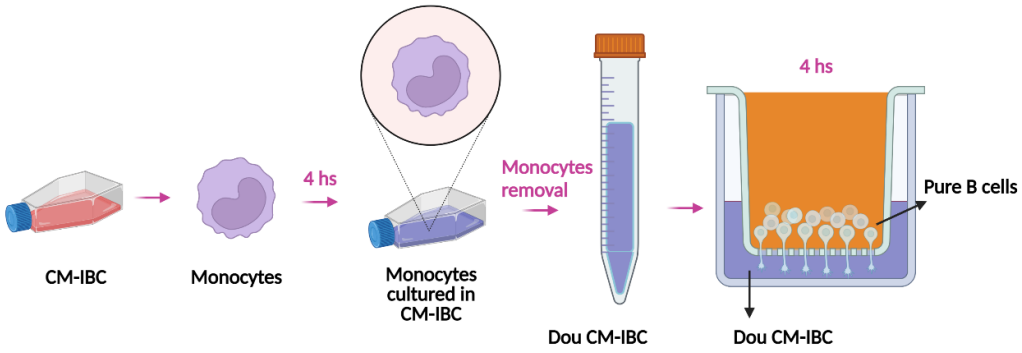

B

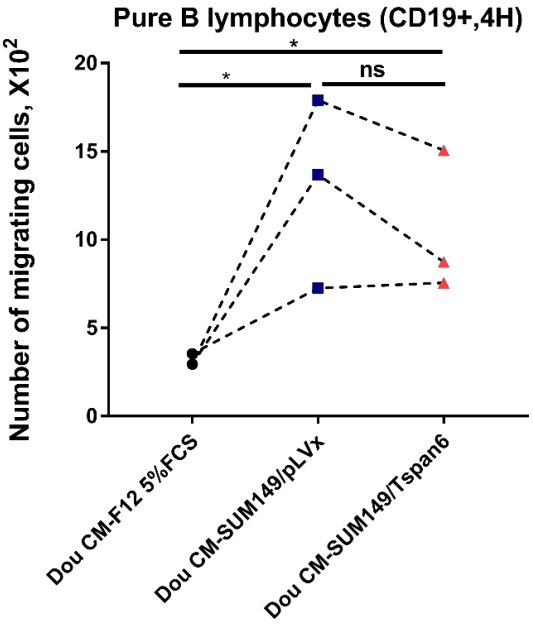

Figure 6-3. The presence of monocytes is required for the Tspan6-induced B cell short-term migration. (A) A flow chart shows the process of double CM generation. Pure monocytes ($2x10^5$ cells/ml) were incubated with CM-SUM149/Tspan6 and CM-SUM149/pLVx for 4 hours to generate Dou CM-SUM149/Tspan6 and Dou CM-SUM149/pLVx; then, monocytes were removed. Dou CM-F12+5% FCS was shown as a blank control. Pure B cells ($2x10^5$ cells/200 µl) were allowed to migrate to double CM above for another 4 hours. **(B)** The comparison between the migration of B cells to Dou CM-SUM149/Tspan6, Dou CM-SUM149/pLVx and Dou CM-F12+5% FCS. Numbers connected by dot lines are donor-matched comparisons. Shown are the results of 3 independent experiments. P values were calculated using a two-tailed t-test and are indicated on the graph, *p<0.05.

6.5. Mutual effect between monocyte-dependent and monocyte-independent B cell migration to CM of Tspan6-expressing IBC cells

Our data have showed that enhanced short-term migration of B cells towards CM-SUM149/Tspan6 involves both monocyte-dependent and monocyte-independent (PTX sensitive mediator(s)) pathways. However, the mutual influence between these two mechanisms remained unknown. To this end, pure B lymphocytes were pretreated with PTX, mixed with monocytes, and allowed to migrate to CM-SUM149/Tspan6 and CM-SUM149/pLVx for 4 hours. Non-pretreated B cells were applied as controls. In agreement with the experiments described above, the migration of pure B cells to CM-SUM149/Tspan6 was decreased after PTX treatment ($p < 0.05$), but these PTX-pretreated B cells became migratory upon monocyte supplementation ($p < 0.05$) (Figure 6-4 A). This suggests that PTX did not affect the stimulatory effect of monocytes on the migration of B cells to CM-SUM149/Tspan6 (Figure 6-4 A). Compared to CM-SUM149/Tspan6, the migration of pure B cells to CM-SUM149/pLVx was not affected by PTX as expected (Figure 6-4 B). Furthermore, in CM-SUM149/pLVx, PTX did not alter the responsiveness of B cells to monocyte-induced chemotactic effect (Figure 6-4 B). These results suggest that PTX-sensitive pathway(s) did not interrupt monocyte-stimulated B cell migration.

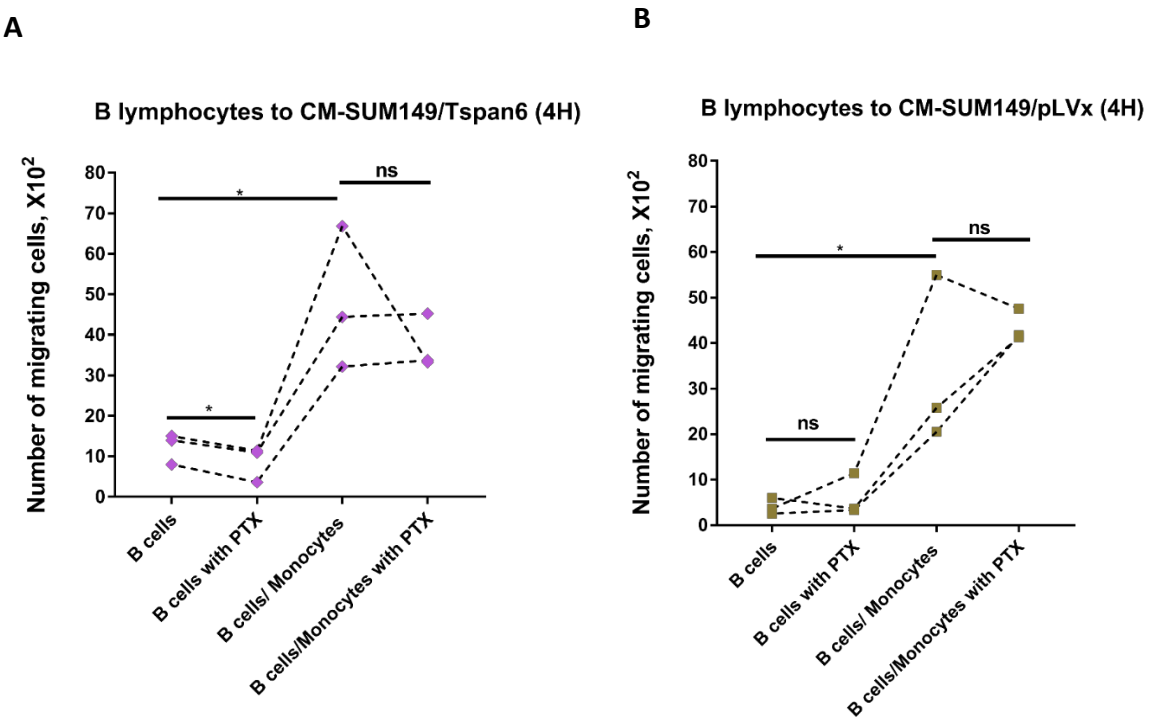

Figure 6-4. PTX-sensitive pathway(s) does (do) not implicate in the monocyte-dependent B cell migration to CM-SUM149/Tspan6. (A-B) Pure B cells ($2x10^5$ cells/100 µl) pretreated with PTX (200 ng/ml) were mixed with monocytes ($2x10^5$ cells/100 µl) and allowed to migrate to CM-SUM149/Tspan6 and CM-SUM149/pLV for 4 hours. Non-pretreated B cells under the same experimental conditions was shown as controls. Numbers connected by dot lines are donor-matched comparisons. Each dot shown here represents a number of migrating B cells in an individual trans-well assay. Shown are the results of 3 independent experiments. P values were calculated using a two-tailed t-test and are indicated on the graph, *$p<0.05$.

6.6. The involvement of CD8+ T cells in Tspan6-dependent short-term migration of B cells

We have found that Tspan6 expression also enhanced the short-term migration of CD8+ T cells (Chapter III Figure 5-4 D), which prompted us to question whether CD8+ T cells contributed to the Tspan6-dependent B cell migration at an early stage. To address this question, we depleted CD8+ T cells from PBMCs (PBMC CD8+ T cells -) and allowed these non-CD8+ T cells to

migrate to CM-SUM149/Tspan6 and CM-SUM149/pLVx for 4 hours. We found that the depletion of CD8+ T cells significantly reduced the number of B cells migrating to CM-SUM149/Tspan6 (Figure 6-5 B) but had no apparent effect on the chemotactic migration of B cells towards CM-SUM149/pLVx (Figure 6-5 A). This suggests that the absence of CD8+ T cells specifically hindered the chemotactic effect of IBC/Tspan6 cells on B cells. To confirm the mediator role of CD8+ T cells, we supplemented CD8+ T cells to pure B cells and allowed this cell mixture to migrate towards CM-SUM149/Tspan6 and CM-SUM149/pLVx for 4 hours. Surprisingly, the addition of pure CD8+ T cells did not boost the migration of B cells to CM-SUM149/Tspan6 (Figure 6-5 E), although this supplementation slightly increased the migration of B cells to CM-SUM149/pLVx (this increase was not statistically significant) (Figure 6-5 D). The discrepancy between the results of these "loss and gain" experiments indicates a third modulator existing in the CD8+ T cell-enhanced B cell migration.

A recent study from our laboratory demonstrated that a higher number of infiltrating B cells was associated with increased accumulation of both macrophages and CD8+ T cells in grade 3 IBC tissues (Badr NM *et al.*, 2022). We, therefore, assumed that monocytes might be the upstream regulators for CD8+ T cells. To our surprise, monocyte depletion significantly increased the migration of CD8+ T cells to CM-SUM149/pLVx (Figure 6-6 A), but did not consistently affect the migration of CD8+ T cells to CM-SUM149/Tspan6 (Figure 6-6 B). Furthermore, the elimination of monocytes negated the difference in the migration of CD8+ T cells towards CM-SUM149/pLVx and CM-SUM149/Tspan6 (Figure 6-6 C).

Collectively, these data show that monocytes play a vital role in the communication between IBC cells and other types of immune cells. More importantly, our results highlight the complexity of the relationships between monocytes, CD8+ T cells and B cells when immune cells are exposed to CM-IBC, particularly to the CM of Tspan6-expressing IBC cells.

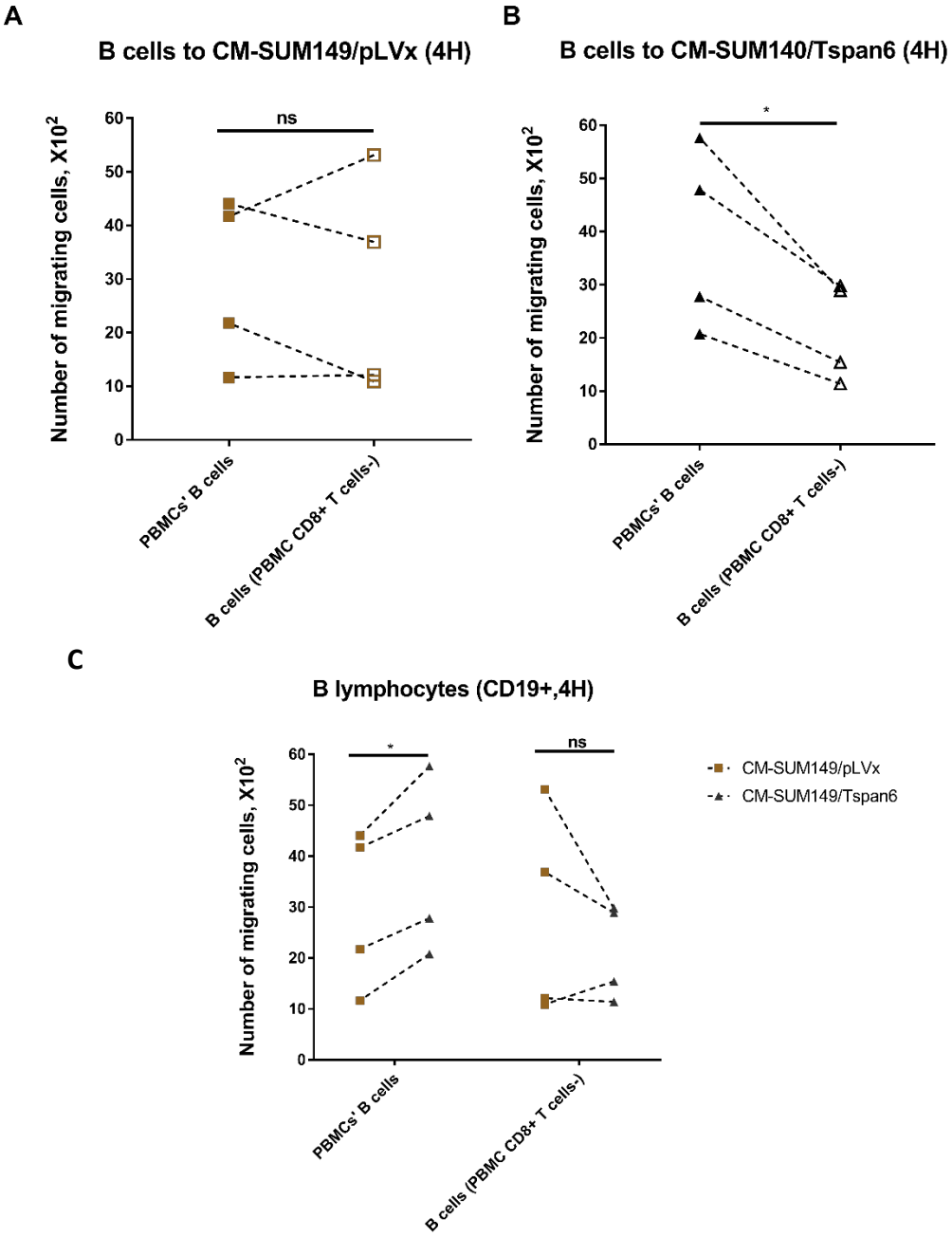

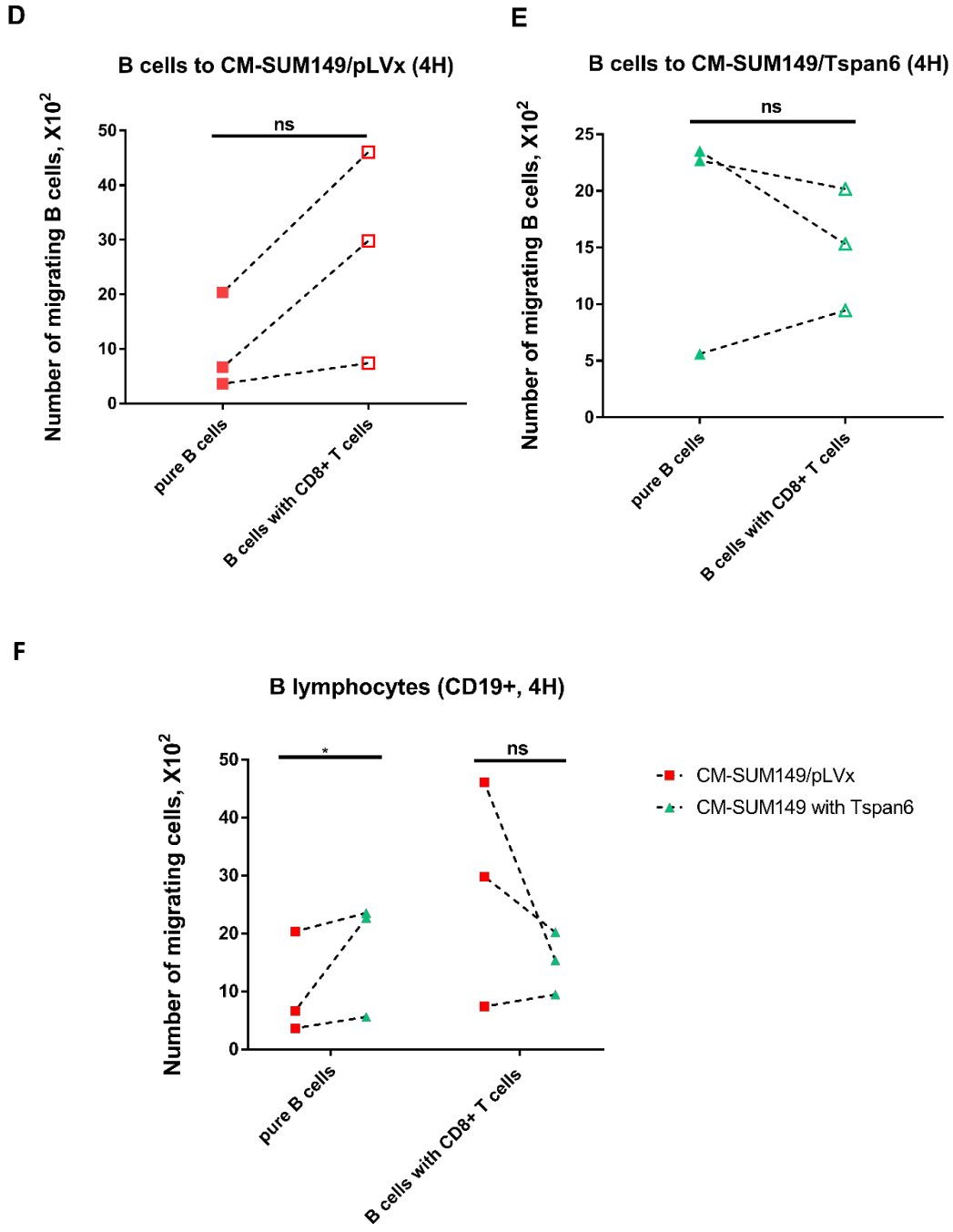

Figure 6-5. CD8+ T cells are important in regulating B cell migration to CM-SUM149/Tspan6. **(A, B)** The depletion of CD8+T cells significantly reduced the migration of B cells to CM-SUM149/Tspan6 but did not affect that to CM-SUM149/pLVx. CD8+T cells were depleted using biotin-conjugated antibody cocktails, followed by magnetic separation. The CD8+T cell-depleted PBMCs ($2x10^6$ cells/200 µl) and donor-matched PBMCs ($2x10^6$ cells/200 µl) were allowed to migrate to CM-SUM149/pLVx (A) and CM-SUM149/Tspan6 (B) for 4 hours. **(C)** The depletion of CD8+ T cells abrogated the advantage of CM-SUM149/Tspan6 in attracting B cells.

Shown are the results of 4 independent experiments. **(D, E)** The supplementation of CD8+ T cells did not significantly promote B cell migration to CM-SUM149/Tspan6 or to CM-SUM149/pLVx. Mixture of B cells ($2x10^5$/100 µl) with CD8+ T cells ($2x10^5$ cells/100 µl) and pure B cells ($2x10^5$ cells/200 µl) were allowed to migrate towards CM-SUM149/pLVx (D) and CM-SUM149/Tspan6 (E) for 4 hours. The numbers of B lymphocytes migrating to individual CM under different conditions were assessed. **(F)** The supplementation of CD8+ T cells did not restore the enhanced chemotactic effect of SUM149/Tspan6 cells on B cells. Numbers connected by dot lines are donor-matched comparisons. Shown are the results of 3 independent experiments. P values were calculated using a two-tailed t-test (normal distribution data) or Mann-Whitney test (non-normal distribution data). The significance of P value is indicated on the graph, *p<0.05.

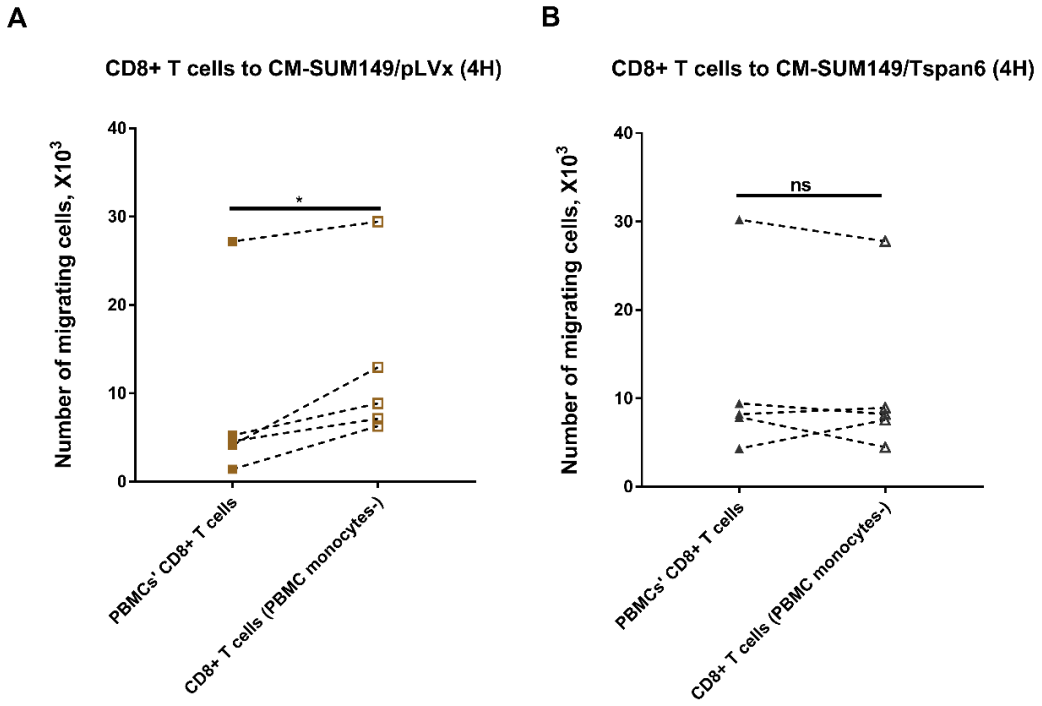

C

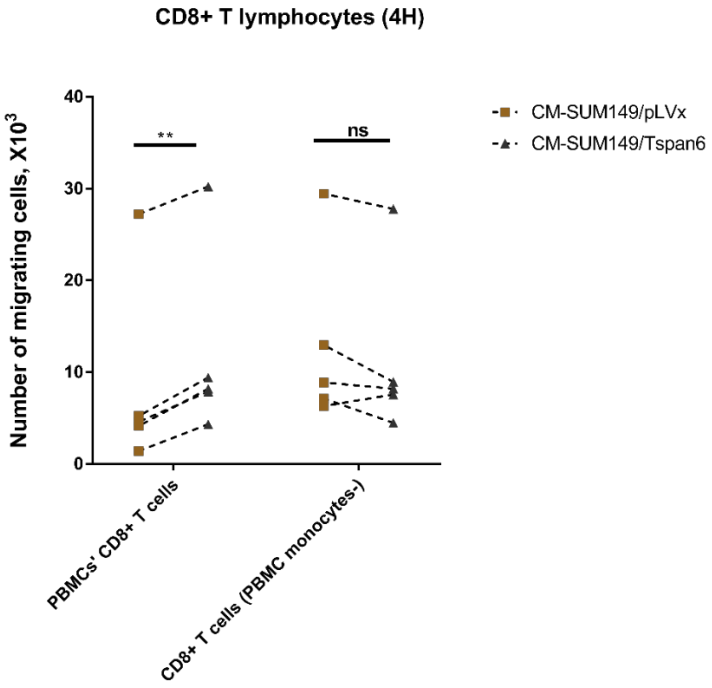

Figure 6-6. Monocytes might be the upstream regulators for CD8+ lymphocytes. (A, B) Removing monocytes increased the migration of CD8+T cells to CM-SUM149/pLVx but did not affect the migration to CM-SUM149/Tspan6. Monocytes were depleted by using biotin-conjugated antibody cocktails, followed by magnetic separation. The non-monocyte PBMCs ($2x10^6$ cells/200 µl) and donor-matched PBMCs ($2x10^6$ cells/200 µl) were allowed to migrate to CM-SUM149/pLVx (A) and CM-SUM149/Tspan6 (B) for 4 hours separately. **(C)** The comparison between CD8+ T cell migration to CM-SUM149/Tsapn6 and CM-SUM149/pLVx before and after monocyte depletion. The numbers of CD8+ T lymphocytes migrating to individual CM under different circumstances were assessed. Numbers connected by dot lines are donor-matched comparisons. Shown are the results of 5 independent experiments. P values were calculated using a two-tailed t-test (normal distribution data) or Mann-Whitney test (non-normal distribution data). The significance of P value is indicated on the graph, *p<0.05, **p<0.01.

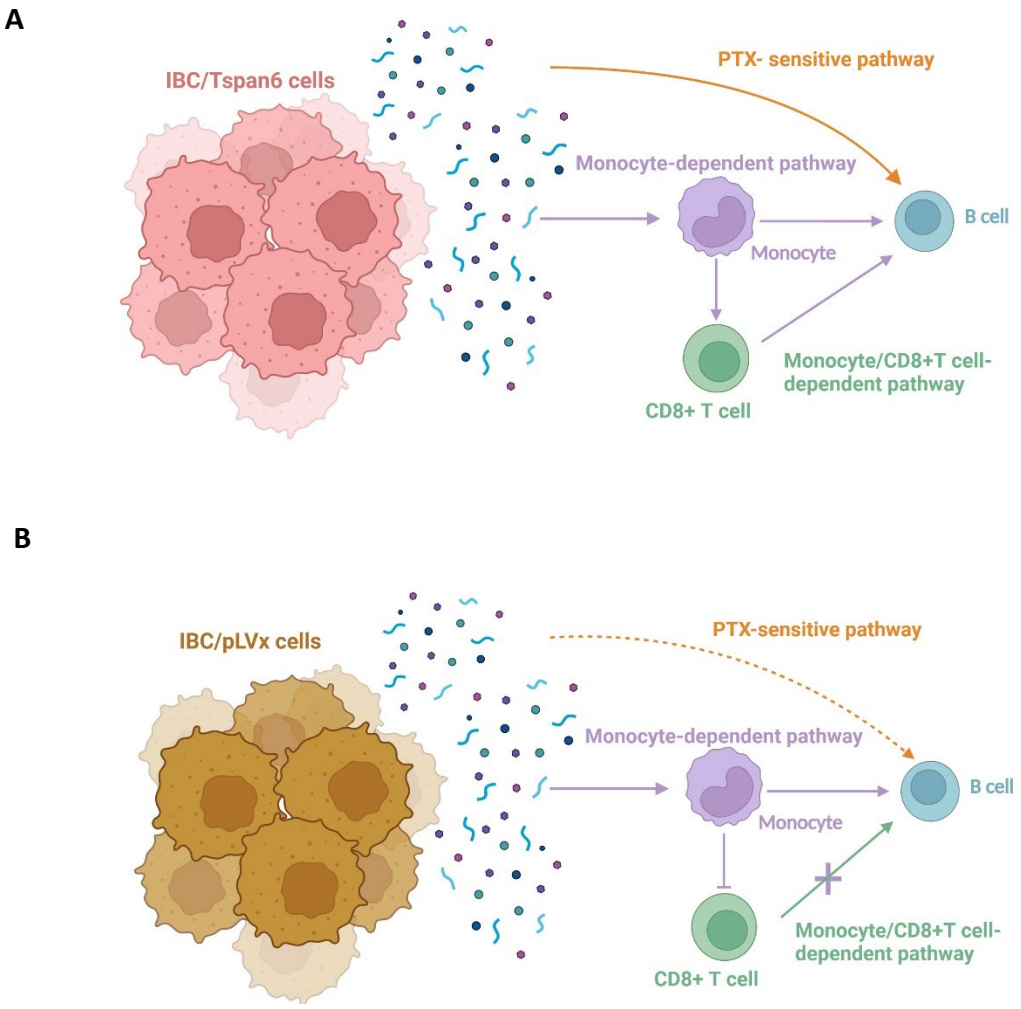

Figure 6-7. Proposed model depicting how Tspan6 regulates the chemoattractive potential of IBC for B cells at the early stage. Three pathways are shown: monocyte-dependent pathway, monocyte/CD8+ T cell-dependent pathway, and PTX-sensitive (monocyte-independent) pathway. **(A)** Monocytes activated by the stimuli from IBC/Tspan6 cells enhance the migration of B cells. In parallel, monocytes confer a pro-migration capability to CD8+ T cells, allowing them to promote the migration of B cells. Apart from the above two pathways, chemotactic factors produced by IBC/Tspan6 cells can also directly regulate the migration of B cells by secreting PTX-sensitive mediator(s). **(B)** While maintaining the monocyte-dependent pathway, IBC/pLVx cells lost the monocyte/CD8+ T cell-dependent regulation. Mechanistically, monocytes activated by the stimuli from IBC/pLVx cells suppress the pro-migration function of CD8+ T cells, which abolishes a CD8+ T cell-stimulated B cell movement. In addition, the involvement of PTX sensitive mediator(s) in regulating B cell migration to CM-IBC/pLVx remained unclear, requiring more experiments to confirm.

6.7. Discussion

Having established the role of Tspan6 in enhancing the chemoattractive potential of IBC cells for B lymphocytes at the early stage, we attempted to understand the underlying mechanisms. In general, the data here demonstrated that Tspan6 promoted the migration of B cells via a combination of monocyte-dependent, monocyte/CD8+ T cell-dependent, and monocyte-independent (PTX-sensitive) pathways.

Our recent data (unpublished) have demonstrated that the cytoplasmic expression of Tspan6 correlated with the co-localisation of stomal B cells and macrophages ($p = 0.04$). Furthermore, the intratumoral co-existence of B cells with macrophages was associated with positive membranous expression of Tspan6 ($p = 0.04$). These data support our *in vitro* findings that Tspan6 expressed by IBC cells enhances the ability of monocytes/macrophages to potentiate B cell migration.

Molecular networks explaining how monocytes contribute to the communication between Tspan6-expressing IBC cells and B lymphocytes are currently unknown. Therefore, we preliminarily assessed the expression of some common B cell chemotaxis-related chemokines (i.e. CXCL10, CXCL12, CXCL13 and CCL20) in double CM (Dou CM-SUM149/Tspan6 and DOU CM-SUM149/pLVx). Our data indicate that monocytes exposed to CM of IBC cells-expressing Tspan6 did not acquire a promoted biosynthesis of these chemokines (Supplementary Figure 1-5). While the role of chemokines warranted more further

investigations, the potential effect of cytokines on B cell migration cannot be neglected. For example, TNF-α, a cytokine abundantly produced by monocytes (Farrokhi M *et al.*, 2015), exhibits the ability to drive the recruitment of B cells in TIME (Shaul ME *et al.*, 2021). In this regard, Ghods *et al*. found that B cells collected from the breast draining lymph nodes highly expressed TNF-α receptor 2 (TNFR2) (Ghods A *et al.*, 2019), and the activation of TNFR2 is known to trigger the migration and proliferation of immune cells (Bradley JR, 2008; Mercogliano MF, Bruni S, Elizalde PV and Schillaci R, 2020). Likewise, monocyte-produced proinflammatory cytokine MIF (Calandra T and Roger T, 2003) has also been reported to enhance the B cell chemotaxis via binding to MIF receptors CXCR4 and CD74 (Klasen C *et al.*, 2014). In addition to their direct promigratory activities, cytokines can modulate the sensitivity of B cells to chemokines, such as IFN-α, which was suggested to promote the chemotaxis of B cells in response to CCL20, CCL21 and CXCL12 (Badr G *et al.,* 2005). Specifically, IFN-α was shown to increase the chemotaxis of B cells by reducing the internalisation of chemokine receptors and promoting the activation of the chemokine-induced signaling pathway (Badr G *et al.*, 2005). Monocytes are an important source of IFN-α (Boyette LB *et al.*, 2017).

Although we do not know the precise mechanism for monocyte-dependent regulation, the results of the cell migration assay using double CM suggest that the presence of monocytes is required for Tspan6-dependent B cell migration. We found that Dou CM-SUM149/Tspan6 was only as chemotactic to B cells as the Dou CM-SUM149/pLVx. Two possibilities could explain

why Dou CM-SUM149/Tspan6 did not attract more B cells than Dou CM-SUM149/pLVx. The first is that the B cell migration is regulated by a direct cell-to-cell contact whereby monocytes physically interact with B cells, directing the B cells to CM-SUM149/Tspan6. For example, B-cell activating factor (BAFF), a member of TNF family, are expressed by monocytes (Tribouley C *et al.*, 1999). It was reported that the membrane-bound form of BAFF was biologically active for B cells, which induced the activation of B cells by binding to the receptos (BAFFR and TACI) (Nicoletti AM *et al.*, 2016). The second possibility is that chemotactic factors secreted by T6-monocytes are short-lived and possibly degraded during four-hour incubation at 37°C (our experimental set-up for short-term migration), such as TNF-α (Ma Y *et al.*, 2015).

To our surprise, monocytes enhance B cell migration not only on their own but also through the cooperation with CD8+ T cells in the context of Tspan6 expression. This phenomenon is particularly interesting as monocytes acquire distinct modulatory abilities when exposed to different types of CM-IBC. While monocytes exposed to CM-IBC/pLVx suppress the migration of CD8+ T cells, monocytes exposed to CM-IBC/Tspan6 do not or exert a minor promotional effect. Based on this, we propose that monocyte-inhibited CD8+ T cells cannot stimulate the migration of B cells, whereas monocyte-activated monocytes can. That said, one cannot exclude a direct impact of different CM-IBC on CD8+ T cells. In this regard, we found that, without monocytes (pure CD8+ T cell supplementation experiments), CD8+ T cells exposed to CM-SUM149/pLVx (Con-CD8+ T cells) appear to enhance the short-term migration of B cells (though this change did not reach a statistical significance). However, CD8+ T cells exposed to

CM-SUM149/Tspan6 (T6-CD8+ T cells) had no such tendency. This observation indicates that lacking of the T6-monocytes' help, T6-CD8+ T cells have no or poor ability to stimulate B cell migration, whereas the absence of pLVx-monocytes alleviated the inhibitory effect on pLVx-CD8+ T cell stimulation of B cell migration. In short, these interesting findings indicate the pleiotropic functions of monocytes and highlight the pivotal role of monocytes/macrophages in the TIME of IBC.

Monocytes are antigen-presenting cells (APCs) that express MHC class I and co-stimulatory molecules, which are important for CD8+ T cell activation (Affandi AJ *et al.*, 2021). Moreover, monocytes/macrophages can produce a diverse range of soluble factors that either activate CD8+ T cells (e.g. IL-12, IL-6, and TNF-α (Rossol M *et al.*, 2011; Mohamed MM *et al.*, 2014; St Paul M and Ohashi PS, 2020)), or suppress their function (e.g. IL-10, TGF-β (Chen ML *et al.*, 2005; Rossol M *et al.*, 2011; Chang LY *et al.*, 2012; Smith LK *et al.*, 2018)). An early study demonstrated that CD14+ monocytes/macrophages collected from the axillary vein tributaries of IBC patients secreted IL-10 and TNF-α (Mohamed MM *et al.*, 2014). As for CD8+ T cells, they are currently recognised as a heterogeneous population of cells with five subtypes identified (St Paul M and Ohashi PS, 2020). Among them, Tc1 cells (the classic CD8+ T cells) have been shown to produce TNF-α (St Paul M and Ohashi PS, 2020) and, therefore, can affect B cell migration as described above. In addition, Tc17 cells characterised by IL-17 production (St Paul M and Ohashi PS, 2020) may also potentially implicate B cell migration. Interestingly, IL-17 does not affect the migration of B cells directly, but it can promote the chemotaxis of B

cells in response to CXCL12 and CXCL13 due to its capability to inhibit the expression of RGS16, the negative regulator for chemokine receptor signalling pathway (Ferretti E, Ponzoni M, Doglioni C and Pistoia V, 2016). Furthermore, Tc17 is often seen in the TIME of breast cancer (Faghih Z *et al.*, 2013).

In contrast to monocyte-dependent regulation that requires non-B cells to function as intermediates, the monocyte-independent pathway (PTX-sensitive mediators) can modulate the B cell migration directly. We discovered that PTX significantly inhibited the short-term migration of pure B cells towards CM-SUM149/Tspan6, but, perhaps due to insufficient experiment replications, the effect of PTX on the direct chemotactic effect of CM-SUM149/pLVx was less pronounced. PTX specifically inhibits the Gαi subunit of trimeric G proteins that are associated with GPCRs for chemokines (Hughes CE and Nibbs R, 2018). Though results of chemokine array and ELISA experiments could not represent all the alterations of chemokine/cytokine biosynthesis that occurred in IBC cells when Tspan6 was expressed, we temporarily do not consider chemokines and cytokines are the main mediators controlling the B cell short-term migration. In addition to chemokines and cytokines, PTX can also block the signal transduction of some bioactive lipids (Li YF *et al.*, 2016; van Jaarsveld MT, Houthuijzen JM and Voest EE, 2016). Recent studies have demonstrated that some lipids are involved in regulating the chemotactic migration of B cells, such as Sphingosine-1 (S1P) (Sic H *et al.*, 2014) and oxysterols (Liu C *et al.*, 2011). Unpublished data from our lab showed that Tspan6 upregulated the chemoattractive potential of non-IBC cells for B cells via increasing

the secretion of several oxysterol species. Thus, further investigation will be required to examine whether these or other bioactive lipids (e.g. prostaglandins) are involved in the Tspan6-dependent IBC-B cell communication axis.

In summary, we identified three types of regulations: monocyte-dependent pathway, monocyte/CD8+ T cell-dependent pathway, and PTX-sensitive (monocyte-independent) pathway, by which IBC/Tspan6 cells could modulate the short-term migration of B cells (Figure 6-7). These different modulations co-exist and represent a key element of the complex communication networks established by the Tspan6-expressing IBC cells, which ultimately develop a specific immune niche found in the Tspan6-positive IBC tissues.

7. RESULTS CHAPTER V: TSPAN6-INVOLVED SIGNALLING PATHWAYS

7.1. Introduction

We have shown that Tspan6 upregulated the chemoattractive potential of IBC cells for B cells *in vitro*, and monocytes, CD8+ T cells and PTX-sensitive factor(s) were involved in this regulation. It has been shown that tetraspanins regulate signalling pathways (e.g. NF-κB, p38 MAPK) that can potentially affect the production of chemotactic factors by cancer cells (Hwang JR *et al.*, 2012; Zhang B *et al.*, 2018; Ding H *et al.*, 2019; Gao C *et al.*, 2021). These tetraspanin-dependent chemoattractants appear to regulate the recruitment of immune cells (Ding H *et al.*, 2019; Gao C *et al.*, 2021). In this chapter, we described the results of the experiments aiming to address the question of how Tspan6 affects intracellular signalling pathways, which may explain the enhanced chemoattractive potential of IBC cells. In addition, we attempted to determine the role of the Tspan6 partner protein, syntenin-1 (Guix FX *et al.*, 2017; Andrijes R *et al.*, 2021), as well as the roles of syntenin-1-associated molecules (Shimada T, Yasuda S, Sugiura H and Yamagata K, 2019) in enhancing the chemoattractive potential of IBC cells.

7.2. Tspan6 and syntenin-1

7.2.1. Tspan6 associates with syntenin-1 in IBC cells but does not alter the endogenous expression and phosphorylation level of syntenin-1

Two studies reported a direct association between Tspan6 and syntenin-1 in human colorectal

cancer cells and embryonic kidney cells (Guix FX *et al.*, 2017; Andrijes R *et al.*, 2021). Firstly, we wanted to confirm the association of Tspan6 and syntenin-1 in our cell models. Flag-tagged Tspan6 was immunoprecipitated using anti-Flag mAb pre-conjugated with agarose. The presence of syntenin-1 in the Tspan6-containing protein complex was detected by western blot. As anticipated, the Tspan6-syntenin-1 complex was detected in both SUM149/Tspan6 and BCX010/Tspan6 cell lines (Figure 7-1 A). Furthermore, the total expression of syntenin-1 in IBC cells was not affected by Tspan6 expression (Figure 7-1 A).

A previous study suggested that the phosphorylation of syntenin-1 could affect the binding of syntenin-1 to its partner proteins (Rajesh S *et al.*, 2011). Thus, three known sites that are identified to be phosphorylated in syntenin-1 (serine 6 S6 (Rajesh S *et al.*, 2011), tyrosine 4 Y4 (Sala-Valdés M *et al.*, 2012), and tyrosine 46 Y46 (Imjeti NS *et al.*, 2017)) were examined using custom-made anti-phospho-syntenin-1 Abs. We only observed a marginal increase in the phosphorylation of Tyr^{46} and a minor decrease in the phosphorylation at Tyr^{4} in SUM149/Tspan6 compared to SUM149/pLVx (Figure 7-1 B and C). However, all the alterations between SUM149/Tspan6 and SUM149/pLVx did not reach statistical significance. Similarly, we observed varied results in the BCX010 cell pair (Figure 7-1 B, D). Therefore, Tspan6 does not consistently affect the phosphorylation of syntenin-1 in IBC cells.

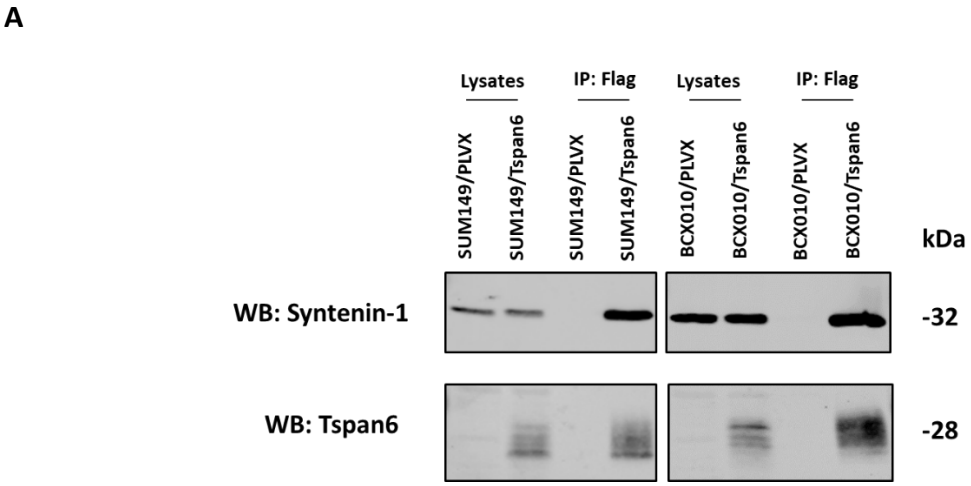
A
Lysates
IP: Flag
Lysates
IP: Flag
SUM149/PLVX
SUM149/Tspan6
SUM149/PLVX
SUM149/Tspan6
BCX010/PLVX
BCX010/Tspan6
BCX010/PLVX
BCX010/Tspan6
kDa
WB: Syntenin-1
-32
WB: Tspan6
-28

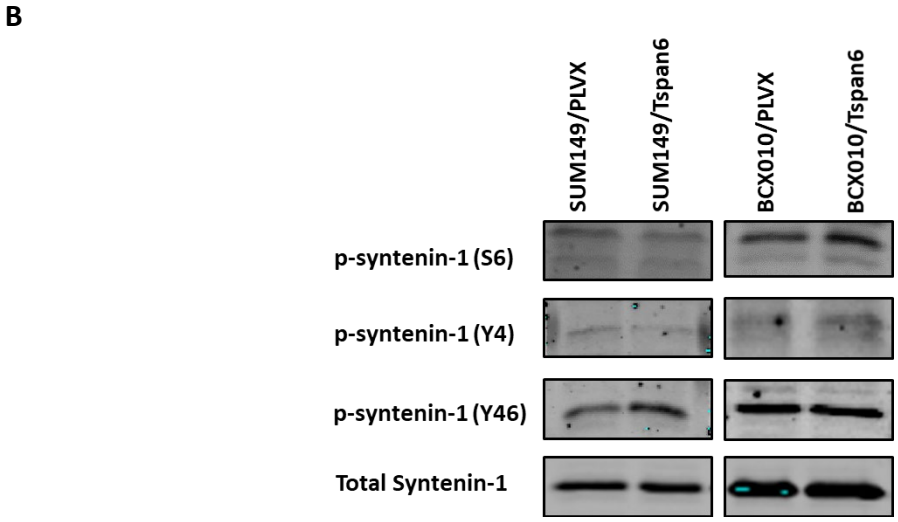
B
SUM149/PLVX
SUM149/Tspan6
BCX010/PLVX
BCX010/Tspan6
p-syntenin-1 (S6)
p-syntenin-1 (Y4)
p-syntenin-1 (Y46)
Total Syntenin-1

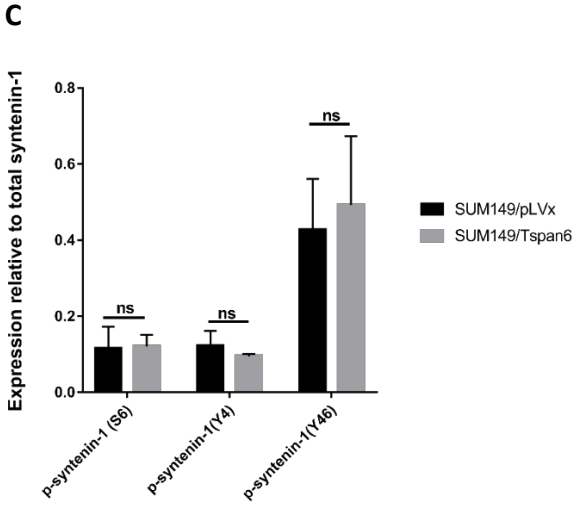
C
Expression relative to total syntenin-1
0.8
0.6
0.4
0.2
0.0
ns
ns
ns
p-syntenin-1 (S6)
p-syntenin-1(Y4)
p-syntenin-1(Y46)
SUM149/pLVx
SUM149/Tspan6

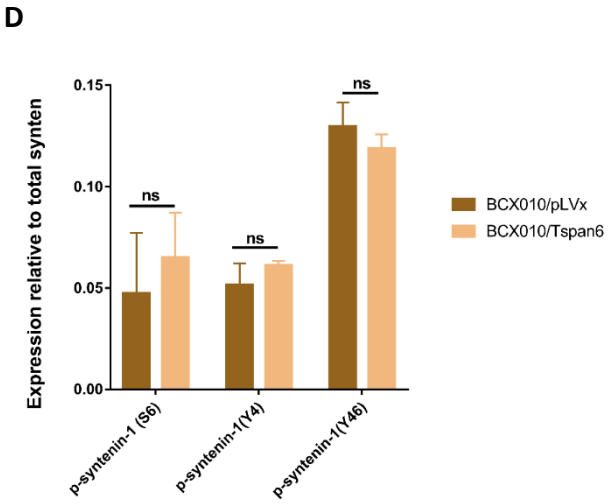
D
Expression relative to total synten
0.15
0.10
0.05
0.00
ns
ns
ns
p-syntenin-1 (S6)
p-syntenin-1(Y4)
p-syntenin-1(Y46)
BCX010/pLVx
BCX010/Tspan6

Figure 7-1. The effects of Tspan6 on syntenin-1. (A) Tspan6 interacted with syntenin-1 but did not alter its endogenous expression level. SUM149 and BCX010 cells expressing Flag-Tspan6 were lysed in immunoprecipitated buffer (1% Brij98) and incubated with monoclonal anti-Flag conjugated-agarose. Lysates of SUM149/pLVx and BCX010/pLVx were applied as controls. Protein complexes were collected and resolved on 12% SDS-PAGE and subsequently were probed with anti-syntenin-1 mAb and anti-Tspan6 polyclonal Ab in western blotting. The lower panel shows the efficiency of Tspan6 precipitation. **(B)** The expression of Tspan6 did not significantly alter the phosphorylation status of syntenin-1. Lysates prepared from SUM149/Tspan6, SUM149/pLVx and BCX010/Tspan6 and BCX010/pLVx were resolved on 12% SDS-PAGE and were subsequently detected with customised anti-phospho-syntenin-1 mAbs in western blotting. Total syntenin-1 was used as a loading control in this blot. **(C, D)** Relative phosphorylation levels of syntenin-1 in IBC cells. The phosphorylation levels of syntenin-1 at different residues were assessed based on the ratio of p-syntenin-1 in total. Shown are means with SD of the results of 3 independent experiments. P values were calculated using a two-tailed t-test and are indicated on the graph, *p<0.05.

7.2.2. Tspan6 promoted the chemoattractive potential of IBC cells via associating with syntenin-1

As the association between Tspan6 and syntenin-1 in IBC cells was confirmed, we wanted to examine whether syntenin-1 was required for Tspan6 to promote the chemoattractive potential of IBC cells. To address this question, we performed siRNA-based knockdown experiments to decrease the expression of endogenous syntenin-1 in SUM149/Tspan6 and SUM149/pLVx cells (SUM149/Tspan6 syn-KD and SUM149/pLVx syn-KD). CM from these cells was used as chemoattractants in the "short-term" migration experiments as described above. We found that the number of B lymphocytes migrating towards CM-SUM149/Tspan6 syn-KD markedly decreased when compared to the number of B cells migrating to CM-SUM149/Tspan6 ($p < 0.05$) (Figure 7-2 B), whereas this reduction was not observed when the expression of syntenin-1 was

suppressed in SUM149/pLVx cells (Figure 7-2 A). As a result, the knockdown of syntenin-1 abolished the difference between the chemoattractive potential of CM-SUM149 /Tspan6 and CM-SUM149/pLVx. (Figure 7-2 C).

It was suggested that the last two C-terminal amino acids were essential for Tspan6 to bind syntenin-1 (Guix FX *et al.*, 2017). Thus, we established SUM149 cells expressing Tspan6 mutant by substituting valine in the C-terminal with glycine (SUM149/Tspan6 V/G). Results of "sustained" cell migration experiments revealed that the number of B cells migrating to CM-SUM149/Tspan6 V/G significantly decreased compared to CM-SUM149/Tspan6 (Figure 7-3 A). Furthermore, the disruption between Tspan6 and syntenin-1 downregulated the chemotactic effect of SUM149/Tspan6 cells to the level of SUM149/pLVx (Figure 7-3 A). These data further confirmed that the association with syntenin-1 was essential for Tspan6 to enhance the chemoattractive potential of IBC cells for B lymphocytes.

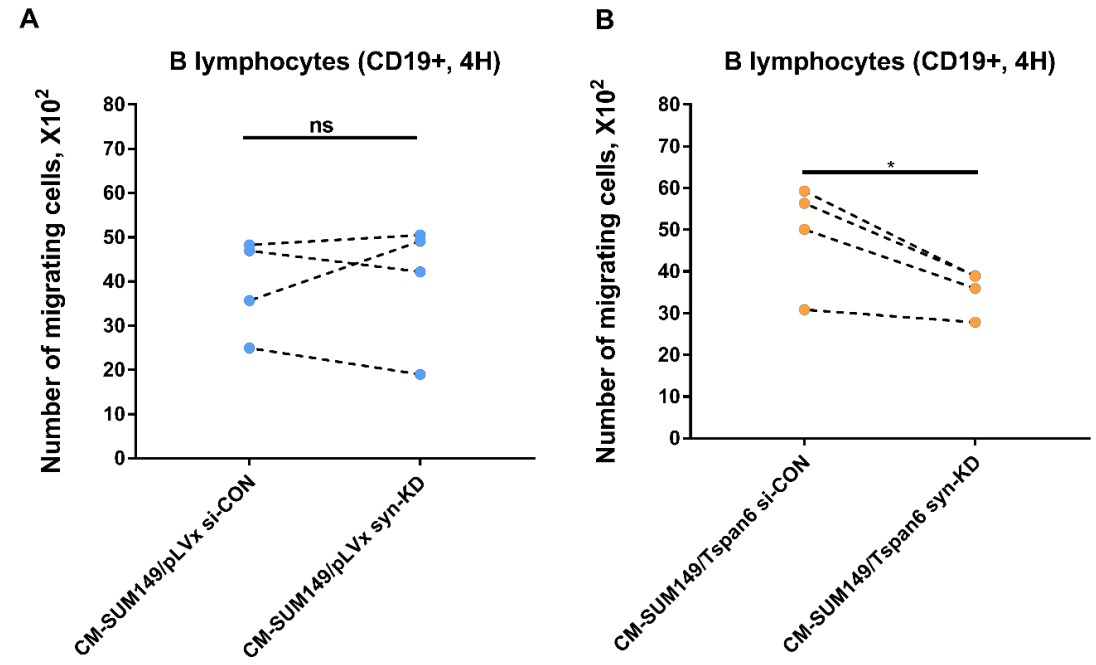
A
B lymphocytes (CD19+, 4H)
Number of migrating cells, X10²
ns
CM-SUM149/pLVx si-CON
CM-SUM149/pLVx syn-KD
B
B lymphocytes (CD19+, 4H)
Number of migrating cells, X10²
*
CM-SUM149/Tspan6 si-CON
CM-SUM149/Tspan6 syn-KD

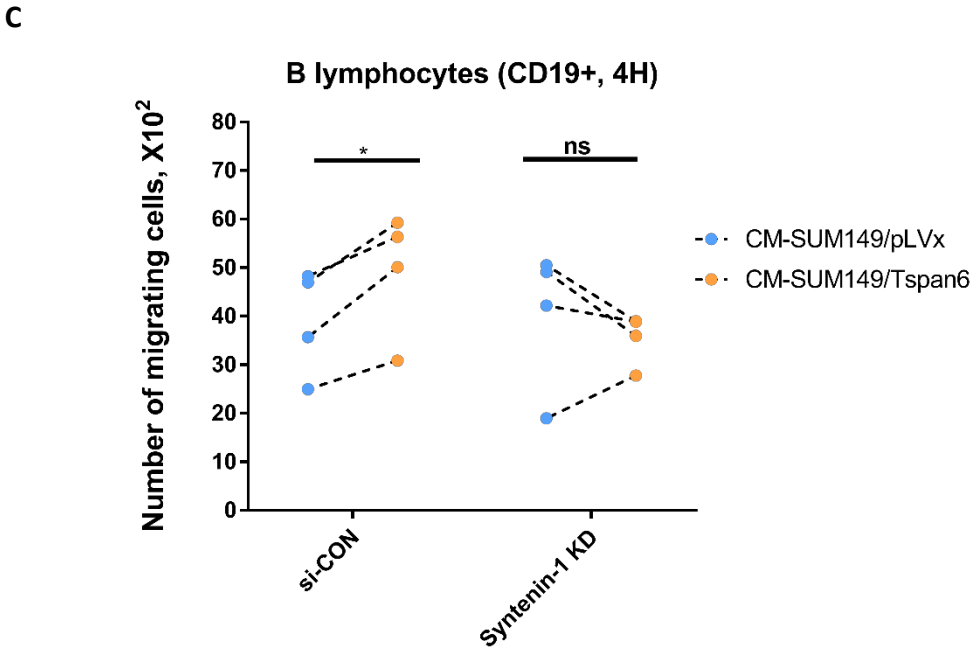
C
B lymphocytes (CD19+, 4H)
Number of migrating cells, X10²
*
ns
si-CON
Syntenin-1 KD
CM-SUM149/pLVx
CM-SUM149/Tspan6

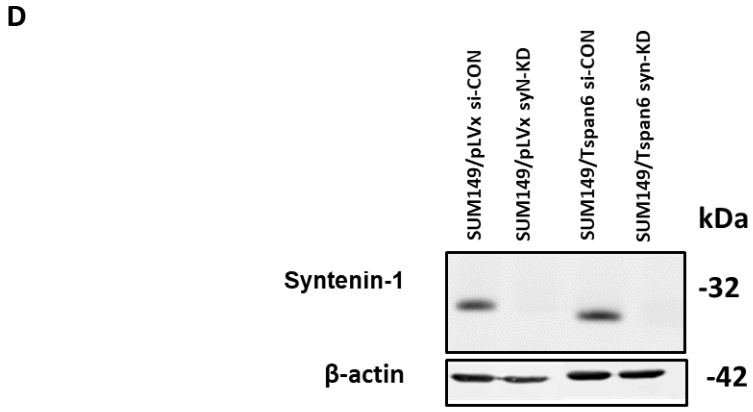

Figure 7-2. Tspan6 enhances the chemoattractive potential of IBC cells for B cells via associating with syntenin-1. (A-B) The short-term migration of B cells to SUM149/pLVX (A) and CM-SUM149/Tspan6 (B) before and after the syntenin-1 knockdown. **(C)** The knockdown of syntenin-1 abrogated the advantage of CM-SUM149/Tspan6 in attracting B cells. The difference between B cell migration to CM-SUM149/Tspan6 and CM-SUM149/pLVx after syntenin-1 knockdown was evaluated. PBMCs ($2x10^6$ cells/200 µl) were allowed to migrate to CM-SUM149/Tspan6 syn-KD and CM-SUM149/pLVx syn-KD, as well as to CM-SUM149/Tspan6 si-CON and CM-SUM149/pLVx si-CON (controls), for 4 hours. Migration of B lymphocytes towards individual CM was assessed. Numbers connected by a dotted line indicate a donor-matched comparison. Shown are the results of 4 independent experiments under each condition. P values were calculated using a two-tailed t-test and are indicated on the graph, *$p<0.05$. **(D)** The efficiency of syntenin-1 knockdown. Representative western blot showing the expression of syntenin-1 in SUM149/Tspan6 and SUM149/pLVx cells treated with control siRNA and syntenin-1 siRNA for 4 days.

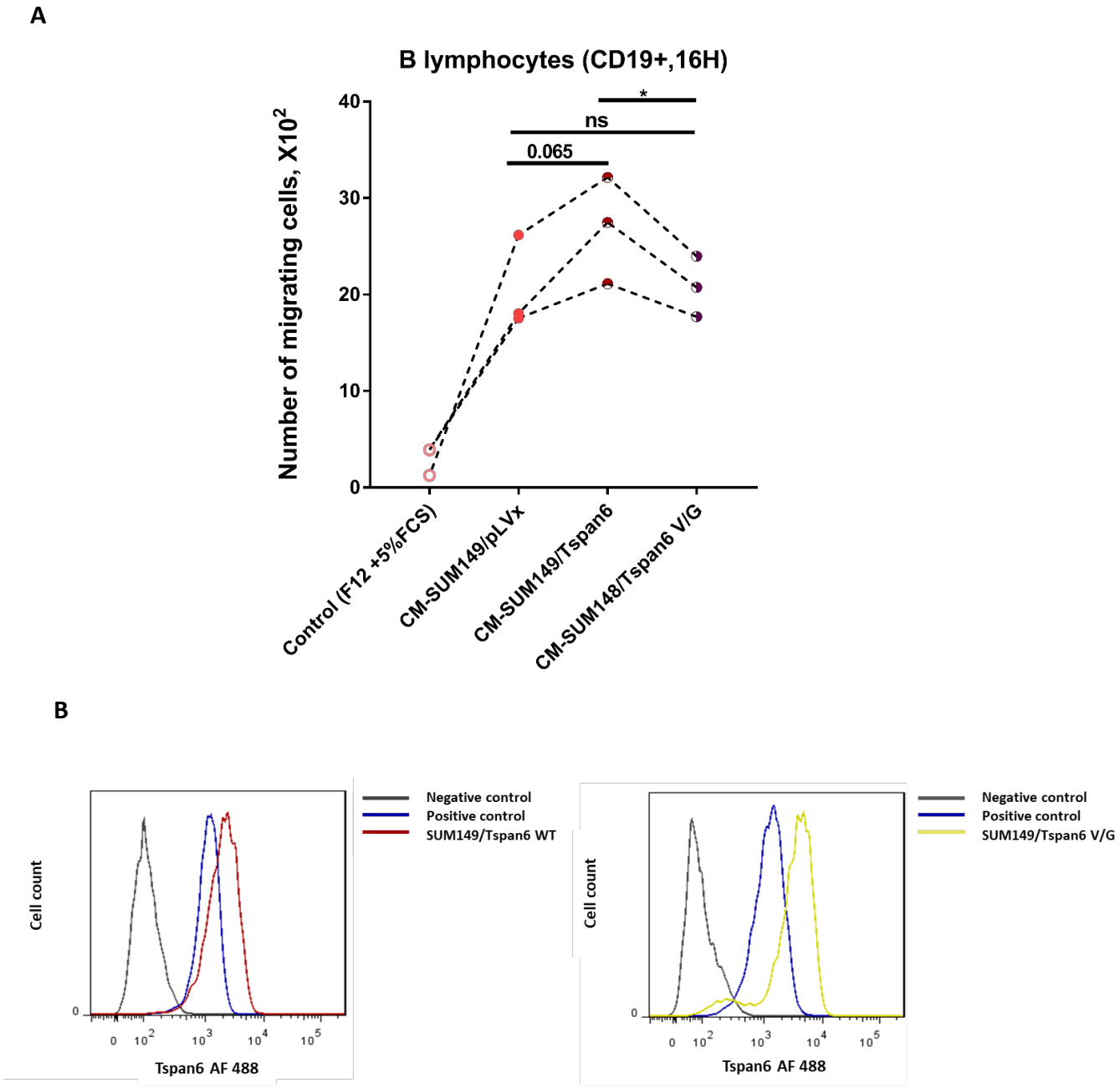

Figure 7-3. The mutation of Tspan6 reduces the Tspan6/syntenin-1 complex-dependent B cell short-term migration. (A) The 4-hour migration to CM-SUM149/Tspan6, CM-SUM149/Tspan6 V/G, CM-SUM149/pLVx and control medium. The interaction between Tspan6 and syntenin-1 was abolished by substituting valine in the C-terminal of Tspan6 with glycine (SUM149/Tspan6 V/G). The sustained migration of B cells to above CM was assessed separately. Numbers connected by dot line indicated donor-matched experiment. Shown are the results of 3 independent experiments under each condtion. P values were calculated using two-tailed t-test are indicated on the graph, *p<0.05. **(B)** Tspan6 expression was assessed by FACS with an in-house generated mouse antibody against Tspan6. Ab M38 (Anti-CD81) and Ab 4C5G (anti-Type II PI 4-kinase) were applied as positive and negative controls.

7.3. Tspan6 and p38 MAP kinase

7.3.1. Tspan6 expression was associated with hyperactivation of p38 MAP Kinase in IBC cells

To determine which signalling pathway is responsible for the Tspan6/syntenin-1-dependent chemotactic effect of IBC cells, we analysed the activation of pathways related to syntenin-1 (Boukerche H *et al.*, 2008; Sun L *et al.*, 2020) and IBC development (X Wang TS, LTH Phi SC and Iwase T, 2020). Specifically, we evaluated the phosphorylation status of proteins from the PKC pathway, PI3K/AKT/mTOR pathway, and MAPKs (ERK, p38, and JNK) pathway, as well as some of the proteins linked to mRNA translation, cellular stress, and cell-adhesion (Supplementary Figure 1-6). Western blotting and densitometric analysis revealed that the phosphorylation level of p38 MAPK was consistently higher in Tspan6-expressing IBC cells than in control IBC cells (Figure 7-4 A, Supplementary Figure 1-6). As p38 MAPK consists of four isoforms (García-Hernández L *et al.*, 2021), p38α (MAPK14), p38β (MAPK11), p38γ (MAPK12 / ERK6), and p38δ (MAPK13 / SAPK4), we firstly assessed the total expression of each isoform in our cellular models. With the exception of p38δ, which did not express in BCX010 cells, p38α, p38β, and p38γ were readily detectable in both IBC cell lines. Importantly, Tspan6 did not change the total expression levels of these p38 isoforms (Figure 7-4 B).

A

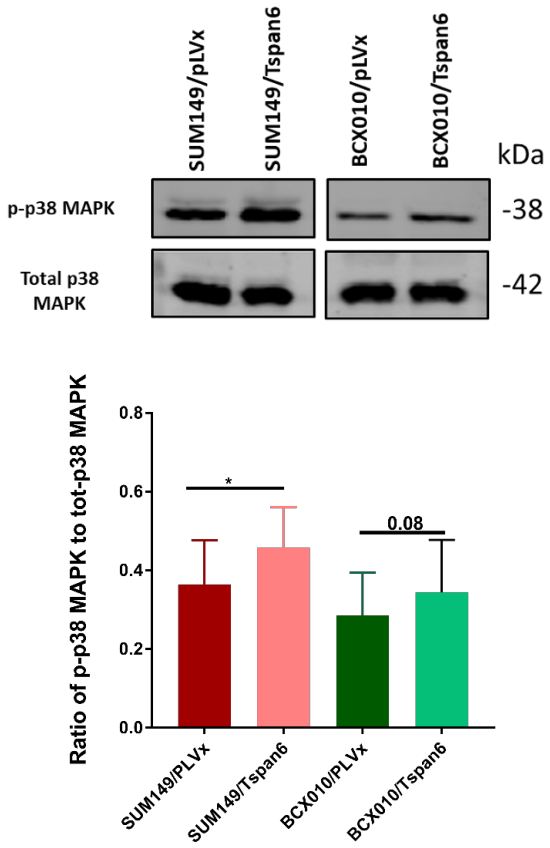
SUM149/pLVx
SUM149/Tspan6
BCX010/pLVx
BCX010/Tspan6
kDa
p-p38 MAPK
-38
Total p38 MAPK
-42
Ratio of p-p38 MAPK to tot-p38 MAPK
0.8
0.6
0.4
0.2
0.0
*
0.08
SUM149/PLVx
SUM149/Tspan6
BCX010/PLVx
BCX010/Tspan6

B

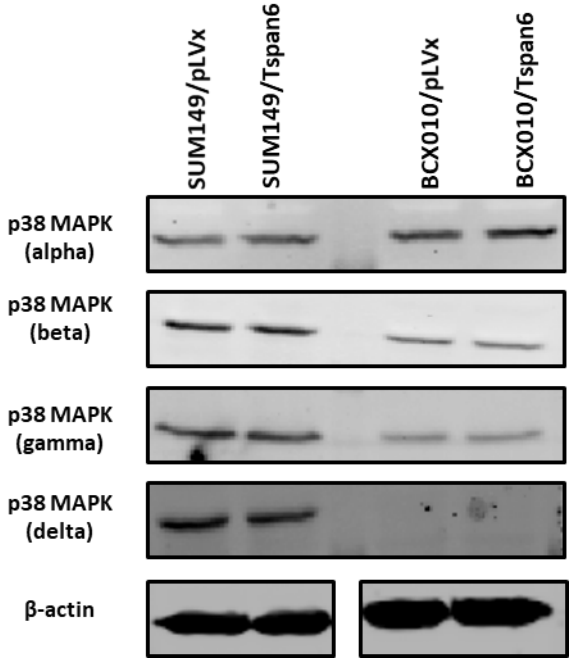
SUM149/pLVx
SUM149/Tspan6
BCX010/pLVx
BCX010/Tspan6
p38 MAPK (alpha)
p38 MAPK (beta)
p38 MAPK (gamma)
p38 MAPK (delta)
β-actin

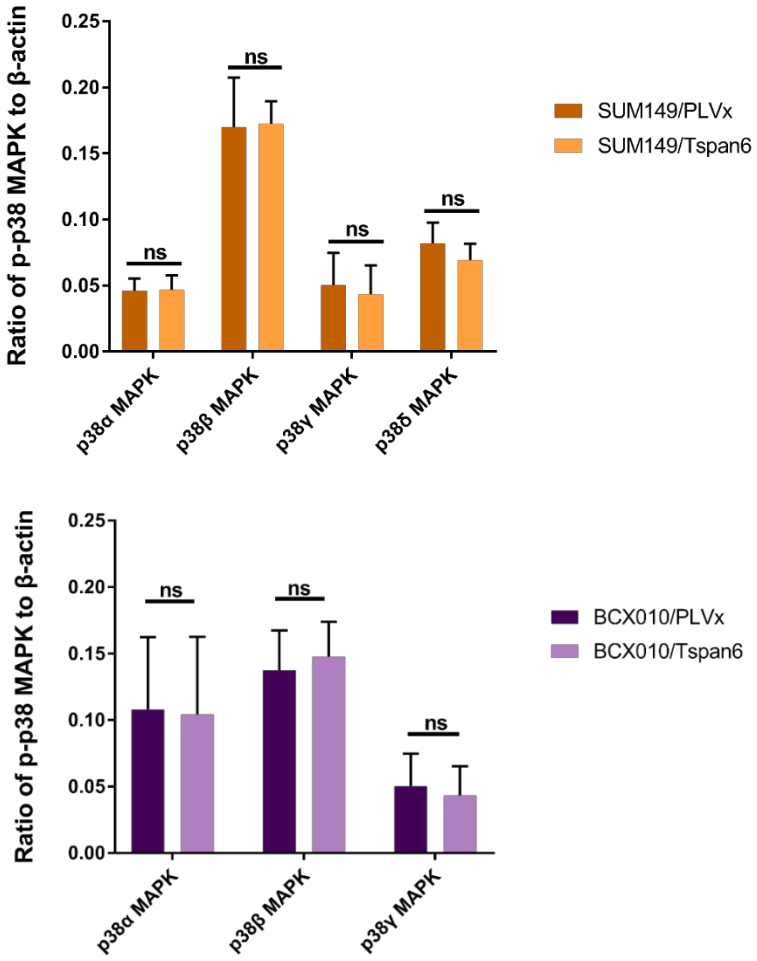

Figure 7-4. The effects of Tspan6 on the expression of p38 MAPKs. (A) Tspan6 expression upregulated the activation of p38 MAPK in IBC cells. The extent of phosphorylation of p38 MAPK was assessed based on the ratio of p38 MAPK in total. **(B)** Tspan6 had no effect on the total expression of any Isoform of p38 MAPK. β-actin was shown as the loading control. Shown are means with SD of the results of 3 independent experiments. P values were calculated using a two-tailed t-test and are indicated on the graph.

7.3.2. Tspan6 enhances the chemoattractive potential of IBC cells via p38β MAPK

Next, we examined the effect of different p38 MAPK isoforms on the Tspan6-dependent B cell migration. The expression of p38α, p38β, and p38γ in SUM149/Tspan6 and SUM149/pLVx was separately decreased using a siRNA-based knockdown protocol as described above. CM

from these cells was used in our short-term migration experiments. We found that the knockdown of p38β MAPK significantly reduced the chemoattractive potential of SUM149/Tspan6 cells for B lymphocytes while having no apparent effect on the migration of B cells to CM-SUM149/pLVx (Figure 7-5 D). Importantly, p38β MAPK knockdown negated the difference between the chemoattractive potential of CM-SUM149/Tspan6 and CM-SUM149/pLVx (Figure 7-5 E). In contrast, the silencing of p38α had no significant impact on the pro-migratory activities of any CM (Figure 7-5 A and B). The influence of p38γ MAPK knockdown remained unclear due to limited replicates (Figure 7-5 G and H). In conclusion, our results show that p38β MAPK is involved in regulating the Tspan6-dependent B cell migration.

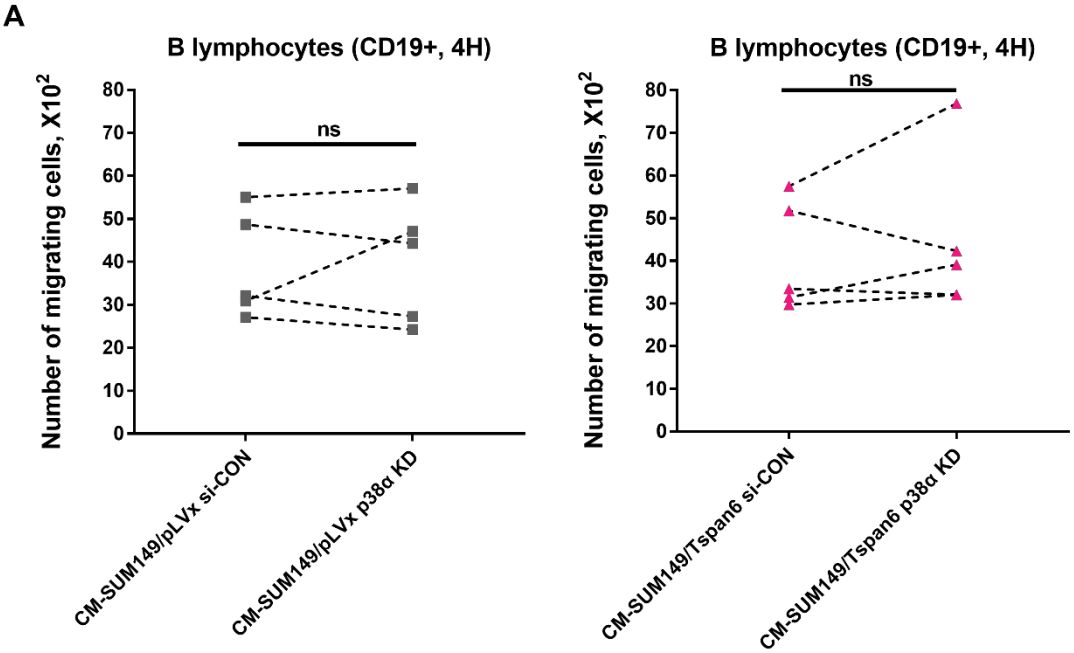

B

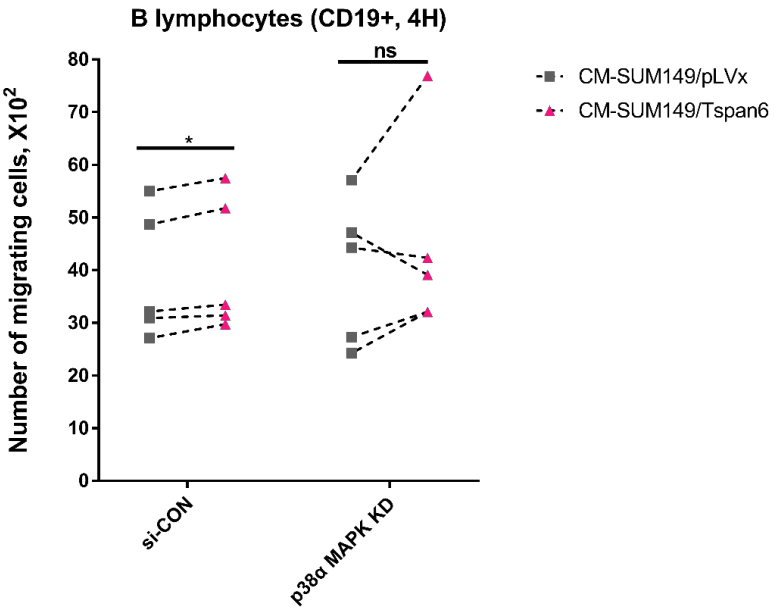
B lymphocytes (CD19+, 4H)
Number of migrating cells, X10²
80
70
60
50
40
30
20
10
0
*
ns
si-CON
p38α MAPK KD
CM-SUM149/pLVx
CM-SUM149/Tspan6

C

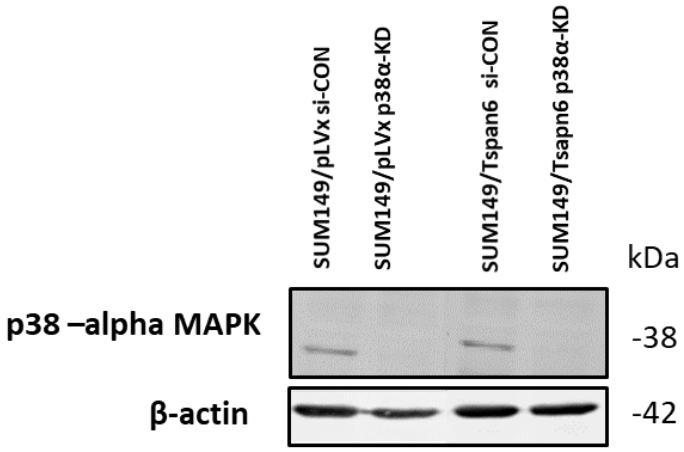
SUM149/pLVx si-CON
SUM149/pLVx p38α-KD
SUM149/Tspan6 si-CON
SUM149/Tsapn6 p38α-KD
kDa
p38 –alpha MAPK
-38
β-actin
-42

D

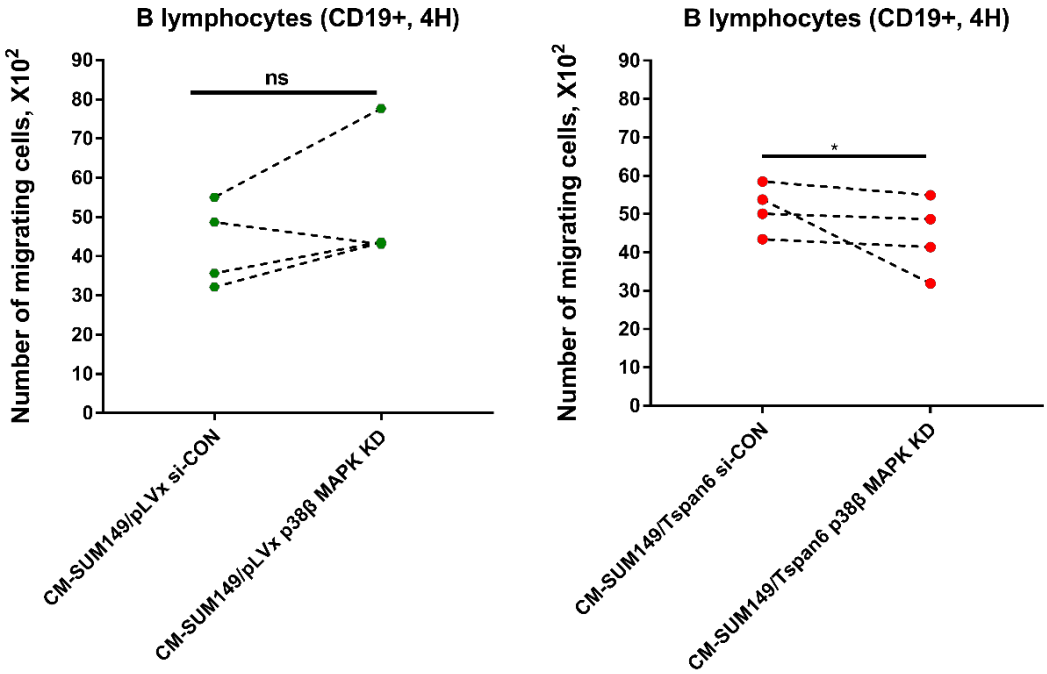
B lymphocytes (CD19+, 4H)
Number of migrating cells, X10²
ns
CM-SUM149/pLVx si-CON
CM-SUM149/pLVx p38β MAPK KD
B lymphocytes (CD19+, 4H)
Number of migrating cells, X10²
*
CM-SUM149/Tspan6 si-CON
CM-SUM149/Tspan6 p38β MAPK KD

E

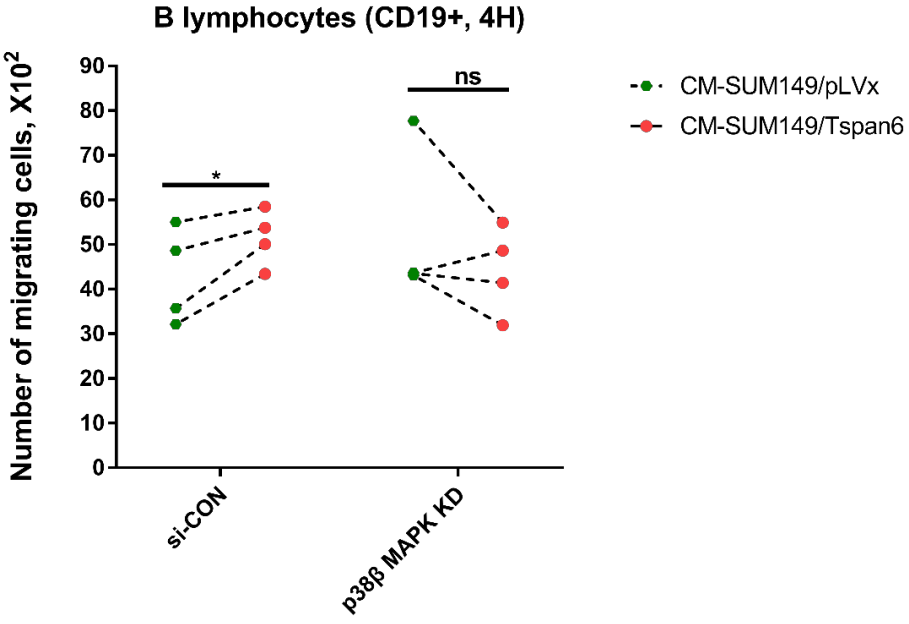
B lymphocytes (CD19+, 4H)
Number of migrating cells, X10²
*
ns
si-CON
p38β MAPK KD
CM-SUM149/pLVx
CM-SUM149/Tspan6

F

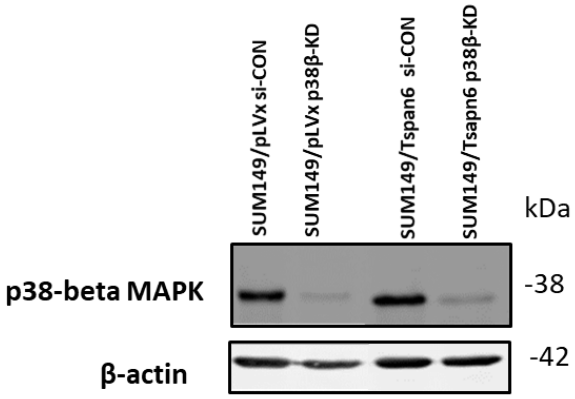
SUM149/pLVx si-CON
SUM149/pLVx p38β-KD
SUM149/Tspan6 si-CON
SUM149/Tsapn6 p38β-KD
kDa
p38-beta MAPK
-38
β-actin
-42

G

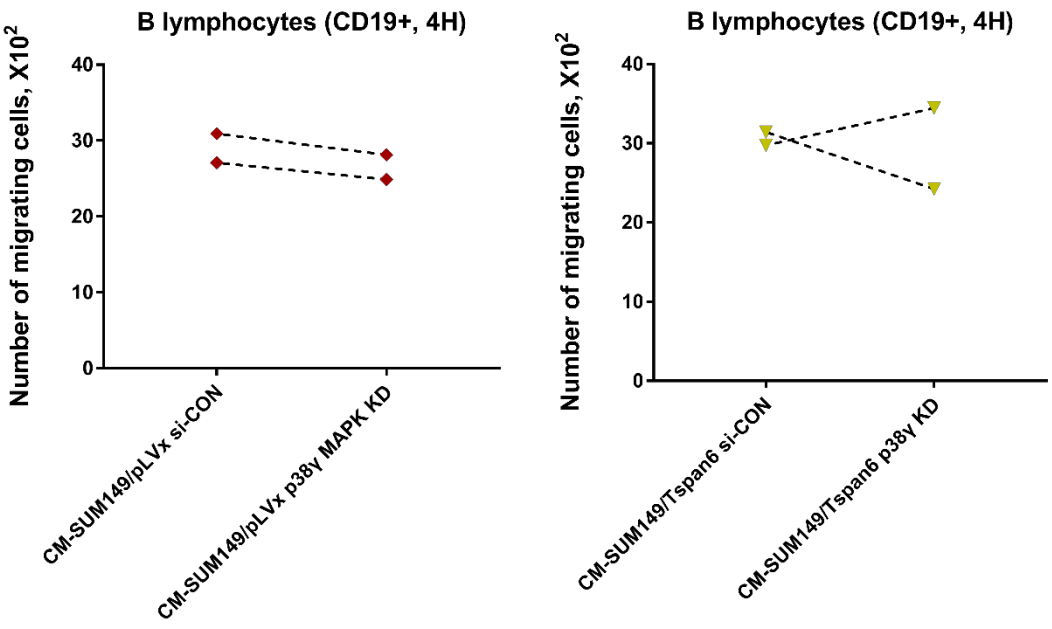
B lymphocytes (CD19+, 4H)
Number of migrating cells, X10²
40
30
20
10
0
CM-SUM149/pLVx si-CON
CM-SUM149/pLVx p38γ MAPK KD
B lymphocytes (CD19+, 4H)
Number of migrating cells, X10²
40
30
20
10
0
CM-SUM149/Tspan6 si-CON
CM-SUM149/Tspan6 p38γ KD

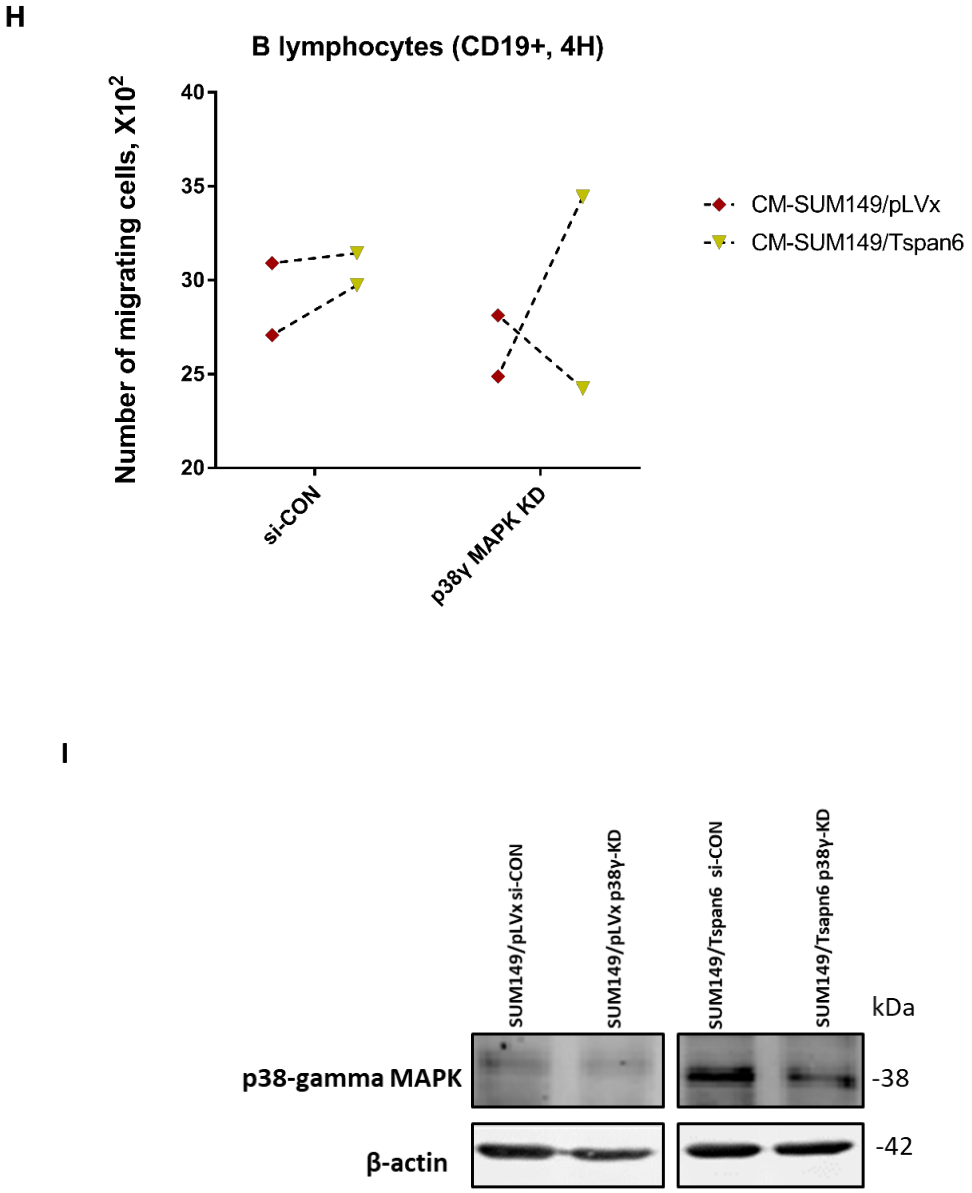

Figure 7-5. Tspan6/Syntenin-1 complex enhances the chemoattractive potential of IBC cells via p38β MAPK. (A-C) The knockdown of p38α MAPK had an inconsistent impact on the Tspan6-dependent migration of B cells. **(D-F)** The knockdown of p38β MAPK significantly downregulated the chemoattractive potential of SUM149/Tspan6 for B cells. **(G-I)** The impact of p38γ MAPK knockdown on B cell migration remained unclear. The expression of p38 MAPK isoforms was downregulated by siRNA to generate SUM149/Tspan6 p38α-KD, SUM149/Tspan6 p38β-KD, and SUM149/Tspan6 p38γ-KD, as well as SUM149/pLVx p38α-KD, SUM149/pLVx p38β-KD, and SUM149/pLVx p38γ-KD. Control siRNA was also applied to generate corresponding knockdown control cells. CM of the above cells was subsequently applied to the PBMC migration assay. Representative western blots (C, F, I) separately showing the expression of p38α, p38β and p38γ MAPKs in SUM149/Tspan6 and SUM149/pLVx cells

treated with control siRNA and MAPK isoform-targeted siRNAs for 4 days. Numbers connected by a dotted line indicate a donor-matched comparison. Two to five independent experiments were performed under each condition. P values were calculated using a two-tailed t-test (normal distribution data) or Mann-Whitney test (non-normal distribution data). The significance of P value is indicated on the graph, *p<0.05.

7.4. Tspan6 and Src kinase

7.4.1. Tspan6 upregulated the activation of Src kinase family

It was reported that syntenin-1 triggered the activation of p38 MAPK via c-Src kinase, one of the most commonly activated pathways in cancer (Boukerche H *et al.*, 2010). Therefore, we proposed that Tspan6/syntenin-1 complex induces the activation of p38 MAPK via c-Src. To prove our hypothesis, we initially assessed the phosphorylation level of the entire Src family kinase in SUM149/Tspan6 and BCX010/Tspan6, and in corresponding control cells (SUM149/pLVx and BCX010/pLVx). Higher expression of phosphorylated Src were detected in SUM149/Tspan6 and BCX010/Tspan6 compared to SUM149/pLVx and BCX010/pLVx, respectively (Figure 7-6 A).

7.4.2. The activation of c-Src is not affected by Tsapn6 expression.

Having identified a hyperactivation of Src family kinase in IBC cells expressing Tspan6, we continue to determine whether this phenomenon attributed to a Tspan6-induced c-Src activation. Due to an absence of the specific antibody against phosphorylated c-Src, we analysed the active level of c-Src by immunoprecipitating total c-Src from whole cell lysates and detecting the phosphorylated c-Src with p-Src family Ab. Compared with SUM149/pLVx, SUM149/Tspan6

cells did not have a hyperactivation of c-Src, and we obtained consistent results of BCX010 pair (Figure 7-6 B and C). The results of these experiments revealed that Tspan6 expression did not change the phosphorylation level of c-Src in IBC cells.

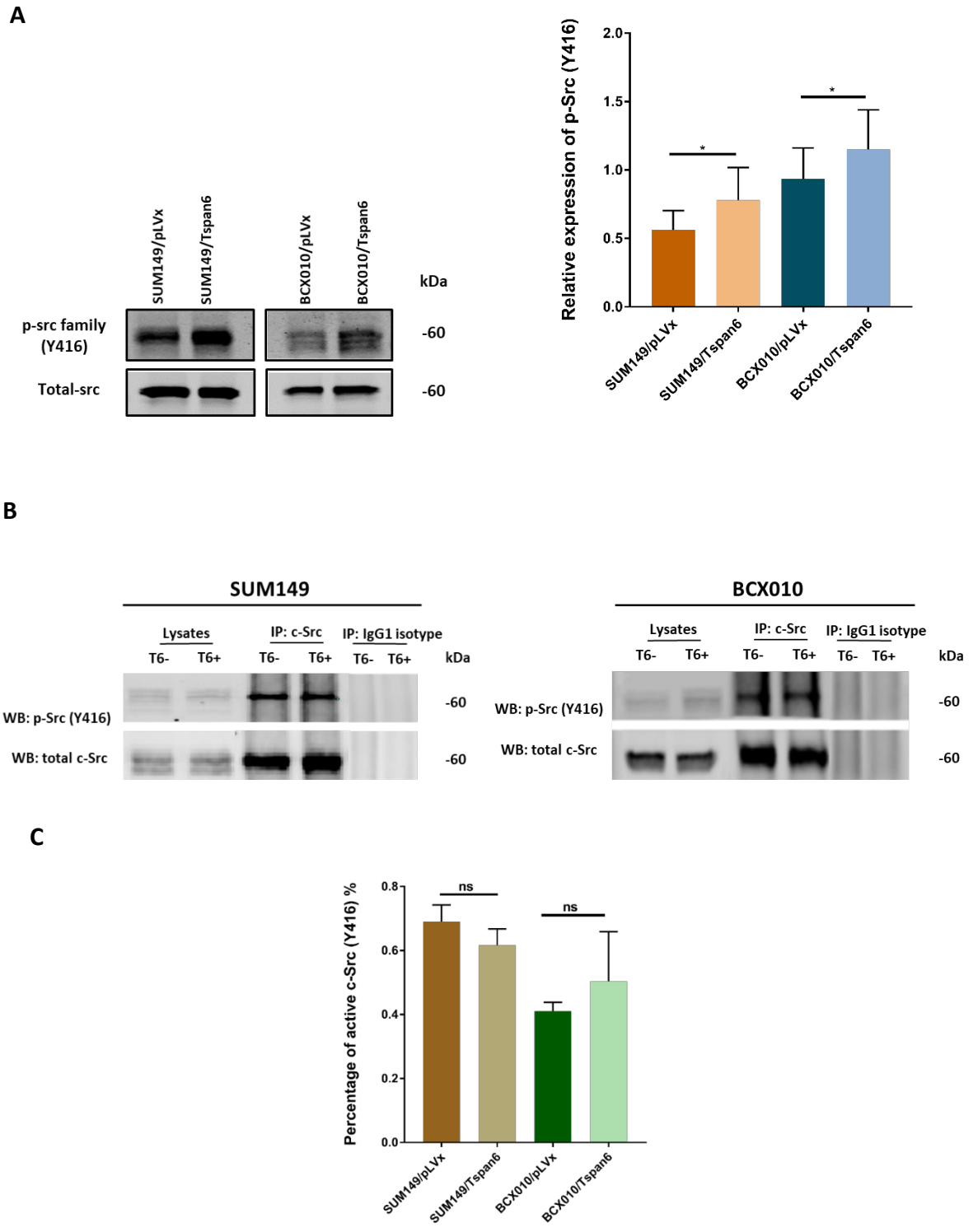

Figure 7-6. Tspan6 does not affect the phosphorylation level of c-Src in IBC cells. (A) The phosphorylation level of Src family kinase in SUM149/Tspan6, BCX010/Tspan6 and corresponding control cells (SUM/pLVx and BCX010/pLVx). Four individual experiments were done. Relative expression of p-Src family kinase was assessed by comparing the readings of pSrc (Y416) to total Src. **(B)** The expression of phosphorylated c-Src at Tyr^{416} in SUM149/Tspan6, SUM149/pLVx cells and BCX010/Tspan6, BCX010/pLVx cells. Three individual immunoprecipitation experiments were done. The c-Src protein from SUM149/Tspan6, SUM149/pLVx cells, and BCX010/Tspan6, BCX010/pLVx cells were immunoprecipitated using anti-c-Src mAb and Protein G PLUS-agarose beads. Proteins were eluted from the beads and resolved on 10% SDS-PAGE, and subsequently probed with anti-$pSrc^{Tyr416}$ in western blotting. Total c-Src was used as a loading control in these blots. **(C)** The Extent of phosphorylated c-Src (Y416) in immunoprecipitated samples was assessed by comparing the readings of pSrc (Y416) to the total c-Src in IP (c-Scr) group.

7.5. NF-κB and Tspan6

7.5.1. Tspan6 increased the chemoattractive potential of IBC cells in an NF-κB-independent way

It was reported that syntenin-1 facilitated the activation of p38 MAPK, which, in turn, triggered the activation of NF-κB, a family of transcription factors that play an important role in various physiological processes, including inflammation (Liu T, Zhang L, Joo D and Sun SC, 2017) and cancer development (Boukerche H *et al.*, 2007, 2010). In this study, we did not find that Tspan6 expression affected the total level or the phosphorylation of RelA (a vital member of the NF-κB family) in SUM149 cells (Figure 7-7 A, Supplementary Figure 1-6). By contrast, the total RelA expression in BCX010 cells was slightly upregulated by Tspan6 (Figure 7-7 A), although the expression of Tspan6 did not change its phosphorylation in BCX010 cells (Supplementary Figure 1-6).

To further determine the role of NF-κB in enhancing the chemoattractive potential of IBC cells for B cells, we silenced RelA in SUM149/Tspan6 and SUM149/pLVx cells with siRNAs (SUM149/Tspan6 RelA-KD and SUM149/pLVx RelA-KD). CM from these cells was used as chemoattractants in the "short-term" migration experiments. Though only two individual experiments were done, we observed consistent results that the knockdown of RelA did not have a suppressive effect on the B cell migration to CM-SUM149/Tspan6 or CM-SUM149/pLVx (Figure 7-7 B and C). Therefore, the enhanced chemotactic effect of SUM149/Tspan6 cells on B cells was maintained (Figure 7-7 D). These data suggest that NF-κB is not required for Tspan6/syntenin-1 complex to enhance the chemoattractive potential of IBC cells for B cells at the early stage.

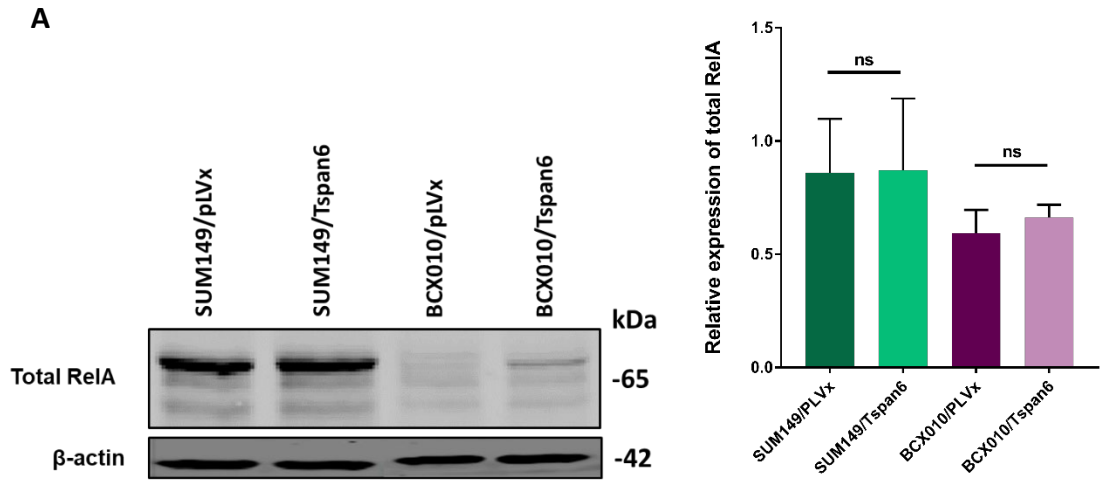

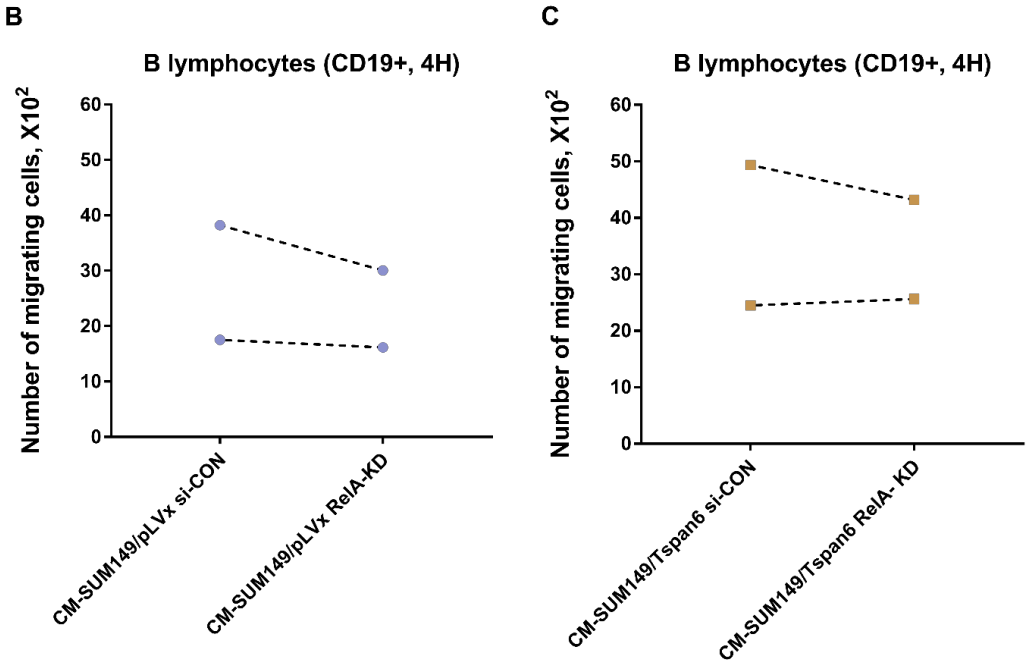
B
B lymphocytes (CD19+, 4H)
Number of migrating cells, X10²
60
50
40
30
20
10
0
CM-SUM149/pLVx si-CON
CM-SUM149/pLVx RelA-KD
C
B lymphocytes (CD19+, 4H)
Number of migrating cells, X10²
60
50
40
30
20
10
0
CM-SUM149/Tspan6 si-CON
CM-SUM149/Tspan6 RelA- KD

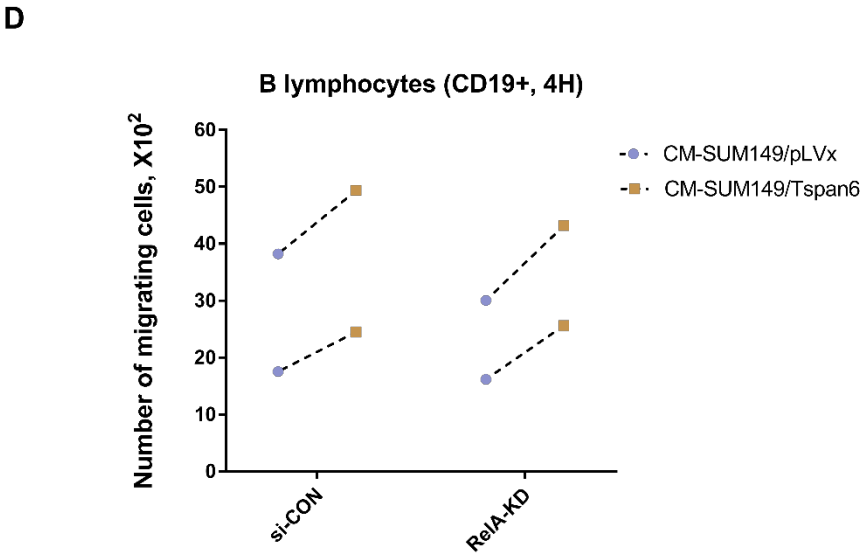
D
B lymphocytes (CD19+, 4H)
Number of migrating cells, X10²
60
50
40
30
20
10
0
si-CON
RelA-KD
CM-SUM149/pLVx
CM-SUM149/Tspan6

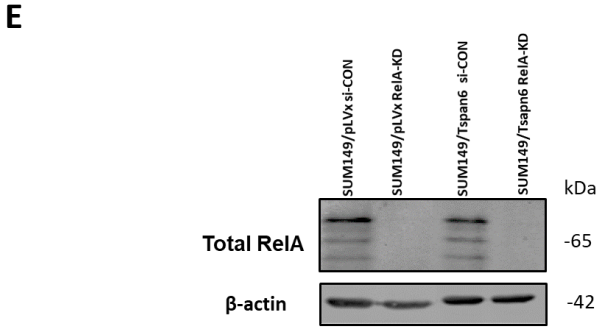
E
SUM149/pLVx si-CON
SUM149/pLVx RelA-KD
SUM149/Tspan6 si-CON
SUM149/Tsapn6 RelA-KD
kDa
Total RelA
-65
β-actin
-42

Figure 7-7. NF-κB is not involved in regulating the Tspan6-enhanced chemoattractive potential of IBC cells for B cells at an early stage. (A) Representative western blotting images showing the total expression of RelA in IBC cells. Shown are means with SD of the results of 3 independent experiments. P values were calculated using a two-tailed t-test and are indicated on the graph. **(B-C)** Knockdown of RelA did not significantly affect the migration of B cells to CM-SUM149/Tspan6 or CM-SUM149/pLVx. **(D)** Comparison between B cell short-term migration to CM-SUM149/Tspan6 and CM-SUM149/pLVx before and after RelA knockdown. The expression of RelA was downregulated by siRNA to generate SUM149/Tspan6 RelA -KD and SUM149/pLVx RelA -KD. Control siRNA was also applied to generate corresponding knockdown control cells. CM of the above cells was subsequently applied to the PBMC migration assay. Each dot in the graph represents the total number of migrating B lymphocytes in an individual trans-well assay. **(E)** The expression of RelA in SUM149/Tspan6 and SUM149/pLVx cells was treated with RelA siRNA and control siRNA for 4 days.

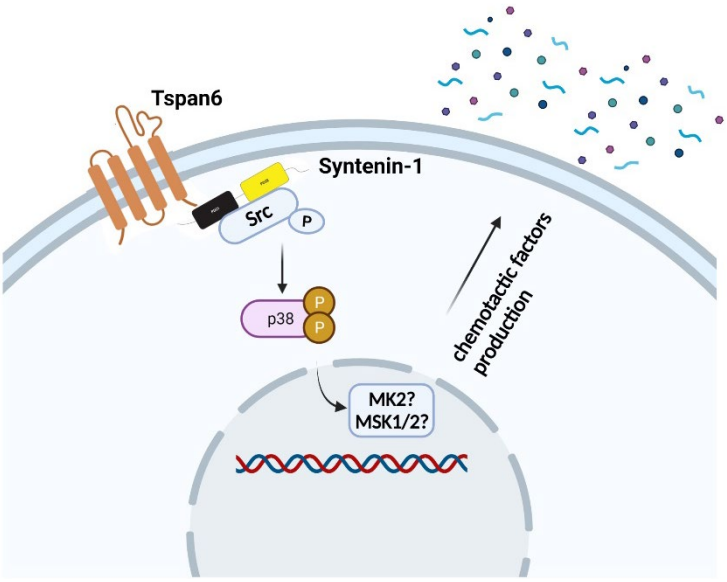

Figure 7-8. Proposed model depicting how Tspan6 increases the chemoattractive potential of IBC cells. Tspan6 promotes the recruitment and activation of Src via associating with syntenin-1, subsequently increasing the activation of p38 MARK. The p38 MAPK activates its downstream kinases, such as MK2 (Ray AL *et al.*, 2018; Soni S, Anand P and Padwad YS, 2019) or MSK1/2 (Reyskens KM and Arthur JS, 2016; McGuire VA *et al.*, 2017) , resulting in increased production or release of chemotactic factors.

7.6. Discussion

Our results show that Tspan6 enhanced the chemoattractive potential of IBC via mechanisms involving syntenin-1. As a scaffolding protein, Tspan6 has been reported to associate (directly or indirectly) with several molecules to exert its functions (Guix FX *et al.*, 2017; Ghossoub R *et al.*, 2020; Andrijes R *et al.*, 2021; Humbert PO *et al.*, 2022), but Syntenin-1 was the only known partner protein for Tspan6 (direct binding) (Guix FX *et al.*, 2017; Andrijes R *et al.*, 2021). Andrijes *et al*. revealed that Tspan6 altered the cellular distribution of a syntenin-1-associated transmembrane form of TGF-α (Andrijes R *et al.*, 2021). Thus, we questioned whether Tspan6 binding to syntenin-1 modifies the localisation or activation of syntenin-1-associated molecules or syntenin-1 downstream effectors, therefore increasing the production of chemotactic factors for B cells.

We discovered that p38 MAPK was involved in the Tspan6-syntenin-1-dependent migration of B cells. Tspan6 expression increased the activity of p38 MAPK in IBC cells but had no apparent effect on its total level (Supplementary Figure 1-6). It has been shown that activation of p38 MAPK was linked to the proliferation, invasion and metastasis of breast cancer cells (Mueller KL *et al.*, 2012; Luo J *et al.*, 2022). Here, we found that p38β MAPK but not the other p38 isoforms contributed to the Tspan6/syntenin-1-dependent B cell migration. Earlier studies suggested that p38α and p38β MAPK possessed similar functions in regulating host responses to cellular stress and production of inflammatory factors, with p38α MAPK taking the lead role, given that the knockout of p38β MAPK did not affect the viability and immune response of

mice while p38α MAPK did (Beardmore VA *et al.*, 2005; B Xing ADB and Van Eldik LJ, 2013). However, one study provided evidence that p38β MAPK was not redundant. Although both activated p38α MAPK and p38β MAPK were detected in breast cancer cells (MDA-MB-231 and MDA-MB-468), only p38β MAPK could promote the production and release of MCP-1/CCL2 of tumour cells (He Z *et al.*, 2014). CCL2 triggered the activation and differentiation of osteoclasts, resulting in osteolytic bone degradation (He Z *et al.*, 2014). The knockdown of p38β MAPK markedly inhibited the CCL2-dependent osteoclast-induced bone destruction but had no apparent effects on tumour growth or survival *in vivo* (He Z *et al.*, 2014), suggesting a specific role of p38β MAPK in regulating the secretion of inflammatory factors.

The oncoprotein, c-Src, was reported to regulate the syntenin-1-dependent phosphorylation of p38 MAPK. Mechanistically, syntenin-1 increases the activation of c-Src (Boukerche H *et al.*, 2008; Mir C *et al.*, 2021) and facilitates the recruitment of c-Src to the plasma membrane via direct binding through its PDZ1 and PDZ2 (Boukerche H *et al.*, 2010). Subsequently, active c-Src induces the phosphorylation of p38 MAPK (Boukerche H *et al.*, 2010). However, we did not observe a Tspan6-dependent hyperactivation of the c-Src IBC cells. Two possibilities could explain the results: 1) Other member(s) of the Src family, such as Fyn or Yes (Roskoski R Jr, 2015), is activated by the Tspan6/syntenin-1 complex. 2) The other explanation is that the activation level of c-Src detected in our experiments demonstrated the total phosphorylation of c-Src in the whole cell but failed to demonstrate the specific contribution from Tspan6/syntenin-1 complex to it. Thus, more investigations are needed to examine molecular links between the

Tspan6/syntenin-1 complex and proteins of Src family.

In our study, we did not find any contribution from NF-κB to Tspan6/syntenin-1-dependent B cell migration, which suggests that other downstream molecules of p38 MAPK may be involved. In fact, p38 MAPK can activate transcription factors via two downstream kinases, MK2 and MSK1/2. MK2 has been reported to regulate the production of some cytokines, such as TNF-α, IL-1β, IL-8, IL-6, and IFNγ, via upregulating the mRNA stability (Soni S, Anand P and Padwad YS, 2019).In contrast, MSK1/2 is likely to exert anti-inflammation effects (e.g. IL-10) via regulating transcription factors, such as Histone H3 and CREB (MacKenzie KF *et al.*, 2013; Elcombe SE *et al.*, 2013; Reyskens KM and Arthur JS, 2016; McGuire VA *et al.*, 2017). Thus, it will be interesting to investigate whether MK2 or MSK1/2 are targeted in Tspan6-expressing IBC cells.

In summary, we propose a model wherein Tspan6 promotes the recruitment and activation of a Src kinase via associating with syntenin-1. This will increase the activation of p38 MARK (particularly p38β MAPK), resulting in increased production or release of chemotactic factors (Figure 7-8). Further research is needed to elucidate the mechanism(s) underlying the Tspan6-enhanced chemoattractive potential of IBC, which may provide more insights into the TIME of IBC and identify more potential targets for IBC anti-tumour therapeutics.

8. GENERAL DISCUSSION AND FUTURE DIRECTIONS

Due to previous clinicopathological data suggesting a positive correlation between B cell infiltration and Tspan6 positivity in IBC tissues, we sought to identify whether there is a chemoattractive potential of IBC cells for B cells and how Tspan6 modulate this phenomenon. In our study, we first demonstrated the chemoattractive potential of IBC for B cells. This IBC's chemotactic effect onsets rapidly (short-term effect) and last durably (sustained effect). Furthermore, we discovered that Tspan6 expression enhanced the IBC's short-term chemotactic effect on B cells by regulating multiple pathways. In the extracellular environment, Tspan6 enhanced the IBC's impact on the pro-migration ability of monocytes, CD8+ T cells and PTX-sensitive factors, which resulted in elevated short-term migration of B cells. In the intracellular environment, Tspan6 promoted the activation of Src and p38β MAKP by associating with syntenin-1, whereby Tspan6 strengthened the chemoattactive potential of IBC for B cells. Further investigations can concentrate on the chemotactic factors controlling the B cell movement, how Tspan6/syntenin-1/Src/p38β MAPK pathway modulates the chemotactic factor production, and the conversion of recruited B cells in the IBC resident microenvironment.

8.1. Chemotactic factors mediating B cell migration

Our study investigated the mechanisms underlying the short-term migration of B cells, but the exact chemotactic factor(s) remained unknown. Whilst we have not exhaustively tested the contribution of chemokines and cytokines (and, therefore, cannot completely rule out their involvement), we cannot neglect the possibility that this process is mediated by other bioactive

molecules, such as lipids. This hypothesis is based on the unprecedented findings in non-IBC cells (unpublished data from our lab) that Tspan6 expression promoted the production of oxysterols (a bioactive lipid) in non-IBC cells, which consequently enhanced the B cell migration. Here, we summarised three bioactive lipids relevant to immune cell recruitment and potentially directly or indirectly modulate B cell migration to IBC.

Lipid mediators have been extensively studied in multiple fields, including allergic disease (Al-Azzam N and Elsalem L, 2020), obesity (Lyer A *et al.*, 2010), chronic inflammatory diseases (Miyabe Y *et al.*, 2017), cancer development (Xi Y *et al.*, 2021; He Y *et al.*, 2022; Zhu Y *et al.*, 2022) and TIME regulation (Eibinger G *et al.*, 2013; Raccosta L *et al.*, 2013; He Y *et al.*, 2022). In this regard, the most well-studied inflammatory bioactive lipid is eicosanoic acid, which represents a heterogenous family of lipid mediators originating from arachidonic acid (AA) (Johnson AM, Kleczko EK and Nemenoff RA, 2020) (Figure 8-1). The Eicosanoid family comprises prostaglandins and thromboxanes, leukotrienes, and epoxidised fatty acids.

AA is converted to prostaglandins and thromboxanes by cyclooxygenases (COX) (Johnson AM, Kleczko EK and Nemenoff RA, 2020). Emerging evidence suggests that prostaglandins, particularly PGE2, are involved in reshaping the TIME (Thumkeo D *et al.*, 2022). Mishra *et al.* discovered that a decreased PGE2 expression by breast cancer cells was associated with decreased migration of M2-TAMs *in vitro* and *in vivo* (Mishra S *et al.*, 2022). Conversely, enhanced expression of PGE2 promoted the migration of Tregs and induced the apoptosis of

cytotoxic T cells (Karavitis J *et al.*, 2012). In addition, blocking EP4 (PGE2 receptors) on TAMs *in vivo* significantly reduced the production and secretion of VEGF-C and VEGF-D by TAMs in the context of breast cancer (Majumder M *et al.*, 2014). These studies highlight a chemotactic effect and a regulatory function of PGE2. Notably, IBC is characterised by a high expression of COX-2 (Lerebours F *et al.*, 2008) and a concomitant expression of PGE2 (Fouad TM *et al.*, 2014). Therefore, this signalling axis may also be in operation in IBC. Further investigation will be necessary to address this question.

Leukotrienes are synthesised by the action of 5-lipoxygenase (5-LO), following the AA synthesis (Johnson AM, Kleczko EK and Nemenoff RA, 2020). Among leukotrienes, LTD4 was discovered to stimulate the migration of B cells, as LTD4 promoted calcium fluxes, actin polymerisation, and chemotaxis by activating the LTD4 receptor CysLTR1 in B cells (both lymphocytic leukaemia cells and normal B cells) (Drost AC *et al.*, 2012). Therefore, examining the production of LTD4 by IBC cells and its contribution to the IBC-induced migration of B lymphocytes may represent another important direction for future research.

As aforementioned, data from our lab (unpublished) showed that oxysterols produced by Tspan6-expressing non-IBC cells promoted the chemotactic migration of B cells. Specifically, we found that Tspan6 facilitated the accumulation of 25-and 27-hydroxycholesterols in EVs produced by IBC cells, resulting in the enhanced chemoattractive potential of cancer cells. Therefore, it will be interesting to investigate whether oxysterols exert a similar effect on B

cells in the context of IBC. Oxysterols are derivatives of cholesterol that undergo oxidisation (de Freitas FA *et al.*, 2022). Growing evidence demonstrates the regulatory function of oxysterols in the immune system (Raccosta L *et al.*, 2016; de Freitas FA *et al.*, 2022). For example, the 7α,25-dihydroxycholeserol directs the migration of B cells to the outer follicle in the second lymphoid organ via binding with its receptor EBI2, a GPCR highly expressed by active B cells (Liu C *et al.*, 2011). To be noted, receptors of oxysterols (EBI2 and liver X receptor (LXR)) are widely expressed by many immune subsets, including monocytes, DCs, T cells and B cells (Sun S and Liu C, 2015; de Freitas FA *et al.*, 2022). These findings indicate a broad influence of oxysterols on immune networks. In this regard, one study reported that the 7β-hydroxycholesterol and 25-hydroxycholesterol induced U937 and THP-1 cells (monocyte cell lines) to produce some chemokines, such as MCP-1, MIP-1β, TNF-α, IL-1 and IL-8 (Prunet C *et al.*, 2006), which may also affect the B cell migration.

It was suggested that the phospholipid sphingosine-1-phosphate (S1P), a ceramide metabolite, was involved in regulating the migration of B cells (Sic H *et al.*, 2014; Olesch C, Brüne B and Weigert A, 2022). There are five S1P receptors, S1P1-5, which are all GPCRs but with distinct subtypes of G proteins (Bryan AM and Del Poeta M, 2018; Olesch C, Brüne B and Weigert A, 2022). Therefore, it is unsurprising that S1P and S1P receptors have distinct roles in regulating different aspects of B cell behaviour (Sic H *et al.*, 2014). S1P1 is the first well-established receptor (G_iPCR) (Bryan AM and Del Poeta M, 2018), which is a key player in coordinating the shuttling of B cells between secondary lymphoid organs (SLOs) and circulating blood

(Olesch C, Brüne B and Weigert A, 2022). B cells migrate along the S1P gradient that displays the highest concentration in the blood, then lymph and lowest in the SLOs. Exposure to a high concentration of S1P induces the internalisation of S1P1, resulting in the desensitisation of B cells and facilitating their return to SLOs (Olesch C, Brüne B and Weigert A, 2022). Interestingly, S1P2 and S1P4 downregulate the S1P1-dependent migration (Sic H *et al.*, 2014), suggesting the complexity of S1P regulation of B cells. Apart from B cells, S1P receptors are widely expressed by monocytes, T cells, DCs, and NK cells. It is worth noting that breast cancer cells overexpress the enzyme for S1P synthesis, sphingosine kinase 1 (SPHK1) (Aoyagi T, Nagahashi M, Yamada A and Takabe K, 2012), which is accompanied by an increased level of S1P in tumour tissues than in normal tissues (Tsuchida J, Nagahashi M, Takabe K and Wakai T, 2017).

Interestingly, some transporters participate in the export of these bioactive lipids from cells. The transporter of prostaglandin and oxysterols is an ATP-binding cassette (ABC), such as multidrug resistance proteins (Park JY, Pillinger MH and Abramson SB, 2006; Ruiz JL, Fernandes LR, Levy D and Bydlowski SP, 2013; Nakamura Y, Nakanishi T and Tamai I, 2018). In contrast, the transporters of S1P are Spinster 2 (SPNS2), ABC, and the major facilitator superfamily transporter 2b (MFSD2B) (Olesch C, Brüne B and Weigert A, 2022). Accordingly, an increase in the expression of transporters by breast cancer cells (e.g. ATP Binding Cassette Subfamily C Member 1, ABCC1) can also facilitate the export of these bioactive lipids (Yamada A *et al.*, 2018). Notably, ABCC1-dependent S1P secretion by breast cancer cells simultaneously

enhanced the transcription of SPHK1 (Yamada A *et al.*, 2018), suggesting a positive feedback loop in the process of S1P production.

In short, the above bioactive lipids possessing pro-migration ability may be the potential mediators of the enhanced B cell migration in our study. More investigations are needed to evaluate their production and secretion by IBC cells and the contribution of Tspan6 to these activities.

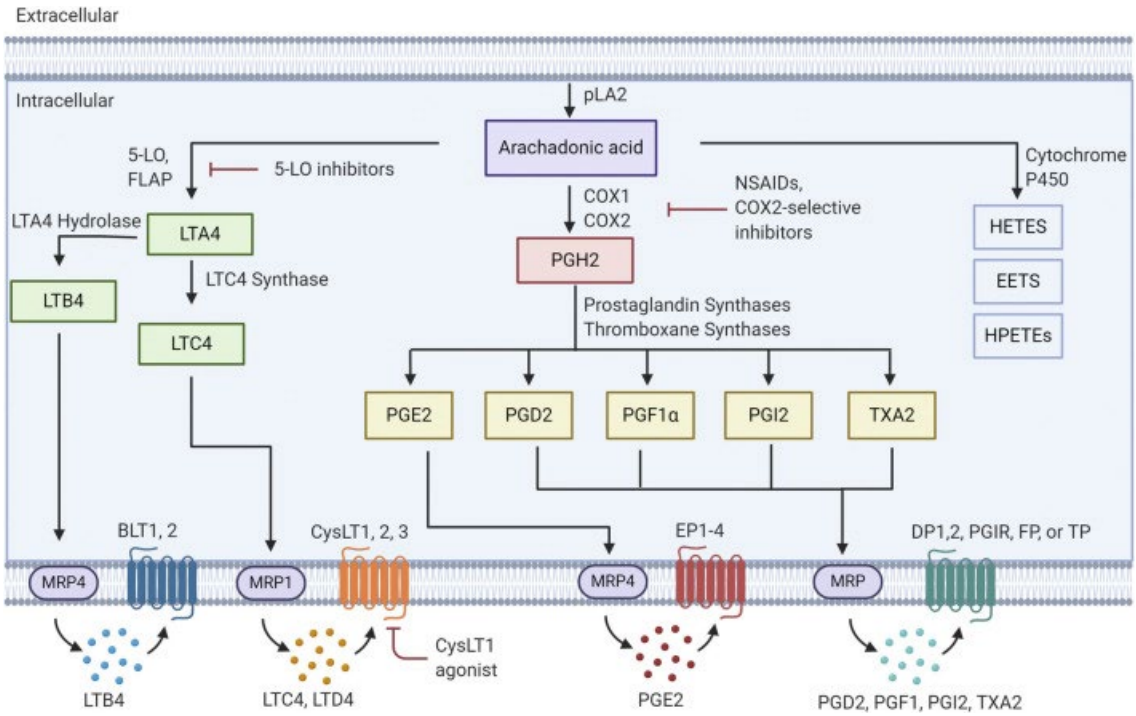

Figure 8-1. A diagram shows distinct pathways for synthesising prostaglandins and thromboxanes, leukotrienes, and epoxidised fatty acids. The figure is adopted from (Johnson AM, Kleczko EK and Nemenoff RA, 2020).

8.2. Downstream effectors of the Tspan6-syntenin-1 axis

Having determined the critical role of syntenin-1 for Tspan6 to promote the migration of B cells,

we sought to identify prospective candidates to serve as their downstream effectors. Our data showed that p38 MAPK represents one class of such molecules. It is well-established that the p38 MAPK signalling pathway regulates the expression of a heterogeneous group of molecules, including enzymes responsible for inflammatory factor production. For example, p38 MAPK activates the cPLA2 by phosphorylating it at Ser505 (Lin LL *et al.*, 1993). This phosphorylation induces a cPLA2-catalyzed AA production (see above), a rate-limiting step for eicosanoid production (Leslie CC, 2004; Nakanishi M and Rosenberg DW, 2006). In addition to cPLA2, p38 MAPK also phosphorylated the 5-LO (a key enzyme for leukotrienes synthesis) via MAPKAPK2 (MK2) and probably MAPKAPK3 (MK3) (Werz O, Klemm J, Samuelsson B and Rådmark O, 2000). The MK2-dependent phosphorylation of 5-LO at Ser271 effectively restrains its nuclear export and facilitates the interaction of 5-LO with FALP (5-LO activating protein) to initiate the synthesis of leukotrienes (Abramovitz M *et al.*, 1993; Mancini JA *et al.*, 1993; Flamand N, Luo M, Peters-Golden M and Brock TG, 2009; Kanaoka Y and Austen KF, 2019). Furthermore, it has been reported that p38 MAPK, acting via MK2, maintained the stability of mRNAs for TNF-α (Kotlyarov A *et al.*, 1999; Hitti E *et al.*, 2006; Chen X *et al.*, 2012) (a chemoattractant for B cells) and matrix metalloproteinase-9 (MMP9) (Van Tubergen EA *et al.*, 2013). As is well known, MMP9 modulates the activation and inactivation of diverse chemokines and cytokines via proteolysis (Young D, Das N, Anowai A and Dufour A, 2019; Augoff K, Hryniewicz-Jankowska A, Tabola R and Stach K, 2022). Although chemokines and cytokines do not appear to be involved in the Tspan6-dependent regulation of B cell migration by IBC cells, the mechanistic link between p38 MAPK and the stability of cellular mRNAs

may be crucial.

While MK2 acts on pro-inflammatory activities, MSK1/2, another p38 MAPK target, is more related to anti-inflammation modulations via its downstream CREB (Reyskens KM and Arthur JS, 2016). Knockout MSK1/2 *in vivo* decreases the expression of IL-10 and increases the expression of pro-inflammatory cytokines, such as TNF, IL-6 and IL-12 (Ananieva O *et al.*, 2008). In addition, MSK1/2 upregulates the production of IL-1ra, which is a natural antagonist of the IL-1 receptor (Darragh J *et al.*, 2010). IFNβ is inversely regulated by MSK1/2 as well, which is mediated by CREB-involved production of DUSP1 (a phosphatase that acts as a suppressor for p38 MAPK and JNK) (Ananieva O *et al.*, 2008), generating negative feedback to IFNβ production (McGuire VA *et al.*, 2017). Except for cytokines, MSK1/2 regulates the transcription of COX-2 via modulating the activity of CREB and TTP, leading to a transient elevation and a delayed decrease in the production of prostaglandins (MacKenzie KF *et al.*, 2013).

Taken together, through its downstream effectors, p38 MAPK is involved in regulating the biosynthesis of various inflammatory factors, including cytokines, chemokines, and bioactive lipids. Further exploration is warranted to assess the activation of these proteins in the Tspan6-expressing IBC cells and how these proteins contribute to the enhanced B cell migration.

8.3. Conversion of B cells in IBC resident microenvironment

Recruitment of immune cells to cancerous tissues is the first step for tumour cells to modulate the TIME. However, the subsequent events remained unclear. Tracking immune cells from their circulating state to their terminal differentiation in cancerous tissue would be the best strategy for unravelling the immune cell recruitment to IBC tissues. Unfortunately, there is no data on this topic. Lacking *in vivo* studies on B cell infiltration in IBC undoubtedly exacerbates this problem, as there are no immune-proficient mouse models for IBC. Canine models may be the optimal animal model in the future (Raposo TP *et al.*, 2017) due to a high proportion (~7.6%) of canine inflammatory mammary carcinoma (CIMC, the corresponding canine disease) in dogs (Pérez Alenza MD, Tabanera E and Peña L, 2001), and CIMC has similar biological and clinical features to IBC (Raposo TP *et al.*, 2017).

In addition to future *in vivo* studies, some non-IBC studies may provide clues. It was shown that when breast cancer tissues were compared with normal breast tissues, there was an increased proportion of memory TIL-Bs and a concomitant decrease in the frequency of naive TIL-Bs. In contrast, circulating B cells from breast cancer patients did not differ significantly from those from healthy donors in terms of all B cell subsets. These observations indicate a tumour-induced local B cell activation (Garaud S *et al.*, 2019). Genetic analysis supports this concept. Hu *et al.* analysed the heterogeneity of TIL-Bs in TNBC tissues and circulating B cells of PBMCs by employing single-cell RNA-sequencing and antigen receptor lineage analysis. Compared to PBMC samples, TNBC tissues displayed an increased frequency of memory B

cells in parallel with a reduced frequency of naïve B cells (Hu Q *et al.*, 2021). Moreover, compared to circulating B cells, TIL-Bs were enriched with higher clonality with more class-switching recombination and somatic hypermutations, the hallmarks of B cell activation (Hu Q *et al.*, 2021). These studies suggest that encountering tumour antigens or being exposed to a tumour environment is a prerequisite for B cell priming, and the differentiation and expansion of memory B cells are the product of this process. Furthermore, breast cancer patients with high memory TIL-Bs were more likely to have a favourable survival (OS: $p = 0.005$; DFS: $p = 0.01$) (Hu Q *et al.*, 2021), emphasising the importance of a resident active humoral immunity in anti-tumour actions.

In our present study, we employed CD19 to distinguish B cells from other immune cells. CD19 is widely expressed by a variety of B cells, ranging from pre-B cells to memory B cells (LeBien TW and Tedder TF, 2008). Because those cells possess the potential for differentiation and conversion (LeBien TW and Tedder TF, 2008), more attention should be paid to the aspects that how these cells behave after infiltration into cancerous tissues and how they adapt themselves to a hostile environment. More importantly, neither differentiation nor survival in the tumour microenvironment could be achieved by B cells alone, which definitely needs assistance from other non-B cells present in the TIME (e.g. macrophages and T cells) (Laumont CM *et al.*, 2022). Therefore, a comprehensive study that aims to characterise the phenotypes of TIL-Bs in IBC and to determine the contribution of non-B cells to B cell retention and activation may provide more insights into the dynamics of TIL-Bs and pave the way to exploring novel tumour

immune targets for IBC.

9. CONCLUSIONS

In general, our research uncovered a B cell-targeted chemotactic effect of IBC cells and Tspan6 strengthened this effect by regulating extrinsic and intrinsic cellular and molecular pathways. Nevertheless, there are some limitations in our study. First, all the results were produced by *in vitro* experiments using IBC cell lines. Standard trans-well migration assay cannot completely recapitulate the features of real tumour microenvironment. Therefore, *in vivo* experiments are warranted, by which we are able to further analyse the tempo-spatial distribution of B cells and the intercellular communication between B cells and other immune cells. Secondly, we only used at most two cell lines (SUM149 and BCX010) to investigate the mechanisms underlying the Tspan6-dependent migration of B cells. Both of them are TN-IBC; thus, more cell lines, such as HR+ or HER2+ IBC cell lines are needed to prove a universal impact of Tspan6 on the chemoattractive potential of IBC for B cells. To be worth noting that our current study is just a preliminary investigation. More *in vitro* and *in vivo* experiments are needed to complete the entire story of B cell recruitment to IBC cancerous tissues.

LIST OF REFERENCES

ABRAMOVITZ M, WONG E, COX ME, RICHARDSON CD, LI C and VICKERS PJ. 1993. 5-lipoxygenase-activating protein stimulates the utilization of arachidonic acid by 5-lipoxygenase. *European journal of biochemistry*. 215(1): 105-11.

AFFANDI AJ, OLESEK K, GRABOWSKA J, NIJEN TWILHAAR MK, RODRíGUEZ E, SARIS A, ZWART ES, NOSSENT EJ, KALAY H, DE KOK M, KAZEMIER G, STöCKL J, VAN DEN EERTWEGH A, DE GRUIJL TD, GARCIA-VALLEJO JJ, STORM G, VAN KOOYK Y and DEN HAAN J. 2021. CD169 Defines Activated CD14+ Monocytes With Enhanced CD8+ T Cell Activation Capacity. *Frontiers in immunology*. 12: 697840.

AL-AZZAM, N and ELSALEM, L. 2020. Leukotriene D4 role in allergic asthma pathogenesis from cellular and therapeutic perspectives. *Life sciences*. 260: 118452.

ALWAN, NAS, KERR, D, AL-OKATI, D, PEZELLA, F, TAWFEEQ, FN. 2018. Comparative study on the clinicopathological profiles of breast cancer among Iraqi and British patients. *The open public health journal*. 11: 177-191.

AMORIM, C, DOCASAR, CL, GUIMARãES-BASTOS, D, FRONY, AC, BARJA-FIDALGO, C, RENOVATO-MARTINS, M and MORAES, JA. 2022. Extracellular Vesicles Derived from MDA-MB-231 Cells Trigger Neutrophils to a Pro-Tumor Profile. *Cells*. 11(12): 1875.

ANANIEVA O, DARRAGH J, JOHANSEN C, CARR JM, MCILRATH J, PARK JM, WINGATE A, MONK CE, TOTH R, SANTOS SG, IVERSEN L and ARTHUR JS. 2008. The kinases MSK1 and MSK2 act as negative regulators of Toll-like receptor signaling. *Nature immunology*. 9(9): 1028-1036.

ANDO T, CHARINDRA D, SHRESTHA M, UMEHARA H, OGAWA I, MIYAUCHI M and TAKATA T. 2018. Tissue inhibitor of metalloproteinase-1 promotes cell proliferation through YAP/TAZ activation in cancer. *Oncogene*. 37(2): 263-270.

ANDRIJES, R, HEJMADI, RK, PUGH, M, RAJESH, S, NOVITSKAYA, V, IBRAHIM, M, OVERDUIN, M, TSELEPIS, C, MIDDLETON, GW, GYőRFFY, B, BEGGS, AD and BERDITCHEVSKI, F. 2021. Tetraspanin 6 is a regulator of carcinogenesis in colorectal cancer. *Proceedings of the National Academy of Sciences of the United States of America*. 118(39): e2011411118.

AOYAGI T, NAGAHASHI M, YAMADA A and TAKABE K. 2012. The role of sphingosine-1-phosphate in breast cancer tumor-induced lymphangiogenesis. *Lymphatic research and biology*. 10(3): 97-106.

ARIAS-PULIDO H, CHAHER N, GONG Y, QUALLS C, VARGAS J and ROYCE M. 2012. Tumor stromal vascular endothelial growth factor A is predictive of poor outcome in inflammatory breast cancer. *BMC cancer*. 12: 298.

ARIAS-PULIDO H, CIMINO-MATHEWS A, CHAHER N, QUALLS C, JOSTE N, COLPAERT C, MAROTTI JD, FOISEY M, PROSSNITZ ER, EMENS LA and FIERING S. 2018. The combined presence of CD20 + B cells and PD-L1 + tumor-infiltrating lymphocytes in inflammatory breast cancer is prognostic of improved patient outcome. Breast cancer research and treatment. 171(2): 273-282.

ARIAS-PULIDO, H, CIMINO-MATHEWS, AM, CHAHER, N, QUALLS, CR, JOSTE, N, COLPAERT, C, MAROTTI, JD, CHAMBERLIN, MD, FOISEY, MG, PROSSNITZ, ER, EMENS, LA and FIERING, S. 2021. Differential effects of CD20+ B cells and PD-L1+ immune cells on pathologic complete response and outcome: comparison between inflammatory breast cancer and locally advanced breast cancer patients. *Breast cancer research and treatment*. 190(3): 477-489.

AUGOFF, K, HRYNIEWICZ-JANKOWSKA, A, TABOLA, R and STACH, K. 2022. MMP9: A Tough Target for Targeted Therapy for Cancer. *Cancers*. 14(7): 1847

BADR, G, BORHIS, G, TRETON, D and RICHARD Y. 2005. IFNα enhances human B-cell chemotaxis by modulating ligand-induced chemokine receptor signaling and internalization. *International immunology*. 17(4): 459-467.

BADR NM, MCMURRAY JL, DANIAL I, HAYWARD S, ASAAD NY, ABD EL-WAHED MM, ABDOU AG, SERAG EL-DIEN MM, SHARMA N, HORIMOTO Y, SIRCAR T, VIDYA R, HOAR F, REA D, JONES JL, STEVENS A, SPOONER D, MERARD R, LEWIS P, HUNTER KJ, BERDITCHEVSKI F and SHAABAN AM. 2022. Characterization of the Immune Microenvironment in Inflammatory Breast Cancer Using Multiplex Immunofluorescence. *Pathobiology: journal of immunopathology, molecular and cellular biology*: 1-13.

BAIETTI MF, ZHANG Z, MORTIER E, MELCHIOR A, DEGEEST G, GEERAERTS A, IVARSSON Y, DEPOORTERE F, COOMANS C, VERMEIREN E, ZIMMERMANN P and DAVID G. 2012. Syndecan-syntenin-ALIX regulates the biogenesis of exosomes. *Nature cell biology*. 14(7): 677-685.

BAILLO A, GIROUX C and ETHIER SP. 2011. Knock-down of amphiregulin inhibits cellular invasion in inflammatory breast cancer. *Journal of cellular physiology*. 226(10): 2691-2701.

BEARDMORE VA, HINTON HJ, EFTYCHI C, APOSTOLAKI M, ARMAKA M, DARRAGH J, MCILRATH J, CARR JM, ARMIT LJ, CLACHER C, MALONE L, KOLLIAS G and ARTHUR JS. 2005. Generation and characterization of p38beta (MAPK11) gene-targeted mice. *Molecular and cellular biology*. 25(23): 10454-10464.

BENSE, RD, SOTIRIOU, C, PICCART-GEBHART, MJ, HAANEN, JBAG, VAN VUGT, MATM, DE VRIES, EGE, SCHRÖDER, CP and FEHRMANN, RSN. 2017. Relevance of tumor-infiltrating immune cell composition and functionality for disease outcome in breast cancer. *Journal of the national cancer institute*. 109(1): 192.

BERDITCHEVSKI F, ODINTSOVA E, SAWADA S and GILBERT E. 2002. Expression of the palmitoylation-deficient CD151 weakens the association of alpha 3 beta 1 integrin with the tetraspanin-enriched microdomains and affects integrin-dependent signaling. *The Journal of biological chemistry*. 277(40): 36991-7000.

BERDITCHEVSKI F, ZUTTER MM and HEMLER ME. 1996. Characterization of novel complexes on the cell surface between integrins and proteins with 4 transmembrane domains (TM4 proteins). *Molecular biology of the cell*. 7(2): 193-207.

BERRAONDO P, SANMAMED MF, OCHOA MC, ETXEBERRIA I, AZNAR MA, PéREZ-GRACIA JL, RODRíGUEZ-RUIZ ME, PONZ-SARVISE M, CASTAñóN E and MELERO I. 2019. Cytokines in clinical cancer immunotherapy. *British journal of cancer*. 120(1): 6-15.

BERTUCCI F, BOUDIN L, FINETTI P, VAN BERCKELAER C, VAN DAM P, DIRIX L, VIENS P, GONçALVES A, UENO NT, VAN LAERE S, BIRNBAUM D and MAMESSIER E. 2021. Immune landscape of inflammatory breast cancer suggests vulnerability to immune checkpoint inhibitors. *Oncoimmunology*. 10(1): 1929724.

BERTUCCI F, FINETTI P, COLPAERT C, MAMESSIER E, PARIZEL M, DIRIX L, VIENS P, BIRNBAUM D and VAN LAERE S. 2015. PDL1 expression in inflammatory breast cancer is frequent and predicts for the pathological response to chemotherapy. *Oncotarget*. 6(15): 13506-13519.

BERTUCCI F, UENO NT, FINETTI P, VERMEULEN P, LUCCI A, ROBERTSON FM, MARSAN M, IWAMOTO T, KRISHNAMURTHY S, MASUDA H, VAN DAM P, WOODWARD WA, CRISTOFANILLI M, REUBEN JM, DIRIX L, VIENS P, SYMMANS WF, BIRNBAUM D and VAN LAERE SJ. 2014. Gene expression profiles of inflammatory breast cancer: correlation with response to neoadjuvant chemotherapy and metastasis-free survival. *Annals of oncology: official journal of the European Society for Medical Oncology*. 25(2): 358-365.

BOUKERCHE H, AISSAOUI H, PRéVOST C, HIRBEC H, DAS SK, SU ZZ, SARKAR D and FISHER PB. 2010. Src kinase activation is mandatory for MDA-9/syntenin-mediated activation of nuclear factor-kappaB. *Oncogene*. 29(21): 3054-3066.

BOUKERCHE H, SU ZZ, EMDAD L, SARKAR D and FISHER PB. 2007. mda-9/Syntenin regulates the metastatic phenotype in human melanoma cells by activating nuclear factor-kappaB. *Cancer research*. 67(4): 1812-1822.

BOUKERCHE H, SU ZZ, PRéVOT C, SARKAR D and FISHER PB. 2008. mda-9/Syntenin promotes metastasis in human melanoma cells by activating c-Src. *Proceedings of the National Academy of Sciences of the United States of America*.

105(41): 15914-15919.

BOYETTE LB, MACEDO C, HADI K, ELINOFF BD, WALTERS JT, RAMASWAMI B, CHALASANI G, TABOAS JM, LAKKIS FG and METES DM. 2017. Phenotype, function, and differentiation potential of human monocyte subsets. *PloS one*. 12(4): e0176460.

BRADLEY JR. 2008. TNF-mediated inflammatory disease. *The Journal of pathology*. 214(2): 149-160.

BRYAN AM and DEL POETA M. 2018. Sphingosine-1-phosphate receptors and innate immunity. *Cellular microbiology*. 20(5): e12836.

CABIOGLU N, GONG Y, ISLAM R, BROGLIO KR, SNEIGE N, SAHIN A, GONZALEZ-ANGULO AM, MORANDI P, BUCANA C, HORTOBAGYI GN and CRISTOFANILLI M. 2007. Expression of growth factor and chemokine receptors: new insights in the biology of inflammatory breast cancer. *Annals of oncology: official journal of the European Society for Medical Oncology*. 18(6): 1021-1029.

CALANDRA T and ROGER T. 2003. Macrophage migration inhibitory factor: a regulator of innate immunity. *Nature reviews. Immunology*. 3(10): 791-800.

CAMPEDEL L, BLANC-DURAND P, BIN ASKER A, LEHMANN-CHE J, CUVIER C, DE BAZELAIRE C, TEIXEIRA L, BECOURT S, LEDOUX F, HOCINI H, BOURSTYN E, MIQUEL C, GUILLERM S, CHARVERIAT P, ESPIé M, DE ROQUANCOURT A, HAMY AS and GIACCHETTI S. 2020. Prognostic Impact of Stromal Immune Infiltration before and after Neoadjuvant Chemotherapy (NAC) in Triple Negative Inflammatory Breast Cancers (TNIBC) Treated with Dose-Dense Dose-Intense NAC. *Cancers*. 12(9): 2657.

CASTRO-SANCHEZ L, SOTO-GUZMAN A, NAVARRO-TITO N, MARTINEZ-OROZCO R and SALAZAR EP. 2010. Native type IV collagen induces cell migration through a CD9 and DDR1-dependent pathway in MDA-MB-231 breast cancer cells. *European journal of cell biology*. 89(11): 843-852.

CHANG LY, LIN YC, MAHALINGAM J, HUANG CT, CHEN TW, KANG CW, PENG HM, CHU YY, CHIANG JM, DUTTA A, DAY YJ, CHEN TC, YEH CT and LIN CY. 2012. Tumor-derived chemokine CCL5 enhances TGF-β-mediated killing of CD8(+) T cells in colon cancer by T-regulatory cells. Cancer research. 72(5): 1092-1102.

CHARRIN S, JOUANNET S, BOUCHEIX C and RUBINSTEIN E. 2014. Tetraspanins at a glance. *Journal of cell science*. 127(Pt 17): 3641-3648.

CHARRIN S, LE NAOUR F, LABAS V, BILLARD M, LE CAER JP, EMILE JF, PETIT MA, BOUCHEIX C and RUBINSTEIN E. 2003. EWI-2 is a new component of the tetraspanin web in hepatocytes and lymphoid cells. *The Biochemical journal*. 373(Pt 2): 409-421.

CHARRIN S, MANIé S, BILLARD M, ASHMAN L, GERLIER D, BOUCHEIX C and RUBINSTEIN E. 2003. Multiple levels of interactions within the tetraspanin web. *Biochemical and biophysical research communications*. 304(1): 107-112.

CHARRIN S, MANIé S, OUALID M, BILLARD M, BOUCHEIX C and RUBINSTEIN E. 2002. Differential stability of tetraspanin/tetraspanin interactions: role of palmitoylation. *FEBS letters*. 516(1-3): 139-144.

CHAUVIN A, WANG CS, GEHA S, GARDE-GRANGER P, MATHIEU AA, LACASSE V and BOISVERT FM. 2018. The response to neoadjuvant chemoradiotherapy with 5-fluorouracil in locally advanced rectal cancer patients: a predictive proteomic signature. *Clinical proteomics*. 15: 16.

CHEANG MC, CHIA SK, VODUC D, GAO D, LEUNG S, SNIDER J, WATSON M, DAVIES S, BERNARD PS, PARKER JS, PEROU CM, ELLIS MJ and NIELSEN TO. 2009. Ki67 index, HER2 status, and prognosis of patients with luminal B breast cancer. *Journal of the National Cancer Institute*. 101(10): 736-750.

CHEN ML, PITTET MJ, GORELIK L, FLAVELL RA, WEISSLEDER R, VON BOEHMER H and KHAZAIE K. 2005. Regulatory T cells suppress tumor-specific CD8 T cell cytotoxicity through TGF-beta signals in vivo. *Proceedings of the National Academy of Sciences of the United States of America*. 102(2): 419-424.

CHEN X, WEI Z, WANG W, YAN R, XU X and CAI Q. 2012. Role of RNA-binding protein tristetraprolin in tumor necrosis factor-α mediated gene expression. *Biochemical and biophysical research communications.* 428(3): 327-332.

CHIANG, SF, TSAI, MH, TANG, R, HSIEH, LL, CHIANG, JM, YEH, CY, HSIEH, PS, TSAI, WS, LIU, YP, LIANG, Y, CHEN, JS and YU, JS. 2014. Membrane proteins as potential colon cancer biomarkers: verification of 4 candidates from a secretome dataset. *Surgical Science*. 5(10): 418-438.

CHOI, C and FINLAY, DK. 2020. Diverse Immunoregulatory Roles of Oxysterols-The Oxidized Cholesterol Metabolites. *Metabolites*. 10(10): 384.

CHOW A, ZHOU W, LIU L, FONG MY, CHAMPER J, VAN HAUTE D, CHIN AR, REN X, GUGIU BG, MENG Z, HUANG W, NGO V, KORTYLEWSKI M and WANG SE. 2014. Macrophage immunomodulation by breast cancer-derived exosomes requires Toll-like receptor 2-mediated activation of NF-κB. *Scientific reports.* 4: 5750.

CHU PY, HOU MF, LAI JC, CHEN LF and LIN CS. 2019. Cell Reprogramming in Tumorigenesis and Its Therapeutic Implications for Breast Cancer. *International journal of molecular sciences*. 20(8): 1827.

CLAAS C, SEITER S, CLAAS A, SAVELYEVA L, SCHWAB M and ZöLLER M. 1998. Association between the rat homologue of CO-029, a metastasis-associated tetraspanin molecule and consumption coagulopathy. *The Journal of cell biology*. 141(1): 267-280.

CLEMENTE M, SáNCHEZ-ARCHIDONA AR, SARDóN D, DíEZ L, MARTíN-RUIZ A, CACERES S, SASSI F, DOLORES PéREZ-ALENZA M, ILLERA JC, DUNNER S and PEñA L. 2013. Different role of COX-2 and angiogenesis in canine inflammatory and non-inflammatory mammary cancer. *The veterinary journal*. 197(2): 427-432.

COHEN EN, GAO H, ANFOSSI S, MEGO M, REDDY NG, DEBEB B, GIORDANO A, TIN S, WU Q, GARZA RJ, CRISTOFANILLI M, MANI SA, CROIX DA, UENO NT, WOODWARD WA, LUTHRA R, KRISHNAMURTHY S and REUBEN JM. 2015. Inflammation Mediated Metastasis: Immune Induced Epithelial-To-Mesenchymal Transition in Inflammatory Breast Cancer Cells. *PloS one*. 10(7): e0132710.

COPSON E, SHAABAN AM, MAISHMAN T, MOSELEY PM, MCKENZIE H, BRADBURY J, BORLEY A, BRZEZINSKA M, CHAN S, CHING J, CUTRESS RI, DANIAL I, DALL B, KERIN M, LOWERY AJ, MACPHERSON IR, ROMICS L, SAWYER E, SHARMAT N, SIRCAR T, VIDYA R, PAN Y, REA D, JONES L, ECCLES DM and BERDITCHEVSKI F. 2018. The presentation, management and outcome of inflammatory breast cancer cases in the UK: Data from a multi-centre retrospective review. *The Breast: official journal of the European Society of Mastology*. 42: 133-141.

CRISTOFANILLI M, GONZALEZ-ANGULO AM, BUZDAR AU, KAU SW, FRYE DK and HORTOBAGYI GN. 2004. Paclitaxel improves the prognosis in estrogen receptor negative inflammatory breast cancer: the M. D. Anderson Cancer Center experience. *Clinical breast cancer*. 4(6): 415-419.

DARRAGH J, ANANIEVA O, COURTNEY A, ELCOMBE S and ARTHUR JS. 2010. MSK1 regulates the transcription of IL-1ra in response to TLR activation in macrophages. *The Biochemical journal*. 425(3): 595-602.

DE ANGELIS C, NAGI C, HOYT CC, LIU L, ROMAN K, WANG C, ZHENG Y, VEERARAGHAVAN J, SETHUNATH V, NUCIFORO P, WANG T, TSIMELZON A, MAO S, HILSENBECK SG, TRIVEDI MV, CATALDO ML, PAVLICK A, WOLFF AC, WEIGELT B, REIS-FILHO JS, PRAT A, GUTIERREZ C, OSBORNE CK, RIMAWI MF and SCHIFF R. 2020. Evaluation of the Predictive Role of Tumor Immune Infiltrate in Patients with HER2-Positive Breast Cancer Treated with Neoadjuvant Anti-HER2 Therapy without Chemotherapy. *Clinical cancer research: an official journal of the American Association for Cancer Research*. 26(3): 738-745.

DE FREITAS FA, LEVY D, REICHERT CO, CUNHA-NETO E, KALIL J and BYDLOWSKI SP. 2022. Effects of Oxysterols on Immune Cells and Related Diseases. *Cells*. 11(8): 1251

DEGNIM AC, HOSKIN TL, ARSHAD M, FROST MH, WINHAM SJ, BRAHMBHATT RA, PENA A, CARTER JM, STALLINGS-MANN ML, MURPHY LM, MILLER EE, DENISON LA, VACHON CM, KNUTSON KL, RADISKY

DC and VISSCHER DW. 2017. Alterations in the Immune Cell Composition in Premalignant Breast Tissue that Precede Breast Cancer Development. *Clinical cancer research: an official journal of the American Association for Cancer Research*. 23(14): 3945-3952.

DENG L, GAO X, LIU B, HE X, XU J, QIANG J, WU Q and LIU S. 2018. NMT1 inhibition modulates breast cancer progression through stress-triggered JNK pathway. *Cell death & disease*. 9(12): 1143.

DENG X, LI Q, HOFF J, NOVAK M, YANG H, JIN H, ERFANI SF, SHARMA C, ZHOU P, RABINOVITZ I, SONNENBERG A, YI Y, ZHOU P, STIPP CS, KAETZEL DM, HEMLER ME and YANG XH. 2012. Integrin-associated CD151 drives ErbB2-evoked mammary tumor onset and metastasis. *Neoplasia: an international journal for oncology research*. 14(8): 678-689.

DETCHOKUL S, WILLIAMS ED, PARKER MW and FRAUMAN AG. 2014. Tetraspanins as regulators of the tumour microenvironment: implications for metastasis and therapeutic strategies. *British journal of pharmacology*. 171(24): 5462-5490.

DHILLON AS, HAGAN S, RATH O and KOLCH W. 2007. MAP kinase signalling pathways in cancer. *Oncogene*. 26(22): 3279-3290.

DING H, DAI Y, LEI Y, WANG Z, LIU D, LI R, SHEN L, GU N, ZHENG M, ZHU X, ZHAO G and HU Y. 2019. Upregulation of CD81 in trophoblasts induces an imbalance of Treg/Th17 cells by promoting IL-6 expression in preeclampsia. *Cellular & molecular immunology*. 16(1): 302-312.

DROST AC, SEITZ G, BOEHMLER A, FUNK M, NORZ KP, ZIPFEL A, XUE X, KANZ L and MöHLE R. 2012. The G protein-coupled receptor CysLT1 mediates chemokine-like effects and prolongs survival in chronic lymphocytic leukemia. *Leukemia & lymphoma*. 53(4): 665-673.

EIBINGER G, FAULER G, BERNHART E, FRANK S, HAMMER A, WINTERSPERGER A, EDER H, HEINEMANN A, MISCHEL PS, MALLE E and SATTLER W. 2013. On the role of 25-hydroxycholesterol synthesis by glioblastoma cell lines. Implications for chemotactic monocyte recruitment. *Experimental cell research*. 319(12): 1828-1838.

EL KHARBILI M, ROBERT C, WITKOWSKI T, DANTY-BERGER E, BARBOLLAT-BOUTRAND L, MASSE I, GADOT N, DE LA FOUCHARDIèRE A, MCDONALD PC, DEDHAR S, LE NAOUR F, DEGOUL F and BERTHIER-VERGNES O. 2017. Tetraspanin 8 is a novel regulator of ILK-driven β1 integrin adhesion and signaling in invasive melanoma cells. *Oncotarget.* 8(10): 17140-17155.

ELCOMBE, SE, NAQVI, S, VAN DEN BOSCH, MWM, MACKENZIE, KF, CIANFANELLI, F, BROWN, GD, and ARTHUR, JSC. 2013. Dectin-1 regulates IL-10 production via a MSK1/2 and CREB dependent pathway and promotes the induction of regulatory macrophage markers. *PloS one*. 8(3): e60086.

ELLIS DL and TEITELBAUM SL. 1974. Inflammatory carcinoma of the breast. A pathologic definition. *Cancer*. 33(4): 1045-1047.

EVANS MK, BROWN MC, GERADTS J, BAO X, ROBINSON TJ, JOLLY MK, VERMEULEN PB, PALMER GM, GROMEIER M, LEVINE H, MORSE MA, VAN LAERE SJ and DEVI GR. 2018. XIAP Regulation by MNK Links MAPK and NFκB Signaling to Determine an Aggressive Breast Cancer Phenotype. *Cancer research.* 78(7): 1726-1738.

FAGHIH, Z, REZAEIFARD, S, SAFAEI, A, GHADERI, A and ERFANI, N. 2013. IL-17 and IL-4 producing CD8+ T cells in tumor draining lymph nodes of breast cancer patients: positive association with tumor progression. *Iranian journal of immunology: IJI*. 10(4): 193-204.

FARROKHI M, ETEMADIFAR M, JAFARY ALAVI MS, ZARKESH-ESFAHANI SH, BEHJATI M, REZAEI A and AMANI-BENI A. 2015. TNF-alpha Production by Peripheral Blood Monocytes in Multiple Sclerosis Patients and Healthy Controls. *Immunological investigations*. 44(6): 590-601.

FEI Y, WANG J, LIU W, ZUO H, QIN J, WANG D, ZENG H and LIU Z. 2012. CD151 promotes cancer cell metastasis via integrins α3β1 and α6β1 in vitro. *Molecular medicine reports*. 6(6): 1226-1230.

FENG Y, SPEZIA M, HUANG S, YUAN C, ZENG Z, ZHANG L, JI X, LIU W, HUANG B, LUO W, LIU B, LEI Y, DU S, VUPPALAPATI A, LUU HH, HAYDON RC, HE TC and REN G. 2018. Breast cancer development and progression: Risk factors, cancer stem cells, signaling pathways, genomics, and molecular pathogenesis. *Genes & diseases*. 5(2): 77-106.

FERNANDEZ SV, MACFARLANE AW 4th, JILLAB M, ARISI MF, YEARLEY J, ANNAMALAI L, GONG Y, CAI KQ, ALPAUGH RK, CRISTOFANILLI M and CAMPBELL KS. 2020. Immune phenotype of patients with stage IV metastatic inflammatory breast cancer. *Breast cancer research: BCR*. 22(1): 134.

FERNANDEZ-MARTINEZ, A, TANIOKA, M, FAN, C, PARKER, JS, HOADLEY, KA, KROP, I, PARTRIDGE, A, CAREY, L and PEROU, CM. 2019. Predictive and prognostic value of b-cell gene-expression signatures and b-cell receptor (BCR) repertoire in HER2+ breast cancer: A correlative analysis of the CALGB 40601 clinical trial (Alliance). *Annals of Oncology*. 30 (5): v55-v98.

FERRETTI E, PONZONI M, DOGLIONI C and PISTOIA V. 2016. IL-17 superfamily cytokines modulate normal germinal center B cell migration. *Journal of leukocyte biology*. 100(5): 913-918.

FILIPPOU PS, KARAGIANNIS GS and CONSTANTINIDOU A. 2020. Midkine (MDK) growth factor: a key player in cancer progression and a promising therapeutic target. *Oncogene*. 39(10): 2040-2054.

FLAMAND N, LUO M, PETERS-GOLDEN M and BROCK TG. 2009. Phosphorylation of serine 271 on 5-lipoxygenase and its role in nuclear export. *The Journal of biological chemistry*. 284(1): 306-313.

FOOT N, HENSHALL T and KUMAR S. 2017. Ubiquitination and the Regulation of Membrane Proteins. *Physiological reviews*. 97(1): 253-281.

FOUAD TM, BARRERA A, REUBEN JM, LUCCI A, WOODWARD WA, STAUDER MC, LIM B, DESNYDER SM, ARUN B, GILDY B, VALERO V, HORTOBAGYI GN and UENO NT. 2017. Inflammatory breast cancer: a proposed conceptual shift in the UICC-AJCC TNM staging system. *The Lancet. Oncology*. 18(4): e228-e232.

FOUAD, TM, KOGAWA, T, REUBEN, JM and UENO, NT. 2014. The role of inflammation in inflammatory breast cancer. *Advances in experimental medicine and biology*. 816: 53-73.

FUNAKOSHI, Y, WANG, Y, SEMBA, T, MASUDA, H, HOUT, D, UENO, NT and WANG, X. 2019. Comparison of molecular profile in triple-negative inflammatory and non-inflammatory breast cancer not of mesenchymal stem-like subtype. *PLoS one*. 14(9): e0222336.

GAGLIARDI M, PITNER MK, PARK J, XIE X, SASO H, LARSON RA, SAMMONS RM, CHEN H, WEI C, MASUDA H, CHAUHAN G, KONDO K, TRIPATHY D, UENO NT, DALBY KN, DEBEB BG and BARTHOLOMEUSZ C. 2020. Differential functions of ERK1 and ERK2 in lung metastasis processes in triple-negative breast cancer. *Scientific reports*. 10(1): 8537.

GAO C, JIA W, XU W, WU Q and WU J. 2021. Downregulation of CD151 restricts VCAM-1 mediated leukocyte infiltration to reduce neurobiological injuries after experimental stroke. *Journal of neuroinflammation*. 18(1): 118.

GARAUD S, BUISSERET L, SOLINAS C, GU-TRANTIEN C, DE WIND A, VAN DEN EYNDEN G, NAVEAUX C, LODEWYCKX JN, BOISSON A, DUVILLIER H, CRACIUN L, AMEYE L, VEYS I, PAESMANS M, LARSIMONT D, PICCART-GEBHART M and WILLARD-GALLO K. 2019. Tumor infiltrating B-cells signal functional humoral immune responses in breast cancer. *JCI insight*. 5(18): e129641.

GARCíA-HERNáNDEZ L, GARCíA-ORTEGA MB, RUIZ-ALCALá G, CARRILLO E, MARCHAL JA and GARCíA MÁ. 2021. The p38 MAPK Components and Modulators as Biomarkers and Molecular Targets in Cancer. *International journal of molecular sciences*. 23(1): 370

GARCíA-TUñóN I, RICOTE M, RUIZ A, FRAILE B, PANIAGUA R and ROYUELA M. 2006. Role of tumor necrosis factor-alpha and its receptors in human benign breast lesions and tumors (*in situ* and infiltrative). *Cancer science*. 97(10): 1044-1049.

GHODS A, GHADERI A, SHARIAT M, TALEI AR and MEHDIPOUR F. 2019. TNFR2 but not TNFR1 is the main TNFR expressed by B and T lymphocytes in breast cancer draining lymph nodes. *Immunology letters*. 209: 36-44.

GHOSSOUB R, CHéRY M, AUDEBERT S, LEBLANC R, EGEA-JIMENEZ AL, LEMBO F, MAMMAR S, LE DEZ F, CAMOIN L, BORG JP, RUBINSTEIN E, DAVID G and ZIMMERMANN P. 2020. Tetraspanin-6 negatively regulates exosome production. *Proceedings of the National Academy of Sciences of the United States of America*. 117(11): 5913-5922.

GIANNI L, EIERMANN W, SEMIGLAZOV V, MANIKHAS A, LLUCH A, TJULANDIN S, ZAMBETTI M, VAZQUEZ F, BYAKHOW M, LICHINITSER M, CLIMENT MA, CIRUELOS E, OJEDA B, MANSUTTI M, BOZHOK A, BARONIO R, FEYEREISLOVA A, BARTON C, VALAGUSSA P and BASELGA J. 2010. Neoadjuvant chemotherapy with trastuzumab followed by adjuvant trastuzumab versus neoadjuvant chemotherapy alone, in patients with HER2-positive locally advanced breast cancer (the NOAH trial): a randomised controlled superiority trial with a parallel HER2-negative cohort. *Lancet*. 375(9712): 377-384.

GOLDBERG AF. 2006. Role of peripherin/rds in vertebrate photoreceptor architecture and inherited retinal degenerations. *International review of cytology*. 253: 131-175.

GOLDHIRSCH A, WOOD WC, COATES AS, GELBER RD, THüRLIMANN B, SENN HJ and Panel members. 2011. Strategies for subtypes--dealing with the diversity of breast cancer: highlights of the St. Gallen International Expert Consensus on the Primary Therapy of Early Breast Cancer 2011. *Annals of oncology: official journal of the European Society for Medical Oncology*. 22(8): 1736-1747.

GOLUBOVSKAYA V and WU L. 2016. Different Subsets of T Cells, Memory, Effector Functions, and CAR-T Immunotherapy. *Cancers*. 8(3): 36.

GONG Y, NAGARATHINAM R, ARISI MF, GERRATANA L, WINN JS, SLIFKER M, PEI J, CAI KQ, HASSE Z, OBEID E, NORIEGA J, SEBASTIANO C, ROSS E, ALPAUGH K, CRISTOFANILLI M and FERNANDEZ SV. 2021. Genetic Variants and Tumor Immune Microenvironment: Clues for Targeted Therapies in Inflammatory Breast Cancer (IBC). *International journal of molecular sciences*. 22(16): 8924.

GUAN H, LAN Y, WAN Y, WANG Q, WANG C, XU L, CHEN Y, LIU W, ZHANG X, LI Y, GU Y, WANG Z and XIE F. 2016. PD-L1 mediated the differentiation of tumor-infiltrating CD19+ B lymphocytes and T cells in Invasive breast cancer. *Oncoimmunology*. 5(2): e1075112.

GUIX FX, SANNERUD R, BERDITCHEVSKI F, ARRANZ AM, HORRé K, SNELLINX A, THATHIAH A, SAIDO T, SAITO T, RAJESH S, OVERDUIN M, KUMAR-SINGH S, RADAELLI E, CORTHOUT N, COLOMBELLI J, TOSI S, MUNCK S, SALAS IH, ANNAERT W and DE STROOPER B. 2017. Tetraspanin 6: a pivotal protein of the multiple vesicular body determining exosome release and lysosomal degradation of amyloid precursor protein fragments. *Molecular neurodegeneration*. 12(1): 25.

GUéRIN M, GABILLOT M, MATHIEU MC, TRAVAGLI JP, SPIELMANN M, ANDRIEU N and RIOU G. 1989. Structure and expression of c-erbB-2 and EGF receptor genes in inflammatory and non-inflammatory breast cancer: prognostic significance. *International journal of cancer*. 43(2): 201-208.

HAMM CA, MORAN D, RAO K, TRUSK PB, PRY K, SAUSEN M, JONES S, VELCULESCU VE, CRISTOFANILLI M and BACUS S. 2016. Genomic and Immunological Tumor Profiling Identifies Targetable Pathways and Extensive CD8+/PDL1+ Immune Infiltration in Inflammatory Breast Cancer Tumors. *Molecular cancer therapeutics*. 15(7): 1746-1756.

HANCE KW, ANDERSON WF, DEVESA SS, YOUNG HA and LEVINE PH. 2005. Trends in inflammatory breast carcinoma incidence and survival: the surveillance, epidemiology, and end results program at the National Cancer Institute. *Journal of the National Cancer Institute*. 97(13): 966-975.

HANSMANN L, GROEGER S, VON WULFFEN W, BEIN G and HACKSTEIN H. 2008. Human monocytes represent a

competitive source of interferon-alpha in peripheral blood. *Clinical immunology: the official journal of the Clinical Immunology Society*. 127(2): 252-264.

HAYWARD S, GACHEHILADZE M, BADR N, ANDRIJES R, MOLOSTVOV G, PANIUSHKINA L, SOPIKOVA B, SLOBODOVá Z, MGEBRISHVILI G, SHARMA N, HORIMOTO Y, BURG D, ROBERTSON G, HANBY A, HOAR F, REA D, ECKHARDT BL, UENO NT, NAZARENKO I, LONG HM, VAN LAERE S, SHAABAN AM and BERDITCHEVSKI F. 2020. The CD151-midkine pathway regulates the immune microenvironment in inflammatory breast cancer. *The Journal of pathology*. 251(1): 63-73.

HE Y, REZAEI S, JúNIOR R, CRUZ LJ and EICH C. 2022. Multifunctional Role of Lipids in Modulating the Tumorigenic Properties of 4T1 Breast Cancer Cells. *International journal of molecular sciences*. 23(8): 4240

HE Z, HE J, LIU Z, XU J, YI SF, LIU H and YANG J. 2014. MAPK11 in breast cancer cells enhances osteoclastogenesis and bone resorption. *Biochimie*. 106: 24-32.

HEMLER ME. 2005. Tetraspanin functions and associated microdomains. *Nature reviews. Molecular cell biology*. 6(10): 801-811.

HENNEL R, BRIX N, SEIDL K, ERNST A, SCHEITHAUER H, BELKA C and LAUBER K. 2014. Release of monocyte migration signals by breast cancer cell lines after ablative and fractionated γ-irradiation. Radiation oncology. 9(1): 85.

HENNESSY BT, GONZALEZ-ANGULO AM, HORTOBAGYI GN, CRISTOFANILLI M, KAU SW, BROGLIO K, FORNAGE B, SINGLETARY SE, SAHIN A, BUZDAR AU and VALERO V. 2006. Disease-free and overall survival after pathologic complete disease remission of cytologically proven inflammatory breast carcinoma axillary lymph node metastases after primary systemic chemotherapy. *Cancer*. 106(5): 1000-1006.

HITTI E, IAKOVLEVA T, BROOK M, DEPPENMEIER S, GRUBER AD, RADZIOCH D, CLARK AR, BLACKSHEAR PJ, KOTLYAROV A and GAESTEL M. 2006. Mitogen-activated protein kinase-activated protein kinase 2 regulates tumor necrosis factor mRNA stability and translation mainly by altering tristetraprolin expression, stability, and binding to adenine/uridine-rich element. *Molecular and cellular biology*. 26(6): 2399-2407.

HOTTA H, ROSS AH, HUEBNER K, ISOBE M, WENDEBORN S, CHAO MV, RICCIARDI RP, TSUJIMOTO Y, CROCE CM and KOPROWSKI H. 1988. Molecular cloning and characterization of an antigen associated with early stages of melanoma tumor progression. *Cancer research*. 48(11): 2955-2962.

HOUCHENS NW and MERAJVER SD. 2008. Molecular determinants of the inflammatory breast cancer phenotype. *Oncology*. 22(14): 1556-61; discussion 1561, 1565-1576.

HU Q, HONG Y, QI P, LU G, MAI X, XU S, HE X, GUO Y, GAO L, JING Z, WANG J, CAI T and ZHANG Y. 2021. Atlas of breast cancer infiltrated B-lymphocytes revealed by paired single-cell RNA-sequencing and antigen receptor profiling. *Nature communications*. 12(1): 2186.

HUANG H, SOSSEY-ALAOUI K, BEACHY SH and GERADTS J. 2007. The tetraspanin superfamily member NET-6 is a new tumor suppressor gene. *Journal of cancer research and clinical oncology*. 133(10): 761-769.

HUANG Y, ZUCKER B, ZHANG S, ELIAS S, ZHU Y, CHEN H, DING T, LI Y, SUN Y, LOU J, KOZLOV MM and YU L. 2019. Migrasome formation is mediated by assembly of micron-scale tetraspanin macrodomains. *Nature cell biology*. 21(8): 991-1002.

HUGHES CE and NIBBS R. 2018. A guide to chemokines and their receptors. *The FEBS journal*. 285(16): 2944-2971.

HUMBERT PO, PRYJDA TZ, PRANJIC B, FARRELL A, FUJIKURA K, DE MATOS SIMOES R, KARIM R, KOZIERADZKI I, CRONIN S, NEELY GG, MEYER TF, HAGELKRUYS A, RICHARDSON HE and PENNINGER JM. 2022. TSPAN6 is a suppressor of Ras-driven cancer. *Oncogene*. 41(14): 2095-2105.

HWANG JR, JO K, LEE Y, SUNG BJ, PARK YW and LEE JH. 2012. Upregulation of CD9 in ovarian cancer is related to the induction of TNF-α gene expression and constitutive NF-κB activation. Carcinogenesis. 33(1): 77-83.

IGLESIA MD, VINCENT BG, PARKER JS, HOADLEY KA, CAREY LA, PEROU CM and SERODY JS. 2014. Prognostic

B-cell signatures using mRNA-seq in patients with subtype-specific breast and ovarian cancer. *Clinical cancer research: an official journal of the American Association for Cancer Research*. 20(14): 3818-3829.

IMJETI NS, MENCK K, EGEA-JIMENEZ AL, LECOINTRE C, LEMBO F, BOUGUENINA H, BADACHE A, GHOSSOUB R, DAVID G, ROCHE S and ZIMMERMANN P. 2017. Syntenin mediates SRC function in exosomal cell-to-cell communication. *Proceedings of the National Academy of Sciences of the United States of America*. 114(47): 12495-12500.

IYER A, FAIRLIE, DP, PRINS, JB, HAMMOCK, BD and BROWN, L. 2010. Inflammatory lipid mediators in adipocyte function and obesity. *Nature Reviews. Endocrinology*. 6(2):71-82.

JOHNSON AM, KLECZKO EK and NEMENOFF RA. 2020. Eicosanoids in Cancer: New Roles in Immunoregulation. *Frontiers in pharmacology*. 11: 595498.

JOLLY MK, BOARETO M, DEBEB BG, ACETO N, FARACH-CARSON MC, WOODWARD WA and LEVINE H. 2017. Inflammatory breast cancer: a model for investigating cluster-based dissemination. *NPJ breast cancer*. 3: 21.

JONES, D, BENJAMIN, RJ, SHAHSAFAEI, A and DORFMAN, DM. 2000. The chemokine receptor CXCR3 is expressed in a subset of B-cell lymphomas and is a marker of B-cell chronic lymphocytic leukemia. *Blood*. 95(2): 627-632.

KANAOKA Y and AUSTEN KF. 2019. Roles of cysteinyl leukotrienes and their receptors in immune cell-related functions. *Advances in immunology*. 142: 65-84.

KARAMATIC CREW V, BURTON N, KAGAN A, GREEN CA, LEVENE C, FLINTER F, BRADY RL, DANIELS G and ANSTEE DJ. 2004. CD151, the first member of the tetraspanin (TM4) superfamily detected on erythrocytes, is essential for the correct assembly of human basement membranes in kidney and skin. *Blood*. 104(8): 2217-2223.

KARAVITIS J, HIX LM, SHI YH, SCHULTZ RF, KHAZAIE K and ZHANG M. 2012. Regulation of COX2 expression in mouse mammary tumor cells controls bone metastasis and PGE2-induction of regulatory T cell migration. *PloS one*. 7(9): e46342.

KIM HJ and CANTOR H. 2014. CD4 T-cell subsets and tumor immunity: the helpful and the not-so-helpful. *Cancer immunology research*. 2(2): 91-98.

KIM M, CHOI HY, WOO JW, CHUNG YR and PARK SY. 2021. Role of CXCL10 in the progression of in situ to invasive carcinoma of the breast. *Scientific reports*. 11(1): 18007.

KLASEN C, OHL K, STERNKOPF M, SHACHAR I, SCHMITZ C, HEUSSEN N, HOBEIKA E, LEVIT-ZERDOUN E, TENBROCK K, RETH M, BERNHAGEN J and EL BOUNKARI O. 2014. MIF promotes B cell chemotaxis through the receptors CXCR4 and CD74 and ZAP-70 signaling. *The Journal of immunology: official journal of the American Association of Immunologists*. 192(11): 5273-5284.

KNOBLICH K, WANG HX, SHARMA C, FLETCHER AL, TURLEY SJ and HEMLER ME. 2014. Tetraspanin TSPAN12 regulates tumor growth and metastasis and inhibits β-catenin degradation. *Cellular and molecular life sciences: CMLS*. 71(7): 1305-1314.

KOHLI K, PILLARISETTY VG and KIM TS. 2022. Key chemokines direct migration of immune cells in solid tumors. *Cancer gene therapy*. 29(1): 10-21.

KOTLYAROV A, NEININGER A, SCHUBERT C, ECKERT R, BIRCHMEIER C, VOLK HD and GAESTEL M. 1999. MAPKAP kinase 2 is essential for LPS-induced TNF-alpha biosynthesis. *Nature cell biology*. 1(2): 94-97.

KUPSTAS AR, HOSKIN TL, DAY CN, BOUGHEY JC, HABERMANN EB and HIEKEN TJ. 2020. Biological subtype, treatment response and outcomes in inflammatory breast cancer using data from the National Cancer Database. *The British journal of surgery*. 107(8): 1033-1041.

KURODA, H, JAMIYAN, T, YAMAGUCHI, R, KAKUMOTO, A, ABE, A, HARADA, O and MASUNAGA, A. 2021. Tumor-infiltrating B cells and T cells correlate with postoperative prognosis in triple-negative carcinoma of the breast. *BMC Cancer*. 21(1): 286.

KURODA H, JAMIYAN T, YAMAGUCHI R, KAKUMOTO A, ABE A, HARADA O, ENKHBAT B and MASUNAGA A. 2021. Prognostic value of tumor-infiltrating B lymphocytes and plasma cells in triple-negative breast cancer. *Breast cancer: the journal of the Japanese Breast Cancer Society*. 28(4): 904-914.

LACERDA L, DEBEB BG, SMITH D, LARSON R, SOLLEY T, XU W, KRISHNAMURTHY S, GONG Y, LEVY LB, BUCHHOLZ T, UENO NT, KLOPP A and WOODWARD WA. 2015. Mesenchymal stem cells mediate the clinical phenotype of inflammatory breast cancer in a preclinical model. *Breast cancer research: BCR*. 17: 42.

LANG T and HOCHHEIMER N. 2020. Tetraspanins. *Current biology: CB*. 30(5): 204-206.

LATYSHEVA N, MURATOV G, RAJESH S, PADGETT M, HOTCHIN NA, OVERDUIN M and BERDITCHEVSKI F. 2006. Syntenin-1 is a new component of tetraspanin-enriched microdomains: mechanisms and consequences of the interaction of syntenin-1 with CD63. *Molecular and cellular biology*. 26(20): 7707-7718.

LAUMONT CM, BANVILLE AC, GILARDI M, HOLLERN DP and NELSON BH. 2022. Tumour-infiltrating B cells: immunological mechanisms, clinical impact and therapeutic opportunities. *Nature reviews. Cancer*. 22(7): 414-430.

LEBIEN TW and TEDDER TF. 2008. B lymphocytes: how they develop and function. *Blood*. 112(5): 1570-1580.

LEE BJ and TANNENBAUM NE. 1924. Inflammatory Carcinoma of the Breast: a report of twenty-eight cases from the breast clinic of Memorial Hospital. *Surg Gynecol Obstet*. 39: 580.

LEHMANN BD, BAUER JA, CHEN X, SANDERS ME, CHAKRAVARTHY AB, SHYR Y and PIETENPOL JA. 2011. Identification of human triple-negative breast cancer subtypes and preclinical models for selection of targeted therapies. *The Journal of clinical investigation*. 121(7): 2750-2767.

LEREBOURS F, VACHER S, ANDRIEU C, ESPIE M, MARTY M, LIDEREAU R and BIECHE I. 2008. NF-kappa B genes have a major role in inflammatory breast cancer. *BMC cancer*. 8: 41.

LESLIE CC. 2004. Regulation of the specific release of arachidonic acid by cytosolic phospholipase A2. *Prostaglandins, leukotrienes, and essential fatty acids*. 70(4): 373-376.

LEVINE PH, PORTERA CC, HOFFMAN HJ, YANG SX, TAKIKITA M, DUONG QN, HEWITT SM and SWAIN SM. 2012. Evaluation of lymphangiogenic factors, vascular endothelial growth factor D and E-cadherin in distinguishing inflammatory from locally advanced breast cancer. *Clinical breast cancer*. 12(4): 232-239.

LI F, TIAN P, ZHANG J and KOU C. 2015. The clinical and prognostic significance of midkine in breast cancer patients. *Tumour biology: the journal of the International Society for Oncodevelopmental Biology and Medicine*. 36(12): 9789-9794.

LI J, GONZALEZ-ANGULO AM, ALLEN PK, YU TK, WOODWARD WA, UENO NT, LUCCI A, KRISHNAMURTHY S, GONG Y, BONDY ML, YANG W, WILLEY JS, CRISTOFANILLI M, VALERO V and BUCHHOLZ TA. 2011. Triple-negative subtype predicts poor overall survival and high locoregional relapse in inflammatory breast cancer. *The oncologist*. 16(12): 1675-1683.

LI J, XU J, LI L, IANNI A, KUMARI P, LIU S, SUN P, BRAUN T, TAN X, XIANG R and YUE S. 2020. MGAT3-mediated glycosylation of tetraspanin CD82 at asparagine 157 suppresses ovarian cancer metastasis by inhibiting the integrin signaling pathway. *Theranostics*. 10(14): 6467-6482.

LI YF, LI RS, SAMUEL SB, CUETO R, LI XY, WANG H and YANG XF. 2016. Lysophospholipids and their G protein-coupled receptors in atherosclerosis. *Frontiers in bioscience (Landmark edition)*. 21(1): 70-88.

LIANG YK, DENG ZK, CHEN MT, QIU SQ, XIAO YS, QI YZ, XIE Q, WANG ZH, JIA SC, ZENG and LIN HY. 2021. CXCL9 Is a Potential Biomarker of Immune Infiltration Associated With Favorable Prognosis in ER-Negative Breast Cancer. *Frontiers in oncology*. 11: 710286.

LIM B, WOODWARD WA, WANG X, REUBEN JM and UENO NT. 2018. Inflammatory breast cancer biology: the tumour microenvironment is key. *Nature reviews. Cancer*. 18(8): 485-499.

LIN JJ, JIANG H and FISHER PB. 1998. Melanoma differentiation associated gene-9, mda-9, is a human gamma interferon

responsive gene. *Gene*. 207(2): 105-110.

LIN LL, WARTMANN M, LIN AY, KNOPF JL, SETH A and DAVIS RJ. 1993. cPLA2 is phosphorylated and activated by MAP kinase. *Cell*. 72(2): 269-278.

LINDE, N, CASANOVA-ACEBES, M, SOSA, MS, MORTHA, A, RAHMAN, A, FARIAS, E, HARPER, K, TARDIO, E, TORRES, IR, JONES, J, CONDEELIS, J, MERAD, M and AGUIRRE-GHISO, JA. 2018. Macrophages orchestrate breast cancer early dissemination and metastasis. *Nature communications*. 9(1): 21.

LINEBERRY N, SU L, SOARES L and FATHMAN CG. 2008. The single subunit transmembrane E3 ligase gene related to anergy in lymphocytes (GRAIL) captures and then ubiquitinates transmembrane proteins across the cell membrane. *The Journal of biological chemistry*. 283(42): 28497-2505.

LITTLE AC, PATHANJELI P, WU Z, BAO L, GOO LE, YATES JA, OLIVER CR, SOELLNER MB and MERAJVER SD. 2019. IL-4/IL-13 Stimulated Macrophages Enhance Breast Cancer Invasion Via Rho-GTPase Regulation of Synergistic VEGF/CCL-18 Signaling. *Frontiers in oncology*. 9: 456.

LIU C, YANG XV, WU J, KUEI C, MANI NS, ZHANG L, YU J, SUTTON SW, QIN N, BANIE H, KARLSSON L, SUN S and LOVENBERG TW. 2011. Oxysterols direct B-cell migration through EBI2. *Nature*. 475(7357): 519-523.

LIU RX, WEI Y, ZENG QH, CHAN KW, XIAO X, ZHAO XY, CHEN MM, OUYANG FZ, CHEN DP, ZHENG L, LAO XM and KUANG DM. 2015. Chemokine (C-X-C motif) receptor 3-positive B cells link interleukin-17 inflammation to protumorigenic macrophage polarization in human hepatocellular carcinoma. *Hepatology: official journal of the American Association for the Study of Liver Diseases*. 62(6): 1779-1790.

LIU T, ZHANG L, JOO D and SUN SC. 2017. NF-κB signaling in inflammation. Signal transduction and targeted therapy. 2:17023.

LIU, X, TSANG, JYS, HLAING, T, HU, J, NI, YB, CHAN, SK, CHEUNG, SY and TSE, GM. 2017. Distinct tertiary lymphoid structure associations and their prognostic relevance in HER2 positive and negative breast cancers. *The oncologist*. 22(11): 1316–1324.

LOURDA M, OLSSON-ÅKEFELDT S, GAVHED D, BJöRNFOT S, CLAUSEN N, HJALMARS U, SABEL M, TAZI A, ARICò M, DELPRAT C, HENTER JI and SVENSSON M. 2014. Detection of IL-17A-producing peripheral blood monocytes in Langerhans cell histiocytosis patients. *Clinical immunology: the official journal of the Clinical Immunology Society*. 153(1): 112-122.

LU J, LI J, LIU S, WANG T, IANNI A, BOBER E, BRAUN T, XIANG R and YUE S. 2017. Exosomal tetraspanins mediate cancer metastasis by altering host microenvironment. *Oncotarget*. 8(37): 62803-62815.

LUO J, ZOU H, GUO Y, TONG T, YE L, ZHU C, DENG L, WANG B, PAN Y and LI P. 2022. SRC kinase-mediated signaling pathways and targeted therapies in breast cancer. *Breast cancer research: BCR*. 24(1): 99.

LYNN KD, ROLAND CL and BREKKEN RA. 2010. VEGF and pleiotrophin modulate the immune profile of breast cancer. *Cancers*. 2(2): 970-988.

MA Y, ZHAO S, SHEN S, FANG S, YE Z, SHI Z and HONG A. 2015. A novel recombinant slow-release TNF α-derived peptide effectively inhibits tumor growth and angiogensis. *Scientific reports.* 5: 13595.

MACKENZIE KF, VAN DEN BOSCH MW, NAQVI S, ELCOMBE SE, MCGUIRE VA, REITH AD, BLACKSHEAR PJ, DEAN JL and ARTHUR JS. 2013. MSK1 and MSK2 inhibit lipopolysaccharide-induced prostaglandin production via an interleukin-10 feedback loop. *Molecular and cellular biology*. 33(7): 1456-1467.

MAEDA K, MATSUHASHI S, HORI K, XIN Z, MUKAI T, TABUCHI K, EGASHIRA M and NIIKAWA N. 1998. Cloning and characterization of a novel human gene, TM4SF6, encoding a protein belonging to the transmembrane 4 superfamily, and mapped to Xq22. *Genomics*. 52(2): 240-242.

MAJUMDER, M, XIN, X, LIU, L, GIRISH, GV and LALA, PK. 2014. Prostaglandin E2 receptor EP 4 as the common target on cancer cells and macrophages to abolish angiogenesis, lymphangiogenesis, metastasis, and stem-like cell functions.

Cancer science. 105(9): 1142-1151.

MAKKI J. 2015. Diversity of Breast Carcinoma: Histological Subtypes and Clinical Relevance. *Clinical medicine insights. Pathology*. 8: 23-31.

MANCINI JA, ABRAMOVITZ M, COX ME, WONG E, CHARLESON S, PERRIER H, WANG Z, PRASIT P and VICKERS PJ. 1993. 5-lipoxygenase-activating protein is an arachidonate binding protein. *FEBS letters*. 318(3): 277-281.

MANTOVANI A, ALLAVENA P, SOZZANI S, VECCHI A, LOCATI M and SICA A. 2004. Chemokines in the recruitment and shaping of the leukocyte infiltrate of tumors. *Seminars in cancer biology*. 14(3): 155-160.

MARTIN F, ROTH DM, JANS DA, POUTON CW, PARTRIDGE LJ, MONK PN and MOSELEY GW. 2005. Tetraspanins in viral infections: a fundamental role in viral biology. *Journal of virology*. 79(17): 10839-10851.

MASUDA H, BREWER TM, LIU DD, IWAMOTO T, SHEN Y, HSU L, WILLEY JS, GONZALEZ-ANGULO AM, CHAVEZ-MACGREGOR M, FOUAD TM, WOODWARD WA, REUBEN JM, VALERO V, ALVAREZ RH, HORTOBAGYI GN and UENO NT. 2014. Long-term treatment efficacy in primary inflammatory breast cancer by hormonal receptor- and HER2-defined subtypes. *Annals of oncology: official journal of the European Society for Medical Oncology*. 25(2): 384-391.

MCAULIFFE PF, EVANS KW, AKCAKANAT A, CHEN K, ZHENG X, ZHAO H, ETEROVIC AK, SANGAI T, HOLDER AM, SHARMA C, CHEN H, DO KA, TARCO E, GAGEA M, NAFF KA, SAHIN A, MULTANI AS, BLACK DM, MITTENDORF EA, BEDROSIAN I, MILLS GB, GONZALEZ-ANGULO AM and MERIC-BERNSTAM F. 2015. Ability to Generate Patient-Derived Breast Cancer Xenografts Is Enhanced in Chemoresistant Disease and Predicts Poor Patient Outcomes. *PloS one*. 10(9): e0136851.

MCGUIRE VA, ROSNER D, ANANIEVA O, ROSS EA, ELCOMBE SE, NAQVI S, VAN DEN BOSCH M, MONK CE, RUIZ-ZORRILLA DIEZ T, CLARK AR and ARTHUR J. 2017. Beta Interferon Production Is Regulated by p38 Mitogen-Activated Protein Kinase in Macrophages via both MSK1/2- and Tristetraprolin-Dependent Pathways. *Molecular and cellular biology*. 37(1): e00454-16.

MERCOGLIANO MF, BRUNI S, ELIZALDE PV and SCHILLACI R. 2020. Tumor Necrosis Factor α Blockade: An Opportunity to Tackle Breast Cancer. *Frontiers in oncology.* 10: 584.

MESA-EGUIAGARAY I, WILD SH, ROSENBERG PS, BIRD SM, BREWSTER DH, HALL PS, CAMERON DA, MORRISON D and FIGUEROA JD. 2020. Distinct temporal trends in breast cancer incidence from 1997 to 2016 by molecular subtypes: a population-based study of Scottish cancer registry data. *British journal of cancer*. 123(5): 852-859.

MIESZKOWSKA M, PIASECKA D, POTEMSKI P, DEBSKA-SZMICH S, RYCHLOWSKI M, KORDEK R, SADEJ R and ROMANSKA HM. 2019. Tetraspanin CD151 impairs heterodimerization of ErbB2/ErbB3 in breast cancer cells. *Translational research: the journal of laboratory and clinical medicine*. 207: 44-55.

MILIGY I, MOHAN P, GABER A, ALESKANDARANY MA, NOLAN CC, DIEZ-RODRIGUEZ M, MUKHERJEE A, CHAPMAN C, ELLIS IO, GREEN AR and RAKHA EA. 2017. Prognostic significance of tumour infiltrating B lymphocytes in breast ductal carcinoma in situ. *Histopathology*. 71(2): 258-268.

MILLER J, DREYER TF, BäCHER AS, SINNER EK, HEINRICH C, BENGE A, GROSS E, PREIS S, ROTHER J, ROBERTS A, NELLES G, MITEVA T and REUNING U. 2018. Differential tumor biological role of the tumor suppressor KAI1 and its splice variant in human breast cancer cells. *Oncotarget*. 9(5): 6369-6390.

MIN G, WANG H, SUN TT and KONG XP. 2006. Structural basis for tetraspanin functions as revealed by the cryo-EM structure of uroplakin complexes at 6-A resolution. *The Journal of cell biology*. 173(6): 975-983.

MIR C, GARCIA-MAYEA Y, GARCIA L, HERRERO P, CANELA N, TABERNERO R, LORENTE J, CASTELLVI J, ALLONCA E, GARCíA-PEDRERO J, RODRIGO JP, CARRACEDO Á and LLEONART ME. 2021. SDCBP Modulates Stemness and Chemoresistance in Head and Neck Squamous Cell Carcinoma through Src Activation.

Cancers. 13(19): 4952.

MISHRA S, CHARAN M, SHUKLA RK, AGARWAL P, MISRI S, VERMA AK, AHIRWAR DK, SIDDIQUI J, KAUL K, SAHU N, VYAS K, GARG AA, KHAN A, MILES WO, SONG JW, BHUTANI N and GANJU RK. 2022. cPLA2 blockade attenuates S100A7-mediated breast tumorigenicity by inhibiting the immunosuppressive tumor microenvironment. *Journal of experimental & clinical cancer research: CR*. 41(1): 54.

MIYABE, Y, MIYABE, C and LUSTER, AD. 2017. LTB4 and BLT1 in inflammatory arthritis. *Seminars in immunology*. 33: 52-57.

MOHAMED HT, EL-GHONAIMY EA, EL-SHINAWI M, HOSNEY M, GöTTE M, WOODWARD WA, EL-MAMLOUK T and MOHAMED MM. 2020. IL-8 and MCP-1/CCL2 regulate proteolytic activity in triple negative inflammatory breast cancer a mechanism that might be modulated by Src and Erk1/2. *Toxicology and applied pharmacology*. 401: 115092.

MOHAMED MM, EL-GHONAIMY EA, NOUH MA, SCHNEIDER RJ, SLOANE BF and EL-SHINAWI M. 2014. Cytokines secreted by macrophages isolated from tumor microenvironment of inflammatory breast cancer patients possess chemotactic properties. *The international journal of biochemistry & cell biology*. 46: 138-147.

MOHAMMED ZM, GOING JJ, EDWARDS J, ELSBERGER B and MCMILLAN DC. 2013. The relationship between lymphocyte subsets and clinico-pathological determinants of survival in patients with primary operable invasive ductal breast cancer. *British journal of cancer*. 109(6): 1676-1684.

MONTPELLIER C, TEWS BA, POITRIMOLE J, ROCHA-PERUGINI V, D'ARIENZO V, POTEL J, ZHANG XA, RUBINSTEIN E, DUBUISSON J and COCQUEREL L. 2011. Interacting regions of CD81 and two of its partners, EWI-2 and EWI-2wint, and their effect on hepatitis C virus infection. *The Journal of biological chemistry*. 286(16): 13954-13965.

MOORE HM, GONZALEZ ME, TOY KA, CIMINO-MATHEWS A, ARGANI P and KLEER CG. 2013. EZH2 inhibition decreases p38 signaling and suppresses breast cancer motility and metastasis. *Breast cancer research and treatment*. 138(3): 741-752.

MUELLER KL, POWELL K, MADDEN JM, EBLEN ST and BOERNER JL. 2012. EGFR Tyrosine 845 Phosphorylation-Dependent Proliferation and Transformation of Breast Cancer Cells Require Activation of p38 MAPK. *Translational oncology*. 5(5): 327-334.

MULLOOLY M, MURPHY J, GIERACH GL, WALSH PM, DEADY S, BARRON TI, SHERMAN ME, ROSENBERG PS and ANDERSON WF. 2017. Divergent oestrogen receptor-specific breast cancer trends in Ireland (2004-2013): Amassing data from independent Western populations provide etiologic clues. *European journal of cancer: official journal for European Organization for Research and Treatment of Cancer (EORTC) [and] European Association for Cancer Research (EACR)*. 86: 326-333.

NAKAMURA Y, NAKANISHI T and TAMAI I. 2018. Membrane Transporters Contributing to PGE2 Distribution in Central Nervous System. *Biological & pharmaceutical bulletin*. 41(9): 1337-1347.

NAKANISHI M and ROSENBERG DW. 2006. Roles of cPLA2alpha and arachidonic acid in cancer. *Biochimica et biophysica acta*. 1761(11): 1335-1343.

NELMS K, KEEGAN AD, ZAMORANO J, RYAN JJ and PAUL WE. 1999. The IL-4 receptor: signaling mechanisms and biologic functions. *Annual review of immunology*. 17: 701-738.

NICOLETTI AM, KENNY CH, KHALIL AM, PAN Q, RALPH KL, RITCHIE J, VENKATARAMANI S, PRESKY DH, DEWIRE SM and BRODEUR SR. 2016. Unexpected Potency Differences between B-Cell-Activating Factor (BAFF) Antagonist Antibodies against Various Forms of BAFF: Trimer, 60-Mer, and Membrane-Bound. *The Journal of pharmacology and experimental therapeutics*. 359(1): 37-44.

NISHIUCHI R, SANZEN N, NADA S, SUMIDA Y, WADA Y, OKADA M, TAKAGI J, HASEGAWA H and SEKIGUCHI K. 2005. Potentiation of the ligand-binding activity of integrin alpha3beta1 via association with tetraspanin CD151.

Proceedings of the National Academy of Sciences of the United States of America. 102(6): 1939-1944.

NOVITSKAYA V, ROMANSKA H, KORDEK R, POTEMSKI P, KUSIńSKA R, PARSONS M, ODINTSOVA E and BERDITCHEVSKI F. 2014. Integrin α3β1-CD151 complex regulates dimerization of ErbB2 via RhoA. *Oncogene.* 33(21): 2779-2789.

ODINTSOVA E, SUGIURA T and BERDITCHEVSKI F. 2000. Attenuation of EGF receptor signaling by a metastasis suppressor, the tetraspanin CD82/KAI-1. *Current biology: CB*. 10(16): 1009-1012.

ODINTSOVA E, VAN NIEL G, CONJEAUD H, RAPOSO G, IWAMOTO R, MEKADA E and BERDITCHEVSKI F. 2013. Metastasis suppressor tetraspanin CD82/KAI1 regulates ubiquitylation of epidermal growth factor receptor. *The Journal of biological chemistry*. 288(36): 26323-26334.

ODINTSOVA E, VOORTMAN J, GILBERT E and BERDITCHEVSKI F. 2003. Tetraspanin CD82 regulates compartmentalisation and ligand-induced dimerization of EGFR. *Journal of cell science*. 116(Pt 22): 4557-4566.

OLESCH C, BRüNE B and WEIGERT A. 2022. Keep a Little Fire Burning-The Delicate Balance of Targeting Sphingosine-1-Phosphate in Cancer Immunity. *International journal of molecular sciences*. 23(3): 1289.

OLINGY CE, DINH HQ and HEDRICK CC. 2019. Monocyte heterogeneity and functions in cancer. *Journal of leukocyte biology*. 106(2): 309-322.

ORDAS L, COSTA L, LOZANO A, CHEVILLARD C, CALOVOULOS A, KANTAR D, FERNANDEZ L, CHAUVIN L, DOSSET P, DOUCET C, HERON-MILHAVET L, ODINTSOVA E, BERDITCHEVSKI F, MILHIET PE and BéNISTANT C. 2021. Mechanical Control of Cell Migration by the Metastasis Suppressor Tetraspanin CD82/KAI1. *Cells*. 10(6): 1545.

ORLIKOWSKY T, DANNECKER GE, WANG Z, HOROWITZ H, NIETHAMMER D and HOFFMANN MK. 1999. Activation or destruction of T cells via macrophages. *Pathobiology: journal of immunopathology, molecular and cellular biology*. 67(5-6): 298-301.

OVSIY I, RIABOV V, MANOUSARIDIS I, MICHEL J, MOGANTI K, YIN S, LIU T, STICHT C, KREMMER E, HARMSEN MC, GOERDT S, GRATCHEV A and KZHYSHKOWSKA J. 2017. IL-4 driven transcription factor FoxQ1 is expressed by monocytes in atopic dermatitis and stimulates monocyte migration. *Scientific reports*. 7(1): 16847.

OZGA AJ, CHOW MT and LUSTER AD. 2021. Chemokines and the immune response to cancer. *Immunity*. 54(5): 859-874.

PAN Q, BAO LW and MERAJVER SD. 2003. Tetrathiomolybdate inhibits angiogenesis and metastasis through suppression of the NFkappaB signaling cascade. *Molecular cancer research: MCR*. 1(10): 701-706.

PARK JY, PILLINGER MH and ABRAMSON SB. 2006. Prostaglandin E2 synthesis and secretion: the role of PGE2 synthases. *Clinical immunology: the official journal of the Clinical Immunology Society*. 119(3): 229-240.

PEDERSON PJ, LIANG H, FILONOV D and MOOBERRY SL. 2021. Eribulin and Paclitaxel Differentially Alter Extracellular Vesicles and Their Cargo from Triple-Negative Breast Cancer Cells. *Cancers*. 13(11): 2783.

PEROU CM, SøRLIE T, EISEN MB, VAN DE RIJN M, JEFFREY SS, REES CA, POLLACK JR, ROSS DT, JOHNSEN H, AKSLEN LA, FLUGE O, PERGAMENSCHIKOV A, WILLIAMS C, ZHU SX, LøNNING PE, BøRRESEN-DALE AL, BROWN PO and BOTSTEIN D. 2000. Molecular portraits of human breast tumours. *Nature*. 406(6797): 747-752.

PIMENTA EM, DE S, WEISS R, FENG D, HALL K, KILIC S, BHANOT G, GANESAN S, RAN S and BARNES BJ. 2015. IRF5 is a novel regulator of CXCL13 expression in breast cancer that regulates CXCR5(+) B- and T-cell trafficking to tumor-conditioned media. *Immunology and cell biology*. 93(5): 486-499.

PLITAS, G, KONOPACKI, C, WU, K, BOS, PD, MORROW, M, PUTINTSEVA, EV, CHUDAKOV, DM and RUDENSKY, AY. 2016. Regulatory T cells exhibit distinct features in human breast cancer. *Immunity*. 45(5): 1122-1134.

POULTER JA, ALI M, GILMOUR DF, RICE A, KONDO H, HAYASHI K, MACKEY DA, KEARNS LS, RUDDLE JB, CRAIG JE, PIERCE EA, DOWNEY LM, MOHAMED MD, MARKHAM AF, INGLEHEARN CF and TOOMES C. 2010. Mutations in TSPAN12 cause autosomal-dominant familial exudative vitreoretinopathy. *American journal of*

human genetics. 86(2): 248-253.

POWNER D, KOPP PM, MONKLEY SJ, CRITCHLEY DR and BERDITCHEVSKI F. 2011. Tetraspanin CD9 in cell migration. *Biochemical Society transactions*. 39(2): 563-567.

PRABHAKARAN S, RIZK VT, MA Z, CHENG CH, BERGLUND AE, COPPOLA D, KHALIL F, MULé JJ and SOLIMAN HH. 2017. Evaluation of invasive breast cancer samples using a 12-chemokine gene expression score: correlation with clinical outcomes. *Breast cancer research: BCR*. 19(1): 71.

PRUNET C, MONTANGE T, VéJUX A, LAUBRIET A, ROHMER JF, RIEDINGER JM, ATHIAS A, LEMAIRE-EWING S, NéEL D, PETIT JM, STEINMETZ E, BRENOT R, GAMBERT P and LIZARD G. 2006. Multiplexed flow cytometric analyses of pro- and anti-inflammatory cytokines in the culture media of oxysterol-treated human monocytic cells and in the sera of atherosclerotic patients. *Cytometry. Part A: the journal of the International Society for Analytical Cytology*. 69(5): 359-373.

PéREZ ALENZA MD, TABANERA E and PEñA L. 2001. Inflammatory mammary carcinoma in dogs: 33 cases (1995-1999). *Journal of the American Veterinary Medical Association*. 219(8): 1110-1114.

QIAN BZ, LI J, ZHANG H, KITAMURA T, ZHANG J, CAMPION LR, KAISER EA, SNYDER LA and POLLARD JW. 2011. CCL2 recruits inflammatory monocytes to facilitate breast-tumour metastasis. *Nature*. 475(7355): 222-225.

QIN Y, PENG F, AI L, MU S, LI Y, YANG C and HU Y. 2021. Tumor-infiltrating B cells as a favorable prognostic biomarker in breast cancer: a systematic review and meta-analysis. *Cancer cell international*. 21(1): 310.

RACCOSTA L, FONTANA R, CORNA G, MAGGIONI D, MORESCO M and RUSSO V. 2016. Cholesterol metabolites and tumor microenvironment: the road towards clinical translation. *Cancer immunology, immunotherapy: CII*. 65(1): 111-117.

RACCOSTA L, FONTANA R, MAGGIONI D, LANTERNA C, VILLABLANCA EJ, PANICCIA A, MUSUMECI A, CHIRICOZZI E, TRINCAVELLI ML, DANIELE S, MARTINI C, GUSTAFSSON JA, DOGLIONI C, FEO SG, LEIVA A, CIAMPA MG, MAURI L, SENSI C, PRINETTI A, EBERINI I, MORA JR, BORDIGNON C, STEFFENSEN KR, SONNINO S, SOZZANI S, TRAVERSARI C and RUSSO V. 2013. The oxysterol-CXCR2 axis plays a key role in the recruitment of tumor-promoting neutrophils. *The Journal of experimental medicine*. 210(9): 1711-1728.

RAGHAV K, FRENCH JT, UENO NT, LEI X, KRISHNAMURTHY S, REUBEN JM, VALERO V and IBRAHIM NK. 2016. Inflammatory Breast Cancer: A Distinct Clinicopathological Entity Transcending Histological Distinction. *PloS one*. 11(1): e0145534.

RAJESH S, BAGO R, ODINTSOVA E, MURATOV G, BALDWIN G, SRIDHAR P, RAJESH S, OVERDUIN M and BERDITCHEVSKI F. 2011. Binding to syntenin-1 protein defines a new mode of ubiquitin-based interactions regulated by phosphorylation. *The Journal of biological chemistry*. 286(45): 39606-39614.

RAPOSO TP, ARIAS-PULIDO H, CHAHER N, FIERING SN, ARGYLE DJ, PRADA J, PIRES I and QUEIROGA FL. 2017. Comparative aspects of canine and human inflammatory breast cancer. *Seminars in oncology*. 44(4): 288-300.

RAY AL, BERGGREN KL, RESTREPO CRUZ S, GAN GN and BESWICK EJ. 2018. Inhibition of MK2 suppresses IL-1β, IL-6, and TNF-α-dependent colorectal cancer growth. *International journal of cancer.* 142(8): 1702-1711.

REA D, FRANCIS A, HANBY AM, SPEIRS V, RAKHA E, SHAABAN A, CHAN S, VINNICOMBE S, ELLIS IO, MARTIN SG, JONES LJ, BERDITCHEVSKI F and UK Inflammatory Breast Cancer Working group. 2015. Inflammatory breast cancer: time to standardise diagnosis assessment and management, and for the joining of forces to facilitate effective research. *British journal of cancer*. 112(9): 1613-1615.

REDDY SM, REUBEN A, BARUA S, JIANG H, ZHANG S, WANG L, GOPALAKRISHNAN V, HUDGENS CW, TETZLAFF MT, REUBEN JM, TSUJIKAWA T, COUSSENS LM, WANI K, HE Y, VILLAREAL L, WOOD A, RAO A, WOODWARD WA, UENO NT, KRISHNAMURTHY S, WARGO JA and MITTENDORF EA. 2019. Poor Response

to Neoadjuvant Chemotherapy Correlates with Mast Cell Infiltration in Inflammatory Breast Cancer. *Cancer immunology research*. 7(6): 1025-1035.

REYSKENS KM and ARTHUR JS. 2016. Emerging Roles of the Mitogen and Stress Activated Kinases MSK1 and MSK2. *Frontiers in cell and developmental biology*. 4: 56.

RICHARD V, KINDT N and SAUSSEZ S. 2015. Macrophage migration inhibitory factor involvement in breast cancer (Review). *International journal of oncology*. 47(5): 1627-1633.

ROBERTSON FM, BONDY M, YANG W, YAMAUCHI H, WIGGINS S, KAMRUDIN S, KRISHNAMURTHY S, LE-PETROSS H, BIDAUT L, PLAYER AN, BARSKY SH, WOODWARD WA, BUCHHOLZ T, LUCCI A, UENO NT, UENO N and CRISTOFANILLI M. 2010. Inflammatory breast cancer: the disease, the biology, the treatment. *CA: a cancer journal for clinicians*. 60(6): 351-375.

ROCHA-PERUGINI V, MONTPELLIER C, DELGRANGE D, WYCHOWSKI C, HELLE F, PILLEZ A, DROBECQ H, LE NAOUR F, CHARRIN S, LEVY S, RUBINSTEIN E, DUBUISSON J and COCQUEREL L. 2008. The CD81 partner EWI-2wint inhibits hepatitis C virus entry. *PloS one*. 3(4): e1866.

ROSKOSKI R Jr. 2015. Src protein-tyrosine kinase structure, mechanism, and small molecule inhibitors. *Pharmacological research*. 94: 9-25.

ROSSOL M, HEINE H, MEUSCH U, QUANDT D, KLEIN C, SWEET MJ and HAUSCHILDT S. 2011. LPS-induced cytokine production in human monocytes and macrophages. *Critical reviews in immunology*. 31(5): 379-446.

RUFFELL, B, AU, A, RUGO, HS, ESSERMAN, LJ, HWANG, ES and COUSSENS, LM. 2012. Leukocyte composition of human breast cancer. *Proceedings of the National Academy of Sciences of the United States of America*. 109(8): 2796-2801.

RUIZ JL, FERNANDES LR, LEVY D and BYDLOWSKI SP. 2013. Interrelationship between ATP-binding cassette transporters and oxysterols. *Biochemical pharmacology*. 86(1): 80-88.

SADEJ R, GRUDOWSKA A, TURCZYK L, KORDEK R and ROMANSKA HM. 2014. CD151 in cancer progression and metastasis: a complex scenario. *Laboratory investigation; a journal of technical methods and pathology*. 94(1): 41-51.

SADEJ R, ROMANSKA H, KAVANAGH D, BALDWIN G, TAKAHASHI T, KALIA N and BERDITCHEVSKI F. 2010. Tetraspanin CD151 regulates transforming growth factor beta signaling: implication in tumor metastasis. *Cancer research*. 70(14): 6059-6070.

SALA-VALDéS M, GORDóN-ALONSO M, TEJERA E, IBáñEZ A, CABRERO JR, URSA A, MITTELBRUNN M, LOZANO F, SáNCHEZ-MADRID F and YáñEZ-Mó M. 2012. Association of syntenin-1 with M-RIP polarizes Rac-1 activation during chemotaxis and immune interactions. *Journal of cell science*. 125(Pt 5): 1235-1246.

SALAS IH, CALLAERTS-VEGH Z, ARRANZ AM, GUIX FX, D'HOOGE R, ESTEBAN JA, DE STROOPER B and DOTTI CG. 2017. Tetraspanin 6: A novel regulator of hippocampal synaptic transmission and long term plasticity. *PloS one*. 12(2): e0171968.

SALEH ME, GADALLA R, HASSAN H, AFIFI A, GöTTE M, EL-SHINAWI M, MOHAMED MM and IBRAHIM SA. 2019. The immunomodulatory role of tumor Syndecan-1 (CD138) on ex vivo tumor microenvironmental CD4+ T cell polarization in inflammatory and non-inflammatory breast cancer patients. *PloS one*. 14(5): e0217550.

SAUTèS-FRIDMAN C, PETITPREZ F, CALDERARO J and FRIDMAN WH. 2019. Tertiary lymphoid structures in the era of cancer immunotherapy. *Nature reviews. Cancer*. 19(6): 307-325.

SCHLICHTING JA, SOLIMAN AS, SCHAIRER C, SCHOTTENFELD D and MERAJVER SD. 2012. Inflammatory and non-inflammatory breast cancer survival by socioeconomic position in the Surveillance, Epidemiology, and End Results database, 1990-2008. *Breast cancer research and treatment*. 134(3): 1257-1268.

SEIGNEURET M. 2006. Complete predicted three-dimensional structure of the facilitator transmembrane protein and hepatitis C virus receptor CD81: conserved and variable structural domains in the tetraspanin superfamily. *Biophysical journal*.

90(1): 212-227.

SHAUL ME, ZLOTNIK A, TIDHAR E, SCHWARTZ A, ARPINATI L, KAISAR-ILUZ N, MAHROUM S, MISHALIAN I and FRIDLENDER ZG. 2021. Tumor-Associated Neutrophils Drive B-cell Recruitment and Their Differentiation to Plasma Cells. *Cancer immunology research*. 9(7): 811-824.

SHI C and PAMER EG. 2011. Monocyte recruitment during infection and inflammation. *Nature reviews. Immunology*. 11(11): 762-774.

SHIMADA T, YASUDA S, SUGIURA H and YAMAGATA K. 2019. Syntenin: PDZ Protein Regulating Signaling Pathways and Cellular Functions. *International journal of molecular sciences*. 20(17): 4171.

SHIRAKAWA K, SHIBUYA M, HEIKE Y, TAKASHIMA S, WATANABE I, KONISHI F, KASUMI F, GOLDMAN CK, THOMAS KA, BETT A, TERADA M and WAKASUGI H. 2002. Tumor-infiltrating endothelial cells and endothelial precursor cells in inflammatory breast cancer. *International journal of cancer*. 99(3): 344-351.

SIC H, KRAUS H, MADL J, FLITTNER KA, VON MüNCHOW AL, PIEPER K, RIZZI M, KIENZLER AK, AYATA K, RAUER S, KLEUSER B, SALZER U, BURGER M, ZIRLIK K, LOUGARIS V, PLEBANI A, RöMER W, LOEFFLER C, SCARAMUZZA S, VILLA A, NOGUCHI E, GRIMBACHER B and EIBEL H. 2014. Sphingosine-1-phosphate receptors control B-cell migration through signaling components associated with primary immunodeficiencies, chronic lymphocytic leukemia, and multiple sclerosis. *The Journal of allergy and clinical immunology*. 134(2): 420-428.

SIGISMUND S, AVANZATO D and LANZETTI L. 2018. Emerging functions of the EGFR in cancer. *Molecular oncology*. 12(1): 3-20.

SMITH LK, BOUKHALED GM, CONDOTTA SA, MAZOUZ S, GUTHMILLER JJ, VIJAY R, BUTLER NS, BRUNEAU J, SHOUKRY NH, KRAWCZYK CM and RICHER MJ. 2018. Interleukin-10 Directly Inhibits CD8+ T Cell Function by Enhancing N-Glycan Branching to Decrease Antigen Sensitivity. *Immunity*. 48(2): 299-312.e5.

SONI S, ANAND P and PADWAD YS. 2019. MAPKAPK2: the master regulator of RNA-binding proteins modulates transcript stability and tumor progression. *Journal of experimental & clinical cancer research: CR*. 38(1): 121.

SORRELLE N, DOMINGUEZ A and BREKKEN RA. 2017. From top to bottom: midkine and pleiotrophin as emerging players in immune regulation. *Journal of leukocyte biology*. 102(2): 277-286.

SQUADRITO ML and DE PALMA M. 2011. Macrophage regulation of tumor angiogenesis: implications for cancer therapy. *Molecular aspects of medicine*. 32(2): 123-145.

ST PAUL M and OHASHI PS. 2020. The Roles of CD8+ T Cell Subsets in Antitumor Immunity. *Trends in cell biology*. 30(9): 695-704.

STANTON, SE and DISIS, ML. 2016. Clinical significance of tumor-infiltrating lymphocytes in breast cancer. *Journal for immunotherapy of cancer*. 4: 59.

STANTON SE, ADAMS S and DISIS ML. 2016. Variation in the Incidence and Magnitude of Tumor-Infiltrating Lymphocytes in Breast Cancer Subtypes: A Systematic Review. *JAMA oncology*. 2(10): 1354-1360.

STREICHER KL, WILLMARTH NE, GARCIA J, BOERNER JL, DEWEY TG and ETHIER SP. 2007. Activation of a nuclear factor kappaB/interleukin-1 positive feedback loop by amphiregulin in human breast cancer cells. *Molecular cancer research: MCR*. 5(8): 847-861.

SUN L, GUO C, YAN L, LI H, SUN J, HUO X, XIE X and HU J. 2020. Syntenin regulates melanogenesis via the p38 MAPK pathway. *Molecular medicine reports*. 22(2): 733-738.

SUN L and YE RD. 2012. Role of G protein-coupled receptors in inflammation. *Acta pharmacologica Sinica*. 33(3): 342-350.

SUN S and LIU C. 2015. 7α, 25-dihydroxycholesterol-mediated activation of EBI2 in immune regulation and diseases. *Frontiers in pharmacology.* 6: 60.

TAN P, SHI M, LAI L, TANG Z, XIE N, XU H, WEI Q, ZHANG X, YANG L and WU L. 2018. Regulative role of the CXCL13-CXCR5 axis in the tumor microenvironment. *Precision clinical medicine*. 1(1): 49-56.

TARIQ M, ZHANG J, LIANG G, DING L, HE Q and YANG B. 2017. Macrophage Polarization: Anti-Cancer Strategies to Target Tumor-Associated Macrophage in Breast Cancer. *Journal of cellular biochemistry*. 118(9): 2484-2501.

TAY RE, RICHARDSON EK and TOH HC. 2021. Revisiting the role of CD4+ T cells in cancer immunotherapy-new insights into old paradigms. *Cancer gene therapy*. 28(1-2): 5-17.

TERMINI CM and GILLETTE JM. 2017. Tetraspanins Function as Regulators of Cellular Signaling. *Frontiers in cell and developmental biology*. 5: 34.

THUMKEO D, PUNYAWATTHANANUKOOL S, PRASONGTANAKIJ S, MATSUURA R, ARIMA K, NIE H, YAMAMOTO R, AOYAMA N, HAMAGUCHI H, SUGAHARA S, TAKEDA S, CHAROENSAWAN V, TANAKA A, SAKAGUCHI S and NARUMIYA S. 2022. PGE2-EP2/EP4 signaling elicits immunosuppression by driving the mregDC-Treg axis in inflammatory tumor microenvironment. *Cell reports*. 39(10): 110914.

TITU S, GRAPA CM, MOCAN T, BALACESCU O and IRIMIE A. 2021. Tetraspanins: Physiology, Colorectal Cancer Development, and Nanomediated Applications. *Cancers*. 13(22): 5662

TOKUNAGA R, ZHANG W, NASEEM M, PUCCINI A, BERGER MD, SONI S, MCSKANE M, BABA H and LENZ HJ. 2018. CXCL9, CXCL10, CXCL11/CXCR3 axis for immune activation - A target for novel cancer therapy. *Cancer treatment reviews*. 63: 40-47.

TOMINAGA N, HAGIWARA K, KOSAKA N, HONMA K, NAKAGAMA H and OCHIYA T. 2014. RPN2-mediated glycosylation of tetraspanin CD63 regulates breast cancer cell malignancy. *Molecular cancer*. 13: 134.

TRIBOULEY C, WALLROTH M, CHAN V, PALIARD X, FANG E, LAMSON G, POT D, ESCOBEDO J and WILLIAMS LT. 1999. Characterization of a new member of the TNF family expressed on antigen presenting cells. *Biological chemistry*. 380(12): 1443-1447.

TSUCHIDA J, NAGAHASHI M, TAKABE K and WAKAI T. 2017. Clinical Impact of Sphingosine-1-Phosphate in Breast Cancer. *Mediators of inflammation*. 2017: 2076239.

UMEDA R, SATOUH Y, TAKEMOTO M, NAKADA-NAKURA Y, LIU K, YOKOYAMA T, SHIROUZU M, IWATA S, NOMURA N, SATO K, IKAWA M, NISHIZAWA T and NUREKI O. 2020. Structural insights into tetraspanin CD9 function. *Nature communications*. 11(1): 1606.

URETMEN KAGIALI ZC, SANAL E, KARAYEL Ö, POLAT AN, SAATCI Ö, ERSAN PG, TRAPPE K, RENARD BY, ÖNDER TT, TUNCBAG N, ŞAHIN Ö and OZLU N. 2019. Systems-level Analysis Reveals Multiple Modulators of Epithelial-mesenchymal Transition and Identifies DNAJB4 and CD81 as Novel Metastasis Inducers in Breast Cancer. *Molecular & cellular proteomics: MCP*. 18(9): 1756-1771.

VALETA-MAGARA A, GADI A, VOLTA V, WALTERS B, ARJU R, GIASHUDDIN S, ZHONG H and SCHNEIDER RJ. 2019. Inflammatory Breast Cancer Promotes Development of M2 Tumor-Associated Macrophages and Cancer Mesenchymal Cells through a Complex Chemokine Network. *Cancer research*. 79(13): 3360-3371.

VAN BERCKELAER C, RYPENS C, VAN DAM P, POUILLON L, PARIZEL M, SCHATS KA, KOCKX M, TJALMA W, VERMEULEN P, VAN LAERE S, BERTUCCI F, COLPAERT C and DIRIX L. 2019. Infiltrating stromal immune cells in inflammatory breast cancer are associated with an improved outcome and increased PD-L1 expression. *Breast cancer research: BCR*. 21(1): 28.

VAN DER AUWERA I, VAN LAERE SJ, VAN DEN EYNDEN GG, BENOY I, VAN DAM P, COLPAERT CG, FOX SB, TURLEY H, HARRIS AL, VAN MARCK EA, VERMEULEN PB and DIRIX LY. 2004. Increased angiogenesis and lymphangiogenesis in inflammatory versus noninflammatory breast cancer by real-time reverse transcriptase-PCR gene expression quantification. *Clinical cancer research: an official journal of the American Association for Cancer Research*. 10(23): 7965-7971.

VAN JAARSVELD MT, HOUTHUIJZEN JM and VOEST EE. 2016. Molecular mechanisms of target recognition by lipid GPCRs: relevance for cancer. *Oncogene*. 35(31): 4021-4035.

VAN LAERE SJ, VAN DER AUWERA I, VAN DEN EYNDEN GG, ELST HJ, WEYLER J, HARRIS AL, VAN DAM P, VAN MARCK EA, VERMEULEN PB and DIRIX LY. 2006. Nuclear factor-kappaB signature of inflammatory breast cancer by cDNA microarray validated by quantitative real-time reverse transcription-PCR, immunohistochemistry, and nuclear factor-kappaB DNA-binding. *Clinical cancer research: an official journal of the American Association for Cancer Research*. 12(11 Pt 1): 3249-3256.

VAN NIEL G, D'ANGELO G and RAPOSO G. 2018. Shedding light on the cell biology of extracellular vesicles. *Nature reviews. Molecular cell biology*. 19(4): 213-228.

VAN TUBERGEN EA, BANERJEE R, LIU M, VANDER BROEK R, LIGHT E, KUO S, FEINBERG SE, WILLIS AL, WOLF G, CAREY T, BRADFORD C, PRINCE M, WORDEN FP, KIRKWOOD KL and D'SILVA NJ. 2013. Inactivation or loss of TTP promotes invasion in head and neck cancer via transcript stabilization and secretion of MMP9, MMP2, and IL-6. *Clinical cancer research: an official journal of the American Association for Cancer Research*. 19(5): 1169-1179.

VAN UDEN D, VAN MAAREN MC, STROBBE L, BULT P, VAN DER HOEVEN JJ, SIESLING S, DE WILT J and BLANKEN-PEETERS C. 2019. Metastatic behavior and overall survival according to breast cancer subtypes in stage IV inflammatory breast cancer. *Breast cancer research: BCR*. 21(1): 113.

VAN ZELM MC, SMET J, ADAMS B, MASCART F, SCHANDENé L, JANSSEN F, FERSTER A, KUO CC, LEVY S, VAN DONGEN JJ and VAN DER BURG M. 2010. CD81 gene defect in humans disrupts CD19 complex formation and leads to antibody deficiency. *The Journal of clinical investigation*. 120(4): 1265-1274.

VENCES-CATALáN F, RAJAPAKSA R, SRIVASTAVA MK, MARABELLE A, KUO CC, LEVY R and LEVY S. 2015. Tetraspanin CD81 promotes tumor growth and metastasis by modulating the functions of T regulatory and myeloid-derived suppressor cells. *Cancer research*. 75(21): 4517-4526.

WANG DY, JIANG Z, BEN-DAVID Y, WOODGETT JR and ZACKSENHAUS E. 2019. Molecular stratification within triple-negative breast cancer subtypes. *Scientific reports*. 9(1): 19107.

WANG X, REYES ME, ZHANG D, FUNAKOSHI Y, TRAPE AP, GONG Y, KOGAWA T, ECKHARDT BL, MASUDA H, PIRMAN DA Jr, YANG P, REUBEN JM, WOODWARD WA, BARTHOLOMEUSZ C, HORTOBAGYI GN, TRIPATHY D and UENO NT. 2017. EGFR signaling promotes inflammation and cancer stem-like activity in inflammatory breast cancer. *Oncotarget*. 8(40): 67904-67917.

WANG, X, SEMBA, T, PHI, LTH, CHAINITIKUN, S, IWASE, T, LIM, B and UENO, NT. 2020. Targeting signaling pathways in inflammatory breast cancer. *Cancers*. 12(9): 2479.

WANG XQ, YAN Q, SUN P, LIU JW, GO L, MCDANIEL SM and PALLER AS. 2007. Suppression of epidermal growth factor receptor signaling by protein kinase C-alpha activation requires CD82, caveolin-1, and ganglioside. *Cancer research*. 67(20): 9986-9995.

WANG Y, SHI T, SONG X, LIU B and WEI J. 2021. Gene fusion neoantigens: Emerging targets for cancer immunotherapy. *Cancer letters*. 506: 45-54.

WANG Y, TONG X, OMOREGIE ES, LIU W, MENG S and YE X. 2012. Tetraspanin 6 (TSPAN6) negatively regulates retinoic acid-inducible gene I-like receptor-mediated immune signaling in a ubiquitination-dependent manner. *The Journal of biological chemistry*. 287(41): 34626-34634.

WEI H, FU P, YAO M, CHEN Y and DU L. 2016. Breast cancer stem cells phenotype and plasma cell-predominant breast cancer independently indicate poor survival. *Pathology, research and practice*. 212(4): 294-301.

WERZ O, KLEMM J, SAMUELSSON B and RåDMARK O. 2000. 5-lipoxygenase is phosphorylated by p38 kinase-dependent MAPKAP kinases. *Proceedings of the National Academy of Sciences of the United States of America*. 97(10): 5261-5266.

WILLMARTH NE, BAILLO A, DZIUBINSKI ML, WILSON K, RIESE DJ 2nd and ETHIER SP. 2009. Altered EGFR localization and degradation in human breast cancer cells with an amphiregulin/EGFR autocrine loop. *Cellular*

signalling. 21(2): 212-219.

WILLMARTH NE and ETHIER SP. 2006. Autocrine and juxtacrine effects of amphiregulin on the proliferative, invasive, and migratory properties of normal and neoplastic human mammary epithelial cells. *The Journal of biological chemistry*. 281(49): 37728-37737.

WOODWARD WA. 2015. Inflammatory breast cancer: unique biological and therapeutic considerations. *The Lancet. Oncology*. 16(15): e568-e576.

XI Y, YANI Z, JING M, YINHANG W, XIAOHUI H, JING Z, QUAN Q and SHUWEN H. 2021. Mechanisms of induction of tumors by cholesterol and potential therapeutic prospects. *Biomedicine & pharmacotherapy = Biomédecine & pharmacothérapie*. 144: 112277.

XIE, X, KAOUD, TS, EDUPUGANTI, R, ZHANG, T, KOGAWA, T, ZHAO, Y, CHAUHAN, GB, GIANNOUKOS, DN, QI, Y, TRIPATHY, D, WANG, J, GRAY, NS, DALBY, KN, BARTHOLOMEUSZ, C and UENO, NT. 2017. c-Jun N-terminal kinase promotes stem cell phenotype in triple-negative breast cancer through upregulation of Notch1 via activation of c-Jun. *Oncogene*. 36(18): 2599-2608.

XING, B, BACHSTETTER, AD and VAN ELDIK, LJ. 2013. Deficiency in p38β MAPK fails to inhibit cytokine production or protect neurons against inflammatory insult in in vitro and in vivo mouse models. *PloS one*. 8(2): e56852.

XU X, WANG B, YE C, YAO C, LIN Y, HUANG X, ZHANG Y and WANG S. 2008. Overexpression of macrophage migration inhibitory factor induces angiogenesis in human breast cancer. *Cancer letters*. 261(2): 147-157.

YAMADA A, NAGAHASHI M, AOYAGI T, HUANG WC, LIMA S, HAIT NC, MAITI A, KIDA K, TERRACINA KP, MIYAZAKI H, ISHIKAWA T, ENDO I, WATERS MR, QI Q, YAN L, MILSTIEN S, SPIEGEL S and TAKABE K. 2018. ABCC1-Exported Sphingosine-1-phosphate, Produced by Sphingosine Kinase 1, Shortens Survival of Mice and Patients with Breast Cancer. *Molecular cancer research: MCR*. 16(6): 1059-1070.

YAN W, HUANG J, ZHANG Q and ZHANG J. 2021. Role of Metastasis Suppressor KAI1/CD82 in Different Cancers. *Journal of oncology*. 2021: 9924473.

YANG J, YAN J and LIU B. 2018. Targeting VEGF/VEGFR to Modulate Antitumor Immunity. *Frontiers in immunology*. 9: 978.

YANG X, CLAAS C, KRAEFT SK, CHEN LB, WANG Z, KREIDBERG JA and HEMLER ME. 2002. Palmitoylation of tetraspanin proteins: modulation of CD151 lateral interactions, subcellular distribution, and integrin-dependent cell morphology. *Molecular biology of the cell*. 13(3): 767-781.

YANG X, KOVALENKO OV, TANG W, CLAAS C, STIPP CS and HEMLER ME. 2004. Palmitoylation supports assembly and function of integrin-tetraspanin complexes. *The Journal of cell biology*. 167(6): 1231-1240.

YOUNG D, DAS N, ANOWAI A and DUFOUR A. 2019. Matrix Metalloproteases as Influencers of the Cells' Social Media. *International journal of molecular sciences*. 20(16): 3847

ZHANG B, ZHANG Z, LI L, QIN YR, LIU H, JIANG C, ZENG TT, LI MQ, XIE D, LI Y, GUAN XY and ZHU YH. 2018. TSPAN15 interacts with BTRC to promote oesophageal squamous cell carcinoma metastasis via activating NF-κB signaling. *Nature communications*. 9(1): 1423.

ZHANG D, LAFORTUNE TA, KRISHNAMURTHY S, ESTEVA FJ, CRISTOFANILLI M, LIU P, LUCCI A, SINGH B, HUNG MC, HORTOBAGYI GN and UENO NT. 2009. Epidermal growth factor receptor tyrosine kinase inhibitor reverses mesenchymal to epithelial phenotype and inhibits metastasis in inflammatory breast cancer. *Clinical cancer research: an official journal of the American Association for Cancer Research*. 15(21): 6639-6648.

ZHANG N, ZUO L, ZHENG H, LI G and HU X. 2018. Increased Expression of CD81 in Breast Cancer Tissue is Associated with Reduced Patient Prognosis and Increased Cell Migration and Proliferation in MDA-MB-231 and MDA-MB-435S Human Breast Cancer Cell Lines In Vitro. *Medical science monitor: international medical journal of experimental and clinical research*. 24: 5739-5747.

ZHANG NN, QU FJ, LIU H, LI ZJ, ZHANG YC, HAN X, ZHU ZY and LV Y. 2021. Prognostic impact of tertiary lymphoid structures in breast cancer prognosis: a systematic review and meta-analysis. *Cancer cell international*. 21(1): 536.

ZHANG, X, KIM, S, HUNDAL, J, HERNDON, JM, LI, S, PETTI, AA, SOYSAL, SD, LI, L, MCLELLAN, MD, HOOG, J, PRIMEAU, T, MYERS, N, VICKERY, TL, STURMOSKI, M, HAGEMANN, IS, MILLER, CA, ELLIS, MJ, MARDIS, ER, HANSEN, T, FLEMING, TP, GOEDEGEBUURE, SP and GILLANDERS, WE. 2017. Breast cancer neoantigens can induce CD8+ T-cell responses and antitumor immunity. *Cancer immunology research*. 5(7): 516-523.

ZHANG Z, ZHU Y, WANG Z, ZHANG T, WU P and HUANG J. 2017. Yin-yang effect of tumor infiltrating B cells in breast cancer: From mechanism to immunotherapy. *Cancer letters*. 393: 1-7.

ZHAO SJ, ZHAO HD, LI J, ZHANG H, GAO DT and WANG Q. 2018. CD151 promotes breast cancer metastasis by activating TGF-β1/Smad signaling pathway. *European review for medical and pharmacological sciences.* 22(21): 7314-7322.

ZHU X and ZHU J. 2020. CD4 T Helper Cell Subsets and Related Human Immunological Disorders. *International journal of molecular sciences*. 21(21): 8011

ZHU Y, GU L, LIN X, ZHANG J, TANG Y, ZHOU X, LU B, LIN X, LIU C, PROCHOWNIK EV and LI Y. 2022. Ceramide-mediated gut dysbiosis enhances cholesterol esterification and promotes colorectal tumorigenesis in mice. *JCI insight*. 7(3): e150607

ZIMMERMAN B, KELLY B, MCMILLAN BJ, SEEGAR T, DROR RO, KRUSE AC and BLACKLOW SC. 2016. Crystal Structure of a Full-Length Human Tetraspanin Reveals a Cholesterol-Binding Pocket. *Cell*. 167(4): 1041-1051.e11.

SUPPLEMENTARY DATA

Table 1-1. The co-migration of B cells with non-B cells to CM-IBCs (4H)

	CM-SUM149 B cells	CM-BCX010 B cells	CM-SUM190 B cells	CM-MD-IBC3 B cells	CM-KPL4 B cells
Monocytes	0.657	-0.600	-0.769	-0.205	-0.386
CD4+ T cells	0.406	0.400	0.003	-0.656	0.929*
CD8+ T cells	0.771	0.300	-0.114	-0.078	0.282

*Correlation is significant below 0.05 (2-tailed).

Table 1-2. The co-migration of B cells with non-B cells to CM-IBCs (16H)

	CM-SUM149 B cells	CM-BCX010 B cells	CM-SUM190 B cells	CM-MD-IBC3 B cells	CM-KPL4 B cells
Monocytes	-0.927*	-0.467	-0.596	-0.500	0.621
CD4+ T cells	0.945*	0.813	-0.652	0.200	0.937
CD8+ T cells	0.921*	0.808	-0.100	0.100	0.960*

*Correlation is significant below 0.05 (2-tailed).

Table 1-3. The co-migration between different subsets to CM-SUM149/pLVx

CM-SUM149/pLVx	Monocytes	CD4+ T cells	CD8+ T cells	B cells
Monocytes	**/**	**<-0.01**	**0.037**	**0.033**
CD4+ T cells	**-0.065**	**/**	**0.487****	**0.475****
CD8+ T cells	**0.086**	**0.487****	**/**	**0.344***
B cells	**0.033**	**0.486****	**0.437***	**/**

** Correlation is significant below 0.01 (2-tailed).

Table 1-4. The co-migration between different subsets to CM-SUM149/Tspan6

CM-SUM149 /Tspan6	Monocytes	CD4+ T cells	CD8+ T cells	B cells
Monocytes	/	0.050	0.088	<-0.001
CD4+ T cells	0.050	/	0.336*	0.566***
CD8+ T cells	0.088	0.336*	/	0.274
B cells	<-0.001	0.566***	0.274	/

** Correlation is significant below 0.01 (2-tailed).

Table 1-5. The co-migration between different subsets to CM-BCX010/pLVx

CM-BCX010/pLVx	Monocytes	CD4+ T cells	CD8+ T cells	B cells
Monocytes	/	0.043	0.335	-0.246
CD4+ T cells	-0.043	/	0.830***	0.223
CD8+ T cells	0.335	0.830***	/	0.073
B cells	-0.246	0.223	0.073	/

** Correlation is significant below 0.01 (2-tailed).

Table 1-6. The co-migration between different subsets to CM-BCX010/Tspan6

CM-BCX010/Tspan6	Monocytes	CD4+ T cells	CD8+ T cells	B cells
Monocytes	/	0.402	0.252	0.161
CD4+ T cells	0.402	/	0.665*	0.052
CD8+ T cells	0.252	0.665*	/	-0.142
B cells	0.161	0.052	-0.142	/

*Correlation is significant below 0.05 (2-tailed).

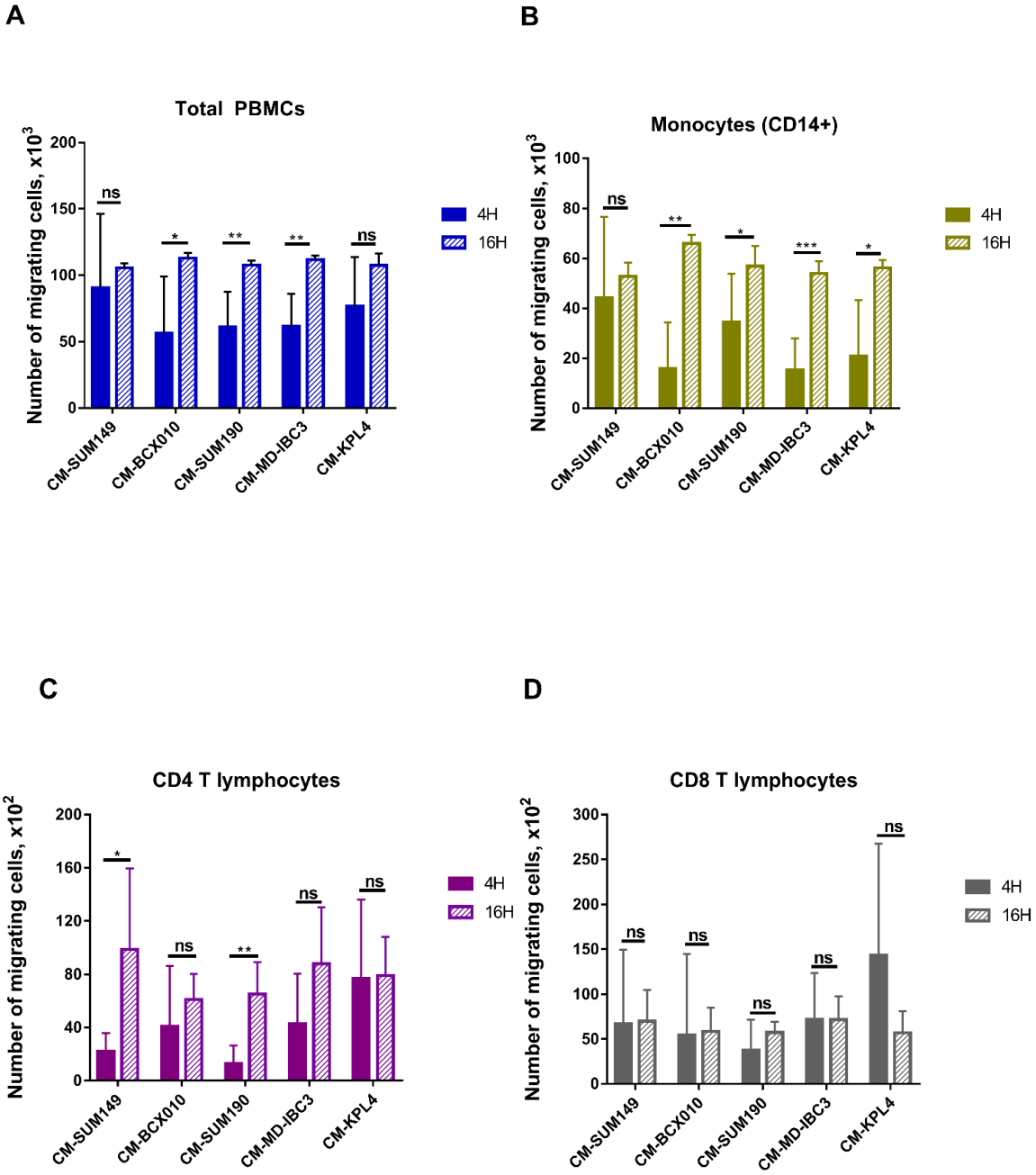
A
Total PBMCs
Number of migrating cells, x10^3
200
150
100
50
0
ns
*
**
**
ns
CM-SUM149
CM-BCX010
CM-SUM190
CM-MD-IBC3
CM-KPL4
4H
16H
B
Monocytes (CD14+)
Number of migrating cells, x10^3
100
80
60
40
20
0
ns
**
*
***
*
CM-SUM149
CM-BCX010
CM-SUM190
CM-MD-IBC3
CM-KPL4
4H
16H
C
CD4 T lymphocytes
Number of migrating cells, x10^2
200
160
120
80
40
0
*
ns
**
ns
ns
CM-SUM149
CM-BCX010
CM-SUM190
CM-MD-IBC3
CM-KPL4
4H
16H
D
CD8 T lymphocytes
Number of migrating cells, x10^2
300
250
200
150
100
50
0
ns
ns
ns
ns
ns
CM-SUM149
CM-BCX010
CM-SUM190
CM-MD-IBC3
CM-KPL4
4H
16H

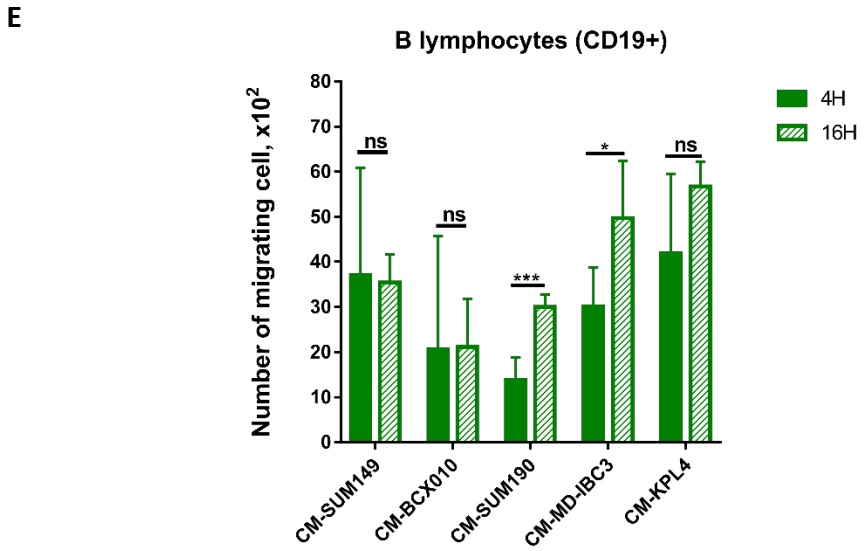

Figure 1-1. The length of migration time differently affects the migration of immune cells. (A-E) The migration of PBMCs (A), monocytes (B), T cells (C, D) and B cells (E) migrating to CM-SUM149, CM-BCX010, CM-SUM190, CM-MD-IBC3, CM-KPL4 under different conditions (4 and 16 hours) were compared. P values are indicated on the graph, *p<0.05, **p<0.01, ***p<0.001.

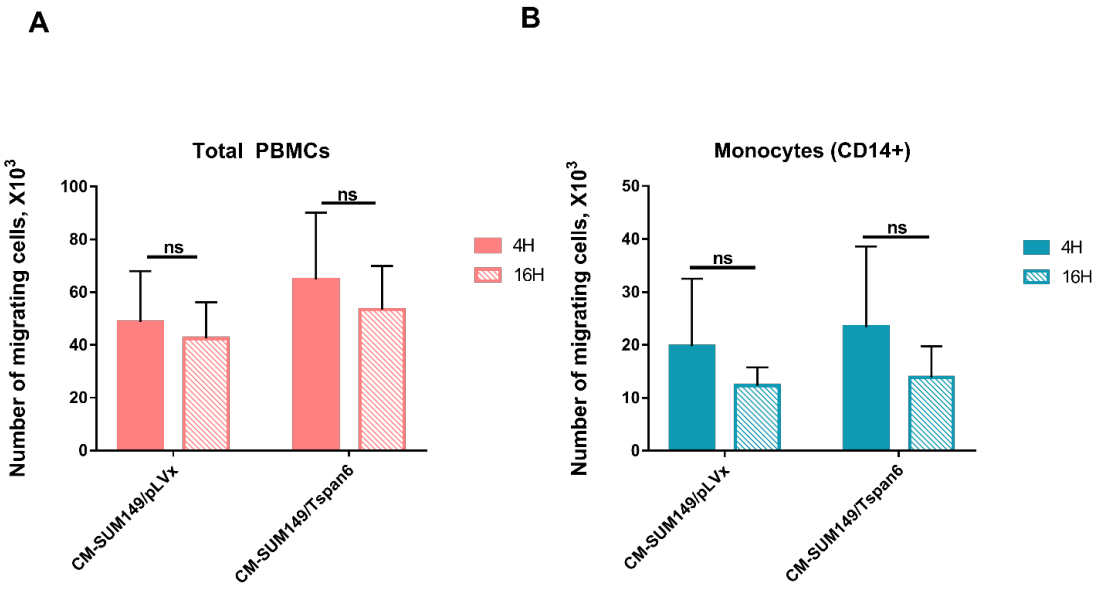

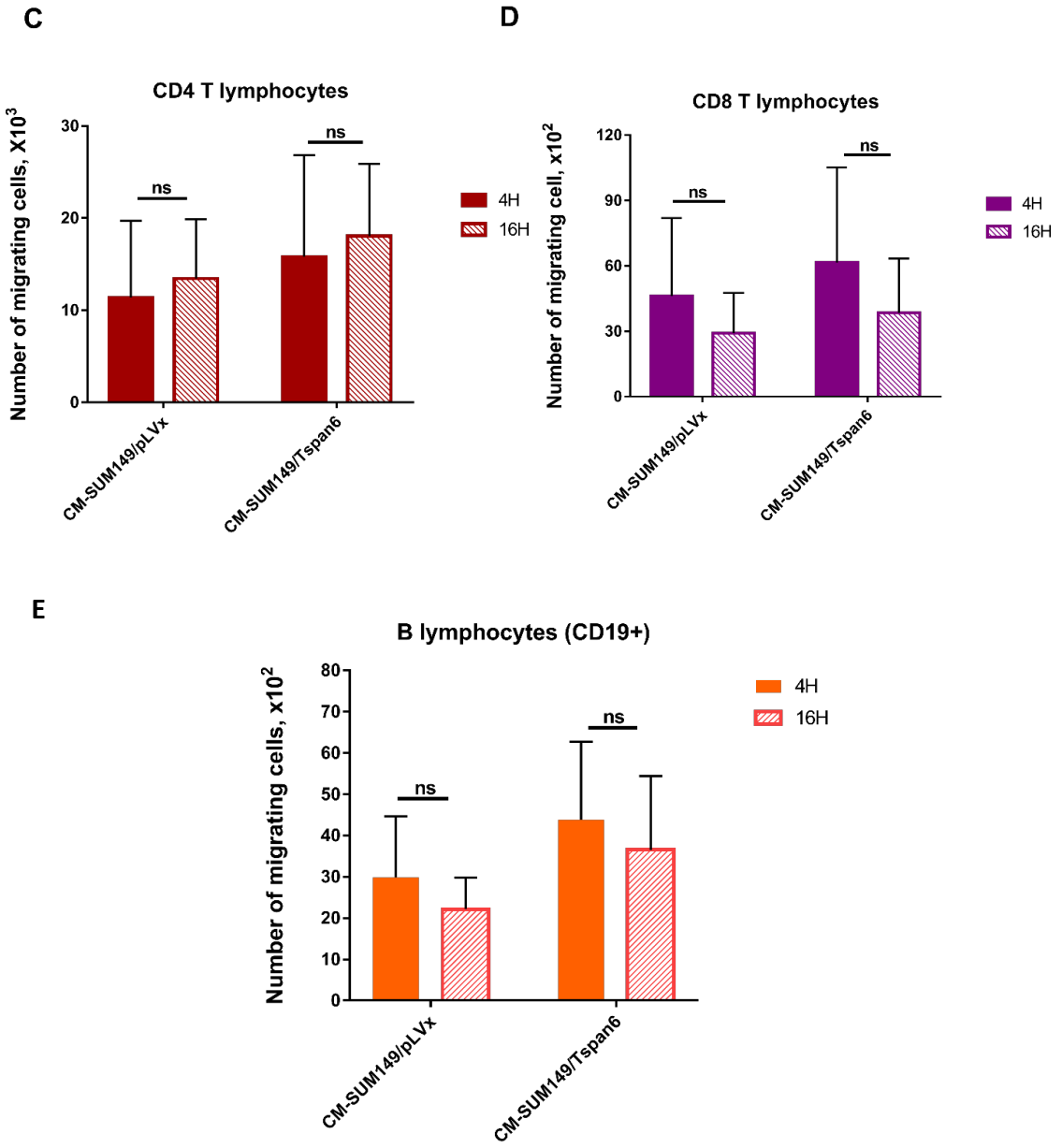

Figure 1-2. The Tspan6-dependent migration of B cells occurs in the early stage. (A-E) The absolute numbers of total PBMCs (A), monocytes (B), CD4 T cells (C), CD8 T cells (D) and B cells (E) migrating to CM-SUM149/Tspan6 within 4 and 16 hours were compared. Cells under the same condition migrating to CM-SUM149/pLVx were controls. P values are indicated on the graph.

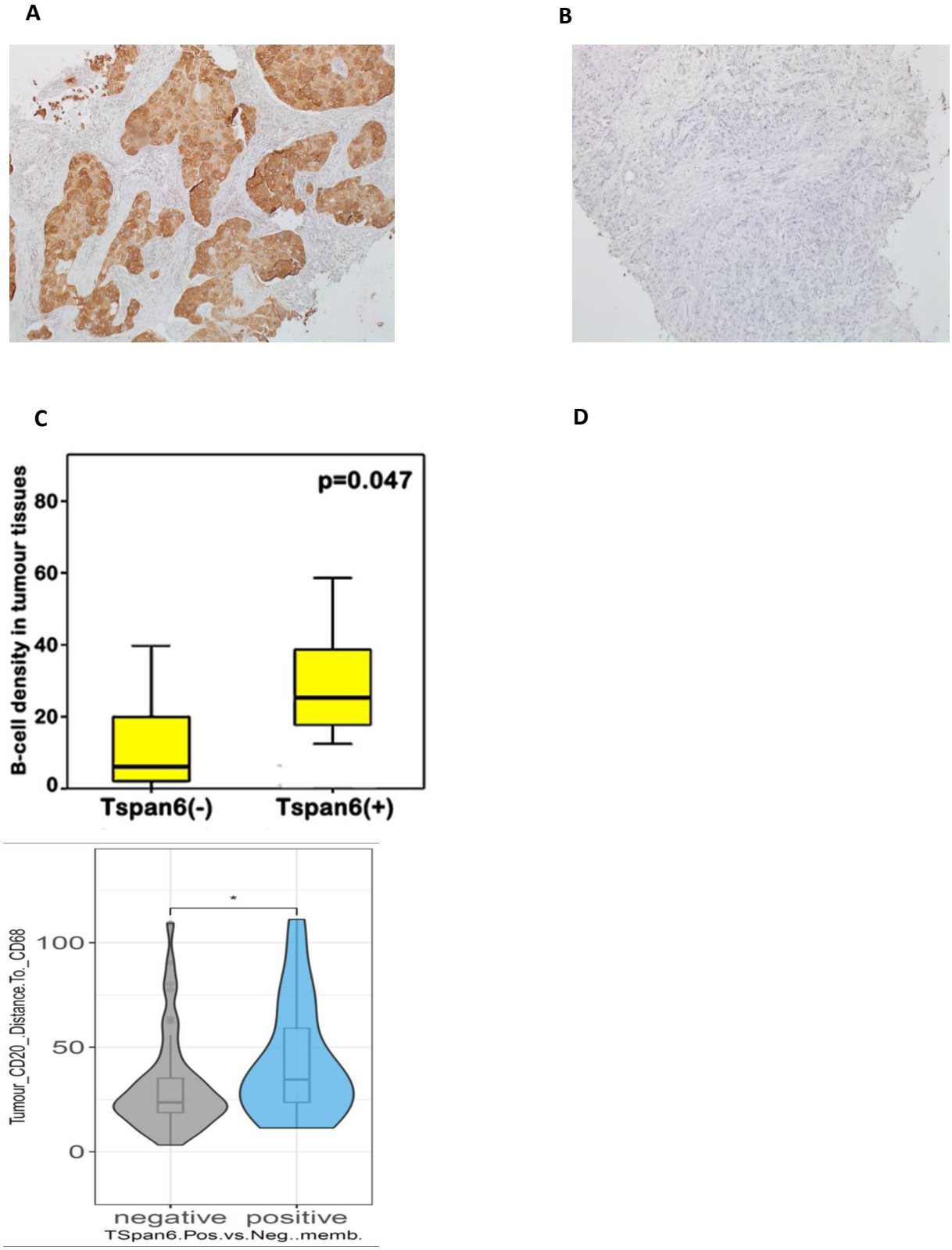

Figure 1-3. Immunostaining for Tspan6 in IBC tissues. **(A)** Positive expression (brown) of Tspan6 in IBC. **(B)** Negative expression of Tspan6 in IBC. **(C)** The expression of Tspan6 positively

correlates with tumour-infiltrating B cells. **(D)** Intratumoural co-existance of CD20+ and CD68+ cells correlated with positive Tspan6 expression. Unpublished data provided by Badr.et.al.

A

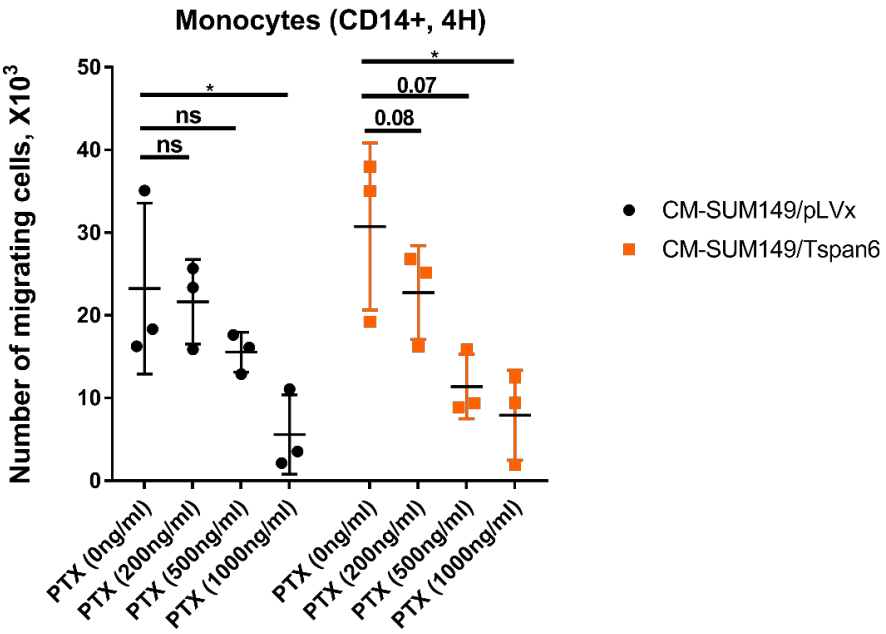

B

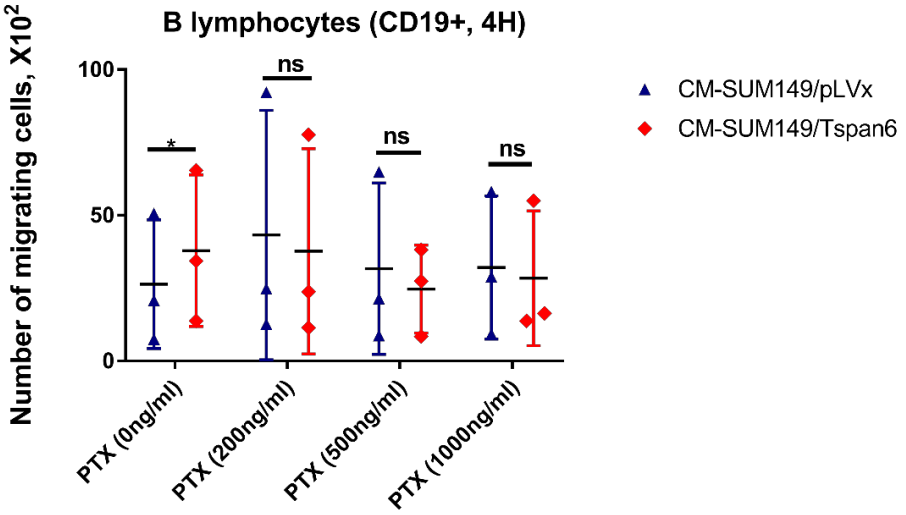

Figure 1-4. PTX partially affects the ability of monocytes to promote the Tspan6-dependent migration of B cells. (A, B) The short-term migration of PBMCs' moncoytes and B cells to CM-SUM149/Tspan6 and CM-SUM149/pLVx after PTX pre-treatment. PBMCs ($2x10^6$ cells/200 µl) were pre-treated with different concentrations of PTX and were allowed to migrate to above CM for 4 hours. P values are indicated on the graph, *p<0.05.

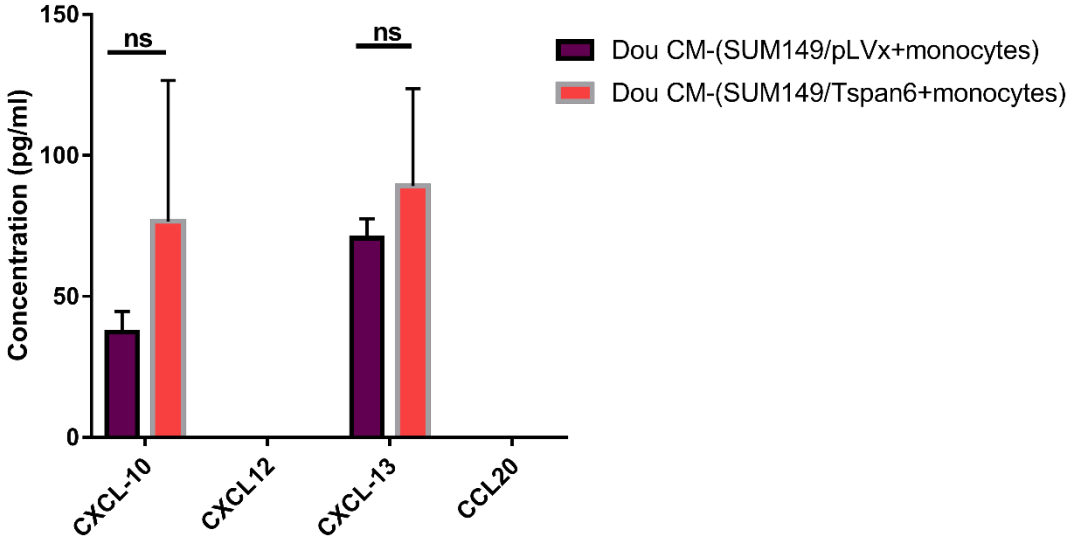

Figure 1-5. Chemokines in double CM. Pure monocytes ($2x10^5$ cells/ml) were cultured in CM-SUM149/Tspan6 and CM-SUM149/pLVx for 4 hours to generate double CM (Dou CM-SUM149/Tspan6 and Dou CM-SUM149/pLVx). Concentrations of chemokines related to B cell chemotaxis in double CM were assessed by ELISA. Shown are means with SD of the results of 2-3 independent experiments. P values are indicated on the graph.

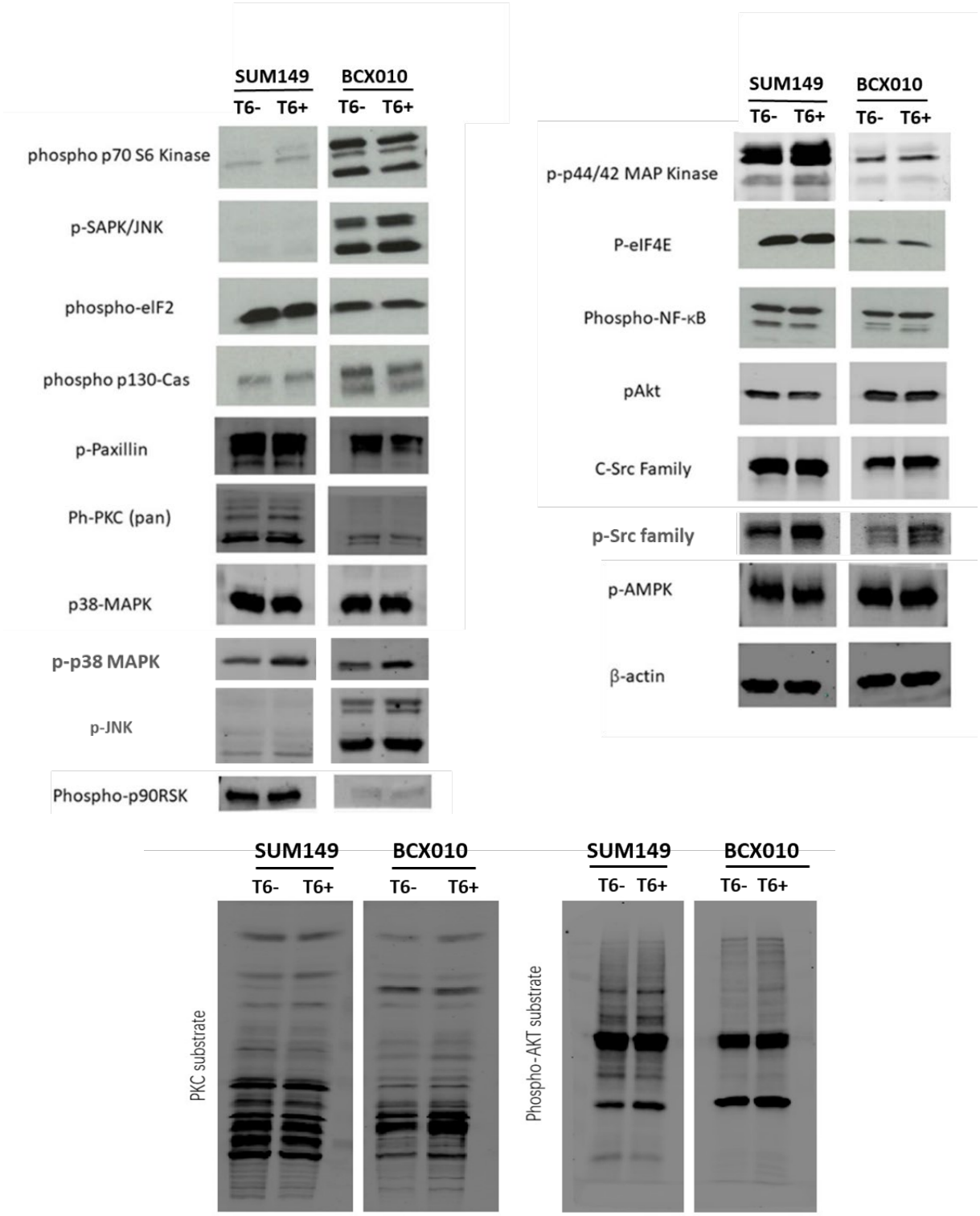

Figure 1-6. The impact of Tspan6 on the signalling pathways of IBC cells. The expression of proteins involved in IBC-related signalling pathways was analyzed by western blot.

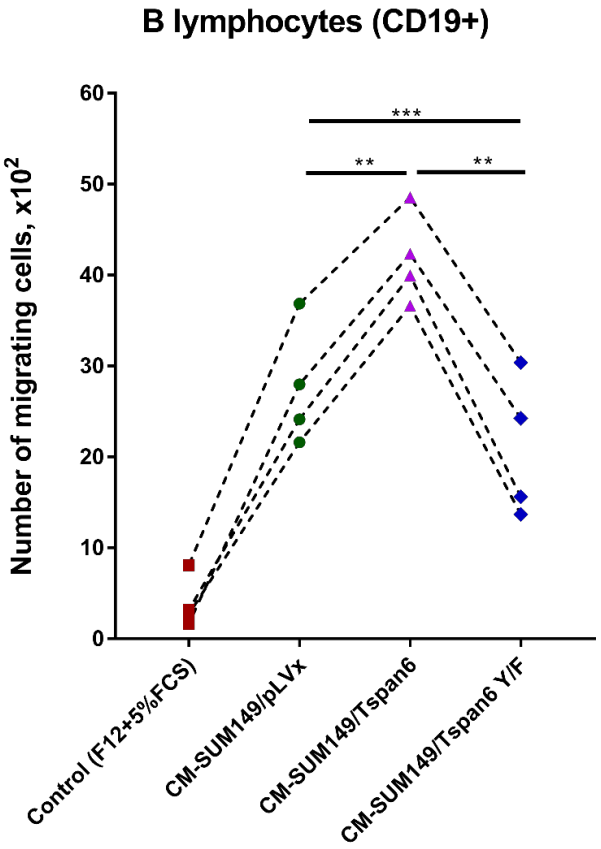

Figure 1-7. Mutation in tyrosin-sorting motif of Tspan6 diminishes the Tspan6-dependent migration of B cells. The mutation of tyrosin-sorting motif of Tspan6 was complished by substituting tyrosine in the C-terminal of Tspan6 with phenylalanine (Y→F). PBMC migration experiments were performed as described in Chapter I section 3.2. B cell migration to CM-SUM149/pLVx, CM-SUM149/Tspan6, CM-SUM149/Tspan6 Y/F, and control medium was assessed separately. Numbers connected by dot line indicated donor-matched experiment. P values are indicated on the graph, *p<0.05, **p<0.01, ***p<0.001.

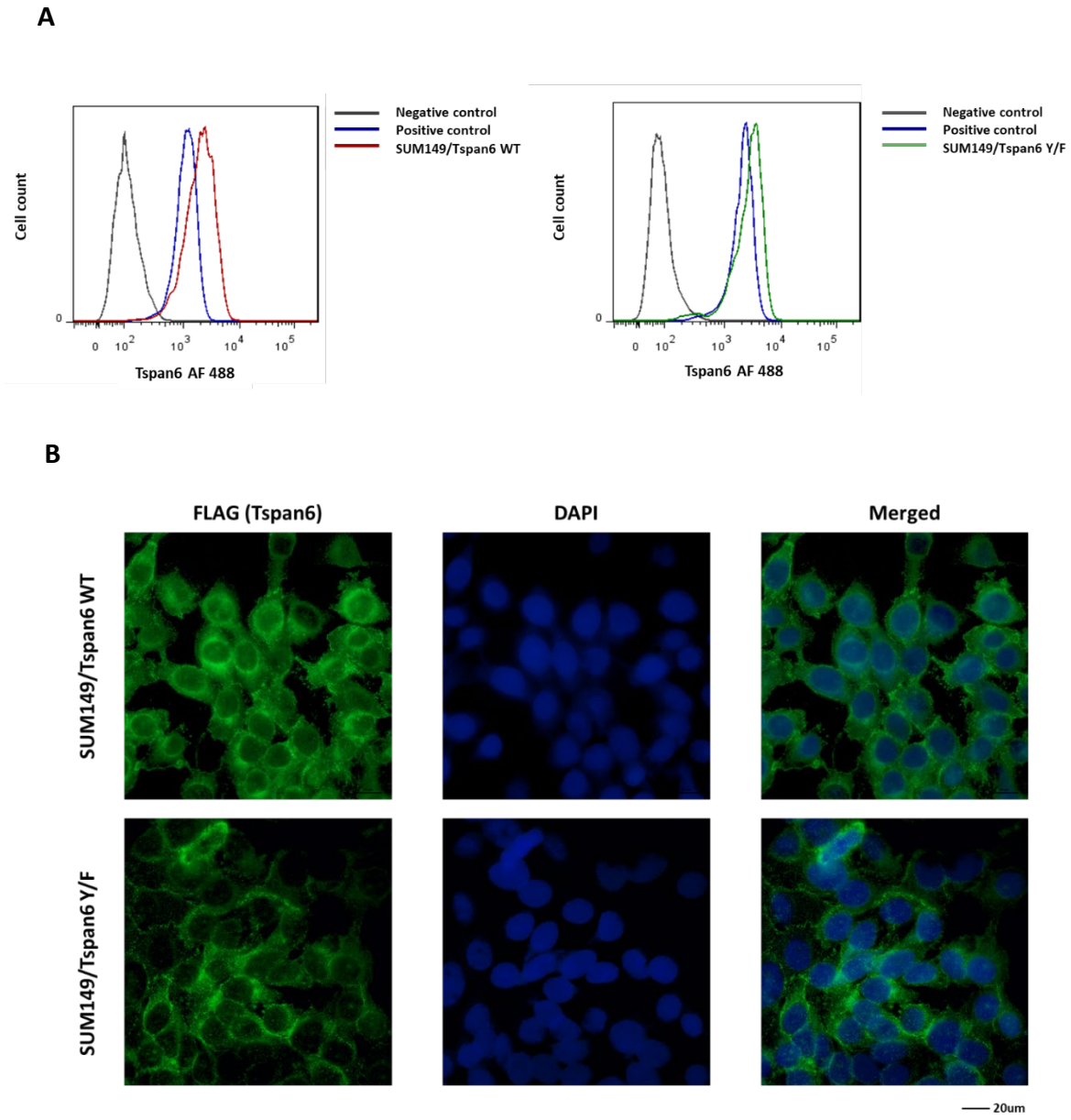

Figure 1-8. Membranous distribution of Tspan6 Y/F on IBC cells. (A) Tspan6 expression was assessed by FACS with an in-house generated mouse antibody against Tspan6. Ab M38 (Anti-CD81) and Ab 4C5G (anti-Type II PI 4-kinase) were applied as positive and negative controls **(B)** Representative Immunofluorescent images of SUM149/Tspan6 and SUM149/Tspan6 Y/F. Flag-tagged Tspan6 was detected by mAb anti-Flag and visualised by goat anti-mouse Ab conjugated with AF488.

APPENDIX

Table of Buffers

Buffer	Composition	Notes
Cell freezing solution	10% (v/v) dimethyl sulfoxide (DMSO) (Sigma-Aldrich) and 90% (v/v) FCS (Gibco)	
1x Phosphate-buffered saline (PBS)	1x PBS tablet in 100ml of dH2O.	
1% Triton X-100 buffer	Dilute 100% TritonX-100 in PBS with 1:99.	
0.1% Triton X-100 buffer	Dilute 1% TritonX-100 in PBS with 1:9.	
10x Tris-buffered saline (TBS)	87.6g NaCl, 60.6g Tris base in 1L of dH2O.	Adjusted to pH 7.6. The working solution was diluted in dH_2O to 1x TBS. 0.05% Tween20 added to 1x TBS for 1x TBS-T
4x Laemmli buffer .	4ml 20% w/v SDS, 4ml 100% glycerol, 3.25ml 1M Tris-Cl pH 6.8, and 1.55ml dH2O	Diluted to 1x with 1:3 of dH2O. If needed, β-mercaptoethanol was added to achieve a final concentration of 5%. Bromophenol blue, if needed, was added to a final concentration of 0.02% w/v.
1% Brij98	1% v/v in 1xPBS. E.g. 1ml Brij98 in 100ml PBS.	
Blocking buffer (5% milk)	5% w/v in 1x TBS-T. E.g. 5g milk in 100ml TBS-T.	Used with antibodies for detecting non-phosphorylated proteins.
Blocking buffer (3%	3% w/v in 1x TBS-T. E.g. 3g	Used with antibodies

Bovine serum albumin)	BSA in 100ml TBS-T.	for detecting phosphorylated proteins.
Blocking buffer (20% goat serum)	4ml goat serum in 16ml PBS	Filtered using 0.2 um membrane prior to using. Used with antibodies for immunofluorescence.
4% Paraformaldehyde (PFA)	2g PFA, and 1.5g sucrose, 25ul 2M $MgCl_2$, 25ul 1M $CaCl_2$ in 50 ml 1x PBS.	
2% Paraformaldehyde (PFA)	0.4 g of paraformaldehyde, 2 ml 10xPBS, 10 ul of 10% w/v NaOH, 10ul of CaCl2 1M, 10ul of MgCl2 2M, 0.6 g of sucrose in 18ml dH2O	Adjusted to pH 7.0 by adding 8.3ul 12M HCl before adding CaCl2, MgCl2 and sucrose.